# Subsurface Stratigraphy and Geochemistry of Late Quaternary Evaporites, Searles Lake, California

GEOLOGICAL SURVEY PROFESSIONAL PAPER 1043


# Subsurface Stratigraphy and Geochemistry of Late Quaternary Evaporites, Searles Lake, California

By GEORGE I. SMITH

With a section on RADIOCARBON AGES OF STRATIGRAPHIC UNITS
By MINZE STUIVER and GEORGE I. SMITH

GEOLOGICAL SURVEY PROFESSIONAL PAPER 1043

*Description of the stratigraphic succession of muds and salts deposited by closed-basin lakes that occupied Searles Valley during late Quaternary time*


UNITED STATES GOVERNMENT PRINTING OFFICE, WASHINGTON : 1979

**UNITED STATES DEPARTMENT OF THE INTERIOR**

**CECIL D. ANDRUS,** *Secretary*

**GEOLOGICAL SURVEY**

**H. William Menard,** *Director*

Library of Congress Cataloging in Publication Data

Smith, George Irving, 1927-
Subsurface stratigraphy and geochemistry of late Quaternary evaporites, Searles Lake, California.

(Geological Survey Professional Paper 1043)
Bibliography: p. 118-122.
Includes index.
1. Evaporites–California–Searles Lake. 2. Geology, Stratigraphic–Quaternary. 3. Geochemistry–California–Searles Lake. 4. Geology–California–Searles Lake. I. Title. II. Series: United States. Geological Survey. Professional paper 1043.
QE471.15.E8S58 551.7'9'0979495 77-10704

For sale by the Superintendent of Documents, U.S. Government Printing Office
Washington, D.C. 20402

Stock Number 024-001-03163-9

# CONTENTS


| | Page |
|---|---|
| Abstract | 1 |
| Introduction | 2 |
| Discovery and economic development of Searles Lake | 4 |
| Geologic environment and history of Searles Lake | 5 |
| Previous geologic studies of Searles Lake | 6 |
| Acknowledgments | 8 |
| Stratigraphy of the evaporite deposits | 8 |
| Mixed Layer | 13 |
| Areal extent and thickness | 13 |
| Mineral composition and lithology | 13 |
| Bottom Mud | 15 |
| Areal extent and thickness | 16 |
| Mineral composition and lithology | 16 |
| Chemical composition of the Bottom Mud | 17 |
| Lower Salt | 18 |
| Areal extent and volume | 20 |
| Saline units | 20 |
| Mud units | 20 |
| Mineral composition and lithology | 34 |
| Saline units | 34 |
| Mud units | 37 |
| Chemical composition | 40 |
| Chemical analyses of the solids | 40 |
| Chemical analyses of the brines | 43 |
| Estimated bulk composition of the unit | 47 |
| Parting Mud | 47 |
| Areal extent and volume | 47 |
| Mineral composition and lithology | 48 |
| Chemical composition | 54 |
| Upper Salt | 56 |
| Areal extent and volume | 56 |
| Mineral composition and lithology | 59 |
| Chemical composition | 60 |
| Chemical analyses of the solids | 60 |
| Chemical composition of the brines | 60 |
| Stratigraphy of the evaporite deposits—Continued | |
| Upper Salt—Continued | |
| Estimated bulk composition of the unit | 64 |
| Overburden Mud | 66 |
| Areal extent and volume | 66 |
| Mineral composition and lithology | 66 |
| Chemical composition | 68 |
| Radiocarbon ages of stratigraphic units, by Minze Stuiver and George I. Smith | 68 |
| Introduction | 68 |
| Reliability of sampled materials | 70 |
| Probable true ages of stratigraphic units | 73 |
| Rates of deposition | 75 |
| Geochemistry of sedimentation | 78 |
| Mud Layers | 79 |
| Saline layers | 82 |
| Phase relations applicable to Searles Lake salts | 83 |
| Salines in the Mixed layers | 84 |
| Salines in the Bottom Mud | 85 |
| Salines in the Lower Salt, Upper Salt, and Overburden Mud | 86 |
| Lower Salt | 86 |
| Upper Salt | 91 |
| Overburden Mud | 95 |
| Geochemical influence on shape and thickness of salt bodies | 96 |
| Source of salt components | 98 |
| Geochemistry of diagenesis | 100 |
| Mud layers | 100 |
| Salt layers | 106 |
| Reconstructed depositional history | 108 |
| Correlations with deposits in other areas | 112 |
| Economic geology | 116 |
| References cited | 118 |


# ILLUSTRATIONS


| | | Page |
|---|---|---|
| PLATE 1. | Subsurface sections showing relations between stratigraphic units of Searles Lake, California. | In pocket |
| 2. | Diagrams showing components in Mixed Layer and Bottom Mud of Searles Lake, California. | In pocket |
| FIGURE 1. | Index map showing location of Searles Lake and other Pleistocene lakes | 3 |
| 2. | Graphs showing average temperature and rainfall, Searles Valley | 4 |
| 3. | Map showing location of core holes | 9 |
| 4. | Stratigraphic column showing units in Searles Lake | 11 |
| 5. | Cross section of Searles Valley showing bedrock profile and stratigraphy of upper part of fill | 12 |
| 6. | Graph showing weight percent acid-insoluble material in Bottom Mud | 18 |
| 7. | Contour map on base of Lower Salt | 19 |

FIGURES 8–20. Isopach maps: Page
8. Unit S–1 21
9. Unit S–2 22
10. Unit S–3 23
11. Unit S–4 24
12. Unit S–5 25
13. Unit S–6 26
14. Unit S–7 27
15. Unit M–2 28
16. Unit M–3 29
17. Unit M–4 30
18. Unit M–5 31
19. Unit M–6 32
20. Unit M–7 33
21. Diagrams showing compositions of brines in Lower Salt in relation to phase boundaries 46
22. Contour map on base of Parting Mud 49
23. Isopach map, Parting Mud 50
24. Graphs showing volume percent of components in Parting Mud 52
25. Graph showing percentage of pore water in samples of Parting Mud 54
26. Contour map on base of Upper Salt 57
27. Isopach map, Upper Salt 58
28. Diagram showing composition of brines in Upper Salt in relation to phase boundaries 65
29. Photograph showing polygonal cracks in lake surface 67
30. Stratigraphic column showing position and age of $^{14}C$ dated samples from cores 69
31. Stratigraphic column showing relation between depth and new $^{14}C$ ages of mud layers in Lower Salt 74
32. Graph showing relation between area, volume, and salinity of Pleistocene Searles Lake 78
33. Phase diagram of $NaHCO_3$–$Na_2CO_3$–$Na_2SO_4$–NaCl–$H_2O$ system at 20° C 83
34. Graph showing percentages of major minerals in Lower Salt and Upper Salt 87
35–39. Phase diagrams showing:
35. Stability fields in $NaHCO_3$–$Na_2CO_3$–$Na_2SO_4$–NaCl–$H_2O$ system at 20° C for crystallization of units S–1 to S–5 87
36. Stability fields in $Na_2CO_3$–$Na_2SO_4$–NaCl–$H_2O$ system at 15° C for crystallization of units S–6 and S–7 89
37. Superimposed 5-component and 4-component systems at 20° C 89
38. Stability fields in $NaHCO_3$–$Na_2CO_3$–$Na_2SO_4$–NaCl–$H_2O$ system at 20° C 91
39. Stability field of hanksite in $NaHCO_3$–$Na_2CO_3$–$Na_2SO_4$–NaCl–$H_2O$ system at 20° C 93
40. Graph showing relation between temperature and depth in sediments of Searles Lake 101
41. Graph showing inferred history of fluctuations in Searles Lake, 0–150,000 years ago 109
42. Diagram showing possible correlations between the history of Searles Lake and the histories of other lakes and glaciers 112
43. Diagram showing possible correlations between the history of Searles Lake and the histories indicated by other climatically sensitive criteria 113
44. Diagram comparing details of Searles Lake fluctuations and Laurentide ice sheet fluctuations 115

# TABLES

TABLE 1. Nonclastic minerals in the Searles Lake evaporites Page 10
2. Chemical analyses of core samples from the Mixed Layer 15
3. Area and volume of units in the Lower Salt 20
4. Estimated mineral compositions of saline layers in the Lower Salt 35
5. Estimated mineral compositions of mud layers in the Lower Salt 38
6. Mineral abundance in mud units of the Lower Salt, core GS–14, determined for total sample and acid-insoluble fraction of sample 40
7. Chemical analyses of solids in the Lower Salt 41
8. Comparison of chemical analyses with composition indicated by visual estimates of mineral percentages 42
9. Chemical analyses of brines in the Lower Salt 44
10. Estimated percentages and total quantities of water soluble components in the upper two and lower five units of the Lower Salt 48
11. Megascopic mineral composition of the Parting Mud 51
12. Size distribution of acid-insoluble material in four samples of the Parting Mud, core L–12 53
13. Partial chemical analyses of samples from core GS–16 in Parting Mud 55
14. Mineral composition of salines in the Upper Salt by contour interval 59
15. Chemical analyses of cores from the Upper Salt and Overburden Mud 61

Page

TABLE 16. Chemical analyses of brines from the Upper Salt and Overburden Mud ---- 62
17. Estimated percentages and total quantities of water-soluble components in the Upper Salt ---- 66
18. Partial chemical analyses of core GS–40 from the Overburden Mud ---- 68
19. New $^{14}C$ dates on disseminated organic carbon in mud layers of the Lower Salt and top of the Bottom Mud, core L–31 70
20. Depositional rates in Parting Mud ---- 77
21. Comparison of amount of selected components carried by Owens River in 24,000 years with amount now in Owens Lake and Upper Salt of Searles Lake ---- 99
22. Analyses of brines pumped to chemical plants, 1938–51 ---- 117

# SUBSURFACE STRATIGRAPHY AND GEOCHEMISTRY OF LATE QUATERNARY EVAPORITES, SEARLES LAKE, CALIFORNIA

By GEORGE I. SMITH

ABSTRACT

Searles Lake is a dry salt pan, about 100 km² in area, that lies on the floor of Searles Valley, in the desert of southeast California. Several salt bodies of late Quaternary age lie beneath the surface, mostly composed of sodium and potassium carbonate, sulfate, chloride, and borate minerals. Mud layers separate the salt bodies, which contain interstitial brine that is the source of large quantities of industrial chemicals. The value of annual production from the deposit exceeds $30 million; total production to date exceeds $1 billion.

The salts and muds were deposited during Pleistocene and Holocene times by a series of large lakes (200 m maximum depth, 1,000 km² maximum area) that fluctuated in size in response to climatic change. Salts were deposited during major dry (interpluvial) episodes, muds during wet (pluvial) episodes that correlate with glacial advances in other parts of North America and the world. Data based on cores from the deposit are used in this paper to establish the stratigraphy of the deposit, the chemical and mineral compositions of successive units, and the total quantities of components contained by them. These parameters are then used to determine the geochemical evolution of the sedimentary layers. The results provide a refined basis for reconstructing the limnology of Searles Lake and the regional climate during late Quaternary time.

Six main stratigraphic units were distinguished and informally named earlier on the basis of their dominant composition:

| *Unit* | *Typical thickness (in meters)* | *$^{14}C$ age, uncorrected (years B.P.)* |
|---|---|---|
| Overburden Mud | 7 | 0 to >3,500 |
| Upper Salt | 15 | >3,500 to 10,500 |
| Parting Mud | 4 | 10,500 to 24,000 |
| Lower Salt | 12 | 24,000 to 32,500 |
| Bottom Mud | 30 | 32,500 to 130,000 |
| Mixed Layer | 200+ | >130,000 |

(The age of 130,000 years for the Mixed Layer is based on extrapolated sedimentation rates.) The Lower Salt is subdivided into seven salt units (S–1 to S–7) and six mud units (M–2 to M–7), the Mixed Layer into six units (A to F). For each salt unit, the areal extent, volume, shape, mineralogy, and chemical composition of the solids and brines have been determined; for each mud unit (which originally extended over much of the basin), the shape and volume within a standard area, and the mineralogy, have been determined. The bulk compositions (brines plus salts) of the combined Lower Salt units S–1 to S–5 and units S–6 and S–7, and the Upper Salt, were determined so that the total quantities and ratios of ions in the initial brines could be reconstructed.

The 74 published $^{14}C$ dates on Searles Lake core samples from all but the oldest unit are supplemented by 14 new dates (determined by Minze Stuiver) on the Lower Salt. Most of the age control comes from dates based on disseminated organic carbon; two dates are on wood; dates on carbonate minerals are less reliable. Although the probable disequilibrium between the carbon in the lake and atmosphere (because of contamination, slow equilibrium rates, and other factors) causes disseminated carbon dates to be an estimated 500–2,500 years "too old," the ages of the major and minor units are relatively well established. The list above indicates rounded and uncorrected ages for the contacts of major units. The age of the only salt bed in the Lower Salt which indicates desiccation (S–5) is about 28,000 years. The average uncorrected sedimentation rate in the Parting Mud is 46 yr/cm. Correcting the indicated Parting Mud sedimentation rate on the basis of the greater acid-insoluble content of the Bottom Mud suggests an average rate for it of 33 yr/cm. Using this figure, the age of the base of the Bottom Mud is estimated to be near 130,000 years.

The stratigraphy and mineralogy, combined with known and inferred dates, provide a basis for reconstructing the climatically controlled history of Searles Lake. The best known part is for the past 150,000 years, for which more than 30 major changes in lake level are reconstructed. Prior to that time, less detail can be determined, but there seems to have been a very long period dominated by dryness.

Close similarities in age exist between the major fluctuations in the levels of Searles Lake and the advances and retreats of glaciers in eastern and western North America, fluctuation in atmospheric and sea surface temperatures, and changes in world sea level. The Upper Salt and Overburden Mud are correlated with Holocene and Valderan deposits of the Laurentide ice sheet in eastern North America, the Parting Mud with Twocreekan and Woodfordian deposits, the upper part of the Lower Salt (S–5 and above) with Farmdalian deposits, the lower part of the Lower Salt and part of the Bottom Mud with Altonian deposits. Thin salt layers in the Bottom Mud that are estimated to be about 105,000 years old are provisionally correlated with Sangamon deposits, the 10 m of mud below them with Illinoian deposits, and most of the Mixed Layer with Yarmouth deposits.

The late Quaternary lakes in Searles Valley contained enough dissolved solids for chemical sediments to form at all times. Relatively insoluble minerals precipitated from the large fresh to brackish lakes and salts precipitated from the small highly saline lakes. The geochemical reconstruction of the sedimentation processes allows many of the chemical, physical, and limnological conditions to be approximated. Primary aragonite, calcite, and

possibly dolomite precipitated from even the largest lakes. Some of their precipitation was caused by temperature change and evaporation, but laminae of aragonite (and possibly some northupite) were apparently caused by mixing along the chemocline between a fresh surface layer and an underlying saline layer of higher density. Diagenesis after burial produced gaylussite and pirssonite (when Na-carbonate brines reacted with Ca-carbonate minerals), analcime, searlesite, K-feldspar, and phillipsite. Primary and secondary carbonate minerals now constitute 60 to 85 percent of most mud units; diagenetic silicates, clastic silicates, and organic material form the balance.

The salt layers contain varying mixtures of saline minerals that are zoned both concentrically and vertically. Published logs provide data that allow quantitative estimates of the saline mineral distribution and volume. In the Mixed Layer, halite, trona, and nahcolite are the dominant saline minerals. In the Lower Salt, trona, halite, and burkeite are most abundant; northupite, thenardite, hanksite, borax, nahcolite, sulfohalite, and tychite occur in minor to trace quantities. In the Upper Salt, halite, trona, and hanksite are most abundant; borax, burkeite, thenardite, aphthitalite (glaserite), and sulfohalite occur in that order of decreasing abundance.

Trona constitutes most of the edge facies of all units; other minerals are more abundant in central or intermediate facies. Vertical zonation reflects the original crystallization sequence modified by diagenesis. Units S–1 to S–5 in the Lower Salt represent one sequence that was interrupted by four deep lakes that deposited mud: trona is the dominant mineral in units S–1, S–2, and S–3; trona and burkeite make up most of S–4; and halite, trona and burkeite occur in S–5, which represents desiccation. This sequence is best explained by the phase relations in the $Na_2CO_3$–$NaHCO_3$–$Na_2SO_4$–NaCl–$H_2O$ system at 20°C which relates these minerals. Units S–6 and S–7 of the Lower Salt represent two episodes of incomplete desiccation; trona and halite make up most of both units. Phase relations in the same system at 15°C best explain the compositions of these units. The Upper Salt represents a single desiccation episode. Borax and trona occur at the base, and halite and hanksite constitute most of the upper part. The initial crystallization sequence was trona (and borax), then thenardite and burkeite, halite, and finally aphthitalite; diagenesis resulted in some hanksite forming at the stratigraphic position of the original thenardite and burkeite, some at the stratigraphically higher position of the aphthitalite. Initial crystallization temperatures were low, causing borax to crystallize, then increased during later stages. Phase relations at 20°C in the 5-component system given and in the $Na_2CO_3$–$Na_2SO_4$–NaCl–KCl–$H_2O$ system satisfactorily explain the observed sequence of primary and diagenetically produced minerals in the Upper Salt. Salts in the Overburden Mud are zoned concentrically because the small lake that formed them shrank and deposited successive assemblages in successively smaller areas.

Diagenetic reactions account for a high percentage of the minerals in the mud layers and some minerals in the salt layers. In the muds, gaylussite and pirssonite formed by reactions between Na-carbonate brines and Ca-carbonate minerals, the species of mineral determined by the chemical activity of $H_2O$ ($a_{H_2O}$). This reflects differences in pore water salinity in the upper 166 m of sediments and temperatures greater than about 35°C in deeper sediments. Small accumulations of trona nahcolite, northupite, and tychite probably reflect postburial changes in the chemical activity of $CO_2$ ($a_{CO_2}$). Moderate to large quantities of microcrystalline halite in the muds probably result from post-depositional increases in salinity during compaction. Aragonite, a thermodynamically unstable form of $CaCO_3$, altered spontaneously to calcite in sediments older than about 50,000 years. Slow reactions between clastic silicates and pore brines produced a suite of authigenic silicate minerals consisting of monoclinic K-feldspar, searlesite, analcime, and phillipsite. Pyrite was noted in one sample.

Diagenesis of minerals in salt layers includes increases in the sizes of crystals. This is probably a result of cycles that cause slight undersaturation and then supersaturation, the smallest crystals being dissolved during undersaturation cycles and their ingredients subsequently added to the larger ones that survived. Hanksite formed by the diagenetic reaction of metastable assemblages of burkeite, thenardite, and aphthitalite. Observations of other saline lakes now forming crystal layers suggests that the values of $a_{CO_2}$ and $a_{H_2O}$ at the surface, where crystals first formed, differ from those found a short time later in the accumulating salt layer. This environmental change results in an almost immediate change in saline mineral suites, but that change in species was generally the last; most saline minerals found in Searles Lake appear to be the same species as those formed after that initial change.

The composition of the interstitial brines changed some time after initial deposition of both salts and muds, apparently as a result of the downward migration of water from the lake surface which produced some solution of the salts. Movement of ground water in this direction is caused by the high hydrostatic head of the brines in the lake relative to the water in the surrounding valley fill.

An estimated $480 \times 10^{12}$ g of brine has been pumped as the source of $57 \times 10^{12}$ g of produced salts. This amount represents about 40 percent of the extractable salts in the original brine, but only about 6 percent of the total commercial salt in the deposit. The pumped brines are replaced by waters that dissolve enough salts to reach local chemical equilibrium, but the ratio of components in the replacement brines is less favorable for commercial operations. The quantity of chemicals that can be extracted depends partly on developments in extraction technology and partly on the level of understanding that can be achieved of the chemical and hydrologic parameters of the deposit that dictate the optimum methods of pumping and recharge.

## INTRODUCTION

The Searles Lake evaporites consist of several layers of flat-lying Quaternary deposits that underlie the dry lake in the middle of Searles Valley, San Bernardino and Inyo Counties, Calif. The valley lies near the southwest corner of the Basin and Range province and just north of the Mojave Desert; Los Angeles is about 200 km to the south-southwest, Bakersfield about 160 km to the west (fig. 1).

Searles Valley has a drainage area of about 1,600 $km^2$. The valley floor, which trends south then curves to the southwest, is about 60 km long and at places 15 km wide. Searles Lake itself is a nearly dry playa about 15 km long and 11 km wide that covers approximately 100 $km^2$; about two-thirds of this area is mud, one-third hard salt.

The climate in the valley is hot and arid. In the 36-year period ending in 1973, rainfall averaged about 96.3 mm (3.79 in.) per year, with extremes (calculated for rain years beginning July 1) ranging from 23 to 291 mm (0.92–11.47 in.). During this period, the mean annual temperature was 19.1°C (66.3°F); record tem-

peratures were 47.8°C (118°F) and −12.2°C (10°F) (fig. 2). The strongest winds come in the spring and fall. During most winters, several centimeters of water stand on Searles Lake for a few weeks or months. In the summer and early fall, the surface is normally free of standing water except for isolated brine pools and areas where the chemical plants and towns have discharged waste water onto the surface.

The surface of Searles Lake supports no vegetation. The surrounding alluvial fans and mountains are covered by a sparse growth of plants typical of the lower Sonoran zone; dominant types include creosote bush (*Larrea tridentata*), hop sage (*Grayia spinosa*), desert holly (*Atriplex hymenelytra*), and burro-bush (*Franseria dumosa*). Pinyon pine grows on the highest parts of the Argus Range; Joshua trees on the highest parts of the Slate Range.

Searles Valley is connected by California State Highway 178 from Ridgecrest to the west, and by the unnumbered continuation of that highway to Panamint and Death Valleys to the northeast. Within Searles Valley, numerous dirt roads allow access to many parts of the valley floor. The Trona Railway, which carries only freight, connects the town of Trona with the Southern Pacific Railroad about 55 km to the southwest. In the valley lie the towns of Pioneer Point,

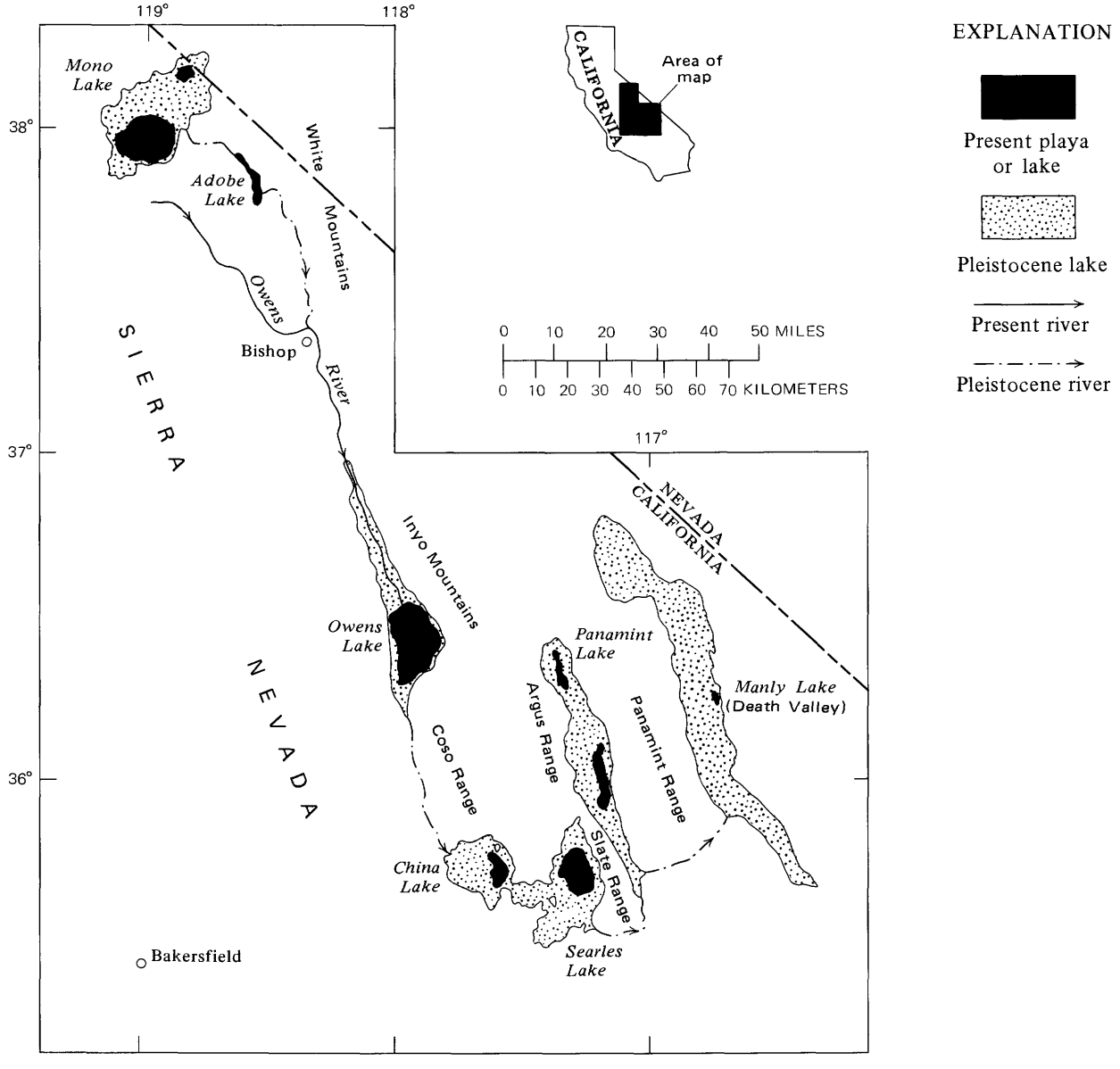


FIGURE 1.—Location of Searles Lake and other lakes connected with it in Pleistocene time.

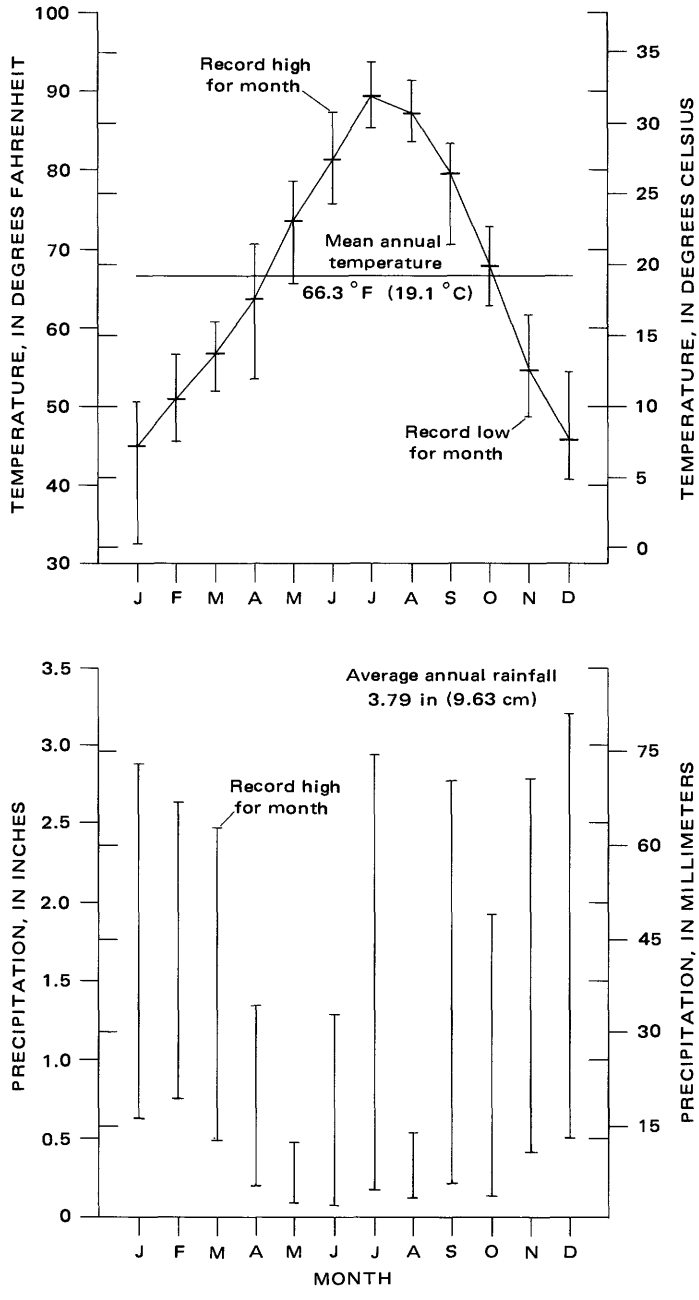


FIGURE 2.—Present climate of Searles Valley. Measurements by weather station at Trona, for period 1937–73. Data from climatological records of U.S. Department of Commerce (Weather Bureau and Environmental Data Service).

Trona, Argus, South Trona, and Westend. Trona, population about 2,000, is the largest.

## DISCOVERY AND ECONOMIC DEVELOPMENT OF SEARLES LAKE

The value of the Searles Lake evaporite deposit is now known to be worth billions of dollars, yet the lake was clearly regarded by the earliest transients as a worthless obstacle. The water was undrinkable and the surface was difficult to traverse. Records of several groups that commented on the nearly dry lake in the valley are available, among them the nearly starved Bennett-Arcane (Manly) party as they left Death Valley in 1849. Soon after 1860, prospectors found a reason for staying in this part of the desert longer than necessary: gold and silver deposits were discovered in the surrounding mountains. These and subsequently discovered deposits were worked intermittently, and their recorded production of gold, silver, lead, zinc, and copper is valued at nearly $3 million (Norman and Stewart, 1951; Smith and others, 1968, p. 28). The mines were small when compared with Darwin, Panamint City, Cerro Gordo, and others nearby, but their discovery did serve to bring prospectors and miners into the valley. Among them were the brothers John and Dennis Searles, for whom the lake was later named.

The discovery of borax occurred on February 14, 1873,[1] when Dennis Searles and E. M. Skillings first noted the similarity of material from the lake to the samples of the Nevada borate playas (Hanks, 1883). After confirming the borate content of the crusts (subsequently found to average about 8 percent), patents for 160 acres were applied for in April 1874 at the U.S. Land Office at Independence by John Searles and J. D. Creigh on behalf of all four men. Production of borax started in that year at a plant on the west side of the lake, and the company holdings were increased in size, eventually covering 2,000 acres (Dyer, 1950). On January 1, 1878, they incorporated under the name San Bernardino Borax Co.

The refining process, which employed about 30 men, operated as follows (De Groot, 1890): The crusts from the lake were collected and dumped into boiling vats of saline solution to dissolve the borax (and other soluble components) and settle out the sediment. The clear liquid was then transferred to wooden crystallizing tanks and allowed to settle for 5 to 9 days. This formed an impure grade of product that was carried in that state, or after further purification, to the Southern Pacific Railroad at Mojave by twenty-mule-team wagons. By 1889, the Searles' refinery had produced 10,500 tons of borax (Hanks, 1889). Production continued until 1895, when the Pacific Coast Borax Co. purchased the operation and closed it.

[1]Some uncertainty exists about the exact dates of these events and the size of the original operation. Hanks (1883, p. 26) is the source of the three dates given here for the discovery of borax, patenting of land, and incorporation of the holding company, and he says that the first patent application was for 160 acres. (His report, however, also describes Searles Lake as lying in T. 30 S., R. 38 E., the site of Koehn Lake.) Teeple (1929, p. 20) and Dyer (1950, p. 39) report 640 acres as the original amount of land under location. Present records of the U.S. Bureau of Land Management show that patent applications were filed by J. W. Searles and others on October 20, 1874, under the company name of Ohio Borax, and that it included 640 acres in section 20 and 21, T. 25 S., R. 43 E. (SE1/4 sec. 20, E1/2NE1/4 sec. 20, W1/2 sec. 21, W1/2NE1/4 sec. 21).

Following this, little activity occurred at Searles Lake until about 1905 or 1906, when the soda ash[2] potential of the lake was realized. This started another episode of economic development that ultimately led to its present state; the first 20 years is described in more detail by Teeple (1929, p. 21–25). By 1908, the California Trona Co. had located claims on most of the deposit and had borrowed a considerable amount of money to develop them, but the firm went into receivership the following year. To keep the property intact, development and exploration were continued by the receiver. By 1914, the reorganized company, called the American Trona Co., had constructed a small plant and completed the Trona Railway, but the new plant never produced. The operation was idled until 1916, when another new plant was finished and commercial production was started at the town of Trona—but the product was potash, not soda ash.

Earlier, in 1913, the U.S. Government had withdrawn the unowned parts of Searles Lake as a potash reserve, realizing that the European supply was about to be cut off. The same realization created a strong incentive to the companies on Searles Lake to start producing potash, known to exist in the brines of the lake at least since 1898 (Gale, 1914, p. 309). Potash production began in 1916 at two plants, one at Trona that had been constructed by the American Trona Co., and one at Borosolvay, constructed in that year as a joint effort of the Pacific Coast Borax Co. and the Solvay Process Co. During the acute potash shortage of World War I, the price increased ten times over the prewar level and both producers flourished. But by the end of 1920, the Borosolvay plant closed for good, and the American Trona Co. continued only with difficulty.

Following the period of readjustment after World War I, the American Trona Co. added borax to its production (in 1919) and began a long period of research on plant design, the details of which are described by Teeple (1921, 1929). In 1926, it merged into the American Potash and Chemical Corp. Production has continued from that time; new processes have been developed and new products added to the list of materials produced.

The West End Chemical Co., at the settlement of Westend, was organized in 1920 by F. M. Smith (widely known as "Borax" Smith), shortly after he lost control of the Pacific Coast Borax Co., which he founded (Hellmers, 1938). The original plant was designed to produce borax and potash but it was found to be inadequate and was redesigned. In 1927, soda ash was first produced, and in 1930, borax was added to the list of products. In 1955, production of sodium sulfate was begun. The production techniques are described by Hellmers (1938) and Ver Planck (1957, p. 480–482).

In 1956, the Stauffer Chemical Co. absorbed the West End Co., and in 1967, the Kerr-McGee Chemical Corp. absorbed the American Potash & Chemical Corp. In 1974, the Kerr-McGee Chemical Corp. purchased Stauffer's West End plant. The chemical plants at Trona and West End now operate under one ownership. Descriptions of the development and present nature of these operations are given by Gale (1938, 1945), Hellmers (1938), Dyer (1950), Hightower (1951), Ryan (1951), Leonardi (1954), Bixler and Sawyer (1957), Ver Planck (1957), Chilton (1958), Garrett (1960), Garrett and Phillips (1960), Goudge and Tomkins (1960), and Hardt, Moyle, and Dutcher (1972). Both plants extract chemicals from brine pumped from the interstices of the saline layers that underlie the dry lake surface. The plant at Trona produces sodium carbonate and sulfate, potassium chloride and sulfate, lithium carbonate, sodium borate, phosphoric acid, and bromine. The plant at West End produces sodium carbonate, sodium borate, and sodium sulfate. Annual production from both plants is now valued at about $30 million, and total production since 1926 exceeds $1 billion.

Leases held by a subsidiary of the Occidental Petroleum Corp., the Searles Lake Chemical Corp., near the south edge of the lake were under development in the early 1970's by two other subsidiary companies, the Garrett Research and Development Co. and the Hooker Chemical Corp. Anticipated production included sodium borate, sodium carbonate, and potassium sulfate (Phosphorus and Potassium, 1971; Industrial Minerals, 1971) by means of a combined solar evaporation and plant process (Kallerud, 1966). Seven large evaporation ponds were completed in 1971 and pumping of brine for test purposes started in 1972 (California Geology, 1972). The operation is inactive at this time (1978).

## GEOLOGIC ENVIRONMENT AND HISTORY OF SEARLES LAKE

Along the west side of the valley, in the southern part of the Argus Range and in the Spangler Hills, most of the rocks are late Mesozoic plutonic bodies cut by numerous dikes. Near the northwest corner of Searles Valley, these rocks are in contact with large areas of Paleozoic limestone and late Cenozoic basalt and pyroclastic rocks. In the Slate Range, along the east side of Searles Valley, rocks representing all geologic eras crop out: Cenozoic lake beds, gravel, pyro-

[2]Soda ash is the industrial mineral term for sodium carbonate; other terms used in this paper are salt cake, for sodium sulfate, borax, for sodium borate, salt, for sodium chloride; and potash, for potassium oxide and other potassium salts.

clastic rocks, and mafic lava, late Mesozoic plutonic rocks, early Mesozoic metavolcanic rocks, Paleozoic limestone, and Precambrian metamorphic rocks. Notable areas of gypsum-bearing fault gouge crop out along the valley edge. The south edge of Searles Valley is bounded by the Lava Mountains and an unnamed range of low hills that consist mostly of late Tertiary sandstone, pyroclastic rocks, and andesite, and Quaternary silt, sand, and gravel. The geology of these ranges is shown on the Geologic Map of California Trona Sheet (Jennings and others, 1962) and on maps by Smith (1964) and Smith and others (1968).

Searles Valley is a closed tectonic depression surrounded by hills and mountains that project 1,000–1,500 m above the valley floor. Gravity and seismic data show that the pre-Cenozoic(?) bedrock floor of the basin is as much as 1,000 m below the present surface and 500 m below sea level (Mabey, 1956). This depth and the structural characteristics of the surrounding ranges indicate that tectonic activity created Searles Valley. Depression of the valley floor and elevation of the surrounding ranges probably began in late Cenozoic time (Smith and others, 1968, p. 13, 25). By late Quaternary time, Searles Valley had evolved into its present form. Water that drained into it either formed a lake that deposited muds or evaporated to form salines. It is the depositional and geochemical record of these late Quaternary lacustrine events, as indicated by the stratigraphy and mineralogy beneath the valley floor, that is described in this report.

The late Quaternary history of Searles Lake was first described in detail by Gale (1914): Searles Lake was third in a chain of five lakes that received water from the Owens River during pluvial periods of the late Pleistocene (see fig. 1). This river received most of its water from the eastern slopes of the Sierra Nevada and transported it to Owens Lake. When the lake had filled to a level about 60 m above the present surface, water overflowed through a narrow gorge to Indian Wells Valley, where it formed China Lake. China Lake, in turn, attained a depth of about 12 m above the present playa and overflowed into Searles Valley to form a lake as much as 200 m above the present playa; during the highest stages, Searles Lake coalesced with China Lake to form a continuous body of water about twice the size of the present-day Lake Tahoe. From Searles Lake, water overflowed around the south end of the Slate Range and into Panamint Valley, where a lake more than 280 m deep formed. This lake spilled over Wingate Pass into Death Valley.

Core holes have been drilled in four of these basins and their logs published (Smith and Pratt, 1957). The cores show that the following lithologies are probably representative of the fill in the central parts of these basins. Owens Lake basin contains fossiliferous fine-grained sediments throughout most of the 280 m tested; the top few meters of evaporites were deposited after 1913, when the Owens River was diverted into the Los Angeles Aqueduct. The 220 m of China Lake basin tested consists of silt- and sand-sized clastic sediments plus some calcite and gaylussite. Searles Lake, cored to a depth of 267 m, contains alternating layers of salines and fine-grained carbonate muds; the details of this sequence are discussed in this paper. Panamint Lake basin, tested to a depth of 303 m, contains clastic deposits ranging from clay to gravel, small amounts of gypsum, and thick layers of nearly pure halite. Death Valley was not cored because logs were available from earlier work (Gale, 1913a, p. 16) that reported alternating layers of mud or clay and rock salt in the upper 30 m of the basin fill.

## PREVIOUS GEOLOGIC STUDIES OF SEARLES LAKE

Searles Lake[3] first received specific attention from geologists and mineralogists after borates were successfully extracted from it in 1874. Early accounts of these commercial operations are given by Hanks (1883, p. 26–28; 1889) and DeGroot (1890). Hanks (1889) described the deposit and speculated on its geologic origin; he suggested that the water in Searles Lake was derived from Owens Lake and the Owens River, but the statement is not clear, and apparently the connection he proposed consisted of underground seepage rather than a series of surface streams and lakes as was subsequently established. Gilbert (1875, p. 103) had previously traced the path of waters that spilled from Owens Lake as far south as Indian Wells Valley, but as his search for an outlet was restricted to the south edge of that valley, he missed its narrow spillway to the east leading into Searles Valley. In 1896, Fairbanks (p. 69) noted that Searles Lake had shorelines as much as 500 feet above the present valley floor, and reported that Owens Lake had drained southward into Indian Wells Valley during pluvial periods, but he did not discuss the possibility of a connection between Indian Wells and Searles Valleys.

Bailey (1902) might be cited as the first to propose a surface waterway connection between Owens Lake and Searles Lake. This proposal was part of a grander concept which postulated (Bailey, 1902, p. 10–12, and map facing p. 32) an extremely large Quaternary lake ("Lake Aubury") that submerged all but the higher

[3]Searles Lake has been known by several other names that are used in older records. The commonest are Slate Range Lake, Alkali Flat, Borax Lake, Borax Marsh, Borax Flat, and Searles Marsh. The name Borax Lake has caused confusion in geologic literature because it is commonly not distinguished from Borax Lake in Lake County, Calif., the site of the earliest borax mining in the State.

peaks in the southwestern Basin Ranges and Mojave Desert of California and unspecified parts of Nevada and Arizona to the east. Bailey further postulated that on partial desiccation, this large lake became fragmented into more modest-sized lakes, and these too are shown on his map (Bailey, 1902, facing p. 32). One of these lakes includes China Lake and Searles Lake, joined as one, and the text (Bailey, 1902, p. 94) indicates this body as the destination of the overflow from Owens Lake, a relation now known to be true. Bailey does not cite the evidence for these smaller lakes—to say nothing of the larger one—and it is not possible to tell whether his correct conclusion regarding the Owens-China-Searles chain was a result of observation or serendipity.

The attempt to commercially extract soda ash (sodium carbonate) from Searles Lake in 1908, and its recognition in 1912 as a domestic supply of potash to replace the European supply being threatened by the events preliminary to World War I stimulated another series of geologic and engineering studies. Reports that include geologic descriptions and interpretations were published by Hamman (1912a, b, c), C. E. Dolbear (1913), Gale (1913b; 1914), S. H. Dolbear (1914), Free (1914, p. 38–40), and Young (1914, p. 48–53). By the time these investigations were made, Searles Lake seems to have been generally recognized as a member of the chain of lakes that received water from the Owens River. Hamman (1912a, p. 373) was the first to clearly state that the salines in Searles Lake were derived from the desiccation of a long-term overflow from Owens Lake, but both Gale (1913b, p. 886; 1914, p. 251, 252) and Free (1914, p. 39), whose fieldwork in the area was started around 1912, also indicated this interrelation.

Of these papers, Gale's report (1914) was the most complete. It is primarily a discussion of the stratigraphy, chemistry, and mineralogy of the Searles Lake deposit but it also presents the factual data on Owens, China, and Panamint Basins that support the geologic history of Searles Lake described herein. This factual support consists chiefly of a systematic record of the shorelines in the several basins as related to the elevations of their spillways. Except for descriptions of the tufas, the lake deposits exposed around the edge of Searles Valley were not described; the possible correlations between the subsurface deposits in Searles Valley and those of other basins or glaciated areas were discussed only indirectly.

At the time of Gale's investigations (1914), about 65 shallow core holes (mostly 15–25 m deep) and one deep hole had been drilled by private organizations, and his knowledge of the stratigraphy of the deposit was based on the results of their work. The shallower holes penetrated only those layers now known as the Overburden Mud and Upper Salt. Chemical analyses of core samples from these units were included in Gale's report, but detailed lithologic and mineralogic logs were not made during drilling. The log of the deep hole, called the "old Searles deep well" and drilled near the west edge of the saline body (see fig. 3), is so generalized that little can be said of the deeper saline and mud layers in the deposit.

Between 1914 and 1952, in the course of commercial development, a wealth of data accumulated. Several new minerals were discovered and new analyses of brines and salines became available. Continued core drilling provided more and better information on the parts of the lake fill investigated by H. S. Gale and has revealed the presence of the deeper saline and mud layers (see Dyer, 1950, p. 41; Ryan, 1951, p. 447 and fig. 2).

In 1952, as part of a study of borates, a new study of Searles Lake was started by the U.S. Geological Survey. The core and analytical data previously obtained by the companies operating on the lake (then the American Potash & Chemical Corp. and the West End Chemical Co.) were made available to the Survey and were used as a basis for a program of core drilling that was carried out between 1953 and 1955. Core logs were later published (Smith and Pratt, 1957; Haines, 1957, 1959).

In 1958, Flint and Gale described the subsurface stratigraphy of the Searles Lake evaporites on the basis of the many cores obtained by the American Potash & Chemical Corp. and the deep core obtained during the Geological Survey's program (Smith and Pratt, 1957). The names used in that paper for the major subsurface units were informal names that had been in use for some years by company geologists and engineers working on the deposit, and those names are used in the present report.

Later, after logs of 41 cores from the upper part of the deposit had been published by Haines (1957, 1959), subdivisions of two of the stratigraphic units described by Flint and Gale (1958) seemed justified and were proposed by Smith (1962). A description of the nonclastic mineral components and a summary of their distribution within these stratigraphic layers was later published by Smith and Haines (1964).

The stratigraphic framework established by Flint and Gale (1958) provided the basis for their own interpretations of $^{14}C$ ages of the sediments and for the later study by Stuiver (1964). The mineral associations described by Smith and Pratt (1957) and Haines (1959) were used by Eugster and Smith (1965) in a study of chemical equilibrium relations in the deposit. Samples of the cores obtained by the Survey were

used in studies by Droste (1961) on clays, Hay and Moiola (1963) on authigenic silicates, and Leopold (1965) on fossil pollen. The stratigraphy and mineralogy described in these papers was later used to interpret the geologic history of the lake and its climatic implications (Smith, 1968, 1976). The deuterium concentration in hydrated minerals of this suite allows estimates of the temperatures of salt crystallization to be made (Smith, Friedman, and Matsuo, 1970).

The ground water in Searles Valley was first studied by Thompson (1929, p. 177–182), who noted the unusually low gradient of the water table near Searles Lake. Moyle (1969) subsequently compiled the much larger volume of well and spring data now available from the valley and confirmed Thompson's earlier observations. These data led to the conclusions presented in a report by Hardt, Moyle, and Dutcher (1972, fig. 10) that even before the activities of the chemical companies on Searles Lake, the hydrostatic head of the high-density brines in the salt body was greater than in the less saline waters in the surrounding parts of the valley. This head means that for much or most of the time since Searles Lake desiccated, brine has migrated, though very slowly, from the central surface of the lake downward and toward its edges, thereby allowing surface waters to move downward and mix with the brines.

#### ACKNOWLEDGMENTS

This report would not have been possible without the complete cooperation of the companies holding land on the Searles Lake deposit. All gave permission for the Geological Survey to drill core holes on their holdings and to publish the factual results of its findings. Data from the past drilling and analytical records of the American Potash and Chemical Corp. and the Stauffer Chemical Co. (and their successor, the Kerr-McGee Chemical Corp.) were made available to me, and written permission was granted to publish those data necessary for this report.

Many individuals associated with those companies participated in helpful discussions and aided in compiling data from Searles Lake. Special thanks are due D. S. Arnold, R. L. Cremer-Bornemann, L. J. Czel, F. J. Dluzak, H. S. Eastman, W. A. Gale, D. E. Garrett, F. C. Hohne, D. A. Holmes, J. F. Phillips, and F. J. Weishaupl, all then on the staff of the American Potash and Chemical Corporation or the Kerr-McGee Chemical Corp., and P. Cortessis, C. F. Cowie, and L. E. Mannion, all then of the Stauffer Chemical Co.

Colleagues with the Geological Survey who provided special help in compiling this report include P. F. Irish, R. J. McLaughlin, J. D. O'Sullivan, and S. Walsh, who did many of the compilations and calculations; R. D. Allen, R. C. Erd, and Beth Madsen, who helped identify some of the uncommon minerals; and the USGS chemists cited in the tables of analyses. Company chemists were not identified on the records of their analyses. D. V. Haines helped compile a preliminary version of this report.

This report is in part the result of a cooperative agreement with the State of California, Department of Natural Resources, Division of Mines and Geology.

## STRATIGRAPHY OF THE EVAPORITE DEPOSITS

The term Searles Lake evaporites[4] is used in this report as an informal term for the sequence of salines and muds beneath the surface of Searles Lake. The stratigraphy of the Searles Lake evaporites described here, with the emphasis on the mineral composition, extent, and stratigraphic arrangement of the units, comes chiefly from published core logs (Smith and Pratt, 1957; Haines, 1957, 1959). Logs and chemical analyses of the Kerr-McGee Chemical Corp. (then the American Potash & Chemical Corp.) were examined as a check on the extent to which the published data apply to other parts of the deposit. With the permission of the company, some of those data are included in this report.

Knowledge of the Searles Lake evaporites is based on samples and logs of cores (fig. 3). The stratigraphy of the upper 120–150 ft (35–45 m)[5] of the deposit was initially determined from 30 logs of cores obtained for the Geological Survey (Haines, 1959), and subsequently applied to about 70 core logs made by the American Potash & Chemical Corp. Samples from several other cores were later obtained from the Kerr-McGee Chemical Corp. for special studies. The stratigraphy of the deeper deposits is determined mostly from the log of the core L-W-D (Smith and Pratt, 1957); six other cores have sampled parts of this inter-

[4]Throughout this report the term "evaporites" is used as a nearly all-inclusive word for chemical sediments that precipitated initially from natural bodies of water. It includes minerals such as calcite, aragonite, and dolomite that precipitated from nearly "fresh" waters, and minerals such as borax, trona, and halite that precipitated from "saline" waters. Solutions containing 1 percent dissolved solids fall near the boundary between "fresh" and "saline" waters as the term is used in this report. The terms "salt," "salts," and "salines" refer to mixtures of solid minerals that crystalized from saline waters; mono-mineralic bodies of halite, though called "salt" in many reports, are referred to as "halite".

[5]In this report, the English system of units (inches, in.; feet, ft; miles, mi; pounds, lbs) has been used in some instances where the data being discussed are directly or indirectly derived from core logs, contour maps, or older publications that use these units; this facilitates relating this report to the original sources of data. When these data are generalized or used in calculations, they are converted and expressed in metric units (millimeters, mm; centimeters, cm; meters, m; kilometers, km; kilograms, kg).

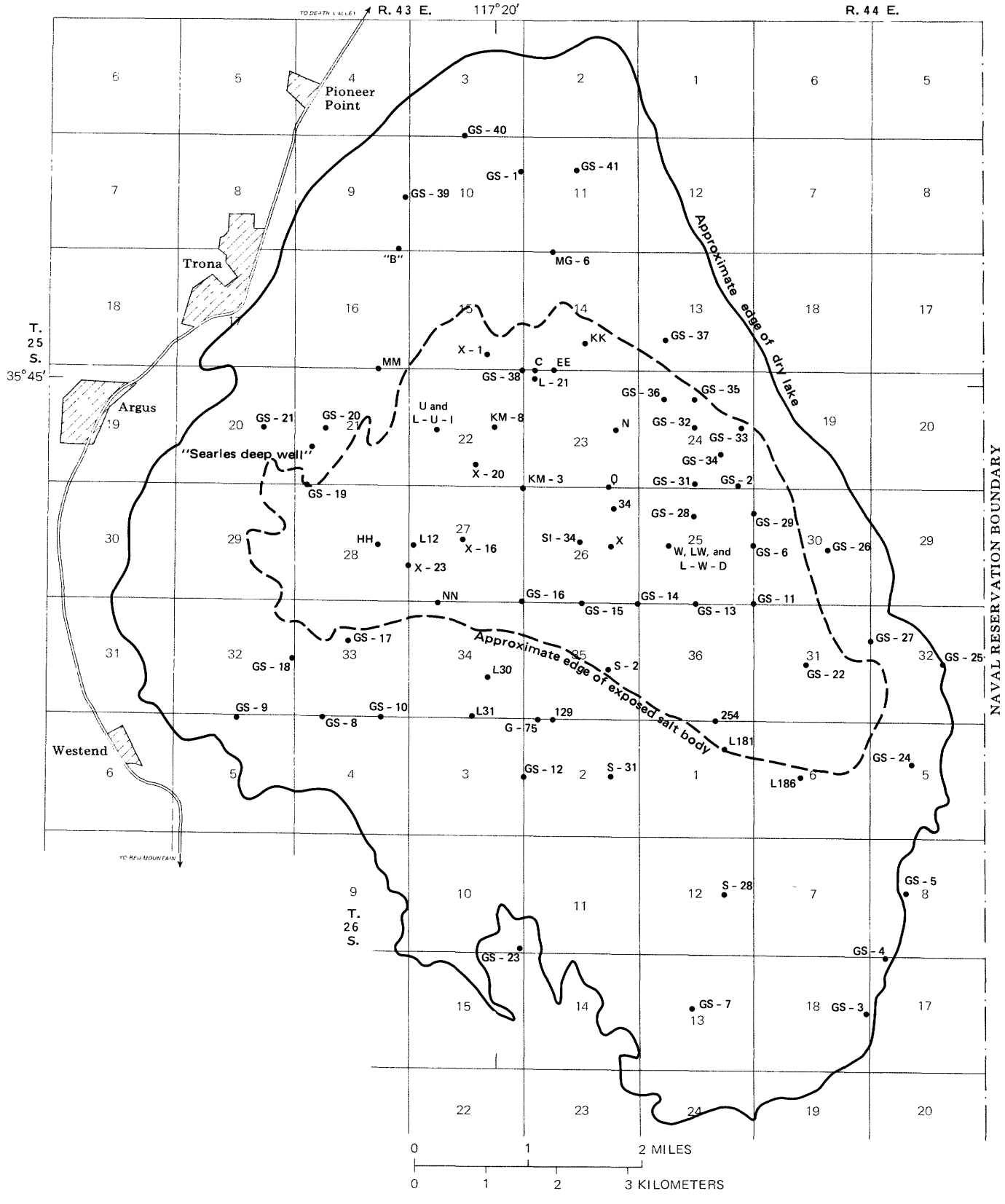


FIGURE 3.—Core holes on Searles Lake discussed in text.

val: core L–30, described in this report, extends to 160 ft (49 m); core 254, described here with permission of Kerr-McGee Chemical Corp., extends to about 260 ft (80 m); cores KK, SL–34, and S–2 (Flint and Gale, 1958, figs. 3, 4) extend to about 300 ft (90 m); a core described by Gale (1914, p 289–290) extends to 628 ft (191 m).

Flint and Gale (1958) described the major stratigraphic units of the deposit and applied the following informal names: Overburden Mud, Upper Salt, Parting Mud, Lower Salt, Bottom Mud, and Mixed Layer. Smith (1962) subdivided the Lower Salt into 13 units and the Mixed Layer into 6 units (fig. 4).

The stratigraphic subdivisions of the Mixed Layer are thick units distinguished by changes in evaporite mineral content that indicate significant differences in the chemical nature of the lake in which they were deposited. The Bottom Mud, Lower Salt, Parting Mud, and Upper Salt are relatively homogeneous units defined on the basis of lithology. Contacts between them are sharp and considered to be about the same age throughout the deposit. The Overburden Mud, which is more heterogeneous, consists of interbedded mud and saline layers. In the central part of the deposit, its basal contact is gradational and consists of a zone having an upward increase in the percentage of clastic-rich mud layers and a decrease in saline layers; around the edges, the contact is at the base of a zone of solid mud that includes near-shore equivalents of horizons in the Upper Salt as well as in the Overburden Mud.

In studying cores, it is generally easy to separate the mud units from the saline units. The muds[6] are mostly dark green to brown, soft, and appear nonporous. They consist chiefly of chemical precipitates made up of Ca, Na, and Mg combined with $CO_3$. The major minerals are fine-grained aragonite and dolomite and fine- or coarse-grained gaylussite and pirssonite (the names and chemical compositions of the nonclastic minerals in the Searles Lake evaporites are given in table 1). A few mud layers have large percentages of clay-sized halite, or small percentages of fine- or coarse-grained borax or northupite. Galeite, schairerite, and tychite occur in traces. Authigenic silicates such as K-feldspar, analcime, phillipsite, and searlesite are locally abundant. Clastic silt and clay, and partially decomposed organic material, are always present but subordinate. Almost all mineral identifications of fine-grained components in the muds are by X-ray diffraction techniques.

The salines are mostly white to dark gray, hard, and porous. They consist chiefly of precipitates made up of Na, K, and Mg combined with $CO_3$, $HCO_3$, $SO_4$, Cl, or $B_4O_7$. The major minerals are coarse-grained halite, trona, hanksite, burkeite, borax, nahcolite, mirabilite, thenardite, northupite, and aphthitalite (glaserite). Small quantities of sulfohalite, teepleite, and tincalconite occur locally. Mineral identifications of saline minerals are by visual inspection (of large crystals) and X-ray diffraction methods.

The identification and correlation of mud and saline units in cores is based upon multiple criteria. Thickness is the most reliable single parameter, but mineralogy, crystal size and habit, bedding character, and the number and positions of thin layers of muds in salines (or, rarely, salines in muds) provide supporting evidence. The Upper Salt, Parting Mud, and units within the Lower Salt generally maintain similar thickness over an extent of a kilometer or so, and these thicknesses form a pattern that can be matched with confidence in nearby cores. The mud beds in these se-

TABLE 1.—*Nonclastic minerals in the Searles Lake evaporites*

| Mineral | Composition |
|---|---|
| Adularia | $KAlSi_3O_8$ |
| Analcime | $NaAlSi_2O_6 \cdot H_2O$ |
| Aphthitalite (glaserite) | $K_3Na(SO_4)_2$ |
| Aragonite | $CaCO_3$ |
| Borax | $Na_2B_4O_7 \cdot 10H_2O$ |
| Burkeite | $2Na_2SO_4 \cdot Na_2CO_3$ |
| Calcite | $CaCO_3$ |
| Dolomite | $CaMg(CO_3)_2$ |
| Galeite | $Na_2SO_4 \cdot Na(F,Cl)$ |
| Gaylussite | $CaCO_3 \cdot Na_2CO_3 \cdot 5H_2O$ |
| Halite | $NaCl$ |
| Hanksite | $9Na_2SO_4 \cdot 2Na_2CO_3 \cdot KCl$ |
| Mirabilite | $Na_2SO_4 \cdot 10H_2O$ |
| Nahcolite | $NaHCO_3$ |
| Northupite | $Na_2CO_3 \cdot MgCO_3 \cdot NaCl$ |
| Phillipsite | $KCa(Al_3Si_5O_{16}) \cdot 6H_2O$ |
| Pirssonite | $CaCO_3 \cdot Na_2CO_3 \cdot 2H_2O$ |
| Schairerite | $Na_2SO_4 \cdot Na(F,Cl)$ |
| Searlesite | $NaBSi_2O_6 \cdot H_2O$ |
| Sulfohalite | $2Na_2SO_4 \cdot NaCl \cdot NaF$ |
| Teepleite | $Na_2B_2O_4 \cdot 2NaCl \cdot 4H_2O$ |
| Thenardite | $Na_2SO_4$ |
| Tincalconite | $Na_2B_4O_7 \cdot 5H_2O$ |
| Trona | $Na_2CO_3 \cdot NaHCO_3 \cdot 2H_2O$ |
| Tychite | $2Na_2CO_3 \cdot 2MgCO_3 \cdot Na_2SO_4$ |

[6]The term "muds" is used throughout this report for the layers having the physical properties listed here. By most conventional sediment terminologies, these muds would be designated as marls rich in organic material. The term "mud" is preferred, however, because it conveys the concept of moist plasticity, one of the striking properties of these materials, better than the conventional sediment term, and because it is an established part of the local terminology for both the sediment itself and the stratigraphic units composed of it.

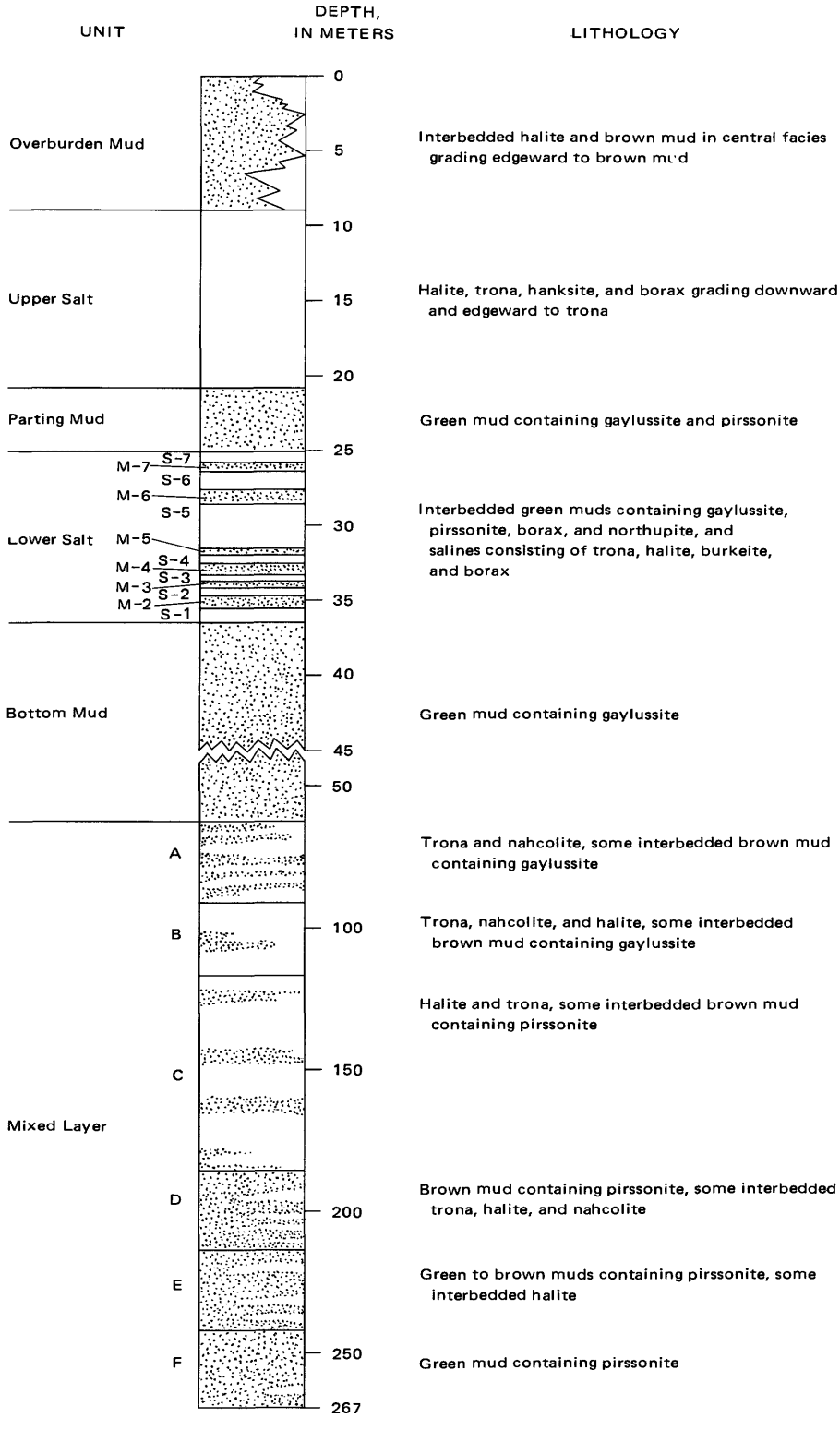


FIGURE 4.—Summary of stratigraphic units in Searles Lake evaporite sequence.

quences are more constant in thickness than the saline beds, and for this reason provide more reliable markers; toward the edges of the deposit, the saline beds pinch out, and the overlying and underlying mud beds are not separable. Detailed correlations have not been attempted between sections of the Bottom Mud and Mixed Layer. Very few cores penetrate complete sections of the Bottom Mud; only one has been examined carefully during this study.

A schematic cross section of the fill in Searles basin is shown in figure 5. The bedrock profile is based on Mabey (1956). The top 45 m of the fill shown in this diagram is based on the data of Haines (1959), Smith (1962), Smith and Haines (1964), and this report. The section between 45 m and 267 m is based on the core log L-W-D from the central part of the basin (Smith and Pratt, 1957) and the "old Searles deep well" from near the west edge (Gale, 1914, p. 275, 289–290); these two logs are so different that correlations are not possible, although the older log reports saline minerals from enough horizons to indicate that some saline layers extend at least that far west.

The cross sections of the upper part of the Searles Lake evaporites, plate 1, are based on core holes described by Haines (1959) and on subsurface data adapted from the isopach maps presented in the following sections (figs. 8–20). Most contacts are drawn at the boundaries between mud and saline material; the base of the Overburden Mud is drawn at the lowermost thick lens of mud in the part of the core considered to represent the Overburden Mud.

The mud layers that can be correlated with the greatest confidence are those near the center of the deposit where the saline layers that separate them are the most distinct and thickest. Near the edges, some saline layers are missing and successive mud layers are combined. Since most of the saline layers have about the same areal extent and position, both the saline units and the mud layers they separate can be recognized over about the same area.

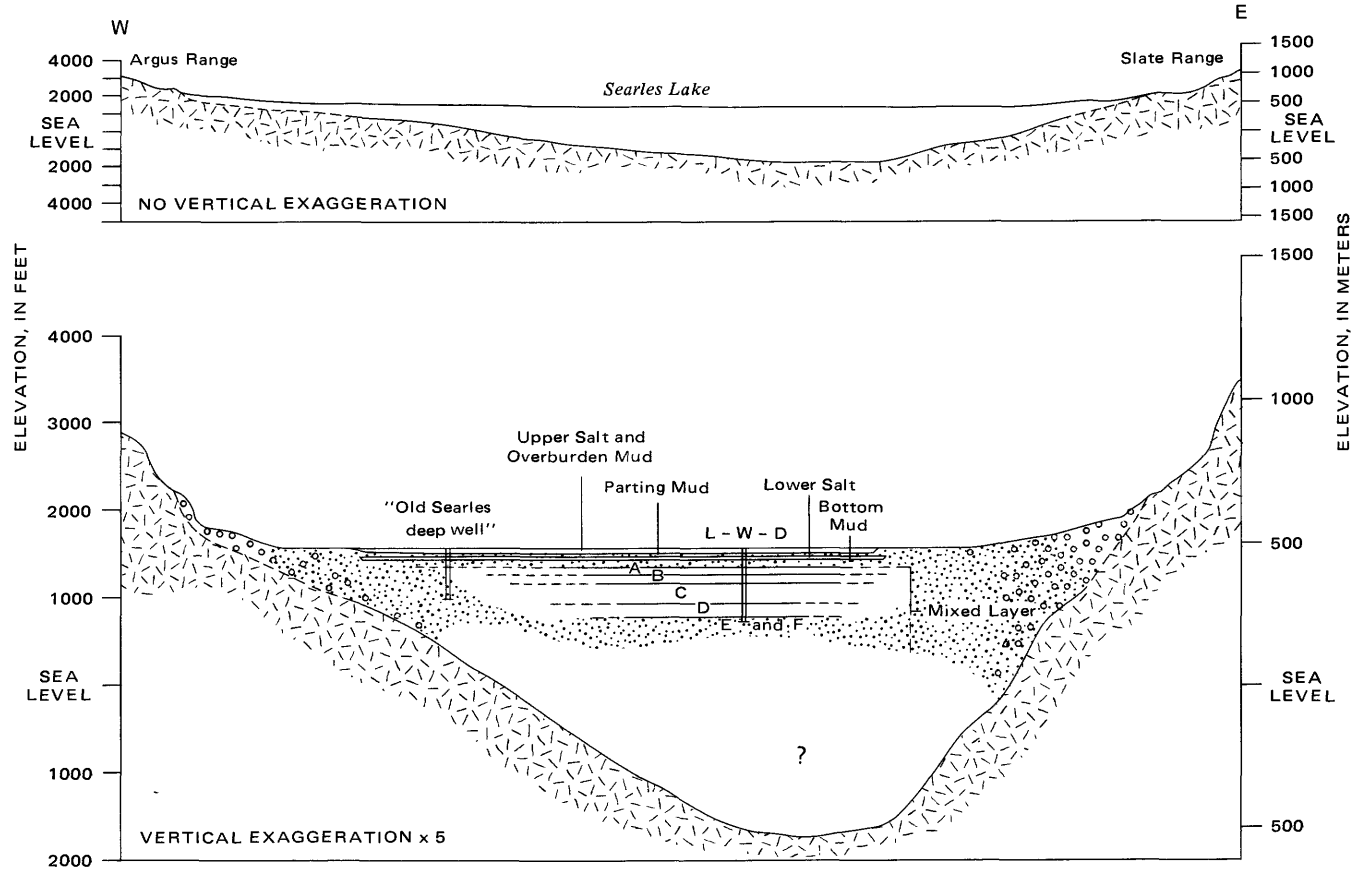


FIGURE 5.—Cross-section of Searles Valley showing bedrock profile (dashed where position uncertain; after Mabey, 1956, fig. 6) and stratigraphy of upper part (top 45 m) of Cenozoic fill (from data of Haines, 1959; Smith, 1962; Smith and Haines 1964; and this report). Profile is east-west and through central part of lake, along section line one mile north of boundary between T. 25 S. and T. 26 S. (see fig. 3). Two deep core holes are projected to this section: "old Searles deep well" (Gale, 1914, p. 289, 290) is 2 km north of this section line, L-W-D (Smith and Pratt, 1957, p. 25–51) 0.8 km north of it.

## MIXED LAYER

All the interbedded salines and lake muds below the Bottom Mud were included in a single stratigraphic unit by Flint and Gale (1958, p. 694) and designated the Mixed Layer. The explored part of this unit, 219 ft–875 ft (66.8–266.7 m) in core L-W-D, was previously inferred by Smith (1962) to be of Illinoian and Sangamon age, but the present paper tentatively revises this correlation, making the Mixed Layer of Yarmouth age and possibly Kansan. Saline layers have an aggregate thickness estimated to be near 280 ft (85 m). This thickness is slightly less than half the entire sequence, but as most of the salines are in the upper 60 percent of it, that part is dominated by them. The salines are mostly trona, nahcolite, and halite that form individual beds several meters thick; small to trace amounts of burkeite, northupite, sulfohalite, thenardite, and tychite are also found. The muds consist of a variable percentage of megascopic crystals of gaylussite or pirssonite, embedded in a silt- to clay-sized matrix of gaylussite, pirssonite, dolomite, calcite, northupite, K-feldspar, analcime, searlesite, clastic silicates, and organic material.

The Mixed Layer has been divided into six stratigraphic units (Smith, 1962) whose boundaries separate deposits characterized by different suites of evaporite minerals that indicate significant changes in the chemical nature of the depositing lake. Relative to the overlying units of the Searles Lake evaporites, these Mixed Layer units are thicker and the contacts between them less sharp because the long periods of distinctive chemical sedimentation that they record changed gradually over a long period of time.

### AREAL EXTENT AND THICKNESS

The interbedded sequence of salines and lake muds that constitute the Mixed Layer grade laterally into alluvial deposits that crop out on the valley sides, but the transition zone between them is not exposed and has not been observed in cores; the areal extent of the lacustrine facies therefore can only be estimated. The three deep cores described by Flint and Gale (1958) and the L-W-D core (Smith and Pratt, 1957) are all in the central part of the basin, and it is clear that all four cores are composed entirely of lake deposits. The log of the "old Searles deep well" (Gale, 1914), near the west edge of the present lake (fig. 5), notes halite, thenardite, trona, and northupite at several horizons within the 628 ft (191 m) of fill tested; although saline layers are apparently few and mud layers predominate, the lower part of that log describes nothing that could be interpreted as the toe of an alluvial fan. The lacustrine deposits of the Mixed Layer appear to be at least as extensive as the present playa lake (100 $km^2$), but outcrops of subaerial gravels considered to be contemporaneous with the Mixed Layer limit the possible extent of most lacustrine deposits to less than 400 $km^2$.

The total thickness of the Mixed Layer has not been determined. Core L-W-D includes 655 ft (200 m) of section assigned to this unit. Three other core holes in the central part of the deposit (Flint and Gale, 1958) penetrate the top 65, 100, and 135 ft (20, 30, and 41 m) of this layer. The "old Searles deep well" penetrated the lateral equivalent of the unit, and, because of its position on the flanks of the bedrock basin (fig. 5), may have included the lateral equivalent of deeper horizons than did L-W-D in the center of the basin. The deepest samples in the old well consist mostly of clay containing halite and calcite; these lithologies indicate that the base of the lake deposits were not reached.

### MINERAL COMPOSITION AND LITHOLOGY

The entire known thickness of the Mixed Layer consists of deposits formed in a moderately to highly saline lake. These have been divided into six zones on the basis of evaporite mineralogy, each zone representing a period when the lake waters, on the average, had a characteristic salinity or composition. The zones of highest salinity are represented by saline layers. Decreases in salinity correspond to increases in the percentage of material logged as mud, but the mud layers themselves are actually composed mostly of evaporite minerals that indicate something of the lake's salinity and composition.

The estimated volume percentages of the main components in the Mixed Layer of core L-W-D (Smith and Pratt, 1957) are plotted quantitatively (pl. 2*A*) such that the horizontal sum of all percentages totals 100. The core that was lost (52 percent) is graphically interpolated by diagonal lines that connect the lithologies plotted for recovered core above and below.

The clastic minerals in the mud (col. 1) and the few beds of sand (col. 2) are mostly quartz, feldspar, and clay, although biotite and amphibole are common. The clastic quartz and feldspar have not been studied in detail, but X-ray patterns of bulk core samples indicate that they are commonly present in about equal quantities. Hay and Moiola (1963, p. 315–320) note that the grains are generally subround to round and pitted or frosted. Cementing materials include calcite, halite, and searlesite. The heavy minerals in the clastic fraction were studied by Gan (1961, table 3). In the Mixed Layer, he found a small but generally persistent percentage of amphibole, opaque mineral, mica,

epidote, apatite, sphene, pyroxene, zircon, and topaz fragments; in a few samples he found rutile, cassiterite, olivine, anatase, corundum, tourmaline, and spinel fragments.

The clay minerals in the Mixed Layer were studied by Droste (1961) who shows (fig. 3) that the illite:montmorillonite:chlorite or kaolinite ratios average about 6:3:1. Estimates by Hay and Moiola (1963, table 1) confirm this ratio. Droste (1961) used the pattern of stratigraphic variation in these ratios to correlate the deposits in Searles Lake with those in the other basins that once contained lakes in the same chain. The field evidence now shows that much of the clastic sediment in each basin was derived locally, the observed variations are likelier to be the result of local factors such as the position of the shoreline of the lake, the pattern of streams relative to the site of the core hole, the circulation pattern of strong currents within the lake, or the nature of local rock-weathering processes.

Of the fine-grained authigenic silica minerals found in the Mixed Layer, and the searlesite(?) reported at 248 ft (75.6 m) by Smith and Pratt (1957), plotted in column 4, K-feldspar is by far the most common; it is estimated by Hay and Moiola (1963) to make up 10–20 percent of many layers and as much as 50 percent of some. Analcime may be slightly more common that K-feldspar in units A and B, but the reverse is clearly true in units C, D, E, and F. Searlesite was reported by Smith and Pratt (1957) from the middle of unit A at 248 ft (75.6 m) and by Hay and Moiola (1963) from units E and F. These three authigenic silicates occur in the overlying Bottom Mud, but only analcime and phillipsite are found in the younger units above it. This stratigraphic distribution suggests either that less time is needed for the formation of analcime and phillipsite than for searlesite and K-feldspar, or that analcime and phillipsite are here precursors to K-feldspar and possibly searlesite as is found elsewhere (Sheppard and Gude, 1968, p. 35, 36).

Eighteen of the X-ray determinations of the fine-grained carbonates (col. 5) were made by Hay and Moiola (1963; R.L. Hay, written commun., 1964) on samples selected for study of authigenic silicates; the rest were made during the present study. Although the samples studied by X-ray are widely spaced, the following observations are probably applicable to the unstudied segments of this unit: northupite, dolomite, pirssonite, and calcite are the only carbonates detected in this fraction; dolomite is more common than calcite; and northupite is most common in zones containing saline layers. Gaylussite and aragonite,[7] though common in overlying units, were not found in the fine-grained fraction of the Mixed Layer.

The percentages of coarse-grained evaporite minerals are plotted in columns 6 to 10 of plate 2*A*. Gaylussite and pirssonite are relatively insoluble Na-Ca carbonates, and their percentages are shown in columns 6 and 7. The percentages of more soluble evaporite minerals—the salines—are plotted in columns 8, 9, and 10. About 45 beds of trona and nahcolite are shown, and these total about 45 ft (14 m) thick. Nearly the same number of beds of halite are shown, but they total about 95 ft (29 m). As about half the core was not recovered, actual thickness of salt beds are likely to be about twice these figures, meaning that a total of about 280 ft (86 m) of salts occur in the Mixed Layer. In terms of the overall composition of the 655-foot (200 m) section of the Mixed Layer discussed here, a little less than 15 percent is trona plus nahcolite and 30 percent is halite.

Chemical analyses of the water-soluble fraction of seven samples of the Mixed Layer are given in table 2. Six of these samples are of salines. These analyses confirm that trona, nahcolite, and halite make up most of the saline portions of the core as reported in the log of L-W-D; they also show that saline minerals containing K and $B_4O_7$ are nearly absent,[8] and sulfate minerals are subordinate to rare. The seventh sample is composed of silt, and the analysis of its water-soluble fraction indicates the presence of small quantities of carbonates, chlorides, and sulfates. Generalized descriptions of the individual stratigraphic units follow:

*Unit A.*—Saline layers composed of trona and nahcolite predominate in unit A. Halite is missing (except near the basal contact), and this characteristic distinguishes unit A from unit B. The mud layers are mostly dark yellowish brown and contain megascopic gaylussite and smaller quantities of pirssonite. Locally there are detectable quantities of megascopic northupite and tychite and microscopic analcime, searlesite(?), and dolomite. A thin bed of basaltic or andesitic volcanic ash lies near the top.

*Unit B.*—Saline layers again predominate in unit B; they consist of both trona and halite with smaller quanitites of nahcolite. Some of the mud layers are dark yellowish brown, others dark olive green. They contain megascopic gaylussite, traces of megascopic pirssonite, sulfohalite, and northupite, and local concentrations of microscopic crystals of analcime, dolomite, K-feldspar, and northupite.

[7]The light-colored laminae in this unit reported by Smith and Haines (1964) to be aragonite are now known to consist of other carbonate minerals.

[8]Core drilling was done with hrine pumped from the top of hole W; table 16 shows the uppermost sample of brine to contain 0.70 percent $B_4O_7$ and 1.39 percent K. Some of the components in this brine must have adhered to the cores that were later analyzed, and some or all of the detected $B_4O_7$ and K could have come from this source.

TABLE 2.—*Chemical analyses of core samples from the Mixed Layer*

[Analyses, by Henry Kramer and Sol Berman, are of material dissolved in boiling water. Samples from core L-W-D described by Smith and Pratt (1957)]

| Depth (ft) | Unit | Lithology | Weight percent | | | | | | | |
|---|---|---|---|---|---|---|---|---|---|---|
| | | | Na | K | Cl | $SO_4$ | $CO_3$ | $HCO_3$ | $B_4O_7$ | Total water soluble |
| 464.0–465.3 | C | Trona with halite, some burkeite. | 32.2 | 0.09 | 11.9 | 3.4 | 18.6 | 20.1 | 0.08 | 86.4 |
| 580.0–583.0 | C | Halite, trona, and thenardite. | 38.2 | .17 | 47.4 | 8.9 | 2.4 | 1.0 | .12 | 98.2 |
| 594.0–597.6 | C | Trona and mud. | 30.0 | .30 | 5.3 | 2.0 | 21.3 | 23.2 | .23 | 82.3 |
| 640.3–650.0 | D | Halite, some trona and pirssonite mud. | 38.8 | .02 | 56.9 | .5 | .9 | 1.4 | .02 | 98.5 |
| 707.0–710.0 | E | Halite and mud. | 33.2 | .06 | 47.9 | .4 | 2.0 | .08 | .06 | 83.7 |
| 722.8–730.0 | E | Halite and pirssonite mud. | 38.3 | .04 | 56.5 | .3 | 1.0 | .08 | .02 | 96.2 |
| 865.0–868.0 | F | Silt cemented by pirssonite and searlesite. | 4.1 | .19 | 1.05 | 1.2 | 3.7 | .08 | .21 | 10.5 |

*Unit C.*—Unit C consists mostly of halite beds, but contains some relatively thin beds of trona. The preponderance of halite over other saline minerals and the virtual lack of gaylussite distinguish this unit from units A and B above it. Traces of nahcolite, burkeite, sulfohalite, and thenardite occur locally. The subordinate mud layers are mostly yellowish to orange brown; they contain megascopic and microscopic crystals of pirssonite and traces of gaylussite, northupite, K-feldspar, analcime, and dolomite.

*Unit D.*—In unit D, pirssonite-bearing yellowish- or greenish-brown mud layers are more common than saline layers, and this distinguishes these deposits from those of unit C above. Most mud layers contain only pirssonite; some contain a little northupite, calcite, and dolomite. Gaylussite is absent from the muds of this and all deeper units. The saline layers consist of about equal percentages of halite and trona, and traces of nahcolite, sulfohalite, and tychite. A 1-cm bed of devitrified glass or andesitic tuff lies near the middle of this unit.

*Unit E.*—About two-thirds of unit E consists of yellowish-green mud containing megascopic crystals of pirssonite and locally northupite and sulfohalite. The saline layers are composed of halite that locally contains traces of included northupite and sulfohalite; trona and nahcolite are absent from the saline layers, and this distinguishes this unit from unit D above it. A thin bed of devitrified andesitic(?) volcanic ash that has been partly altered to K-feldspar, analcime, and searlesite, occurs near the upper contact. Microscopic crystals of analcime, K-feldspar, searlesite, northupite, dolomite, and calcite make up small to major percentages of some beds in the unit.

*Unit F.*—Unit F consists chiefly of mud containing pirssonite. Megascopic crystals of northupite and microscopic crystals of K-feldspar and dolomite are common to abundant, crystals of analcime, searlesite, and calcite less common. A few thin beds of fibrous trona and cubic halite are found, but the rarity of such beds distinguishes unit F from other units in the Mixed Layer.

Brine samples from the Mixed Layer were not collected for analysis during the drilling of core hole L-W-D because they were contaminated during coring by the surface brines forced down into these deep layers. However, the general composition of the brines that permeate the saline bodies of the Mixed Layer can be inferred from the mineral phases present. The saline layers are composed predominantly of minerals made up of Na, $CO_3$, $HCO_3$, and Cl. Minerals containing Mg and $SO_4$ are rare. Saline minerals containing B and K have not been noted although the authigenic silicates searlesite and K-feldspar do contain these components. As the brines in contact with these minerals appear to be in equilibrium, limits can be placed on their chemical compositions by use of phase diagrams (Smith and Haines, 1964, fig. 14) or relative chemical activity diagrams (Eugster and Smith, 1965). Estimates based on these data indicate, in qualitative terms, that the brines in the Mixed Layer have high percentages of Na, low to high percentages of Cl, $HCO_3$, and $CO_3$, (with the ratio of $HCO_3/CO_3$ mostly low), and very low percentages of K, $SO_4$, and B. The chemical activity of $H_2O$ is higher in unit A, and possibly in unit B, than in older units; the activity of $CO_2$ varies but may be higher in units B, C, and the upper part of D than in other units.

## BOTTOM MUD

The Bottom Mud is a unit deposited by a series of perennial lakes that occupied Searles Valley throughout most of early Wisconsin, Sangamon, and Illinoian

times. It consists largely of dark-green to black mud that contains megascopic crystals of gaylussite. The muds consist of fine-grained carbonates and other evaporite minerals, authigenic silicates, clastic silicates, and partially decomposed organic debris. Thin lenticular beds of nahcolite and mirabilite are found at several horizons, and a few thin layers of trona, thenardite, and borax have been noted near the top. These represent low stands of the lake but not desiccation.

### AREAL EXTENT AND THICKNESS

The Bottom Mud has been penetrated by only a few test holes. Core hole L-W and its downward extension L-W-D (Smith and Pratt, 1957, p. 25–51) is in the east-central part of the deposit. Core holes S–2, KK, and SL–34, which extend to depths of about 300 ft (90 m), penetrated the entire unit (Flint and Gale, 1958, figs. 2, 3, and 4); their core logs are not published, but two were examined during this study. The "old Searles deep well," drilled near the west edge of the deposit (Gale, 1914, p. 289), penetrated the Bottom Mud, but its upper and lower limits cannot be identified in the log. Core hole 254, drilled in the southeast part of the lake by the Kerr-McGee Chemical Corp., is described here with their written permission.

In most parts of the deposit, the thickness of the Bottom Mud is about 30 m. Flint and Gale (1958, figs. 3 and 4) show Bottom Mud thicknesses in cores SL–34, S–2, and KK ranging from about 65 to 90 ft (20–27 m), but application of the criteria used by Smith (1962) to the original logs of SL–34 and S–2 indicates Bottom Mud thicknesses in these cores of about 94 and 100 ft (28 and 30 m) respectively. In core L-W-D, the Bottom Mud is 101 ft (31 m) thick; in core 254, 97 ft (29 m) thick. Near the edge of the lake and outside of it, the areal variation in thickness cannot be measured; unpublished mapping shows that the layer was at one time continuous with sections of coarser lake sediments now preserved as remnants around the sides of the valley.

### MINERAL COMPOSITION AND LITHOLOGY

The Bottom Mud consists mostly of mud that contains megascopic gaylussite crystals. About a quarter of the unit has faint or widely spaced laminae or thin beds, but most of it is massive. The mud is clay- to silt-sized material that is moist and plastic. It is composed, in major to minor percentages, of microcrystalline gaylussite, dolomite, aragonite, calcite, analcime, searlesite, authigenic K-feldspar, halite, and clastic minerals plus a few percent organic material. Thin lenticular beds of nahcolite and mirabilite are found at several horizons, and small amounts of trona, burkeite, and borax occur locally. The mirabilite and borax dehydrated to thenardite and tincalconite prior to logging and X-ray identification.

Plate 2*B* shows graphically the distribution of saline layers in three cores of the Bottom Mud, and the mineral composition of the mud fraction. Core 254 represents samples collected from the entire thickness of Bottom Mud, core L–30 and core L-W-D samples from the upper third and lower two thirds. The stratigraphic intervals represented by the two partial cores probably overlap slightly, and the beds of nahcolite at about 152 ft (46.3 m) in both are probably correlative and equivalent to the one at 155 ft (47.2 m) in core 254. The bed of nahcolite at 134 ft (40.8 m) in core 254 may be equivalent to one or both of the beds of mirabilite[9] reported in core L-W. The other nahcolite beds are not found in the correlative cores, either because not present or not recovered during coring.

The top of the Bottom Mud is at 123.4, 116.8, and 120.7 ft (37.61, 35.60, and 36.79 m) in the cores plotted (pl. 2*B*). The base of the Bottom Mud in core 254 is at 226.8 ft (69.13 m) and in L-W-D at 219.3 ft (66.84 m). The top of the unit is placed at the base of the salts that make up unit S–1 of the Lower Salt, and the base at the top of the uppermost saline layer in unit A of the Mixed Layer, a closely spaced series of nahcolite beds.

The Bottom Mud, as represented by the cores plotted, consists mostly of mud containing as much as 70 percent gaylussite crystals. The crystals are subhedral to anhedral, and generally cut across bedding, demonstrating that they grew after burial (see Smith and Haines, 1964, fig. 15; Eugster and Smith, 1965, pl. 1). Crystal sizes range from a fraction of a millimeter to 20 mm, and inclusions of mud similar to the host material occur in most crystals. The largest crystals commonly are found in the top few meters.

Beds and lenses of highly soluble saline minerals are critical in reconstructing the history of the lake inasmuch as they represent periods of low lake levels. A thin bed of borax occurs about 3 ft (1 m) below the top of the Bottom Mud in the core L–30, and thin discontinuous beds and pods of northupite, borax, trona, nahcolite, and thenardite are found in this zone in cores GS–8, 10, 11, 15, 16, 17, 18, 19, and 27 (Haines, 1957, 1959). Beds of mirabilite were reported 10–20 ft (3–6 m) below the top contact in core L-W (Smith and Pratt, 1957, p. 30) and traces of mirabilite and borax were found in core 254 although none were detected in this zone in core L–30. In cores shown in figure 9, nah-

[9]Samples of the mirabilite reported in the log of core L-W were not available for confirmation by X-ray diffraction. However, chemical analyses and descriptions in other logs of the rapid dehydration character of the minerals that constitute saline layers in the Bottom Mud show that mirabilite is probably present in some parts of the unit.

colite forms prominent beds 35–45 ft (10–14 m) below the top, and traces of mirabilite and borax were found in core 254. Core 254 penetrated several beds of nahcolite at depths 60–70 ft (18–21 m) below the top, and core L-W-D contained nodules of trona and borax at this depth. Two thin beds of nahcolite occur near the base of the unit in core L-W-D, 1–4 ft (0.3–1.2 m) above several thicker beds of nahcolite assigned to the Mixed Layer.

The mineralogy of the fine-grained fraction of the segments logged as mud in cores 254, L–30, and L-W-D was studied by X-ray diffraction and found to consist chiefly of carbonate minerals, halite, and authigenic silicates. Clastic minerals are generally subordinate. Figure 9 shows the mineral composition of the samples studied. Determinations on 10 of the X-rayed samples from core L-W-D are by Hay and Moiola (1963, table 1, R. L. Hay, written commun., 1964); the remaining determinations from L-W-D and all the determinations from cores 254 and L–30 are products of this study. Although the abundances of mineral components are only relative, their presence or near-absence is generally certain, and the indicated changes in relative concentrations for any component in a given core are probably reliable.

Gaylussite (G, on pl. 2*B*) is a component in about 90 percent of the samples. Except for the top few meters, its abundance tends to be less in the upper third of the unit, the zone containing the largest amount of calcite (C). Dolomite (D) is a component in half to two-thirds of the unit, but it may be slightly less abundant in the zones containing salines. Aragonite (A) is found in samples from the upper 20 ft (6 m), but it has not been detected below those depths in this unit or in underlying deposits. Analcime (An) is concentrated in two zones, one about 40 ft (12 m) thick near the middle of the unit and one about 10 ft (3 m) thick at the base. A concentration of another zeolite, phillipsite, is reported by Hay and Moiola (1963, table 1) from a tuff bed 8 ft (2.4 m) below the top of the Bottom Mud in core GS–2. Searlesite (Sl) is detected in significant amounts in a 10-ft (3 m) zone a little below the middle of the unit. Monoclinic K-feldspar (K) that is presumed to be authigenic is present in detectable concentrations in three zones that lie above the main saline beds, and its abundance is roughly proportional to the percentage of clastic minerals (Cm); possibly some of the monoclinic feldspar is clastic rather than authigenic, but its diffraction patterns resemble those described by Hay and Moiola (1963, fig. 3) and by Sheppard and Gude (1968, fig. 2; 1969, fig. 2) from authigenic material. The halite (H) concentration may partially reflect the amount of NaCl-saturated interstitial brines in the core sample which dried before X-raying rather than crystalline material in the original core, but crystalline material can be shown to exist in the Parting Mud and may be present in these samples also; its concentration may increase toward the top of the unit. The small amounts of other saline materials (Sx) may also come from the dried brines, but where shown present in minor amounts, the minerals were observed as crystals. The concentration of clastic minerals (Cm) seems highest in the zones deposited immediately after the main saline layers were deposited, a time when the lakes were smaller and the shores nearer the center of the basin.

Traces of microscopic crystals of pyrite were found in greenish-gray silts from a depth of 152.3 ft (46.4 m) in core L-W-D. None were found in four other samples of similar-appearing mud from cores L–30 and L-W-D, which were studied in comparable detail.

## CHEMICAL COMPOSITION OF THE BOTTOM MUD

Complete chemical analyses of samples from the Bottom Mud are not available. Determinations of the acid-insoluble percentage of 41 samples from the Bottom Mud (fig. 6) range from 11 to 65; the average of all determinations is 31. The acid-insoluble fraction includes clastic and authigenic silicates (plus the much smaller organic fraction); the fraction that dissolved in the acid or water consists of Na, Ca, and Mg carbonates plus any salts. As each portion contains several components, the variations cannot be attributed to increases or decreases in any one. Comparing these data with the X-ray data plotted for this core (pl. 2*B*) shows that the zones containing the highest percentages of acid-insoluble material are those containing the highest percentages of authigenic silicates, chiefly analcime (138–176 ft, 219–227 ft) and K-feldspar (176–196 ft). Clastic mineral percentages tend to be high in these zones, which presumably originally included much higher concentrations of clastic silicates that provided the Si and Al now contained in the authigenic minerals. In the parts of the core that do not contain authigenic silicates in abundance, the percentages of acid-insoluble material are mostly between 10 and 30 and average about 20.

The mineral components plotted in figure 9 provide a more detailed estimate of the chemical composition of the unit. Megascopic crystals of gaylussite ($Na_2CO_3 \cdot CaCO_3 \cdot 5H_2O$) were estimated visually to constitute about 10 percent of core L–30 and 55 percent of L-W-D. The finely crystalline gaylussite in the mud determined from the X-ray data appears to be more abundant and consistently present than any other component. Finely crystalline dolomite ($CaCO_3 \cdot$

$MgCO_3$) appears to be next most abundant; halite (NaCl) is third. Less persistent and abundant quantities of analcime ($NaAlSi_2O_6 \cdot H_2O$), authigenic K-feldspar ($KAlSi_3O_8$), and calcite ($CaCO_3$) are indicated. Relatively minor amounts of searlesite ($NaBSi_2O_6 \cdot H_2O$), aragonite ($CaCO_3$), trona ($NaHCO_3 \cdot Na_2CO_3 \cdot 2H_2O$), burkeite ($2Na_2SO_4 \cdot Na_2CO_3$), and borax ($Na_2B_4O_7 \cdot 10H_2O$) are present. Thin beds of nahcolite ($NaHCO_3$) and mirabilite ($Na_2SO_4 \cdot 10H_2O$) make up 5–10 percent of the unit.

This balance of mineral components shows that the authigenic and evaporite minerals in the mud portions of the Bottom Mud are predominantly made up of Ca, Na, Mg, and $CO_3$, with smaller quantities of Cl, and still smaller quantities of Si, K, B, and $HCO_3$. The salts are dominat<d by Na, $CO_3$ or $HCO_3$, and $SO_4$; they probably came from brines that were dominated by these ions plus Cl and probably some B and K (indicated by searlesite and K-feldspar).

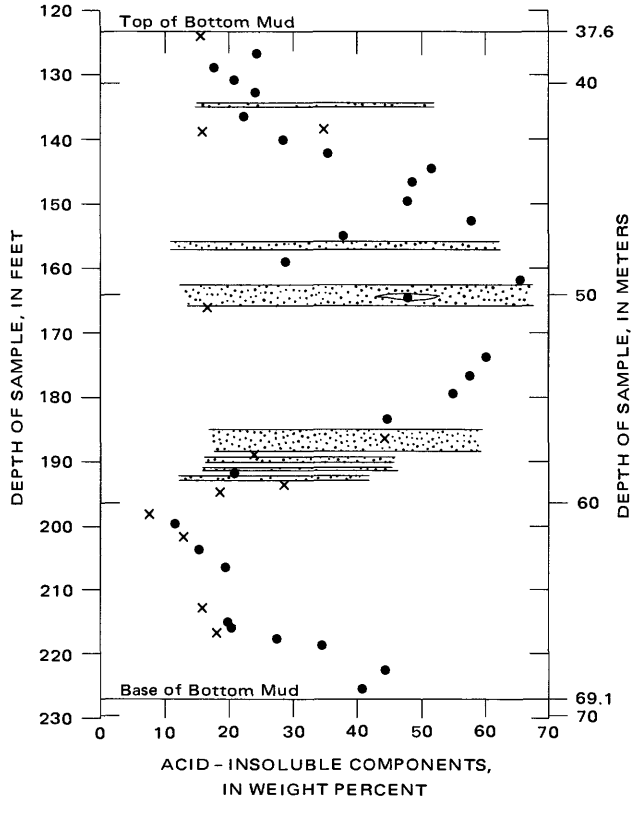


FIGURE 6.—Weight percent of acid-insoluble components in Bottom Mud. Samples were those logged as mud in core 254. Interbedded salt layers in this core shown by horizontal stippled bars. Samples were weighed, treated with dilute (20 percent) HCl at room temperature, washed, dried, and reweighed. Samples shown by circles considered accurate within 1 percent; samples shown by x, within 5 percent.

## LOWER SALT

The Lower Salt, of middle Wisconsin age, consists of a series of interbedded layers of salines and muds, mostly a meter or so thick, that lie nested in a deep basin formed in the top of the Bottom Mud (fig. 7; pl. 1). The Lower Salt has been subdivided into thinner stratigraphic subdivisions than any of the other units, and each of these subdivisions has been studied individually. The sequence thus affords a detailed reconstruction of the lake's history during this period—a history that was characterized by several short episodes of dryness or near-dryness separated by much longer episodes of perennial lakes.

The Lower Salt has been subdivided informally into seven saline layers (designated S–1 to S–7) separated by six mud layers (designated M–2 to M–7). The volumes of the saline units (S–1 to S–7) total about $550 \times 10^6$ m$^3$, the interbedded mud layers (M–2 to M–7) within a similar area total $425 \times 10^6$ m$^3$. The total volume of interbedded muds and salts in the Lower Salt is about 1 km$^3$. Salines form about 56 percent of this total, mud layers about 44 percent. In the central part of the deposit, where the saline layers are thickest and the mud layers thinnest, salines account for about 65 percent of the total volume.

The salines in the Lower Salt are mostly trona, halite, and burkeite, with smaller quantities of northupite, thenardite, hanksite, and borax. Still smaller quantities of nahcolite, sulfohalite, and tychite occur locally. Most of the saline layers contain thin beds of mud, and some of these contain a little gaylussite or pirssonite. Trona makes up most of the lower three saline units (S–1 to S–3); trona, burkeite, and halite dominate in the next two (S–4 and S–5); and trona and halite constitute most of the upper two (S–6 and S–7).

The muds in the Lower Salt are composed mostly of silt- to clay-sized carbonates, silicates, and organic material. Megascopic gaylussite and pirssonite constitute subordinate percentages; the lower four units (M–2 to M–5) generally contain gaylussite, the upper two (M–6 and M–7) both gaylussite and pirssonite. Some units contain a little borax, northupite, thenardite, burkeite, hanksite, halite, trona, nahcolite, schairerite, sulfohalite, tychite, and aragonite.

An appreciable percentage of the brine pumped from Searles Lake to the chemical plants is drawn from the Lower Salt. Densities range from 1.27 near the edges to 1.30 near the center. The major dissolved components are Na, $CO_3$, $SO_4$, Cl, and $B_4O_7$; relative to those of the Upper Salt, these brines are somewhat higher in $B_4O_7$ and $CO_3$, and lower in K.

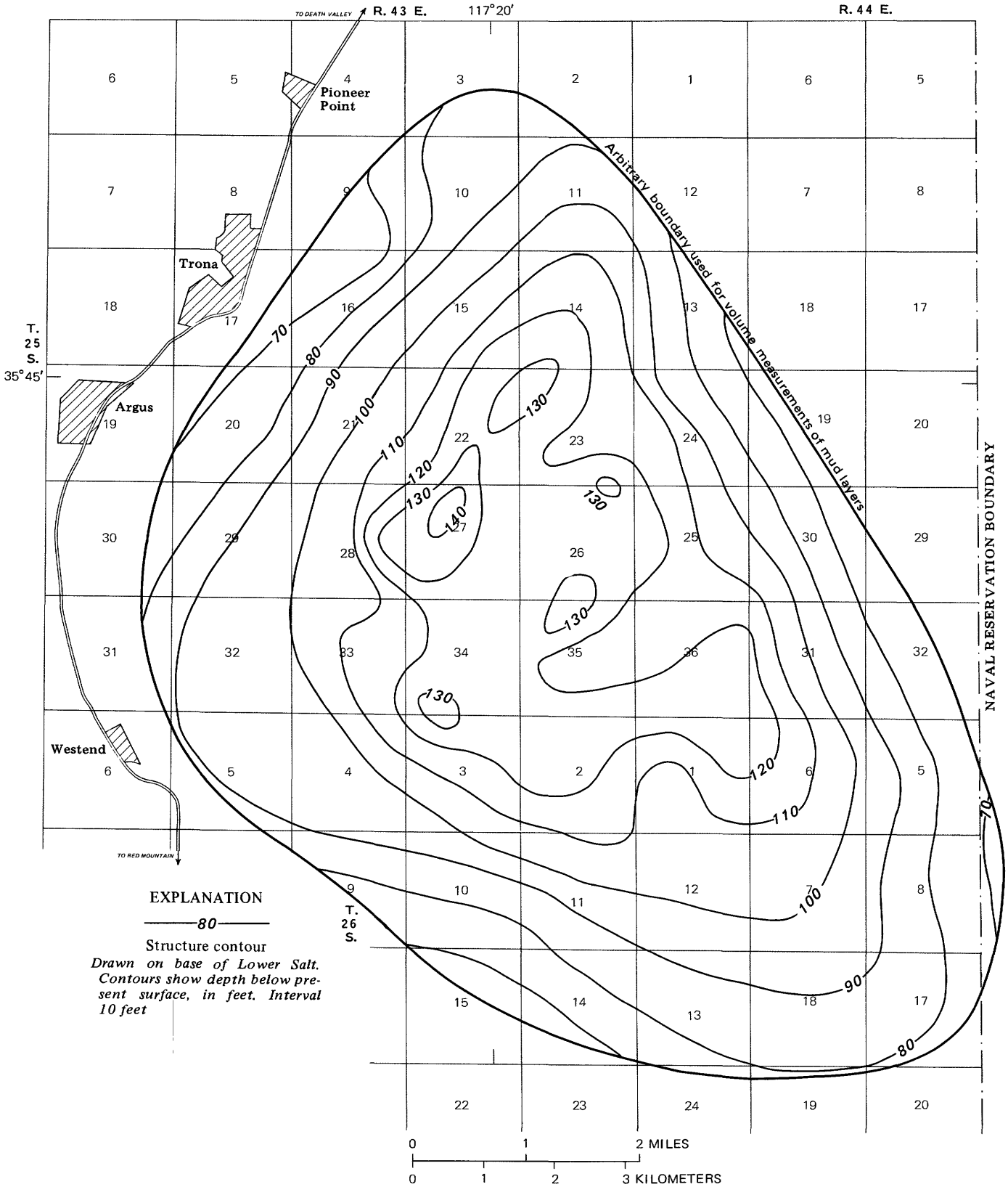


FIGURE 7.—Contour map on base of Lower Salt, Searles Lake.

## AREAL EXTENT AND VOLUME

### SALINE UNITS

The seven saline layers included in the Lower Salt underlie about 114 km² of the present playa. No single bed covers more than 103 km² (table 3), but as the layers are not perfectly superimposed, some of the smaller beds extend beyond the edge of the largest.

Isopach maps of units S–1, S–2, S–3, S–4, S–5, S–6, and S–7 (figs. 8–14) are based on interpretations of the core data presented by Haines (1957, 1959) and the records of the American Potash & Chemical Corp., which were generously made available for study. The combined sources furnish thickness data from about a hundred core holes scattered around the deposit, or an average of about one per square kilometer. The isopach map of each unit was constructed by plotting the thicknesses of the unit (in ft) at each core-hole site, then contouring the data. The zero line represents the estimated edge of the salt layer and always falls inside, not on, points plotted as having zero thickness.

TABLE 3.—*Area and volume of units in the Lower Salt*

[Based on isopach maps (figs. 11–17 and 18–23). Mud unit volumes measured within arbitrary boundary shown on maps ]

| Stratigraphic unit | Area (km²) | Volume | |
|---|---|---|---|
| | | m³x10⁶ | Percent of total volume |
| **Saline units** | | | |
| S–7 | 102.8 | 62 | 11 |
| S–6 | 102.8 | 133 | 24 |
| S–5 | 99.2 | 215 | 38 |
| S–4 | 94.3 | 40 | 7 |
| S–3 | 92.7 | 28 | 5 |
| S–2 | 95.8 | 40 | 7 |
| S–1 | 93.0 | 45 | 8 |
| Total | — | 563 | 100 |
| **Mud units** | | | |
| M–7 | >100 | 93 | 22 |
| M–6 | >100 | 116 | 27 |
| M–5 | >100 | 28 | 7 |
| M–4 | >100 | 59 | 14 |
| M–3 | >100 | 57 | 13 |
| M–2 | >100 | 74 | 17 |
| Total | — | 427 | 100 |

The contouring of these data is a subjective process, and in some areas the actual distribution of thicknesses may be quite different from that shown. This is most likely to be true near the edges, where control points are few. Furthermore, compaction of material or core losses during drilling makes some reported thicknesses uncertain over a range of several tenths of a foot. Many parts of the deposit have closely spaced control points that are fairly consistent; it seems probable that the thicknesses represented by the contours in these areas are essentially correct.

The volumes of saline units were calculated from these isopach maps. Planimeter measurements were first made of the areas bounded by successive contours. The area between each of the crudely concentric contours was then calculated, the volume of the vertical zone beneath each area was computed, and the volumes of all zones were added together. This calculation, expressed as a formula, is as follows:

$$V = h_1(A_0 - A_1) + h_2(A_1 - A_2) + h_3(A_2 - A_3)$$

where

$V$ is total volume,

$A_0$, $A_1$, $A_2$, and $A_3$ are areas bounded by the zero, first, second, and third contours, and $h_1$, $h_2$, and $h_3$ are the midpoints between the zero and first, first and second, and second and third contours (so that maps with a 1-ft contour interval thus have $h_1 = 0.5$, $h_2 = 1.5$, $h_3 = 2.5$, etc.).

The volumes obtained in this way, given in table 3, are a few percent larger than if calculated from formulas for the prismoid or frustrum of a cone[10], but this technique is preferred because the volume of each vertical zone is subsequently used to estimate mineral zonation and bulk mineral composition of the unit.

### MUD UNITS

The six mud units that separate the salt layers in the Lower Salt extend beyond the edges of those layers. Their lateral equivalents crop out in some parts of the valley, mostly a kilometer or more outside of the limits of the salts. Within the cored area, though, the individual mud layers can be identified in virtually every core, and their variations in thickness plotted as isopach maps (figs. 15–20). The contours are terminated at an arbitrary boundary which approximates the limits of the salt layers. Volume measurements have been made in the same manner as the measurements on the salt layers; the results are given in table 3.

[10]For example, the volume of unit S–7 by the technique used is calculated to be $62.3\times10^6$ m³. Applying the formula for the prismoid in the form:

$$V = \frac{1}{6}C\left[A_0 + 4\left(\frac{A_0+A_1}{2}+A_1\right)\right] + \frac{1}{6}C\left[A_1 + 4\left(\frac{A_1+A_2}{2}+A_2\right)\right]\ldots$$

where

C = contour, interval, and

$A_0$, $A_1$, $A_2$, etc. = total areas bounded by each contour,

the volume of S–7 is calculated to be $60.3\times10^6$ m³.

Applying the formula for the frustrum of a cone:

$$V = \tfrac{1}{3}C[A_0 + A_1 (A_0A_1)^{1/2}] + \tfrac{1}{3}C[A_1+A_2+(A_1A_2)^{1/2}]\ldots$$

where symbols are as above, the volume of S–7 is calculated to be $60.0\times10^6$ m³.

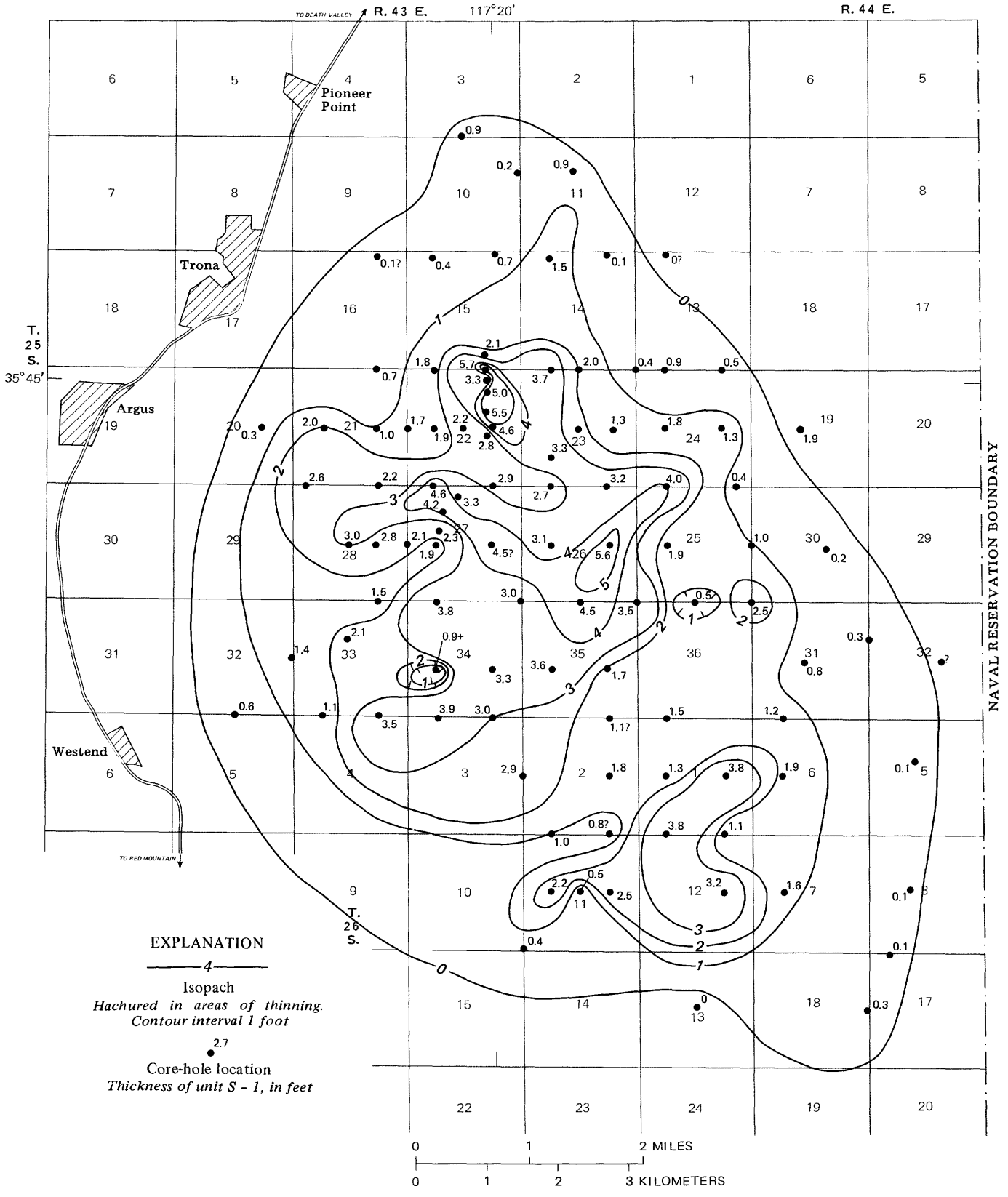


FIGURE 8.—Isopach map of unit S–1, Searles Lake.

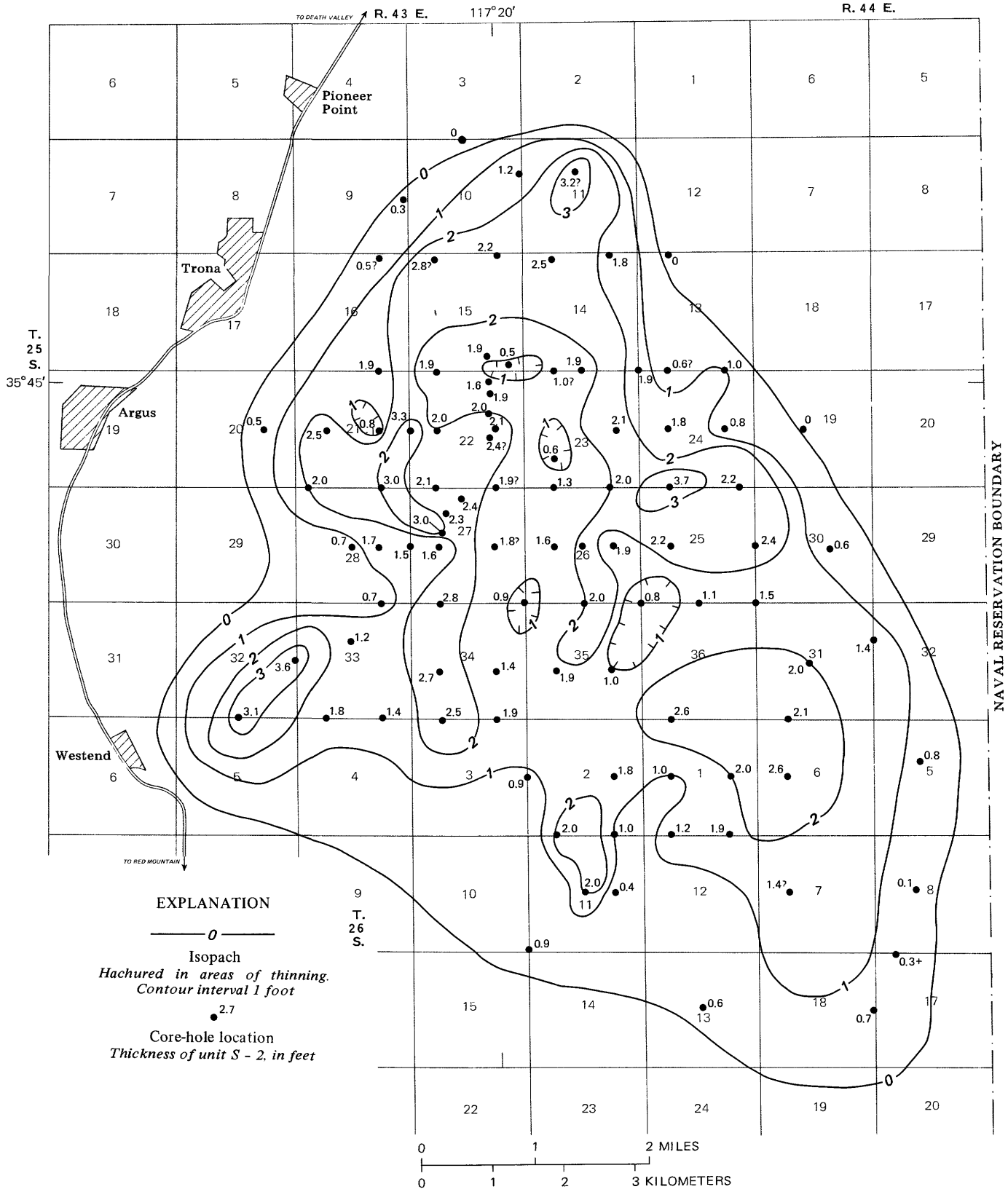


FIGURE 9.—Isopach map of unit S–2, Searles Lake.

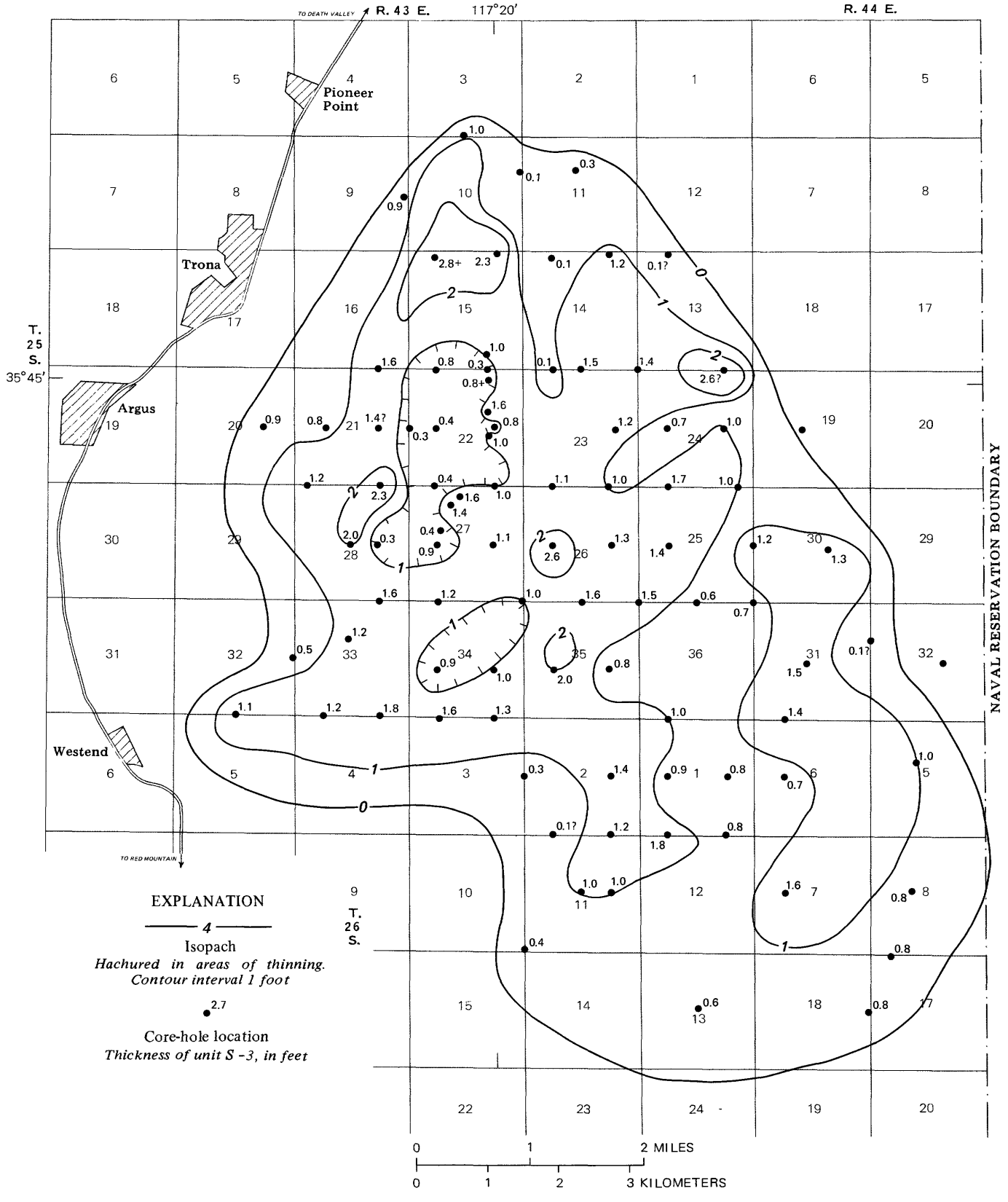


FIGURE 10.—Isopach map of unit S–3, Searles Lake.

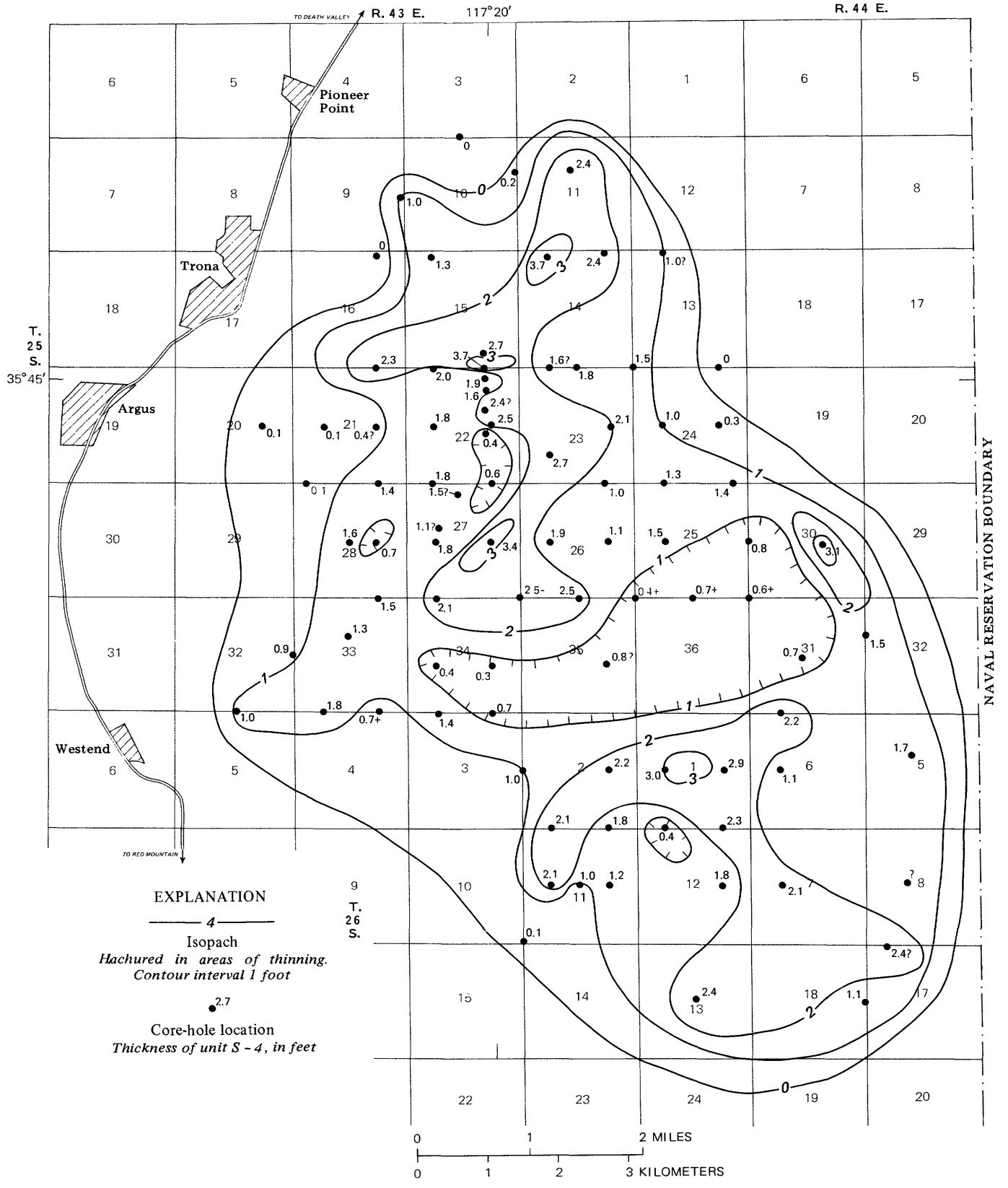


FIGURE 11.—Isopach map of unit S–4, Searles Lake.

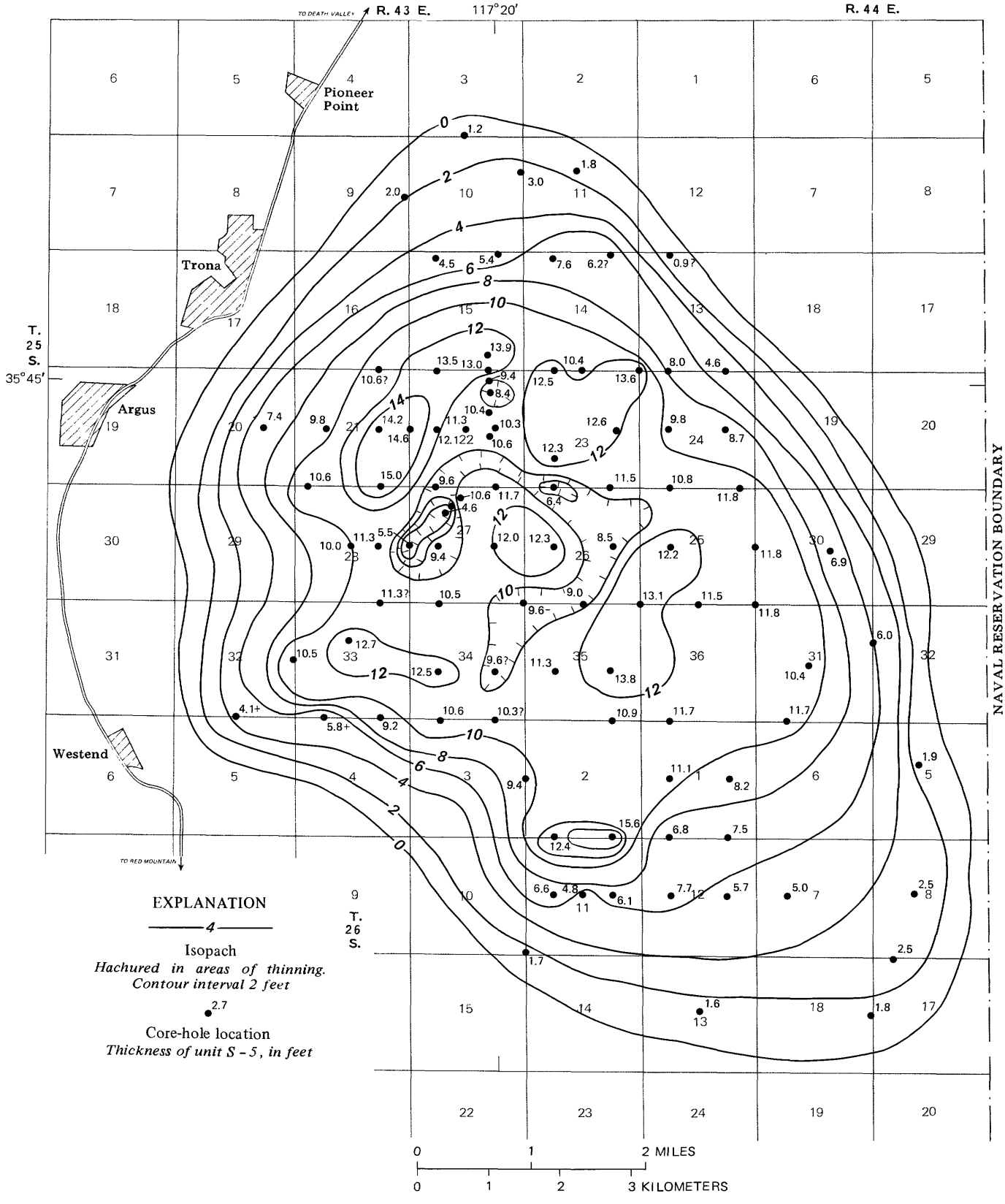


FIGURE 12.—Isopach map of unit S–5, Searles Lake.

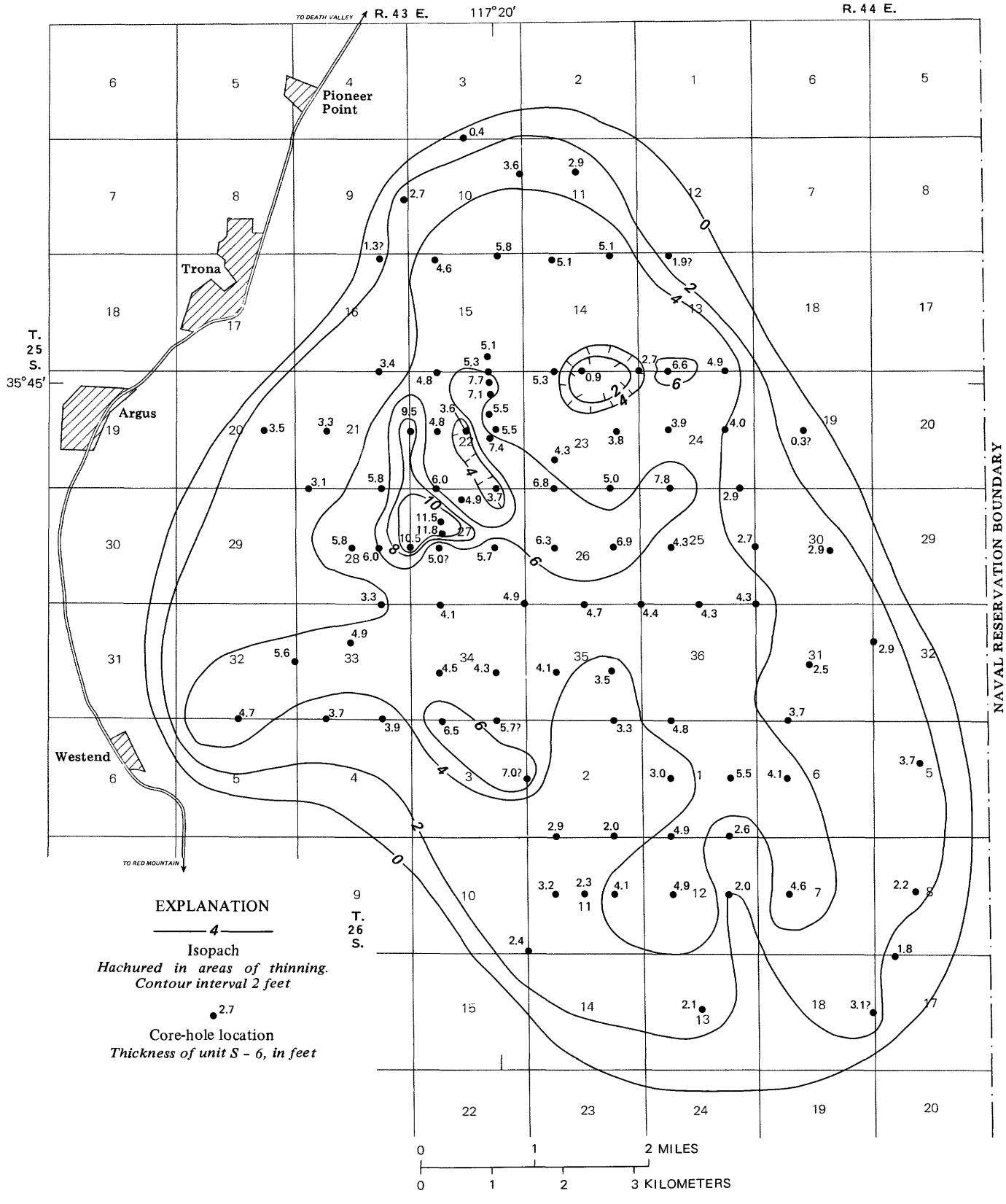


FIGURE 13.—Isopach map of unit S–6, Searles Lake.

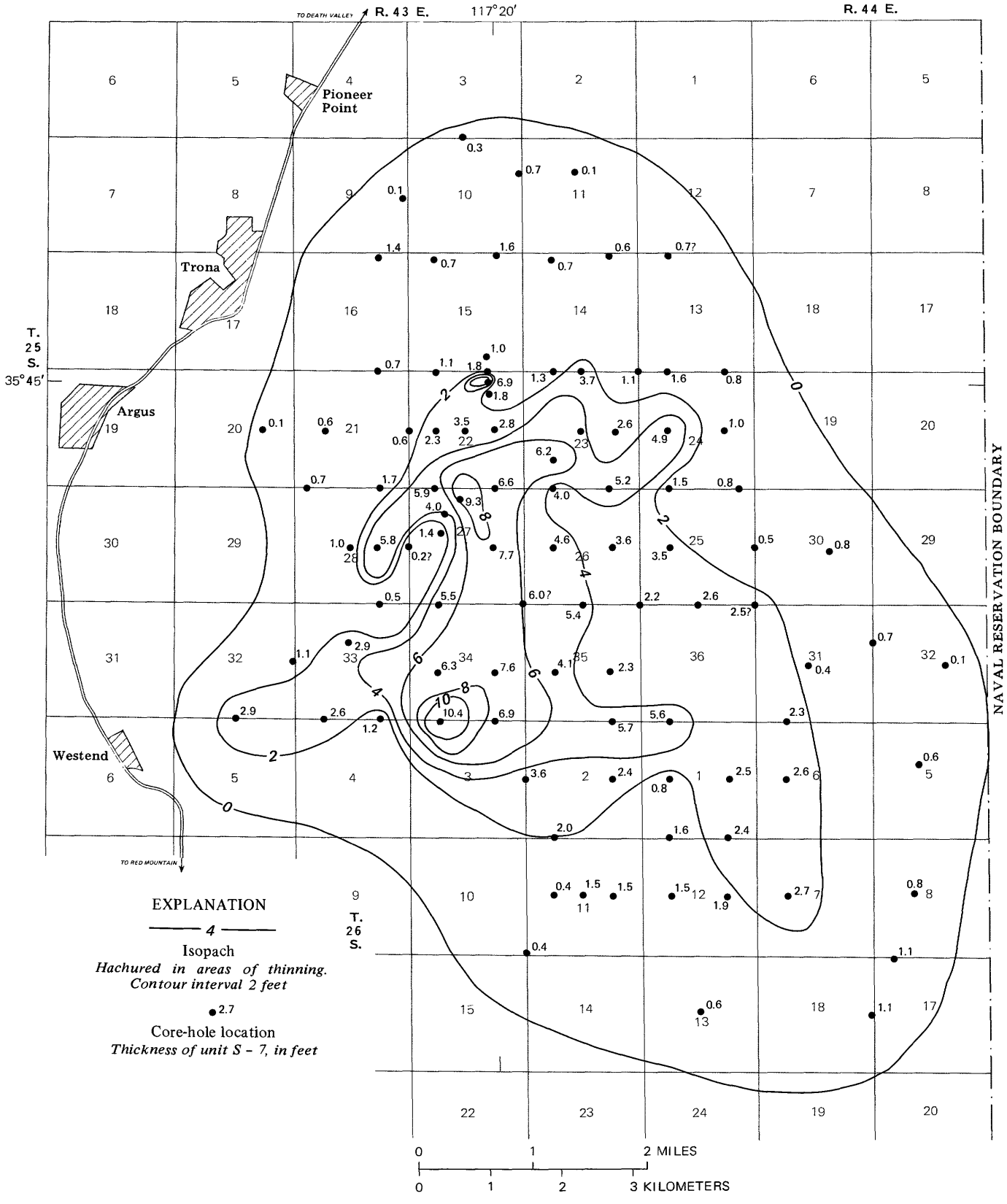


FIGURE 14.—Isopach map of unit S–7, Searles Lake.

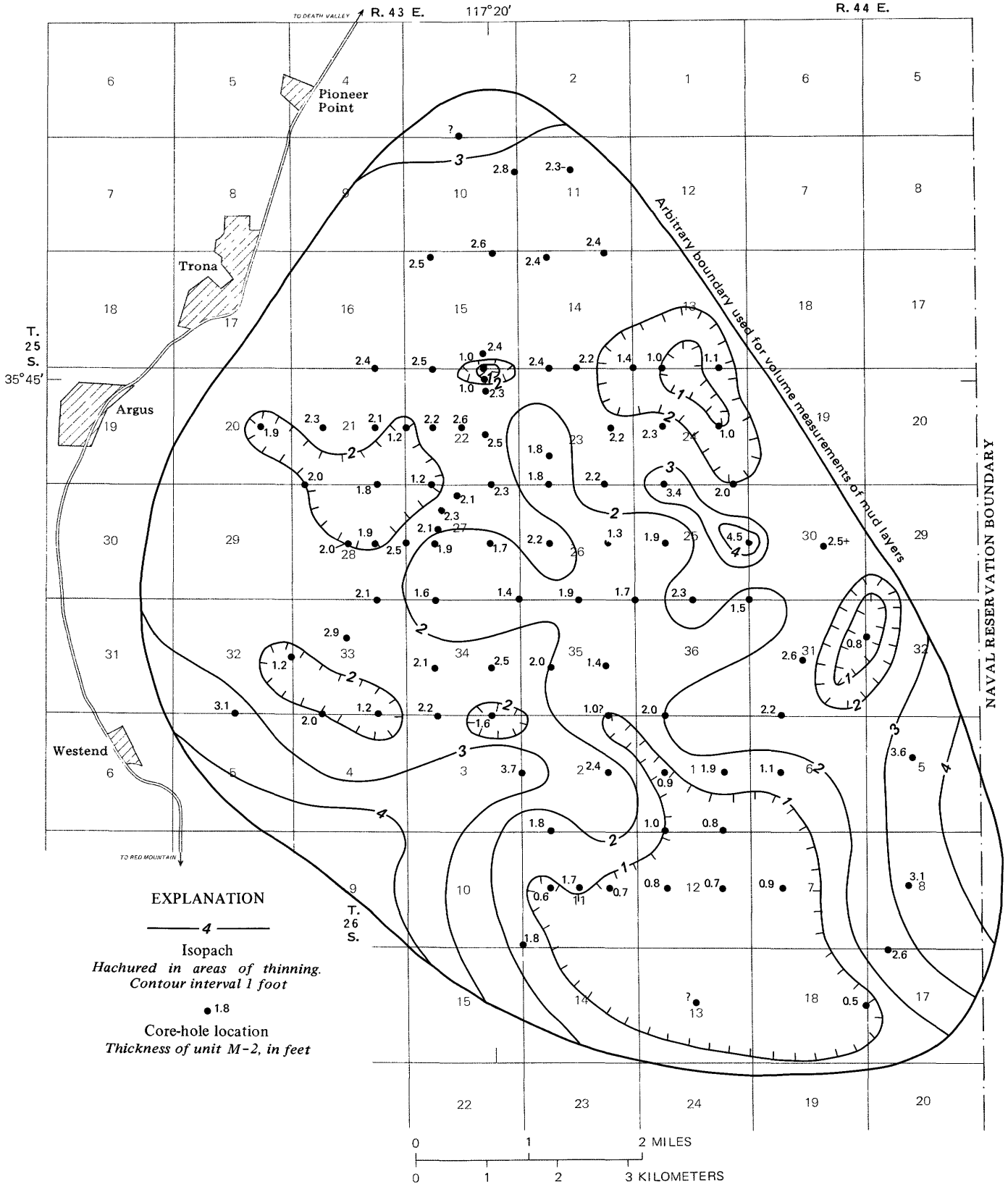


FIGURE 15.—Isopach map of unit M–2, Searles Lake.

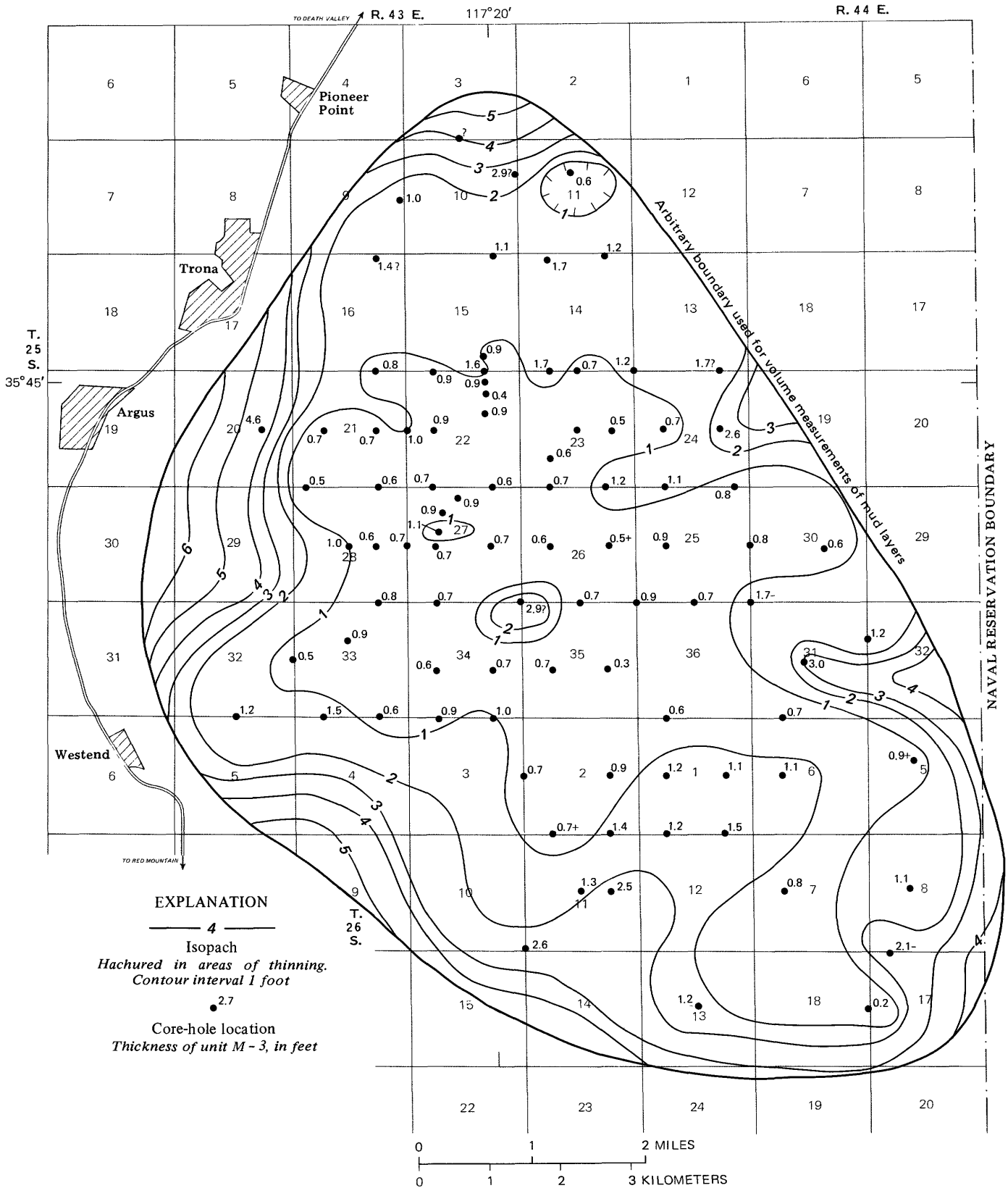


FIGURE 16.—Isopach map of unit M–3, Searles Lake.

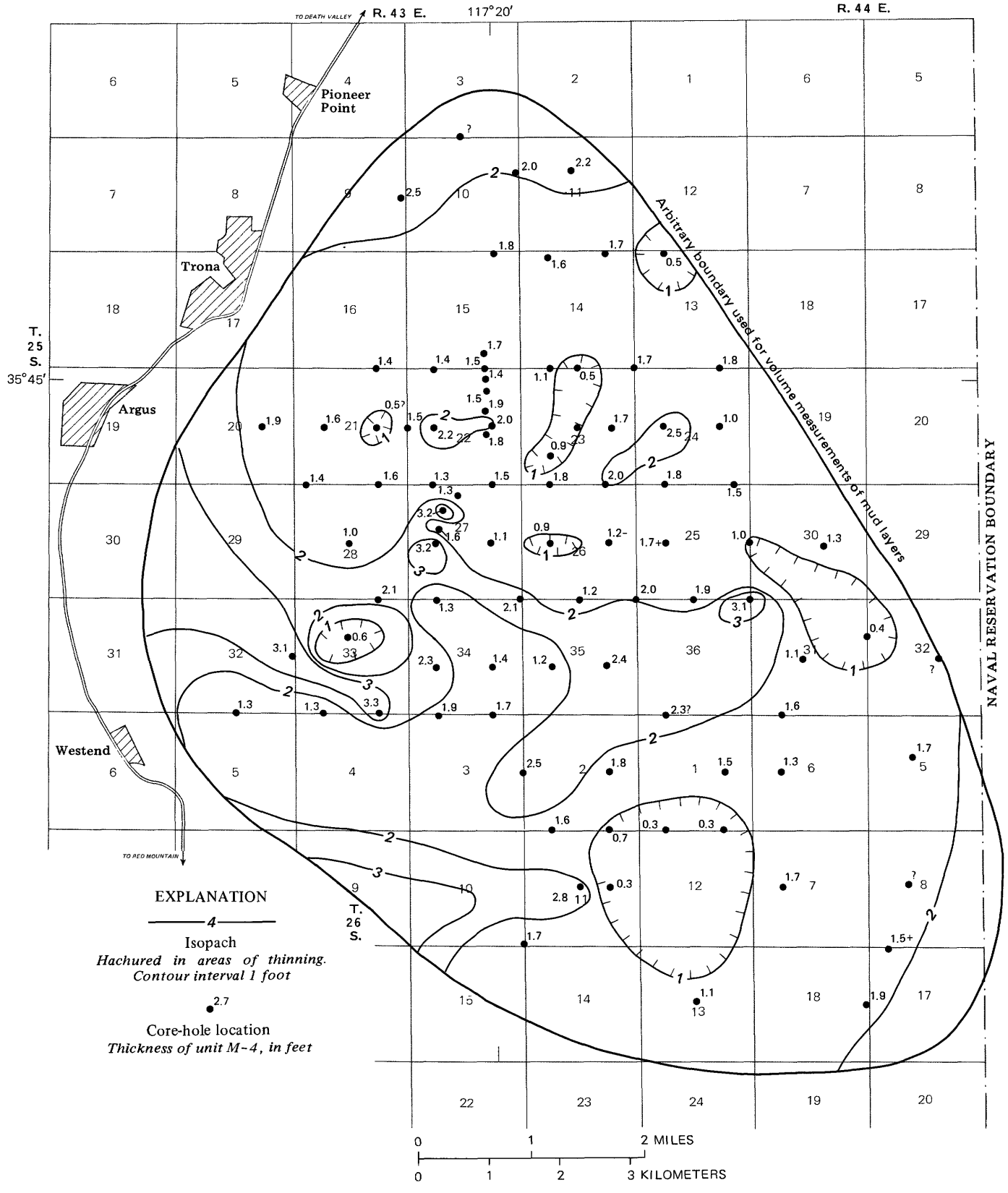


FIGURE 17.—Isopach map of unit M–4, Searles Lake.

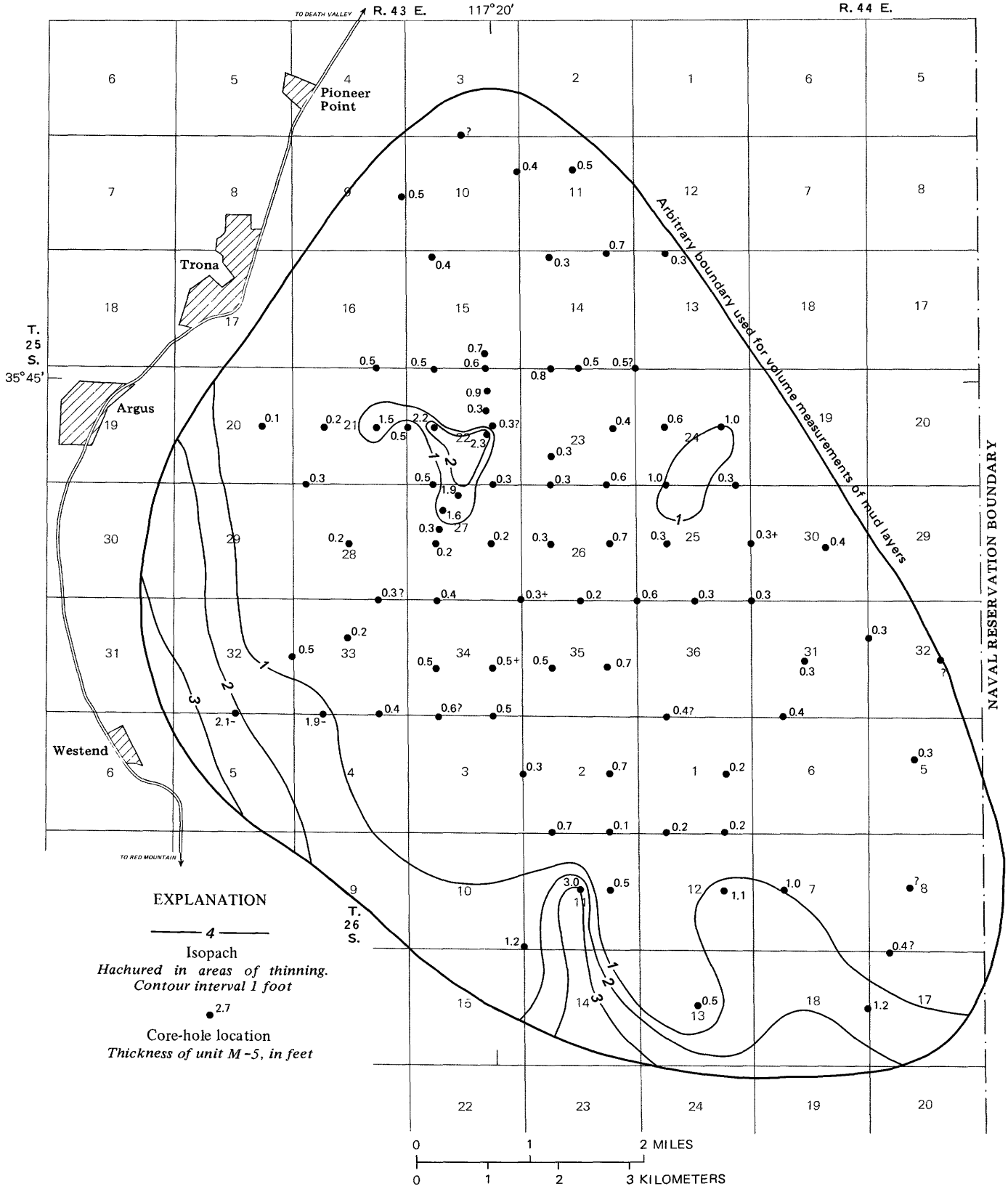


FIGURE 18.—Isopach map of unit M–5, Searles Lake.

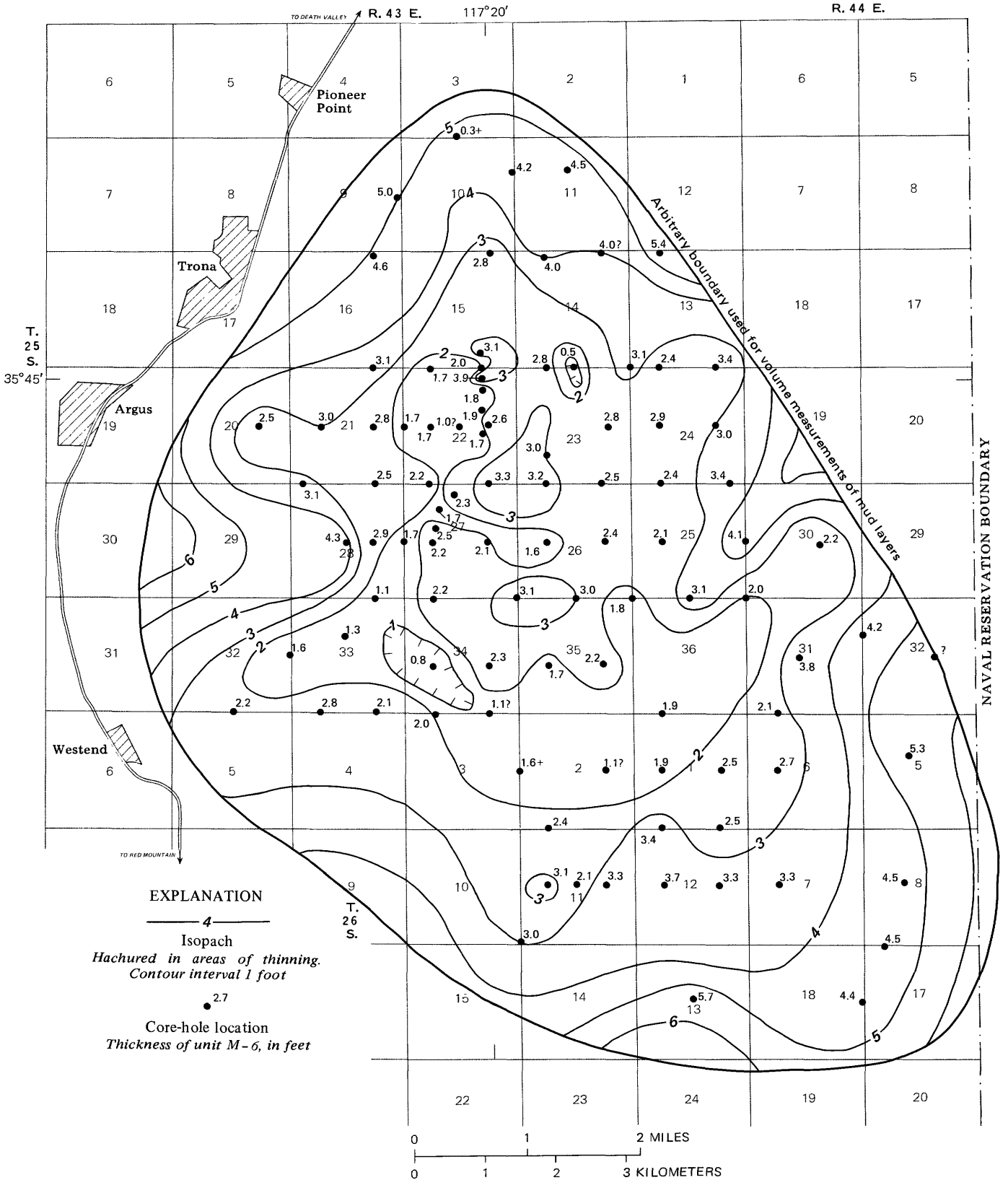


FIGURE 19.—Isopach map of unit M–6, Searles Lake.

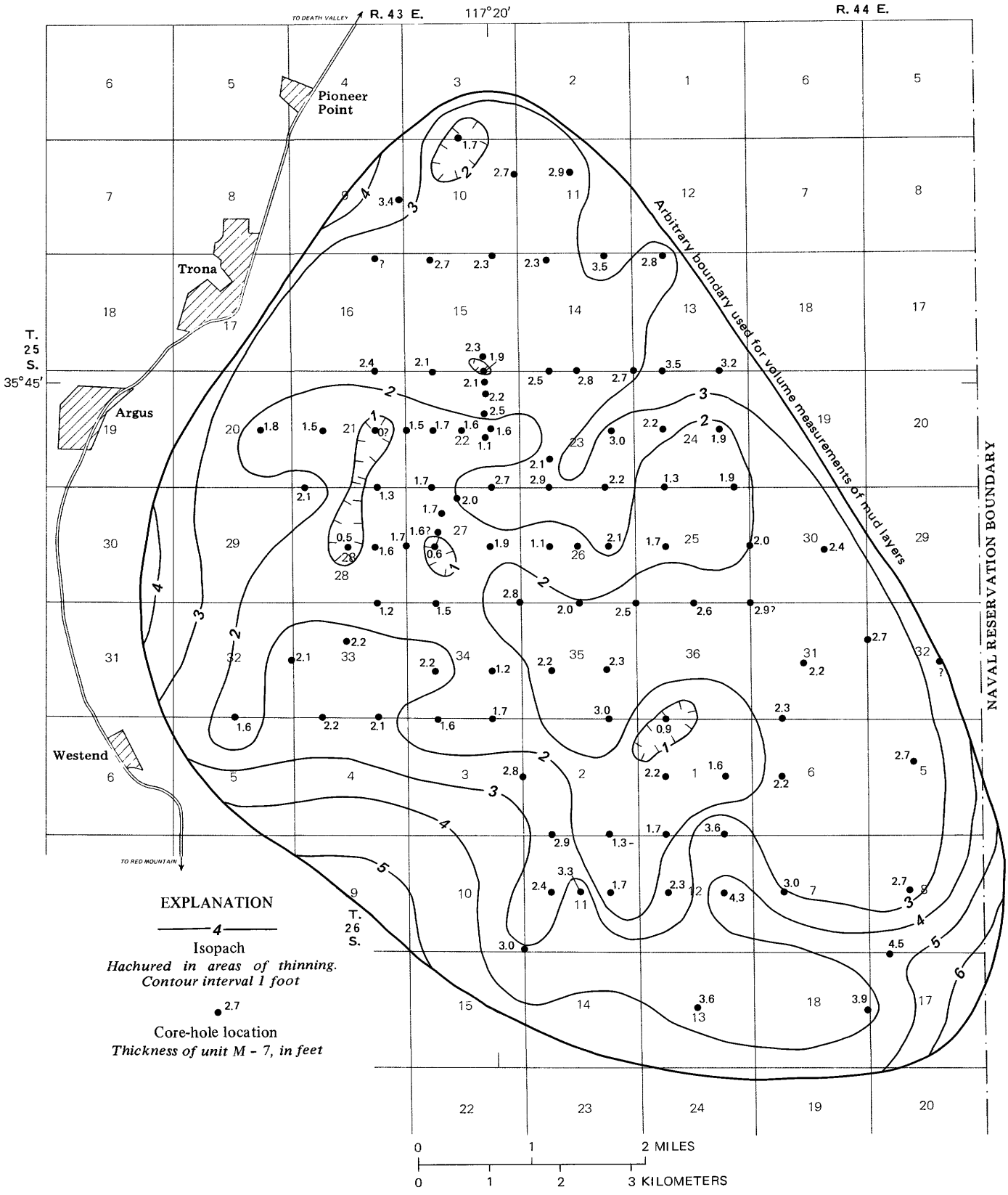


FIGURE 20.—Isopach map of unit M–7, Searles Lake.

## MINERAL COMPOSITION AND LITHOLOGY

The Lower Salt is composed of alternating saline layers and mud layers. The salines are mostly hard, white or light gray, porous, and composed of megascopic crystals. The muds are generally soft, black to dark greenish gray, impervious, and composed mostly of microscopic or submicroscopic components that form a matrix for megascopic crystals of gaylussite, pirssonite, borax, and northupite. Thin discontinuous beds of mud occur locally in the saline units, and lenses and small clusters of saline minerals occur in the mud units, but they do not make up significant percentages and generally the horizons containing them cannot be traced throughout the deposit.

### SALINE UNITS

The main mineral components of the saline units in the Lower Salt are, in approximate order of decreasing abundance, trona, halite, burkeite, northupite, borax, and thenardite. Small amounts of hanksite, nahcolite, sulfohalite, tychite, and tincalconite are found mixed with the other salines, and gaylussite and pirssonite are found in some of the thin interbeds of mud.

The volume percentages of megascopic minerals in the saline units given in table 4 are based on visual estimates of mineral percentages (Haines, 1957, 1959). As described later, these estimates have systematic but moderately sized errors; on the average, they overestimate trona by about 14 percent and underestimate halite by 8 percent, burkeite and hanksite by 5 percent, borax by 2 percent, and gaylussite and pirssonite by 1 to 2 percent.

The volume percentage estimates of the mineral content are made as follows: The isopach map of each stratigraphic unit is considered to represent a solid body that has a base that is flat and a top that is divided into "steps" of different heights along the contours. It is treated as if the steps are a series of nested and crudely concentric rings that have rectangular cross sections. The inner and outer edges of each irregular ring are vertical and defined by successive isopach contours, and the top and base are flat with the height of the top surface being midway between the thicknesses represented by the bounding contours. The area of each of these concentric bodies is calculated from planimeter measurements as described in the previous section, and the volume computed on the basis of their height. The relative volume percentages of the saline minerals in each of these concentric bodies are then calculated. First, the volume percentages of all minerals in that particular stratigraphic unit in each core are computed. These data are then grouped according to the isopach contours the core falls between and averaged. Where there are no core holes between a given pair of contours, a reasonable value is interpolated or extrapolated (shown in table 4 in parentheses). The average composition of each of the rings making up the isopach map body is then weighted according to the percentage of the unit's total volume it accounted for, and then all are added.

The data in table 4 clearly show two types of compositional variation, lateral and vertical. Lateral variation of the minerals trona, halite, and burkeite is marked; borax, thenardite, and nahcolite also appear to change systematically. The minerals halite and burkeite are clearly concentrated in the thicker central parts of the units, and trona, nahcolite, and thenardite are concentrated near the thinner edges. This distribution, a function of the relative solubilities of these minerals, is discussed in a later section.

Vertical variation in composition is evident from the data in this table. The most marked vertical changes are as follows: the lower three units (S–1, S–2, and S–3) consist almost entirely of trona; the next unit (S–4) is mostly trona and burkeite; the next (S–5), the thickest, consists of trona and halite with some burkeite; the upper two (S–6 and S–7) contain large percentages of both trona and halite but are relatively low in burkeite. Several other vertical changes are evident. Northupite is most abundant in S–2, S–3, and S–4. Borax becomes gradually more abundant from S–1 to S–5 and is notably abundant in S–7. Nahcolite is restricted to S–1 and S–7. More complete descriptions of the saline units, based on the above data and on the mineralogical and textural details presented by Haines (1959) and Smith and Haines (1964), follow.

*S–1.*—Unit S–1 consists chiefly of bladed and fine-grained trona with subordinate amounts of the fibrous form. In the central and thicker parts of the body, few other minerals are associated with this bed except for some massive northupite in the interstices of trona blades in GS–11 and 12. Toward the thinner marginal areas, there are local pockets of borax crystals (in GS–18 and 21) and nahcolite (in GS–9, 27, and 41). Tincalconite is reported from this layer (Pabst and Sawyer, 1948; see also Smith and Haines, 1964). Visible halite is absent. Mud as impurities in the trona and as thin beds is common, especially near the lower and upper contacts; in the central areas, mud rarely forms as much as 10 percent of the unit, but nearer the edges it commonly forms more than 20 percent.

TABLE 4.—*Estimated mineral compositions of saline layers in the Lower Salt*

[Numbers in parentheses either interpolated or extrapolated. t = trace]

| Stratigraphic unit | Mineral | Composition (in volume percent) indicated between contour lines | | | | | | | | Weighted total percent |
|---|---|---|---|---|---|---|---|---|---|---|
| | | 0–2 | 2–4 | 4–6 | 6–8 | 8–10 | 10–12 | 12–14 | 14+ | |
| S–7 | Halite | -- | 13 | 35 | 38 | (40) | (40) | -- | -- | 18 |
| | Trona | 84 | 80 | 58 | 61 | (60) | (60) | -- | -- | 73 |
| | Borax | 3.5 | 3.7 | -- | -- | -- | -- | -- | -- | 2.2 |
| | Thenardite | 1.7 | -- | -- | -- | -- | -- | -- | -- | .6 |
| | Sulfohalite | -- | -- | .1 | .2 | -- | -- | -- | -- | .05 |
| | Pirssonite | .1 | .8 | .1 | .2 | -- | -- | -- | -- | .3 |
| | Burkeite | -- | -- | 5.7 | -- | -- | -- | -- | -- | 1.1 |
| | Nahcolite | t | -- | -- | -- | -- | -- | -- | -- | t |
| | Mud | 11 | 2.7 | .8 | .4 | -- | -- | -- | -- | 4.6 |
| Number of cores between contours | | 21 | 7 | 2 | 1 | 0 | 0 | -- | -- | |
| Percentage of unit volume lying between indicated contours | | 35 | 27 | 18 | 15 | 3 | 2 | -- | -- | |
| S–6 | Halite | -- | 5.4 | 30 | 36 | (40) | (40) | -- | -- | 21 |
| | Trona | 92 | 93 | 68 | 64 | (59) | (59) | -- | -- | 77 |
| | Borax | -- | .8 | -- | -- | -- | -- | -- | -- | .3 |
| | Burkeite | -- | -- | 1.2 | -- | -- | -- | -- | -- | .6 |
| | Sulfohalite | -- | t | -- | -- | -- | -- | -- | -- | t |
| | Mud | 7.5 | .6 | .3 | -- | (1.0) | (1.0) | -- | -- | .7 |
| Number of cores between contours | | 2 | 18 | 8 | 1 | 0 | 0 | -- | -- | |
| Percentage of unit volume lying between indicated contours | | 5 | 34 | 49 | 10 | 1 | 1 | -- | -- | |
| S–5 | Halite | 9.5 | 17 | 40 | 66 | 43 | 61 | 49 | (50) | 51 |
| | Trona | 79.9 | 71 | 50 | 31 | 33 | 31 | 35 | (35) | 37 |
| | Hanksite | -- | -- | -- | -- | -- | t | t | -- | t |
| | Borax | -- | -- | .1 | -- | 2.2 | -- | .8 | (1.0) | .5 |
| | Burkeite | -- | -- | 8.0 | 1.5 | 20 | 5.3 | 12 | (13) | 8.1 |
| | Thenardite | 1.5 | -- | -- | -- | -- | -- | -- | -- | .03 |
| | Sulfohalite | .2 | -- | t | t | -- | t | -- | -- | t |
| | Northupite | .3 | 0.4 | t | t | t | -- | -- | -- | .03 |
| | Tychite | -- | -- | t | t | -- | -- | -- | -- | t |
| | Pirssonite | -- | -- | .3 | -- | .1 | .3 | .8 | -- | .3 |
| | Mud | 8.6 | 12 | 2.0 | 2.0 | 1.1 | 1.8 | 3.1 | (1.0) | 2.6 |
| Number of cores between contours | | 7 | 4 | 3 | 3 | 5 | 7 | 2 | 0 | |
| Percentage of unit volume lying between indicated contours | | 2 | 6 | 8 | 13 | 16 | 38 | 14 | 3 | |
| Contour lines | | 0–1 | 1–2 | 2–3 | 3–4 | 4–5 | 5+ | | | |
| S–4 | Trona | 49 | 82 | 45 | 72 | (60) | -- | -- | -- | 64 |
| | Hanksite | -- | 1.7 | -- | -- | -- | -- | -- | -- | 8 |
| | Borax | 5.3 | 1.2 | .2 | 11 | (1.0) | -- | -- | -- | 1.7 |
| | Burkeite | 32 | 12 | 52 | 6.2 | (35) | -- | -- | -- | 29 |
| | Northupite | 3.5 | .6 | .3 | 2.5 | (1.0) | -- | -- | -- | 1.0 |
| | Pirssonite | -- | .2 | -- | -- | -- | -- | -- | -- | .1 |
| | Halite | .3 | -- | -- | -- | -- | -- | -- | -- | .03 |
| | Sulfohalite | .2 | — | — | — | — | — | — | — | .03 |
| | Mud | 9.6 | 2.2 | 2.5 | 7.5 | (3.0) | -- | -- | -- | 3.5 |
| Number of cores between contours | | 15 | 9 | 5 | 1 | 0 | -- | -- | -- | |
| Percentage of unit volume lying between indicated contours | | 14 | 46 | 36 | 3 | 1 | -- | -- | -- | |

TABLE 4.—*Estimated mineral compositions of saline layers in the Lower Salt*—Continued

| Stratigraphic unit | Mineral | Composition (in volume percent) indicated between contour lines | | | | | | | | Weighted total percent |
|---|---|---|---|---|---|---|---|---|---|---|
| | | 0–2 | 2–4 | 4–6 | 6–8 | 8–10 | 10–12 | 12–14 | 14+ | |
| S–3 | Trona | 88 | 86 | (86) | -- | -- | -- | -- | -- | 87 |
| | Hanksite | -- | 2.0 | (2.0) | -- | -- | -- | -- | -- | 1.5 |
| | Borax | 3.7 | 1.1 | (1.0) | -- | -- | -- | -- | -- | 1.8 |
| | Northupite | .8 | 1.5 | (2.0) | -- | -- | -- | -- | -- | 1.3 |
| | Gaylussite | .3 | -- | -- | -- | -- | -- | -- | -- | .08 |
| | Burkeite | — | .6 | (2.0) | — | — | — | — | — | .5 |
| | Mud | 7.1 | 8.8 | (7.0) | -- | -- | -- | -- | -- | 8.2 |
| Number of cores between contours | | 19 | 14 | 0 | -- | -- | -- | -- | -- | |
| Percentage of unit volume lying between indicated contours | | 27 | 65 | 8 | -- | -- | -- | -- | -- | |
| S–2 | Trona | 98 | 93 | 89 | 91 | -- | -- | -- | -- | 92 |
| | Borax | -- | .1 | 2.2 | -- | -- | -- | -- | -- | .9 |
| | Burkeite | .5 | .7 | 1.3 | -- | -- | -- | -- | -- | .9 |
| | Thenardite | -- | -- | 1.3 | -- | -- | -- | -- | -- | .5 |
| | Northupite | .8 | .6 | 1.4 | .3 | -- | -- | -- | -- | .9 |
| | Mud | .9 | 5.2 | 4.5 | 8.8 | -- | -- | -- | -- | 4.6 |
| Number of cores between contours | | 11 | 11 | 6 | 3 | -- | -- | -- | -- | |
| Percentage of unit volume lying between indicated contours | | 12 | 43 | 40 | 5 | -- | -- | -- | -- | |
| S–1 | Trona | 71 | 92 | 97 | 98 | 85 | (100) | -- | -- | 92 |
| | Borax | .3 | 1.2 | t | -- | -- | -- | -- | -- | .3 |
| | Northupite | .4 | -- | .3 | -- | -- | -- | -- | -- | .1 |
| | Tychite | t | -- | -- | -- | -- | -- | -- | -- | t |
| | Nahcolite | 4.5 | -- | -- | -- | -- | -- | -- | -- | .6 |
| | Pirssonite | -- | .4 | .4 | -- | -- | -- | -- | -- | .2 |
| | Mud | 24 | .6 | 2.5 | 1.9 | 14 | -- | -- | -- | 7.1 |
| Number of cores between contours | | 16 | 4 | 5 | 3 | 1 | 0 | -- | -- | |
| Percentage of unit volume lying between indicated contours | | 14 | 24 | 23 | 29 | 8 | 2 | -- | -- | |

*S–2.*—Unit S–2 is in many respects similar to S–1; they are similar in area and volume and both consist largely of trona in the fine-grained and bladed forms, but the fibrous form is subordinate. Locally S–2 has pockets containing major percentages of burkeite (in the central facies, GS–15 and 16), borax (in the east edge facies, GS–2 and 27), and thenardite (in GS–6). In about a third of the cores, small quantities of fine-grained northupite form beds or interstitial fillings. Visible halite is absent. Impurities of mud are less common than in S–1 and seem to be concentrated in the central areas.

*S–3.*—Like the underlying two saline beds, unit S–3 consists primarily of trona, although it is slightly smaller in volume and covers less area. Local pockets contain uncommonly high percentages of burkeite (in GS–15), hanksite (in GS–10), and borax (in GS–15, 19, 22, and 27). Northupite occurs in about a quarter of the cores. Visible halite is absent. Thin beds and impurities of mud make up several percent of the unit in most cores; their distribution does not seem to be related to areal position.

*S–4.*—In bulk composition, unit S–4 is largely trona plus major amounts of burkeite; their relative percentages do not seem related to the thickness of the unit. Halite is present but in very small quantities (in GS–10 and 18). Hanksite (in GS–2 and 27) is present but in smaller quantities than in S–3. Borax (in GS–2, 8, 15, 17, 20, and 26) and northupite (in GS–23, 24, 26, 27, 39, and 41) are commonly found in percentages similar to those of the two underlying units. Mud layers are generally subordinate, especially in the central areas, and most of them contain neither pirssonite nor gaylussite.

*S–5.*—Unit S–5 has the largest volume of saline layers in the Lower Salt, although its areal extent is about the same as the other units. Halite is the chief component, but trona approaches the same concentration. Burkeite is subordinate to halite. Borax forms about half a percent. Minor amounts of hanksite, thenardite, sulfohalite, and northupite occur sporadically. In many areas, burkeite and halite show a tendency to be more abundant in the lower three-quarters of the bed, trona to be more abundant in the

upper one-quarter, but the layering within the unit is not consistent. With respect to thickness, trona percentages show a clear tendency to diminish toward the thick parts of the saline body, whereas halite percentages complement this trend. Both burkeite and borax are clearly concentrated near the central part of the deposit. A 2- 3-cm mud layer is generally present about half a meter above the base of the unit, and a small percentage of mud, much of which contains pirssonite, occurs throughout.

*S–6.*—Trona is clearly the predominant mineral in S–6. The relative percentage of halite is less than half that of the underlying saline unit. The percentages of borax and burkeite are small. In the thicker central facies, the lower two-thirds of the layer contains high percentages of halite that is mixed with trona, and the upper third of this layer is mostly trona; the thinner edge facies are almost exclusively trona. A little borax is found near the edges (GS–6, 19, and 20), burkeite near the center (GS–15). Very small quantities of sulfohalite and mud occur in this unit.

*S–7.*—The preponderant mineral in unit S–7 is trona. As in S–6, halite is concentrated in the lower part of the central thicker facies, whereas trona forms the upper part; trona becomes very common toward the edges. Borax is found locally in the west, central, and eastern parts of the body. A little nahcolite (GS–40), burkeite (GS–15), thenardite (GS–3), sulfohalite (GS–16), and aphthitalite (GS–15) are noted. Mud beds, some of which contain pirssonite, are more abundant in this unit than in S–6 and become more predominent toward the edges.

## MUD UNITS

The six mud units in the Lower Salt are dark organic-rich marls in which megascopic carbonate minerals are embedded. Quantitative estimates of the megascopic mineralogy of these mud layers (within the area sampled by cores) given in table 5, have been made by the same techniques used for the saline layers. These data clearly show that the percentages of these minerals vary according to stratigraphic position. In units M–2 – M–5, megascopic crystals of gaylussite are uniformly distributed and form percentages diminishing from about 18 to 2; small quantities of pirssonite occur in M–4 and M–5. In M–6 and M–7, gaylussite forms 30–40 percent of cores from the edge facies but is subordinate to pirssonite in the central facies. Crystals of borax locally form pockets in most of these layers, but are most abundant in M–4, M–5, and M–6. Northupite forms a small amount of all units but is most concentrated in M–3. Schairerite, tychite, and sulfohalite form fractions of a percent of some units. In addition, some layers have lenses or small pods of megascopic saline minerals such as halite, trona, nahcolite, burkeite, thenardite, or hanksite that were probably formed by postdepositional crystallization of migrating brine.

The microscopic size fraction of these muds consists predominantly of smaller crystals of most of these same minerals plus aragonite, analcime, clastic silicates, and partly decomposed organic material. An X-ray study by R. C. Erd (written commun., 1958) of eight samples of muds from the Lower Salt in GS–14 is summarized in table 6. Gaylussite, pirssonite, northupite, and halite are the major evaporite components of the microscopic fraction. These data show that fine-grained gaylussite and pirssonite coexist; northupite is a prominant component of some units; dolomite is not detected; and halite is present in only minor amounts. Studies of the fine-grained fraction of mud samples from GS–2 by Hay and Moiola (1963, table 1) report small quantities of analcime in units M–6 and M–7. The small percentages of saline minerals found in many of these samples may come from the evaporation of brine that was in the pores or entered the core during drilling.

The mineralogy of these mud layers differs from that of the underlying Bottom Mud and the overlying Parting Mud, which contain larger percentages of aragonite, dolomite, and halite, smaller percentages of clastic minerals, and almost no northupite.

Summaries of the megascopic lithology of the mud layers follow.

*M–2.*—Unit M–2 is the lowest mud layer within the Lower Salt sequence. It most commonly consists of mud that contains 15–20 percent gaylussite crystals. Fine laminar bedding is well-developed in most cores. A few parts of the bed contain disseminated crystals of trona, but halite is not reported. Other minerals found are nodules and thin beds of northupite (in about a third of the cores), disseminated crystals of borax (in GS–8 and 21), and small pockets of crystalline galeite (in GS–17,22, and 41) (misidentified in original logs as schairerite; see Smith and Haines, 1964, p. P32), tychite (in GS–1, 3, and 24), thenardite (in GS–6 and 10), hanksite (in GS–26), and sulfohalite (in GS–11). The northupite is concentrated around the edges of the deposit; thenardite may be also. Unit M–2 is generally 1–3 ft (0.3–1 m) thick and is thinnest near the south end of the deposit (fig. 15); the only marked thickening is to the southeast and southwest, and this thickening is probably a reflection of the clastic contribution coming from the large drainages of these areas.

*M–3.*—Unit M–3 is similar to M–2, consisting chiefly of euhedral gaylussite in mud, although the average percentage of gaylussite is slightly lower. Lam-

TABLE 5.—*Estimated mineral compositions of mud layers in the Lower Salt*

[Compositions, in volume percent, estimated within arbitrary boundaries shown in figs. 15–20]

| Stratigraphic unit | Mineral | Composition (in volume percent) between indicated contour lines | | | | | | | Weighted total percent |
|---|---|---|---|---|---|---|---|---|---|
| | | 0-1 | 1-2 | 2-3 | 3-4 | 4-5 | 5-6 | 6-7 | |
| M–7 | Mud | (62) | 62 | 63 | 67 | 62 | 60 | 60 | 63 |
| | Gaylussite | (18) | 21 | 19 | 33 | 38 | 40 | 40 | 28 |
| | Pirssonite | (20) | 16 | 15 | -- | -- | -- | -- | 8.0 |
| | Northupite | -- | -- | t | -- | -- | -- | -- | t |
| | Borax | -- | -- | .6 | -- | -- | -- | -- | .2 |
| | Trona | -- | .1 | 2.6 | .1 | -- | -- | -- | 1.1 |
| | Sulfohalite | -- | -- | t | -- | -- | -- | -- | t |
| Number of cores between contours | | 0 | 7 | 20 | 5 | 1 | 0 | 0 | |
| Percentage of unit volume, within arbitrary boundary shown on map, lying between indicated contours | | 1 | 11 | 41 | 18 | 24 | 4 | 2 | |
| M–6 | Mud | (56) | 59 | 62 | 65 | 69 | 66 | (65) | 65 |
| | Gaylussite | (2.0) | 3.5 | 16 | 9.8 | 26 | 33 | (34.0) | 20 |
| | Pirssonite | (39) | 34 | 21 | 23 | 4.2 | -- | -- | 13 |
| | Northupite | -- | -- | .1 | t | .2 | .4 | -- | .1 |
| | Borax | (1.0) | 1.0 | .8 | 1.9 | .6 | .9 | (1.0) | 1.1 |
| | Halite | (1.0) | 1.0 | -- | -- | -- | -- | -- | .1 |
| | Trona | (1.0) | 1.1 | -- | -- | .2 | -- | -- | .1 |
| Number of cores between countours | | 0 | 5 | 9 | 8 | 9 | 3 | 0 | |
| Percentage of unit volume, within arbitrary boundary shown on map, lying between indicated contours | | 1 | 6 | 21 | 23 | 25 | 18 | 6 | |
| M–5 | Mud | 86 | 95 | (98) | (98) | -- | -- | -- | 92 |
| | Gaylussite | 2.6 | 2.5 | (2.0) | (2.0) | -- | -- | -- | 2.4 |
| | Pirssonite | 1.5 | -- | -- | -- | -- | -- | -- | .7 |
| | Northupite | 4.2 | -- | -- | -- | -- | -- | -- | 1.9 |
| | Borax | 3.3 | -- | -- | -- | -- | -- | -- | 1.5 |
| | Trona | 2.3 | 2.5 | -- | -- | -- | -- | -- | 1.7 |
| | Tychite | .1 | -- | -- | -- | -- | -- | -- | 0.5 |
| | Sulfohalite | .1 | -- | -- | -- | -- | -- | -- | .05 |
| Number of cores between contours | | 25 | 2 | 0 | 0 | -- | -- | -- | |
| Percentage of unit volume, within arbitrary boundary shown on map, lying between indicated contours | | 46 | 26 | 18 | 10 | -- | -- | -- | |
| M–4 | Mud | 85 | 85 | 84 | 83 | -- | -- | -- | 84 |
| | Gaylussite | 11 | 11 | 11 | 13 | -- | -- | -- | 11 |
| | Pirssonite | -- | .1 | .2 | -- | -- | -- | -- | .1 |
| | Northupite | 3.0 | 1.1 | 1.9 | 1.6 | -- | -- | -- | 1.5 |
| | Borax | .2 | .9 | 1.4 | 1.2 | -- | -- | -- | 1.1 |
| | Trona | .5 | 2.0 | 1.9 | -- | -- | -- | -- | 1.7 |
| | Burkeite | -- | t | -- | 1.3 | -- | -- | -- | .1 |
| | Tychite | -- | t | -- | -- | -- | -- | -- | t |
| | Hanksite | -- | .5 | -- | -- | -- | -- | -- | .3 |
| Number of cores between contours | | 3 | 19 | 7 | 3 | -- | -- | -- | |
| Percentage of unit volume, within arbitrary boundary shown on map, lying between indicated contours | | 2 | 53 | 34 | 11 | -- | -- | -- | |

inar bedding is well-developed in most cores, and, after partial drying, the beds separate into paper-thin layers that have a marked flexibility. Laminae near the base are commonly contorted. Northupite forms massive white nodules or thin beds in more than half the cores, and averages about 2 percent of the unit. A few crystals of trona are found in many cores; crystals of halite are not found. Tychite crystals have been

TABLE 5.—*Estimated mineral compositions of mud layers in the Lower Salt*—Continued

| Stratigraphic unit | Mineral | Composition (in volume percent) 0-1 | 1-2 | 2-3 | 3-4 | 4-5 | 5-6 | 6-7 | Weighted total percent |
|---|---|---|---|---|---|---|---|---|---|
| M-3 | Mud | 84 | 83 | 84 | 82 | 83 | 83 | 83 | 83 |
| | Gaylussite | 13 | 14 | 9.2 | 11 | 17 | 15 | 15 | 13 |
| | Northupite | 1.5 | 1.2 | 2.9 | 5.9 | -- | 2.0 | 2.0 | 2.2 |
| | Borax | -- | t | -- | -- | -- | -- | -- | t |
| | Trona | 2.1 | 2.3 | 2.4 | 1.4 | -- | -- | -- | 1.5 |
| | Tychite | .2 | -- | 1.1 | -- | -- | -- | -- | .2 |
| Number of cores between contours | | 16 | 6 | 5 | 2 | 1 | 0 | 0 | |
| Percentage of unit volume, within arbitrary boundary shown on map, lying between indicated contours | | 11 | 30 | 18 | 15 | 14 | 8 | 4 | |
| M-2 | Mud | 82 | 82 | 81 | 76 | 69.2 | -- | -- | 79 |
| | Gaylussite | 17 | 17 | 18 | 21 | 13.6 | -- | -- | 18 |
| | Northupite | -- | .1 | .4 | 2.2 | t | -- | -- | .6 |
| | Trona | -- | .4 | .4 | .6 | 14 | -- | -- | 1.6 |
| | Tychite | 1.3 | -- | t | .2 | -- | -- | -- | .1 |
| | Galeite | -- | -- | .1 | -- | -- | -- | -- | .05 |
| | Thenardite | -- | .7 | -- | -- | 3.6 | -- | -- | .4 |
| | Borax | -- | .2 | .1 | -- | -- | -- | -- | .1 |
| | Sulfohalite | -- | t | -- | -- | -- | -- | -- | t |
| | Hanksite | -- | -- | t | -- | -- | -- | -- | t |
| Number of cores between contours | | 3 | 11 | 12 | 5 | 1 | -- | -- | |
| Percentage of unit volume, within arbitrary boundary shown on map, lying between indicated contours | | 3 | 16 | 54 | 18 | 9 | -- | -- | |

found only in the southeast part of the deposit (in GS-3 and 4). A trace of borax is reported from GS-27. Current marks were noted in GS-17. Generally, this unit has a thickness of a foot or less (fig. 16), but it thickens rapidly toward the edges of the contoured area.

*M-4.*—Like the underlying two mud units, M-4 consists of dark mud containing gaylussite, but the gaylussite percentage has fallen to about 10 percent. Small euhedral crystals of pirssonite occur locally (in GS-20 and 41). Faint laminar bedding is noted in most cores. Northupite, as white massive nodules or thin beds, forms about 1.5 percent, the maximum concentration in any mud layer in the Lower Salt; its distribution is probably random but it may be more concentrated in the thin central facies. Euhedral, subhedral, anhedral, and massive borax crystals lie in an irregular east-west belt through the center of the deposit. Crystals of trona are embedded in the muds of this unit in about a third of the cores. A little tychite (GS-3), hanksite (GS-26), and burkeite (GS-18 and 22) are noted. The thickness of this unit is commonly between 1 and 2 ft (0.3-0.6 m), but the areal pattern of the variations in thickness is erratic (fig. 17); the unit thickens toward the west and southwest edges but maintains a nearly uniform thickness to the other edges of the drilled area.

*M-5.*—Unit M-5 is normally the thinnest mud unit in the Lower Salt. Faint to indistinct laminar bedding is noted in most cores. Gaylussite crystals, generally much smaller than in other units, are reported from only about a third of the cores studied by Haines (1959) and are estimated here to constitute only 2-3 percent of the unit. Pirssonite crystals are reported from less than half as many cores. Northupite was found in three cores (GS-20, 21, and 26). A little trona (in GS-5, 15, 23, and 39), tychite (in GS-26), and sulfohalite (in GS-26) are reported, but halite is not found. Borax reaches a higher concentration in this mud unit than in any other, most of it being in the elongate prismatic form (see Smith and Haines, 1964, p. P10-P12 and fig. 5); much of the borax is concentrated near the base of the unit and in the central part of the deposit. Ripplemarks were noted in the mud at GS-16. The thickness of this unit is generally less than 1 ft (0.3 m) (fig. 18); except for an anomalous area in the northwest-central part, greater thicknesses are found only very near the west and south edges of the evaporite body.

TABLE 6.—*Mineral abundance in mud units of the Lower Salt, core GS–14, determined for total sample and acid-soluble fraction of sample*

[Semiquantitative determination from X-ray diffraction charts; M = major, I = intermediate to minor, t = trace, ? = determination uncertain, – = not detected. Determinations by R. C. Erd, R. J. McLaughlin, G. I. Smith]

| | | Total Sample | | | | | | | Acid-soluble fraction | | | | |
|---|---|---|---|---|---|---|---|---|---|---|---|---|---|
| Depth (ft) | Unit | Halite | Gaylussite | Pirssonite | Northupite | Calcite | Aragonite | Acid insoluble minerals | Quartz | Feldspar | Mica | Clay | Amphibole |
| 86.1 | M–7 | M[1] | I | I | I | – | – | I | – | M | I | – | M |
| 93.0 | M–6 | I | – | M | – | – | t? | I | t | M | I | – | I |
| 94.4 | M–6 | I | – | – | – | t | – | M | I | M | I | – | I |
| 108.0 | M–5 | t | M | – | – | – | – | I | t? | M | I | t | – |
| 110.0 | M–4 | M | – | – | – | – | – | I | – | I | M | – | – |
| 110.6 | M–4 | I | M | – | M | – | – | I | – | M | M | – | – |
| 112.6 | M–3 | I | M | – | – | – | – | t | – | M | M | – | – |
| 114.3 | M–2 | I | – | – | – | – | – | M | – | M | I | – | – |
| 115.3 | M–2 | I | M | – | – | – | – | I | t? | M | I | – | – |

[1]Sample also contains intermediate amounts of trona.

*M–6.*—About two-thirds of unit M–6 consists of mud, one-third of gaylussite or pirssonite. Laminar bedding is almost nonexistent. In 11 cores, gaylussite exists alone; in 13, pirssonite exists alone; and in 5, both exist in the same unit. The cores that contain megascopic gaylussite in this unit are mostly from the edge facies, whereas the pirssonite-bearing cores are from the more central facies, and the cores containing both come from a transitional zone between them. These zones, though distinctly concentric, do not follow closely the isopachous patterns of the unit; they do, however, approximately follow the present-day depth contours on the top of the mud layer (which are similar to those on the base of the Parting Mud shown in fig. 25). Disseminated crystals of euhedral borax are found in about half of the cores described by Haines (1959), most of which are from the central and eastern parts of the deposit. Northupite is found in this layer in six cores, all from areas near the edges. The total volume of unit M–6 (within the boundary used for measurements) is about $1.2 \times 10^8 m^3$; this volume makes it the largest of any mud unit in the Lower Salt. Its pattern of thickness variation, shown in figure 19, is notable because it varies more symmetrically around a central thin area than the other mud units, probably because the surface on which it was deposited was nearly flat (see p. 97), whereas the other mud units were deposited on irregular surfaces. Typical thicknesses are mostly between 1 and 3 ft (0.3–0.9 m), but some are nearly 6 ft (almost 2 m).

*M–7.*—In most respects, unit M–7 is similar to M–6. Indistinct laminar bedding is found in this unit in about half the cores. Mud, gaylussite, and pirssonite form most of the layer. The percentage of gaylussite is slightly higher than in M–6 and the areal distribution slightly wider, the average percentage of pirssonite correspondingly lower and the distribution more restricted. The pattern of mineral zonation is broadly the same. Borax is found sporadically along the east and west edges of the deposit. Northupite is almost nonexistent. A little trona (in GS–7, 14, and 17), sulfohalite (in GS–8), and nahcolite (in GS–40) are noted. The volume of this unit (table 3) is a little less than unit M–6 but still greater than any of the lower four mud units of the Lower Salt. The thickness of the unit is commonly between 1 and 3 ft (0.3–0.9 m) (fig. 20), somewhat less than M–6, and it shows only a slight thickening toward the west and south.

## CHEMICAL COMPOSITION

### CHEMICAL ANALYSES OF THE SOLIDS

Chemical analyses were made of 34 samples from four cores of the Lower Salt (table 7). The 11 samples from GS–16 are representative of the area near the central part of the deposit, the 6 samples from GS–21 of the parts near the edge, and the 9 samples from GS–11 and the 8 from GS–12 of facies between the edges and center. At the time these samples were taken for chemical analyses, the stratigraphic subdivisions of the Lower Salt had not been established. The intervals chosen for sampling and analysis thus bear no relation to them.

The samples were taken from large-diameter cores (Haines, 1959, p. 147–148, pls. 9 and 10) by sawing a uniform wedge from one side of the core. This entire sample, which represented approximately 5 percent of the volume of the core, was then crushed and split to get a representative sample for analysis.

Table 7 lists both chemical and X-ray analyses. The X-ray data are not quantitative, but when combined with the chemical analyses, allow one to verify and semiquantify the stratigraphic trends in mineral composition inferred from the visual estimates and summarized in table 4. The dominant trends verified are the tendencies for the lower saline units (S–1, S–2, and S–3) to contain larger amounts of $CO_2$ in the form of trona; for the middle units (S–4 and S–5) to contain larger amounts of $SO_3$ in the form of burkeite and Cl in

## TABLE 7.—*Analyses of solids in the Lower Salt*

[Chemical analyses by L. B. Schlocker, H. C. Whitebread, and W. W. Brannock. Analytical techniques: (1) CaO, MgO, $Na_2O$, $K_2O$, and $B_2O_3$ were determined in solutions prepared by boiling portions of samples in 1+9HCl; (2) Cl solutions prepared by boiling portions of samples in distilled water; (3) $SO_3$ by X-ray fluorescence of whole samples; (4) acid insoluble was residue obtained by boiling portions of samples in 1+9HCl, dried at 110°C; (5) $H_2O$ was determined by measuring weight of H expelled during combustion. X-ray analyses of total untreated sample by R. J. McLaughlin and G. I. Smith]

| Sample No. | Depth in core (ft) | Stratigraphic units included | CaO | MgO | $Na_2O$ | $K_2O$ | $CO_2$ | $SO_3$ | $B_2O_3$ | Cl | $H_2O$ | Acid insoluble | (Oxygen equivalent of Cl) | Sum | Minerals identified by X-ray (in approximate order of decreasing abundance) |
|---|---|---|---|---|---|---|---|---|---|---|---|---|---|---|---|
| GS–11–F | 83.5– 87.5 | S7 | 1.2 | 0.64 | 47.5 | 0.43 | 10.4 | 1.0 | 0.19 | 40.5 | 5.7 | 1.5 | (9.14) | 99.9 | Halite, trona, pirssonite? |
| G | 87.5– 92.0 | M7 + S6 | 3.8 | 2.1 | 36.9 | 1.0 | 16.3 | 1.3 | 2.0 | 26.0 | 9.6 | 5.9 | (5.87) | 99.0 | Halite, trona, gaylussite, northupite, pirssonite. |
| H | 92.0– 94.2 | S6 + M6 | 6.4 | 1.6 | 35.8 | 1.1 | 18.7 | 3.7 | .85 | 21.5 | 10.1 | 5.8 | (4.85) | 100.7 | Halite, trona, pirssonite, gaylussite, hanksite? |
| I | 94.2–100.0 | M6 + S5 | 2.9 | 1.0 | 41.0 | .89 | 14.2 | 5.3 | .78 | 27.3 | 7.6 | 4.8 | (6.16) | 99.6 | Halite, trona, burkeite, pirssonite? |
| J | 100.0–104.8 | S5 | .05 | .03 | 50.7 | .27 | 3.8 | 6.2 | .41 | 46.5 | 1.7 | .08 | (10.49) | 99.2 | Halite, trona, burkeite. |
| K | 104.8–109.7 | S5 + M5 + S4 | 1.5 | .40 | 46.2 | .44 | 9.4 | 9.2 | .29 | 33.2 | 5.1 | 1.6 | (7.49) | 99.8 | Halite, trona, burkeite, gaylussite. |
| L | 109.7–113.4 | M4 + S3 | 6.0 | 1.0 | 29.4 | 1.2 | 26.6 | 1.9 | 1.3 | 4.0 | 20.0 | 8.1 | (.90) | 98.6 | Trona, gaylussite, northupite, halite. |
| M | 113.4–116.8 | S2 + M2 + S1 | 4.7 | 1.6 | 31.8 | .87 | 28.9 | 3.2 | .32 | 3.6 | 17.9 | 6.1 | (.81) | 98.2 | Trona, gaylussite, northupite, halite, tychite? |
| N | 116.8–120.8 | S1 + Bot. Mud | .51 | .46 | 39.5 | .51 | 35.6 | 3.7 | .20 | 2.7 | 17.8 | .50 | (.61) | 100.9 | Trona, halite, northupite?, tychite? |
| GS–12–E | 86.9– 88.1 | S7 | .37 | .17 | 30.5 | .17 | 18.9 | .33 | 22.8 | .93 | 24.5 | .26 | (.21) | 98.7 | Tincalconite,[1] trona, halite. |
| F | 88.1– 94.9 | S7 + M7 + S6 | 3.2 | .92 | 38.8 | .72 | 20.1 | 10.0 | .34 | 12.4 | 10.0 | 3.8 | (2.80) | 97.5 | Trona, halite, burkeite, pirssonite? |
| G | 94.9– 98.0 | S6 | .34 | .44 | 47.2 | .33 | 11.3 | 3.3 | .18 | 39.1 | 5.8 | 3.4 | (8.82) | 102.6 | Halite, trona, northupite? |
| H | 98.0–102.4 | M6 + S5 | 7.2 | 2.0 | 33.6 | .95 | 17.0 | 6.5 | 1.5 | 15.3 | 9.6 | 8.3 | (3.45) | 98.5 | Halite, pirssonite, trona. |
| I | 102.4–110.0 | S5 | .16 | 0.4 | 48.6 | .20 | 7.6 | 8.3 | 1.5 | 37.1 | 4.0 | .12 | (8.37) | 99.2 | Halite, trona, burkeite. |
| J | 110.0–114.3 | S5 + M5 + S4 + M4 | 2.1 | .58 | 42.5 | .33 | 12.4 | 14.6 | 1.1 | 20.4 | 7.0 | 2.1 | (4.60) | 98.5 | Halite, burkeite, trona, gaylussite. |
| K | 114.3–119.3 | M4 + S3 + M3 + S2 + M2 | 6.3 | 2.0 | 29.6 | .49 | 25.6 | 5.2 | .49 | 3.3 | 18.2 | 6.7 | (.74) | 97.1 | Trona, gaylussite, northupite?, halite. |
| L | 119.3–121.9 | M2 + S1 | 4.0 | 1.5 | 33.4 | .35 | 31.2 | 2.6 | .28 | 2.2 | 19.4 | 4.2 | (.50) | 98.6 | Trona, gaylussite, northupite?, halite. |
| GS–16–F | 81.1– 83.7 | Parting Mud + S7 | 4.8 | 1.8 | 28.3 | .90 | 23.0 | 1.3 | 10.2 | 3.5 | 18.8 | 6.0 | (.79) | 97.8 | Trona, tincalconite,[1] gaylussite, halite, northupite? |
| G | 83.7– 86.8 | S7 | .20 | .08 | 43.5 | .38 | 26.2 | 1.6 | .15 | 17.1 | 13.4 | .23 | (3.86) | 99.0 | Trona, halite. |
| H | 86.8– 91.4 | S7 + M7 | 5.3 | 1.8 | 35.8 | .99 | 13.2 | 3.4 | 1.3 | 25.3 | 9.6 | 6.6 | (5.71) | 97.6 | Halite, trona, gaylussite, thenardite? |
| I | 91.4– 92.6 | M7 + S6 | 3.5 | .78 | 35.2 | 1.2 | 32.7 | 2.0 | .38 | 4.9 | 15.7 | 5.0 | (1.11) | 100.2 | Trona, halite, pirssonnite. |
| J | 92.6– 97.1 | S6 | .16 | .12 | 48.7 | .35 | 9.8 | 1.0 | .10 | 44.0 | 4.8 | .09 | (9.93) | 99.2 | Halite, trona. |
| K | 97.1–101.9 | M6 + S5 | 7.0 | 2.2 | 31.6 | 1.3 | 17.1 | 2.3 | 1.5 | 18.6 | 10.2 | 10.0 | (4.20) | 97.6 | Pirssonite, halite, trona, tincalconite?[1] |
| L | 101.9–105.6 | S5 | .22 | .08 | 47.4 | .25 | 11.0 | 13.0 | 1.7 | 26.9 | 5.2 | .18 | (6.07) | 99.9 | Halite, trona, burkeite, tincalconite?[1] |
| M | 105.6–111.3 | S5 + M5 | .46 | .14 | 46.2 | .23 | 9.8 | 16.2 | 2.2 | 24.6 | 4.8 | .20 | (5.55) | 99.3 | Halite, burkeite, trona, tincalconite.[1] |
| N | 111.3–113.8 | S4 + M4 | 4.0 | 2.0 | 35.8 | .55 | 16.7 | 19.2 | 1.8 | 4.3 | 9.7 | 4.1 | (.97) | 97.2 | Burkeite, gaylussite, northupite, trona, halite. |
| O | 113.8–117.8 | M4 + S3 + M3 | 4.3 | 1.5 | 29.9 | .57 | 27.2 | 1.5 | 5.3 | 2.5 | 18.6 | 6.0 | (.56) | 96.8 | Trona, gaylussite, tincalconite,[1] northupite, halite. |
| P | 117.8–119.8 | M3 + S2 + M2 | 2.5 | 1.1 | 36.2 | .50 | 30.2 | 4.6 | .28 | 2.7 | 17.3 | 2.6 | (.61) | 97.4 | Trona, gaylussite, northupite, halite. |
| G–21–D | 53.0– 56.8 | S6 | .32 | 0.8 | 39.2 | .53 | 35.2 | 1.5 | .23 | 3.4 | 18.3 | .97 | (.76) | 99.0 | Trona, halite, gaylussite. |
| E | 56.8– 61.2 | S6 + M6 + S5 | 6.5 | 2.3 | 28.6 | .92 | 25.8 | 2.1 | .43 | 5.4 | 17.5 | 8.8 | (1.22) | 97.1 | Trona, gaylussite, northupite?, halite. |
| F | 61.2– 65.9 | S5 | .40 | .22 | 40.5 | .55 | 35.4 | 2.6 | .24 | 3.6 | 17.7 | .31 | (.81) | 100.7 | Trona, halite. |
| G | 65.9– 69.9 | S5 + M5 + S4 + M4 + S3 | 4.7 | 1.6 | 31.3 | .83 | 27.8 | 2.2 | .40 | 5.3 | 17.5 | 6.3 | (1.20) | 96.7 | Trona, gaylussite, halite, northupite. |
| H | 69.9– 74.2 | S3 + M3 | 9.4 | 4.0 | 20.4 | 1.06 | 24.6 | 2.8 | 1.4 | 5.0 | 15.1 | 13.7 | (1.13) | 96.3 | Gaylussite, tincalconite,[1] halite, trona. |
| I | 74.2– 77.8 | M3 + S2 + M2 + S1 | 7.3 | 2.0 | 26.7 | .84 | 25.9 | 2.0 | .84 | 4.5 | 18.8 | 9.2 | (1.01) | 97.1 | Trona, gaylussite, northupite, halite. |

[1]Occurrences of tincalconite represent borax before dehydration in atmosphere.

the form of halite (as well as $CO_2$ in the form of trona); and for the upper units (S–6 and S–7) to contain Cl and $CO_2$ in the forms of halite and trona. The analytical data also confirm that the edge facies (exemplified by GS–21) are low in Cl- and $SO_3$-bearing minerals relative to central (GS–16) and intermediate (GS–11 and GS–12) facies. It is difficult to assess the vertical variations in CaO, MgO, $K_2O$, and $B_2O_3$ because the statigraphic composition of the analyzed intervals is so variable. Horizontal variations are more marked; the central and intermediate facies appear to have about three times as much $B_2O_3$ as the edge facies, about half as much CaO and MgO, and about the same $K_2O$. The acid-insoluble material averages about 4 percent; because about 45 percent of the Lower Salt consists of material logged as mud, more than 90 percent of most mud layers is soluble in acid.

The chemical analyses provide a way to check the reliability of the visually estimated mineral compositions. Table 8 compares the visual estimates of mineral volume percentages (converted to weight percentages of major element oxides) with the chemical analyses of the same intervals. In compiling table 8, the chemical analyses of cores from both the Lower Salt and Upper Salt, given in tables 7 and 15, were combined into a single list and the analysis percentages compared with the modal percentages calculated from the estimated mineral composition of the same intervals cited in the published logs (Haines, 1959). Differences were tabulated, with a positive sign used for differences where the chemical analyses gave higher values, and a negative sign used for those where the chemical analyses gave lower values. To test for systematic errors in visual estimates, these positive and negative values were added algebraically, and the sum divided by the number of analyses. Results of these computations are shown in table 8 both for the four individual cores and for all 51 analyses for Lower and Upper Salt combined. Also listed are mean deviations and standard deviations.

Although the analyses provide a more accurate measure of the composition of the cores, not all differences are attributable to errors in the visual estimates. The chemical analyses are of a relatively small wedge cut from one side, whereas the visual estimates were based on the surface area of the entire core. Because of crystal sizes and the lateral variability in composition found in most cores, the large surface is likely to provide a different, and possibly better, sample of the layer than the small wedge. The chemical analyses were of samples that included the fractured material logged as "probably cuttings, not core," whereas the modal estimates omit these segments. And the analyses include the components that were in the brine entrapped in the pores and were not actually present as salts.

Nevertheless, it is clear that the visual estimates have small but consistent errors which should be taken into account when evaluating the bulk mineral compositions of the saline units given in table 4. The 5.0 percent negative error in $CO_2$ and negative error in $H_2O$ probably means that trona was overestimated in the cores by about 14 percent (assuming that some of the analyzed $CO_2$ came from underestimated or unde-

TABLE 8—*Comparison of chemical analyses with composition indicated by visual estimates of mineral percentages*

[Positive values indicate components for which chemical analyses were higher, negative values indicate chemical analyses lower. All values in weight percent. Data for chemical analyses from tables 7 and 15, visual estimates of mineral percentages from Haines (1959)]

| | CaO | MgO | $Na_2O$ | $K_2O$ | $CO_2$ | $SO_3$ | $B_2O_3$ | Cl | $H_2O$ | Oxygen equivalent of Cl | Sum[2] |
|---|---|---|---|---|---|---|---|---|---|---|---|
| Average error[1] | | | | | | | | | | | |
| GS–11 | +0.4 | +0.7 | −0.8 | +0.6 | −4.6 | +0.8 | +0.5 | +5.2 | −1.6 | (−1.7) | −0.5 |
| GS–12 | 0.0 | +0.8 | +0.3 | +0.5 | −5.7 | +3.3 | +0.6 | +4.7 | −3.2 | (−1.1) | −0.2 |
| GS–16 | +0.6 | +0.7 | −1.8 | +0.9 | −3.8 | +1.6 | +1.1 | +2.2 | −1.1 | (−0.5) | −0.1 |
| GS–21 | +1.1 | +1.3 | −2.2 | +0.9 | −6.5 | +3.8 | +0.6 | +5.1 | −3.0 | (−1.2) | −0.1 |
| All samples | +0.5 | +0.8 | −1.1 | +0.7 | −5.0 | +2.2 | +0.7 | +4.8 | −2.1 | (−1.1) | −0.4 |
| Mean deviation[3] | 1.2 | 0.8 | 2.4 | 0.8 | 5.9 | 4.0 | 0.9 | 6.4 | 3.0 | | |
| Standard deviation[4] | 2.0 | 1.2 | 3.1 | 1.0 | 6.9 | 5.5 | 1.7 | 8.2 | 3.9 | | |

[1] $\frac{\Sigma d}{N}$ where $d$ = difference between chemical analysis value and visual estimates value, sign retained
N = number of analyzed samples; 14 in GS–11, 12 in GS–12, 16 in GS–16, and 9 in GS–21, total of 51.

[2] Algebraic Sums are negative because sums of chemical analyses (tables 8 and 15) are mostly less than 100.

[3] $\frac{\Sigma |d|}{N'}$ $|d|$ = same but sign ignored.

[4] $\left(\frac{\Sigma d^2}{N}\right)^{1/2}$

tected gaylussite or pirssonite as the positive error in CaO suggests). The 4.8 percent positive error in Cl suggests that halite was underestimated by an average of 8 percent; the 2.2 percent positive error in $SO_3$ may mean that burkeite or hanksite was underestimated by about 5 percent; and the 0.7 percent error in $B_2O_3$ means that borax was underestimated by 2 percent. Positive errors in CaO may mean that megascopic gaylussite or pirssonite were underestimated by 1–2 percent, but the CaO may also represent small amounts of microcrystalline minerals in the mud. Similarly, the 0.8 percent MgO may represent about 5 percent megascopic northupite or about 4 percent microscopic dolomite. The 0.7 percent error in $K_2O$ theoretically suggests an error of nearly 25 percent hanksite, but probably indicates about 2 percent aphthitalite or contamination by the entrapped brine.

The errors in visual estimates indicated by these data are of the type easily made while logging core. Fine-grained trona, burkeite, and halite in a core may be very similar in appearances, and when in doubt, the core logger generally chooses the mineral that most commonly has this habit—trona. Borax, prior to dehydration of the surface to white powdery tincalconite, is easily misidentified as one of the other glassy conchoidal-fracturing minerals such as hanksite or gaylussite. Small amounts of northupite (especially the fine-grained variety), thenardite, aphthitalite, and other saline minerals are easily overlooked. All fine-grained components in the muds—mostly aragonite, calcite, dolomite, or halite are not identifiable visually.

## CHEMICAL ANALYSES OF THE BRINES

The current economic value of Searles Lake lies in its brine content. The major commercial operations on the deposit pump the brines from the interstices of the Upper and Lower Salts and process them to extract chemicals. The brine varies in composition from place to place and from depth to depth, and an understanding of these variations is essential for the optimum utilization of the deposit.

Table 9 gives 68 brine analyses from the Lower Salt portion of 11 core holes, 10 in the central and intermediate parts of the deposit, 1 (GS–1) in the outer parts. All samples were taken by lowering a hose to the desired level, pumping brine from that level until an equilibrium was established, then taking a sample. Much of the brine in samples collected in this way undoubtedly came from levels well above and below the bottom of the collection hose. The contribution from each salt horizon exposed in the uncased drill holes depended on its permeability and its proximity to the point of collection. The samples thus approximate moving averages of the brines that existed at successive levels, but these averages overrepresent, to an unknown degree, the brines in the more permeable zones. The analyses from core L–31, however, represent definite stratigraphic units because a packer was used during their collection.

The compositions of the brines given in table 9 are plotted in figure 21. It shows their compositions projected to one face of the tetrahedrons that represent 5-component systems. Figure 21*A* shows projected boundaries of the mineral stability fields in the $Na_2CO_3$-$NaHCO_3$-$Na_2SO_4$-NaCl-$H_2O$ system at 20°C; figure 21*B*, projected boundaries in the $Na_2CO_3$-$Na_2SO_4$-NaCl-KCl-$H_2O$ system at 20°C. Many of the points in figure 21*A* are alined along zones parallel to the burkeite-thenardite and burkeite-halite boundaries. They are probably exactly on these boundaries; the burkeite field expands with increasing temperatures, and temperatures in the Lower Salt are mostly 20°–24°C which would cause the burkeite boundary to move toward the alined points. The points in figure 21*B* show more scatter although most are within the boundaries of the hanksite field; the small amount of hanksite in the Lower Salt means that the removal of much of the K-bearing brines from the unit would result in the phase disappearing. The remaining points lie a short distance away in the adjoining fields.

The specific gravities of brines from the central areas of Searles Lake lie mostly between 1.29 and 1.31 and tend to increase with depth. Those from the edges are as low as 1.25. Except for samples from sites near the edges, the total percentages of dissolved solids, calculated by summation of the percentages, mostly lie between 33 and 35 percent.

Values of pH given for brines from four holes (table 9) range from 9.1 to 9.9; those from GS–4 (which is nearest the edge and higher in sulfate and lower in carbonate) are the lowest. These values may be slightly in error because they were measured several days after collection, and it is likely that some $CO_2$ was lost, thereby changing the pH value.

The brine analysis given in table 9 shows some vertical variation in the weight percentages of the dissolved components. The Na percentages of brines in the upper seven analyses in the table are calculated by equivalent difference; the percentages in the lower four are based on analysis. The Na percentages in most core holes increase downward. The percentage of K increases upward in 9 of the 11 wells analyzed and increases downward in two (GS–1 and GS–10). Seven of the eight analyses wherein K increases upward come from near the center of the deposit, but neither

TABLE 9.—*Chemical analyses of brines in the Lower Salt*

[Analyses of core holes HH, MM, U, W, X, S–28 and S–31, by chemists of American Potash & Chemical Corp., published with permission of company. Analyses of GS–1, GS–4, and GS–10 by Henry Kramer and Sol Berman, U.S. Geological Survey, of L–31 by Shirley L. Rettig, U.S. Geological Survey. Compositions in weight percent except where indicated as parts per million (ppm)]

| Core hole (depths in feet to top and base of Lower Salt) Date of Sampling | Brine sample depth (feet) | Specific gravity | Total dissolved solids (by summation) | pH | Na | K | Li (ppm) | $CO_3$ | $SO_4$ | Cl | $B_4O_7$ | $PO_4$ (ppm) | F (ppm) | Br (ppm) | S (ppm) | As (ppm) | Si (ppm) | I (ppm) |
|---|---|---|---|---|---|---|---|---|---|---|---|---|---|---|---|---|---|---|
| HH | 95 | 1.300 | 34.75 | | 11.05 | 2.40 | ____ | 2.39 | 4.98 | 12.20 | 1.06 | 960 | 20 | 910 | 200 | ____ | ____ | ____ |
| (90.7–129.8) | 100 | 1.310 | 34.98 | ____ | 12.04 | 1.69 | ____ | 4.53 | 3.22 | 11.26 | 1.83 | 400 | ____ | 550 | 1300 | ____ | ____ | ____ |
| November 1949 | 105 | 1.310 | 34.99 | ____ | 12.01 | 1.74 | ____ | 4.57 | 3.20 | 11.19 | 1.85 | 400 | 16 | 550 | 1300 | ____ | ____ | ____ |
| | [1]110 | 1.311 | 35.02 | ____ | 12.04 | 1.73 | ____ | 4.66 | 3.15 | 11.14 | 1.88 | 400 | 23 | 540 | 1300 | ____ | ____ | ____ |
| | 115 | 1.314 | 35.12 | ____ | 12.18 | 1.61 | ____ | 4.93 | 3.04 | 10.95 | 1.99 | 400 | 13 | 520 | 1400 | ____ | ____ | ____ |
| | 120 | 1.317 | 35.33 | ____ | 12.31 | 1.56 | ____ | 5.24 | 2.91 | 10.78 | 2.12 | 380 | 18 | 510 | 1300 | ____ | ____ | ____ |
| | 125 | 1.320 | 35.40 | ____ | 12.34 | 1.54 | ____ | 5.52 | 2.83 | 10.53 | 2.24 | 360 | 23 | 460 | 1300 | ____ | ____ | ____ |
| MM | 70 | 1.297 | 34.37 | ____ | 11.34 | 2.08 | ____ | 2.76 | 4.50 | 12.06 | 1.13 | 580 | ____ | 840 | 980 | ____ | ____ | ____ |
| (66.5–98.3) | 75 | 1.299 | 34.46 | ____ | 11.46 | 1.96 | ____ | 2.88 | 4.50 | 11.95 | 1.20 | 580 | ____ | 780 | 1080 | ____ | ____ | ____ |
| November 1949 | [1]80 | 1.300 | 34.52 | ____ | 11.47 | 1.96 | ____ | 2.91 | 4.52 | 11.88 | 1.23 | 660 | ____ | 810 | 1060 | ____ | ____ | ____ |
| | 85 | 1.301 | 34.57 | ____ | 11.49 | 1.95 | ____ | 2.95 | 4.53 | 11.84 | 1.24 | 700 | ____ | 810 | 1050 | ____ | ____ | ____ |
| | 90 | 1.301 | 34.64 | ____ | 11.51 | 1.96 | ____ | 2.97 | 4.52 | 11.84 | 1.26 | 700 | ____ | 810 | 1110 | ____ | ____ | ____ |
| | 95 | 1.301 | 34.60 | ____ | 11.48 | 1.96 | ____ | 2.97 | 4.52 | 11.84 | 1.26 | 700 | ____ | 810 | 1040 | ____ | ____ | ____ |
| U | 80 | 1.292 | 33.95 | ____ | 11.23 | 2.03 | ____ | 2.43 | 4.35 | 12.24 | 1.13 | 580 | ____ | 800 | 1400 | ____ | ____ | ____ |
| (78.4–114.6) | 85 | 1.294 | 34.22 | ____ | 11.35 | 2.01 | ____ | 2.55 | 4.44 | 12.16 | 1.17 | 580 | ____ | 780 | 1400 | ____ | ____ | ____ |
| December 1949 | [1]90 | 1.294 | 34.11 | ____ | 11.33 | 1.99 | ____ | 2.60 | 4.39 | 12.09 | 1.16 | 600 | ____ | 760 | 1400 | ____ | ____ | ____ |
| | 95 | 1.299 | 34.45 | ____ | 11.58 | 1.85 | ____ | 3.09 | 4.11 | 11.84 | 1.42 | 600 | ____ | 690 | 1600 | ____ | ____ | ____ |
| | 100 | 1.300 | 34.42 | ____ | 11.59 | 1.82 | ____ | 3.17 | 4.05 | 11.77 | 1.46 | 600 | | 660 | 1600 | ____ | ____ | ____ |
| | 105 | 1.300 | 34.47 | ____ | 11.62 | 1.80 | ____ | 3.24 | 4.03 | 11.74 | 1.48 | 620 | ____ | 650 | 1600 | ____ | ____ | ____ |
| | 110 | 1.300 | 34.47 | ____ | 11.65 | 1.77 | ____ | 3.25 | 4.10 | 11.66 | 1.47 | 620 | ____ | 660 | 1600 | ____ | ____ | ____ |
| W | 85 | 1.301 | 34.84 | ____ | 11.37 | 2.10 | ____ | 2.81 | 5.31 | 11.52 | 1.11 | 860 | ____ | 770 | 700 | ____ | ____ | ____ |
| (85.0–120.1) | 90 | 1.304 | 35.99 | ____ | 11.52 | 1.92 | ____ | 2.91 | 5.76 | 11.12 | 1.13 | 860 | ____ | 770 | 800 | ____ | ____ | ____ |
| March 1950 | 95 | 1.304 | 34.85 | ____ | 11.50 | 1.89 | ____ | 2.91 | 5.73 | 11.07 | 1.12 | 860 | ____ | 790 | 800 | ____ | ____ | ____ |
| | [1]100 | 1.304 | 34.91 | ____ | 11.52 | 1.89 | ____ | 2.92 | 5.76 | 11.07 | 1.13 | 840 | ____ | 790 | 800 | ____ | ____ | ____ |
| | 105 | 1.303 | 34.86 | ____ | 11.49 | 1.89 | ____ | 2.92 | 5.81 | 10.99 | 1.13 | 860 | ____ | 770 | 800 | ____ | ____ | ____ |
| | 110 | 1.303 | 34.76 | ____ | 11.43 | 1.92 | ____ | 2.93 | 5.84 | 10.89 | 1.13 | 820 | ____ | 790 | 900 | ____ | ____ | ____ |
| | 115 | 1.302 | 34.57 | ____ | 11.39 | 1.89 | ____ | 2.93 | 5.87 | 10.77 | 1.12 | 800 | ____ | 790 | 800 | ____ | ____ | ____ |
| | 120 | 1.302 | 34.59 | ____ | 11.38 | 1.90 | ____ | 2.93 | 5.87 | 10.77 | 1.12 | 820 | ____ | 770 | 900 | ____ | ____ | ____ |
| X | 90 | 1.304 | 35.00 | ____ | 11.47 | 2.13 | ____ | 3.07 | 4.58 | 11.84 | 1.29 | 840 | ____ | 870 | 700 | ____ | ____ | ____ |
| (89.2–127.2) | 95 | 1.304 | 35.04 | ____ | 11.48 | 2.13 | ____ | 3.07 | 4.58 | 11.84 | 1.30 | 860 | ____ | 890 | 800 | ____ | ____ | ____ |
| March 1950 | 100 | 1.305 | 35.00 | ____ | 11.45 | 2.14 | ____ | 3.07 | 4.56 | 11.84 | 1.30 | 860 | ____ | 890 | 800 | ____ | ____ | ____ |
| | [1]105 | 1.305 | 35.01 | ____ | 11.46 | 2.14 | ____ | 3.07 | 4.56 | 11.84 | 1.30 | 860 | ____ | 890 | 800 | ____ | ____ | ____ |
| | 110 | 1.305 | 35.05 | ____ | 11.47 | 2.14 | ____ | 3.07 | 4.60 | 11.84 | 1.29 | 860 | ____ | 890 | 800 | ____ | ____ | ____ |
| | 115 | 1.306 | 34.97 | ____ | 11.50 | 2.10 | ____ | 3.23 | 4.43 | 11.74 | 1.33 | 860 | ____ | 870 | 800 | ____ | ____ | ____ |
| | 120 | 1.306 | 34.94 | ____ | 11.49 | 2.10 | ____ | 3.24 | 4.43 | 11.70 | 1.35 | 840 | ____ | 850 | 900 | ____ | ____ | ____ |
| | 125 | 1.306 | 34.91 | ____ | 11.52 | 2.05 | ____ | 3.41 | 4.62 | 11.01 | 1.38 | 820 | ____ | 810 | 900 | ____ | ____ | ____ |
| S–28 | 80 | 1.289 | 33.50 | ____ | 11.51 | 1.46 | ____ | 2.39 | 4.58 | 12.06 | 1.03 | 500 | ____ | 560 | 1400 | ____ | ____ | ____ |
| (77.4–102.1) | 85 | 1.290 | 33.50 | ____ | 11.54 | 1.43 | ____ | 2.51 | 4.58 | 11.93 | 1.04 | 480 | ____ | 550 | 1500 | ____ | ____ | ____ |
| September 1950 | [1]90 | 1.293 | 33.94 | ____ | 11.74 | 1.39 | ____ | 2.72 | 4.60 | 11.93 | 1.08 | 520 | ____ | 530 | 1400 | ____ | ____ | ____ |
| | 95 | 1.295 | 34.11 | ____ | 11.80 | 1.35 | ____ | 2.88 | 4.70 | 11.67 | 1.16 | 620 | ____ | 520 | 1600 | ____ | ____ | ____ |
| | 100 | 1.295 | 33.97 | ____ | 11.75 | 1.34 | ____ | 2.89 | 4.70 | 11.58 | 1.16 | 660 | | 520 | 1400 | ____ | ____ | ____ |
| S–31 | 85 | 1.297 | 34.27 | ____ | 11.72 | 1.60 | ____ | 2.89 | 4.43 | 11.95 | 1.21 | 500 | ____ | 630 | 1400 | ____ | ____ | ____ |
| (84.0–117.1) | 90 | 1.297 | 34.23 | ____ | 11.74 | 1.55 | 11 | 2.93 | 4.42 | 11.88 | 1.23 | 500 | ____ | 630 | 1500 | ____ | ____ | ____ |
| December 1950 | [1]95 | 1.298 | 34.29 | ____ | 11.81 | 1.52 | 11 | 3.08 | 4.25 | 11.88 | 1.29 | 460 | ____ | 600 | 1500 | ____ | ____ | ____ |
| | 100 | 1.303 | 34.50 | ____ | 12.04 | 1.39 | 32 | 3.66 | 3.81 | 11.63 | 1.48 | 500 | ____ | 570 | 1600 | ____ | ____ | ____ |
| | 105 | 1.305 | 34.48 | ____ | 12.07 | 1.35 | ____ | 3.89 | 3.68 | 11.42 | 1.57 | 500 | ____ | 570 | 1700 | ____ | ____ | ____ |
| | 110 | 1.305 | 34.50 | ____ | 12.09 | 1.33 | 32 | 3.92 | 3.67 | 11.42 | 1.58 | 500 | ____ | 570 | 1600 | ____ | ____ | ____ |
| | 115 | 1.305 | 34.62 | ____ | 12.12 | 1.35 | ____ | 3.93 | 3.67 | 11.45 | 1.59 | 520 | ____ | 550 | 1600 | ____ | ____ | ____ |
| GS–1 | 68 | 1.253 | 29.8 | 9.3 | 10.2 | 0.95 | 8.8 | 3.98 | 5.34 | 8.50 | 0.79 | | | | | | | |
| (65.0–88.6) | 70 | 1.255 | 30.1 | 9.3 | 10.3 | .96 | 8.8 | 4.12 | 5.44 | 8.48 | .79 | | | | | | | |
| July 1954 | 75 | 1.253 | 30.5 | 9.3 | 10.7 | 1.06 | 12 | 3.72 | 5.37 | 8.84 | .81 | | | | | | | |
| | [1]80 | 1.265 | 31.3 | 9.3 | 10.6 | 1.36 | 21 | 3.14 | 5.11 | 10.14 | .95 | | | | | | | |
| | 85 | 1.264 | 31.6 | 9.3 | 10.8 | 1.36 | 22 | 3.12 | 5.14 | 10.20 | .95 | | | | | | | |
| | 86 | 1.263 | 31.7 | 9.3 | 10.7 | 1.42 | 20 | 3.29 | 5.19 | 10.19 | .91 | | | | | | | |
| GS–4 | 64.6 | 1.275 | 31.8 | 9.15 | 11.2 | 0.93 | 11 | 2.96 | 5.94 | 10.16 | 0.59 | | | | | | | |
| (64.6–89.5) | 70 | 1.274 | 31.9 | 9.19 | 11.1 | 1.01 | 11 | 3.00 | 5.81 | 10.41 | .59 | | | | | | | |
| September 1954 | 75 | 1.274 | 31.8 | 9.12 | 11.1 | .94 | 11 | 2.81 | 5.90 | 10.39 | .61 | | | | | | | |
| | [1]80 | 1.276 | 31.5 | 9.18 | 10.8 | .90 | 11 | 3.11 | 6.30 | 9.82 | .57 | | | | | | | |
| | 85 | 1.274 | 32.0 | 9.15 | 11.1 | .92 | 11 | 3.11 | 6.36 | 9.91 | .57 | | | | | | | |
| | 86 | 1.272 | 31.3 | 9.10 | 11.0 | .58 | 7 | 3.91 | 8.20 | 7.17 | .45 | | | | | | | |
| GS–10 | 85 | 1.280 | 33.0 | 9.32 | 10.7 | 1.70 | 23 | 2.58 | 4.53 | 12.34 | 1.10 | | | | | | | |
| (83.1–114.5) | 90 | 1.281 | 33.3 | 9.41 | 10.9 | 1.85 | 23 | 2.70 | 4.49 | 12.24 | 1.16 | | | | | | | |
| January 1955 | [1]95 | 1.288 | 34.6 | 9.37 | 11.8 | 1.95 | 51 | 2.66 | 4.73 | 12.24 | 1.19 | | | | | | | |
| | 100 | 1.288 | 33.7 | 9.39 | 11.0 | 2.00 | 51 | 2.58 | 4.70 | 12.20 | 1.22 | | | | | | | |
| | 105 | 1.288 | 33.6 | 9.42 | 11.0 | 1.95 | 52 | 2.56 | 4.71 | 12.22 | 1.20 | | | | | | | |
| | 110 | 1.286 | 34.0 | 9.38 | 11.0 | 2.02 | 50 | 2.69 | 4.71 | 12.22 | 1.38 | | | | | | | |
| L–31[2] | 102 | 1.299 | 33.0 | 9.75 | 11.1 | 2.39 | ____ | 3.23 | 3.78 | 11.70 | 1.23 | 536 | 23 | 704 | ____ | 102 | 40 | 27 |
| (91.5–129.1) | 127 | 1.302 | 32.2 | 9.90 | 11.1 | 1.77 | ____ | 4.32 | 4.08 | 9.82 | 1.45 | 357 | 35 | 449 | ____ | 98 | 33 | 22 |
| November 1964 | | | | | | | | | | | | | | | | | | |

[1]Uppermost brine sample used to calculate composition of brine in units S1 + S2 + S3 + S4 + S5.

[2]Sample from depth of 102 feet represents brine from unit S7; sample from 127 feet represents brine from S1, S2, and S3.

the areal position in the deposit nor the total thickness of the Lower Salt bears a consistent relation to the K content. Ryan (1951, p. 449) reports 1.5 percent K as typical of brine pumped from the central part of Lower Salt; Dyer (1950, p. 41) reports 1.4 percent K as typical.

In most wells in the central part of the deposit, total carbonate in the Lower Salt brines, expressed in the analyses as $CO_3$ percentage, increases downward; toward the edges, the vertical variation is small, reflecting the more nearly monomineralic composition of this zone. The percentages of $SO_4$ are generally between 3 and 6. The percentages of $SO_4$ in the brines increase toward the top in four core holes, increase to-

ward the bottom in five, and are nearly constant in two.[11] Brines in core holes GS–4 have abnormally high percentages of $SO_4$ although the associated salines are not high in sulfate minerals. This high $SO_4$ content in the brine may result from the relatively large quantities of sulfate that were contained by the waters draining from the gypsum-bearing lake deposits near the south end of the Slate Range, and the gypsiferous gouge of the Sand Canyon thrust fault along the nearby edge of the Slate Range (Smith and others, 1968, p. 14, 21). The percentages of Cl mostly fall between 10.5 and 12 except near the edges, where the brines have a lower total salinity. The Cl content of the brines generally increases upward. The $B_4O_7$ percentage normally increases downward; most percentages lie between 1 and 2 except near some parts of the edge, where they are substantially less.

Analyses of minor elements are available for some sets of samples. The brine wells for which $PO_4$ analyses are available come from the central part of the deposit. Although there is appreciable variation in $PO_4$ content of brines from different wells, the percentages in brine from a single well are relatively uniform. Ryan (1951, p. 449) reports an average of 590 ppm $PO_4$ and W. A. Gale (written commun., 1952) reports 535 ppm in brines from the central part of the Lower Salt. The analyses for F and Br are all of brines from the central parts of the deposit. The amount of F shows no clear trend; Br tends to increase toward the base of the layer. Ryan reports 30 ppm Li and 540 ppm Br, and Gale estimates 30 ppm Li and 580 ppm Br in the brines pumped by the American Potash and Chemical Corp. The amounts of S may increase downward, although the total range of variation is small. The values are mostly between 1,000 and 1,500 ppm. Ryan and Gale report average quantities of about 1,500 and 1,800 ppm S, respectively. Data on the As, Si, and I content are given in table 9 for core hole L–31. Estimates by Ryan and Gale of the I content of brines pumped from the central part of the Lower Salt are the 20 ppm and 25 ppm. The Sr content of a brine sample from the top part of the Lower Salt in GS–26 is 1.5 ppm (J. D. Hem, analyst, written commun., 1960). The W content of brine in the Lower Salt is reported by Ryan and W. A. Gale to be about 32 ppm. Samples from GS–1, GS–4, GS–10, and L–31 were analyzed for Ca and Mg, but the concentrations were below the limit of detection.

[11]Analyses showing higher percentages of $SO_4$ in the upper part of the Lower Salt may be of brines that were largely or entirely drawn from units S–4 and S–5, as those units are more porous and were not blocked off during sampling of most cores. Analysis of a brine from core L–31, which was collected when that layer was blocked off from other layers, show lower $SO_4$ values for brine from S–7 than from units S–1 through S–3 in that core; although not sampled, units S–4 and S–5 are almost certainly higher in $SO_4$ than S–1, S–2, and S–3.

The vertical variations in brine composition follow a broad pattern but do not bear a close relation to the mineral composition of the surrounding solids. The inconsistency of relations result in part from post-depositional changes in the brines caused by the following processes: (1) fresh waters from the surface and the ground water of surrounding valley sediments have encroached on the salt bodies, probably affecting each salt layer somewhat differently; (2) the brines were allowed to mix when the mud layers that separated the Lower Salt salt layers were perforated by drill holes; (3) additional mixing occurred when these brines were pumped for processing by the chemical companies; and (4) the brine sampling procedure provides a sample for analysis that is still more mixed because it draws brines into the sample from porous zones above and below the sampled depth in the uncased hole.

Of the brines represented by analyses in table 9, those from S–31 are probably least affected by post-depositional changes as that core hole is well away from the edges of the body, and is in the southern part of the deposit, which, at the time of sampling and analysis, was not so extensively drilled nor as heavily pumped as other areas represented by analysis. In S–31, the depths sampled for brine lie near or within the following salt units:

| | |
|---|---|
| 85 ft (25.9 m) | S–7 |
| 90 ft | S–6 |
| 95 ft | S–5 |
| 100 ft | S–5 |
| 105 ft | S–4 |
| 110 ft | S–3 |
| 115 ft (35.1 m) | S–1 |

The brines in S–31 show their greatest change above and below the sample from 95 ft. This change is as expected because, as noted in earlier papers (Smith and Haines, 1964, p. 47–50, 54; Smith, 1968, fig. 4), the only dry-lake stage inferred during deposition of the Lower Salt is represented by the top of unit S–5. The two samples representing S–7 and S–6 have greater percentages of K, $SO_4$, Cl and Br. The five samples representing S–5, S–4, S–3, S–2, and S–1 have greater percentages of Na, $CO_3$, $B_4O_7$, Li, S, and total dissolved solids. Of these lower five samples, the lowest three (representing S–1, S–2, S–3, and S–4) have the greatest concentrations of these components, and the two above them (representing S–5) have intermediate concentrations.

*A*

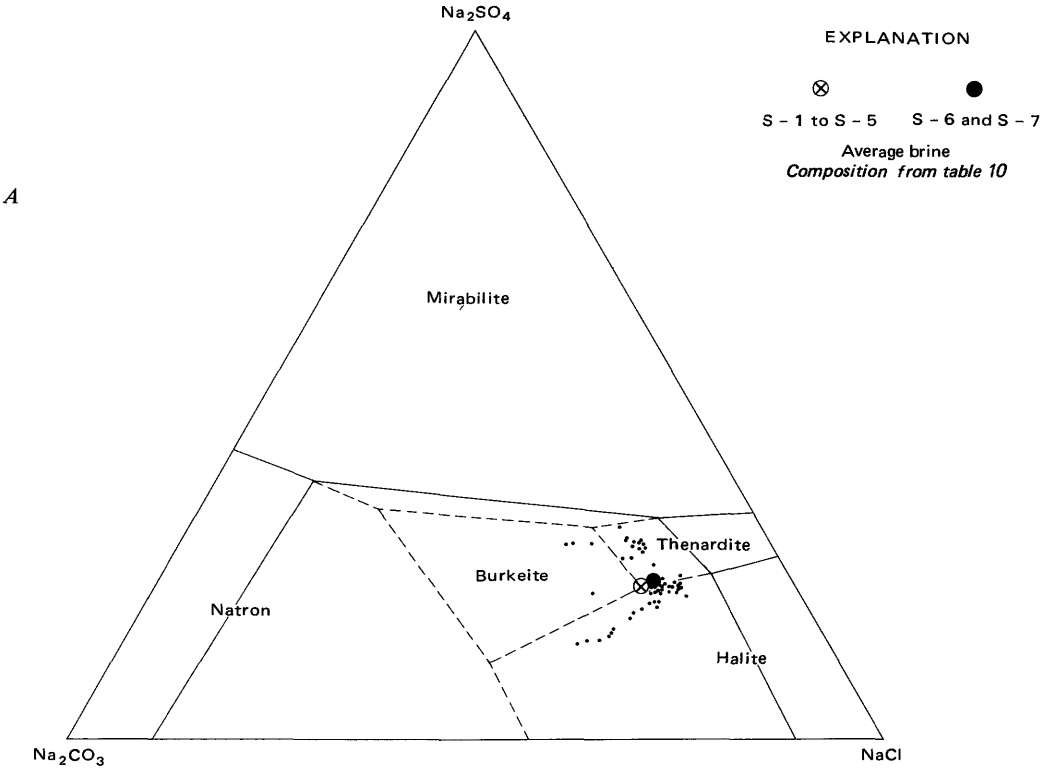
$Na_2SO_4$
EXPLANATION
S - 1 to S - 5
S - 6 and S - 7
Average brine
*Composition from table 10*
Mirabilite
Thenardite
Burkeite
Natron
Halite
$Na_2CO_3$
NaCl

*B*

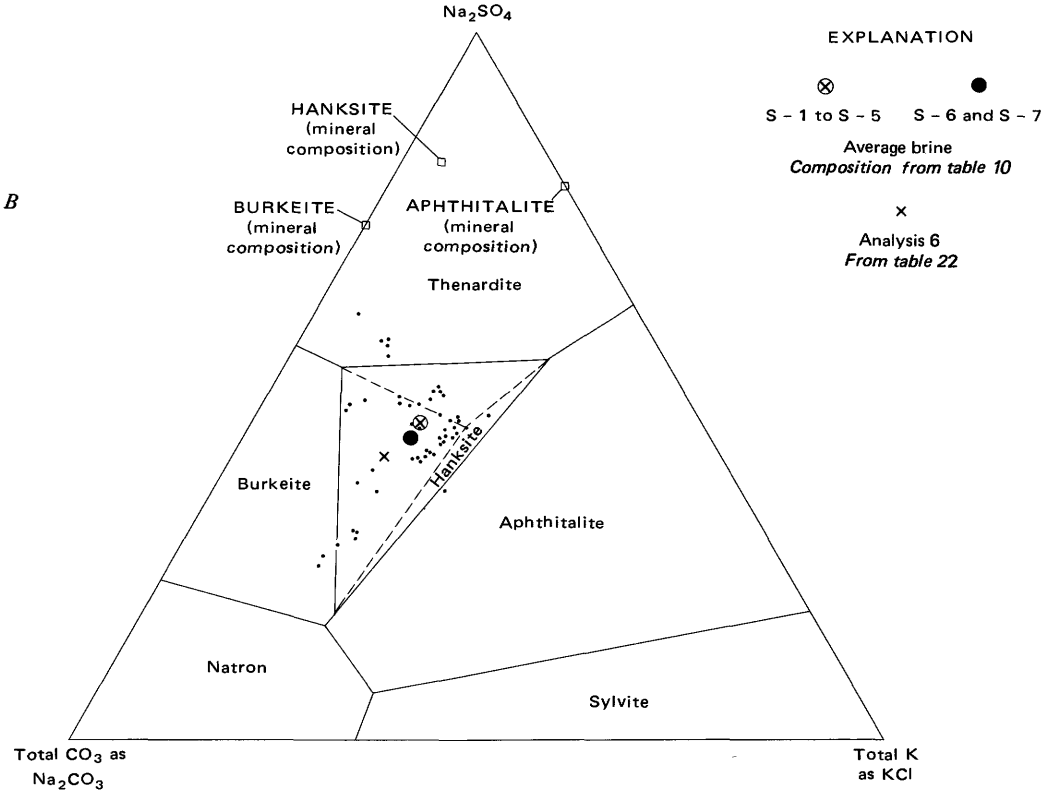
$Na_2SO_4$
EXPLANATION
S - 1 to S - 5
S - 6 and S - 7
Average brine
*Composition from table 10*
Analysis 6
*From table 22*
HANKSITE
(mineral composition)
BURKEITE
(mineral composition)
APHTHITALITE
(mineral composition)
Thenardite
Hanksite
Burkeite
Aphthitalite
Natron
Sylvite
Total $CO_3$ as $Na_2CO_3$
Total K as KCl

ESTIMATED BULK COMPOSITION OF THE UNIT

The estimates of mineral composition of the salt layers (table 4), the measure of the probable error in those visual estimates (table 8), and analyses of the brines (table 9) provide a basis for calculating the relative percentage and total quantity of the major water-soluble components in the Lower Salt. Because the top of S–5 represents a depositional break, the percentage and total quantities are calculated for the layers above and below this level. Table 10 tabulates the steps followed in the calculation. Combining these data and weighting them according to the volumes they represent yields these totals for the Lower Salt:

| | *Total quantity (grams × $10^{12}$)* | *Relative amounts (percent, water-free)* |
|---|---|---|
| Na | 234 | 35.1 |
| K | 9 | 1.4 |
| Mg | 3 | 0.4 |
| $CO_3$ | 99 | 14.9 |
| $HCO_3$ | 83 | 12.4 |
| $SO_4$ | 56 | 8.4 |
| Cl | 171 | 25.7 |
| $B_4O_7$ | 11 | 1.7 |
| $H_2O$ | 312 | — |

In a much more extensive study of the boron in Searles Lake, D. V. Haines, (unpub., 1956) estimated the total amount of $B_4O_7$ in the Lower Salt to be 17.1 × $10^{12}$ g. That amount, based on chemical analyses of brines from 155 wells and cores from 86 core holes, includes the $B_4O_7$ that was in borax in the interbedded mud layers of the Lower Salt and is predictably larger. Calculations based on tables 3, 4, and 5 show that about 63 percent of the solid borax observed in the Lower Salt is in salt layers and 37 percent in mud layers. As about 8.6 × $10^{12}$ of the 11 × $10^{12}$ g of $B_4O_7$ listed in table 10 comes from solid crystals in the salt layers, the amount of additional $B_4O_7$ in borax crystals embedded in M–2 to M–7 is estimated to be near 5.0 × $10^{12}$ g. The resulting total of 16 × $10^{12}$ g $B_4O_7$ in the salt and mud layers in the Lower Salt can be compared with Haines' 17.1 × $10^{12}$ g to give a measure of the probable accuracy of the amounts given here.

◀ FIGURE 21—Composition of brines given in table 9 plotted on diagrams that indicate phase relations in two 5-component systems. *A*, Shows phase boundaries in, and projected from, $Na_2CO_3$–$Na_2SO_4$–NaCl–$NaHCO_3$–$H_2O$ system. *B*, Those boundaries in, and projected from, $Na_2CO_3$–$Na_2SO_4$–KCl–NaCl–$H_2O$ system. Brines are plotted on the basis of their compositions as projected to plane of diagram; some points represent more than one analysis. See figures 35 and 39 and associated text for explanation of phase boundaries and method of plotting.

PARTING MUD

The Parting Mud, of late Wisconsin age, is a layer generally 12–14 ft (3.7–4.3m) thick that rests on the top of the Lower Salt. It is composed chiefly of mud that contains megascopic crystals of gaylussite, pirssonite, and a little borax. Gaylussite is found in almost every core hole, commonly forming 5–15 percent of the unit. Pirssonite is less abundant, commonly 2–5 percent of the unit. In about half the core holes, a layer of megascopic crystals of borax is present near the top or bottom of the unit. The mud matrix consists of a dark-green to black mixture of microscopic crystals of halite, dolomite, clastic silicates, authigenic silicates, organic debris, and entrapped brine. In the upper one- to two-thirds of the unit, thin laminae of white aragonite are numerous.

The Parting Mud has for many years been recognized as a stratigraphic unit by members of the chemical companies operating on the deposit. This unit separates the Lower Salt and the Upper Salt, which differ chemically, and the Parting Mud helps maintain those differences so that they can be utilized in the commercial operations.

AREAL EXTENT AND VOLUME

The outer limits of the Parting Mud are well beyond the limits of the area sampled by cores; mapping in progress shows that its lateral equivalents once extended over an area of about 1,000 $km^2$. Scattered remnants of it crop out around the edges of the basin, and it forms a persistent and unbroken layer in subsurface sections.

The Parting Mud is easily identified in almost all cores from Searles Lake. Its top is most commonly 15–25 m below the present lake surface, its thickness generally 3–4 m. Variations in the depth to the base and top of the unit are shown by contour maps (figs. 22 and 26); variations in its thickness are shown by an isopach map (fig. 23). The isopach contours show that the unit has a large area of relatively uniform thickness in the center and a zone of rapid thickening around the edges. Toward the southwest, a zone of thickening is shown, despite the lack of core evidence, because the outcropping equivalent of the Parting Mud is abnormally thick southwest of the lake.

TABLE 10.—*Estimated percentages and total quantities of water soluble components in the upper two and lower five units of the Lower Salt*

| | Units S–1 + S–2 + S–3 + S–4 + S–5 | | | | | | | | | Units S–6 + S–7 | | | | | | | | |
|---|---|---|---|---|---|---|---|---|---|---|---|---|---|---|---|---|---|---|
| | Na | K | Mg | $CO_3$ | $HCO_3$ | $SO_4$ | Cl | $B_4O_7$ | $H_2O$ | Na | K | Mg | $CO_3$ | $HCO_3$ | $SO_4$ | Cl | $B_4O_7$ | $H_2O$ |
| Chemical composition of solids inferred from visual estimate[1] | 33.7 | trace | trace | 17.1 | 15.7 | 5.0 | 18.8 | 0.2 | 9.5 | 32.2 | 0 | 0 | 20.7 | 21.0 | 0.7 | 12.3 | 0.3 | 12.8 |
| Average error of visual estimates[2] | −0.8 | +0.6 | +0.5 | −3.4 | [3]−3.4 | +2.6 | +4.8 | +0.8 | −[4]1.6 | −0.8 | +0.6 | +0.5 | −3.4 | [3]−3.4 | +2.6 | +4.8 | +0.8 | [4]1.6 |
| Chemical composition of solids, weight percent adjusted for probable error | 32.9 | 0.6 | 0.5 | 13.7 | 12.3 | 7.6 | 23.6 | 1.0 | 7.9 | 31.4 | 0.6 | 0.5 | 17.3 | 17.6 | 3.3 | 17.1 | 1.1 | 11.2 |
| Chemical composition of brine[5] | 11.5 | 1.7 | 0 | 3.3 | [6]0 | 4.6 | 11.3 | 1.3 | 66.3 | 11.3 | 1.7 | 0 | 3.1 | [6]0 | 4.8 | 11.3 | 1.1 | 66.7 |
| Chemical composition of combined solids and brines[7] | 24.3 | 1.0 | 0.3 | 9.5 | 7.4 | 6.4 | 18.7 | 1.1 | 31.3 | 23.4 | 1.0 | 0.3 | 11.6 | 10.6 | 3.9 | 14.8 | 1.1 | 33.4 |
| Total quantity of component in included salt layers, grams × $10^{12}$[8] | 161 | 6 | 2 | 6 | 49 | 43 | 124 | 7 | 207 | 73 | 3 | 1 | 36 | 34 | 13 | 47 | 4 | 105 |

[1]Data in table 4, converted to weight percent.
[2]Based on comparison of visual estimates and chemical analyses of cores (converted to ions), data from table 8, average of all samples; table 8 also lists error in Ca of +0.4, reducing totals in this and underlying columns to 99.6.
[3]Error in $CO_2$ listed in table 8 divided equally between $CO_3$ amd $HCO_3$.
[4]Reduced by amount of H in $HCO_3$.
[5]Arithmetic average of brine analyses given in table 9; averages exclude nalyses from core hole L–31.
[6]Percentage of $HCO_3$ is low, assumed to be 0.
[7]In weight percent, assumed porosity, 40 percent.
[8]Assumed specific gravity of salt plus brine-filled pores, 1.80; volumes from table 3.

The volume of the unit, calculated within the arbitrary boundary by the methods described previously, is about $480 \times 10^6$ $m^3$, about 10 percent more than the combined volumes of the mud layers M–2 to M–7 in the Lower Salt.

## MINERAL COMPOSITION AND LITHOLOGY

The chief megascopic components of the Parting Mud are mud, gaylussite, pirssonite, and borax, in decreasing order of abundance. Thin beds and isolated crystals of trona, halite, and northupite are found locally. Prominent laminar beds of microscopic argonite crystals characterize the upper one- to two-thirds of the layer. The weighted average composition of the megascopic minerals, based on the visual estimates of mineral percentages and calculated by the method described in the section on the Lower Salt, is given in table 11.

The data in table 11 indicate a tendency for the percentage of megascopic gaylussite to increase laterally toward the thinner (more central) areas and the percentages of pirssonite to remain nearly constant. Borax has its highest percentages in the edge and central facies, its lowest percentages in the intermediate zone. Trona and northupite, which occur as thin beds and isolated pods of crystals, are mostly in the intermediate zones. Megascopic crystals of halite occur sporadically in the central zones. In general, though, areal variations in the megascopic mineralogy of this unit are not great because the area sampled by cores represents only the most central facies of the entire unit which originally covered much of the floor of Searles Valley.

Although there is local variation within and between cores, megascopic gaylussite and pirssonite commonly form a higher percentage in the top and bottom meter of the Parting Mud, lower percentages in the middle. In more than half of the pirssonite-bearing cores, this mineral is concentrated near the upper or lower contact, possibly indicating the penetration of more saline waters from the enclosing saline layers which would tend to alter gaylussite to pirssonite (Eugster and Smith, 1965, p. 478–483). Borax is concentrated in the top few centimeters of the unit, but some occurs 20–60 cm up from the base. Aragonite, mostly in the form of white laminar beds composed of microscopic crystals, is common in the upper 55–60 percent of the section except for the uppermost 30–50 cm of the unit.

Variations in the color, abundance of gaylussite and pirssonite, the spacing and color (mineralogy) of laminae, and the chemical composition of the organic components were used by Mankiewicz (1975, p. 7–8) to subdivide the Parting Mud into five parts. In his core B, which came from the northwest part of the lake, the Parting Mud had a thickness of 5.4 m, and changes in lithology were noted at levels 0.30, 0.75, 1.65, and 2.70 m below the top of the unit. The top unit (0.30 m thick) is characterized by laminae and abundant large gaylussite and pirssonite crystals; the next (0.45 m) contains fewer crystals but is finely laminated; the third (0.90 m) is finely laminated but contains more widely spaced yellowish-white (dolomite?) laminae and also contains two rhyolitic tuff beds; the fourth (1.05 m) contains more abundant and closely spaced dolomite(?) layers and some gaylussite (or borax?) vugs, and it is lighter colored, and the fifth (2.70 m) which is light gray and faintly laminated, is characterized by an absence of yellowish and white laminae and the presence of numerous reddish-orange

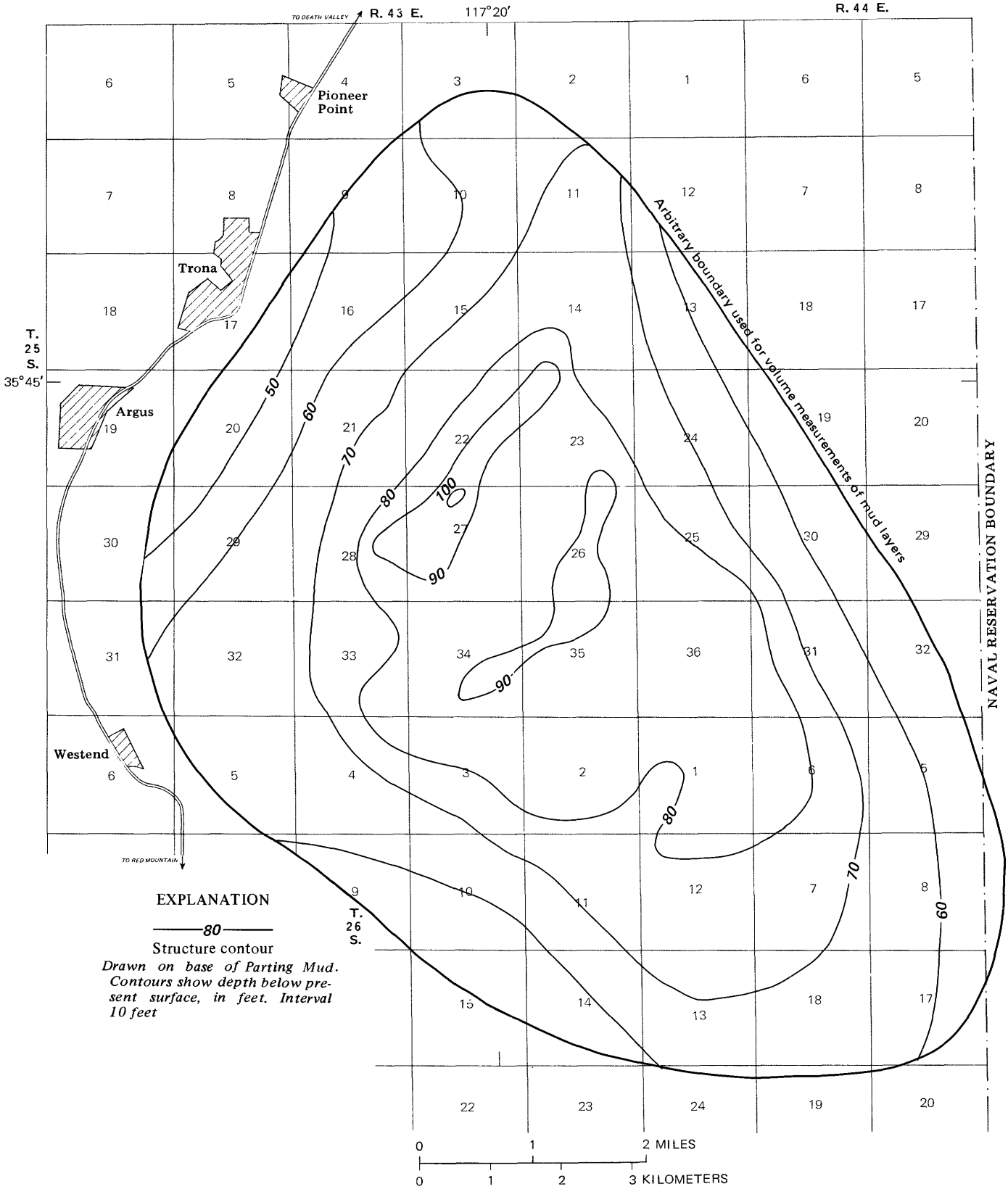


FIGURE 22.—Contour map on base of Parting Mud, Searles Lake.

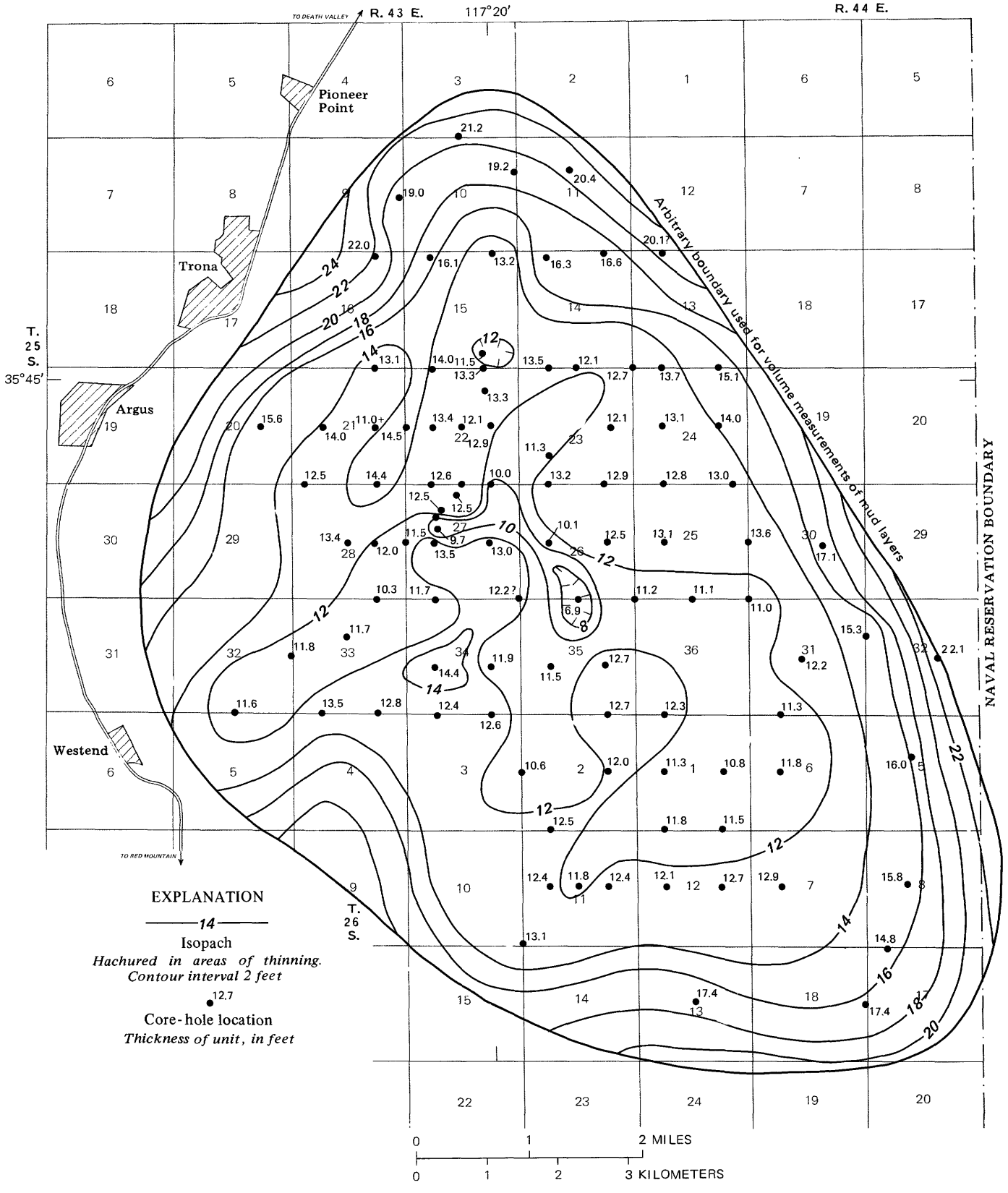


FIGURE 23.—Isopach map of Parting Mud, Searles Lake.

TABLE 11.—*Megascopic mineral composition of the Parting Mud*

[Based on visual estimates of Haines (1959), compositions in volume percent; estimated for intervals without cores shown in parentheses; calculated for contours and within boundary shown in figure 23; t = trace]

| Mineral | Between contours | | | | | | | | | | Weighted total percent |
|---|---|---|---|---|---|---|---|---|---|---|---|
| | 24+ | 24–22 | 22–20 | 20–18 | 18–16 | 16–14 | 14–12 | 12–10 | 10–8 | 8–6 | |
| Mud | (90) | 79 | 91 | 89 | 90 | 88 | 86 | 88 | (76) | 68 | 88 |
| Gaylussite | (6.0) | 14 | 5.6 | 5.9 | 7.5 | 9.0 | 9.5 | 9.8 | (20) | 25 | 8.7 |
| Pirssonite | (3.0) | 3.2 | 3.6 | 3.4 | 2.6 | 3.3 | 3.3 | 1.7 | (3.0) | 4.2 | 3.0 |
| Northupite | -- | -- | -- | -- | -- | -- | t | -- | -- | -- | t |
| Borax | (1.0) | 3.2 | -- | 1.1 | .1 | .1 | .4 | .6 | (1.0) | 3.1 | .5 |
| Halite | -- | -- | -- | -- | -- | -- | .1 | -- | -- | -- | .03 |
| Trona | -- | -- | -- | .3 | .1 | .1 | .3 | -- | -- | -- | .2 |
| Number of cores between contours | 0 | 1 | 2 | 2 | 4 | 6 | 9 | 7 | 0 | 1 | -- |
| Percentage of volume between contours | 1 | 5 | 8 | 11 | 14 | 14 | 32 | 14 | 1 | t | -- |

laminae. These units can be identified in most logs of the Parting Mud cores described by Haines (1959), and a sixth unit, composed of about 0.5 m of faintly laminated green mud, is found above the other five in cores from many parts of the lake.

Hand-specimen and thin-section studies of these muds indicate that most of the megascopic gaylussite and pirssonite crystals grew after burial. Large crystals generally cut directly across bedding planes. Where such crystals cut aragonite laminae, the laminae are not bent (Smith and Haines, 1964, fig. 15; Eugster and Smith, 1965, pl. 1); this shows that most of the mud's compaction occurred prior to crystal growth, and that the growth was by volume-for-volume replacement.

Thin-section studies of the textural characteristics of muds are useful in the laminated segments of the Parting Mud. Sections show that the aragonite laminae are thin bands produced by variations in the purity of calcium carbonate. Where laminae pairs are closely spaced, thickest beds may be either pure or impure. Where laminae pairs are thicker, the dark impure beds are thicker and the light beds of nearly pure calcium carbonate are thinner, rarely exceeding 1 mm. The top and bottom contacts of the laminae are usually sharp, even on a microscopic scale. Laminae defined by slight differences in carbonate percentage are commonly lenticular, and most laminae cannot be traced more than a few millimeters before pinching out. Beds of nearly pure carbonate tend to be continuous at least over the width of the core, and distinctive sequences of them could probably be recognized in cores from an area of several square kilometers.

The thickness of calcium carbonate laminae ranges from several hundredths of a millimeter to about a millimeter. Several series of measurements give average thicknesses for pairs of beds (one light bed and one associated dark bed) ranging from an average of 3.5 mm per pair in zones that represent sections of widely spaced types of laminar beds to an average of 0.75 mm per pair for zones that typify sections of fine laminar bedding. The finest laminae are in beds that average 0.35 mm per pair. If these laminae are interpreted as annual cycles, sedimentation rates represented by these three sets of measurements would be about 3, 13, and 29 yrs/cm, respectively. Sedimentation rates implied for these muds by $^{14}C$ dating average 38 yrs/cm. Presumably the discrepancy results from the lack of distinct episodes of rapid calcium carbonate deposition during some years.

The mineralogy of the fine-grained muds of this unit cannot be determined satisfactorily with a petrographic microscope. Study with immersion oils permits identification of some crystals of carbonates, halite, clay, and silicates, but most of these minerals are coated with submicroscopic crystals of carbonates making consistent identifications impossible.

The abundance of minerals in Parting Mud samples from L–12 and KM–3, as determined by X-ray diffractometer studies, is schematically represented in figure 24. Comparable data for the analyzed core GS–16 are given in table 13. The amounts of gaylussite and pirssonite are variable, but they tend to be more concentrated near the top and base. In core L–12, microscopic gaylussite and pirssonite crystals occur in beds also containing microscopic crystals of the same species. Dolomite is found in major or intermediate amounts at the top of two cores and at the base of all three, but it is also found in detectable amounts in other parts of the core. Aragonite is most abundant in the middle and upper parts; it is mixed with calcite in many samples. Halite, as microscopic and submicroscopic crystals, is a major constituent throughout most of the section in all three cores. The origin of this soluble salt is problematical, but the lower abundances near the top and base of the Parting Mud (at its contacts with salt bodies containing sodium chloride-rich brines) is the opposite of what should be found if the

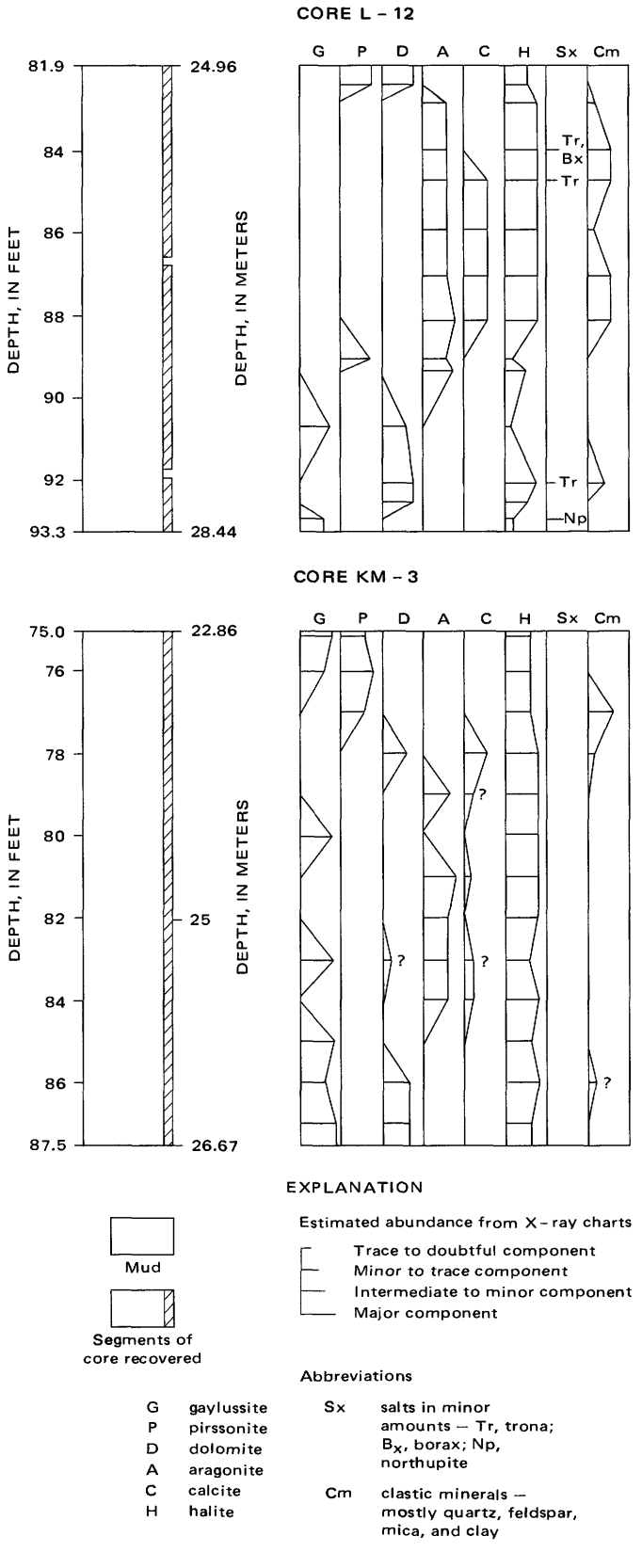


halite formed after burial from brines that migrated into the mud layer. The smaller amounts of trona and borax occurring sporadically in core L–12 may come from the desiccation of entrapped brines. The quantity of northupite at the base of the unit in L–12 is notable and is similar to the quantities noted by Mankiewicz (1975, p. 87) in the top centimeter of the Parting Mud. Clastic silicates form minor to intermediate amounts of the muds in the middle and upper middle parts of the section.

Authigenic silicates are not so abundant in the Parting Mud as in underlying layers. Hay and Moiola (1963, table 1) report traces of analcime from the lower part of the Parting Mud in GS–2, and a thin zone of tuff altered to phillipsite from 1–2 ft (0.3–0.6 m) below the top of the Parting Mud in GS–14 and 17.

The acid-insoluble fraction of these muds is largely composed of clastic fragments plus organic material that is amorphous to X-rays. The mineralogy of this fraction of a sample from the interval between 86.7 and 87.3 ft (26.43 and 26.61 m) in core hole L–12 was studied by R. C. Erd (written commun., 1957). The clay minerals were found to be mostly montmorillonite with a little hydrous mica. About 10–15 percent of the sample was composed of the following, in the approximate order of abundance: biotite (subangular to subrounded grains, dark green), chlorite, feldspar (fresh subangular grains of albite-oligoclase and some fresh subangular microcline), quartz (subangular), hornblende (angular, blue green), glass shards (*n* below 1.51), zircon (traces, subround, prismatic, colorless), sphene (traces, subround), epidote (traces, subround), magnetite (traces).

Four Parting Mud samples from core L–12 were studied by Paul D. Blackmon, of the Geological Survey, for grain-size distribution of the clastic minerals; the results are shown in table 12. Coarse sand and gravel grains are absent. Except for the uppermost sample, medium sand grains are nearly absent. Fine sand and very fine sand consistently form about 15 percent of the total, but most of the clastic material is silt or clay sized.

The quantities of sand seem greater than would be transported by lake waters to this location. Core L–12 is in Parting Mud sediments that were mostly deposit-

◂FIGURE 24.—Mineral abundance in samples from two cores of Parting Mud. Samples from core L–12 represent only silt- and clay-sized components; samples from KM–3 include both megascopic and microscopic components. Determinations for L–12 by R. C. Erd; for KM–3 by R. J. McLaughlin and G. I. Smith.

TABLE 12.—*Size distribution of acid-insoluble material in four samples of the Parting Mud, core L–12*

[Original 350 g samples digested in cold diluted (4:1) HCl; washed in cold water by decanting; dried on a steam bath. Each residue was then treated as follows: the sample was quartered to an appropriate size and stirred vigorously in distilled water for 15 minutes utilizing a milkshake-type stirrer. Sodium metaphosphate was added as a dispersing agent. After stirring, each sample was further dispersed in an ultrasonic separator for approximately ½ hour. Sand-sized particles were then removed by wet seiving, dried, and seived using screen sizes of Wentworth's scale. Percentages of silt and clay were determined by standard pipette analyses. Analyses by P. D. Blackmon. All values are in weight percent]

| Interval sampled (ft below ground surface) | Percent acid insoluble | Size distribution (sizes in mm) | | | | | |
|---|---|---|---|---|---|---|---|
| | | Coarse sand to gravel (>0.5) | Medium sand (0.25–0.5) | Fine sand (0.10–0.25) | Very fine sand (0.0625–0.10) | Silt (0.002–0.0625) | Clay (<0.002) |
| 82.2–82.6 | 20.7 | 0.0 | 4.2 | 10.5 | 8.2 | 50.2 | 27.0 |
| 86.7–87.3 | 28.9 | .0 | .5 | 4.8 | 11.2 | 61.4 | 22.0 |
| 89.4–89.9 | 23.9 | .0 | .8 | 4.7 | 10.3 | 55.0 | 29.2 |
| 91.1–91.7 | 22.9 | .0 | .0 | 2.9 | 5.4 | 66.5 | 25.1 |

ed in 100 m or more of water, 5 km from the nearest shore, and several times that distance from the inlet for most of the water that flowed into the basin during high stands of the lake. It seems unlikely that fine and very fine sand grains could have been transported by current to that area. Transport by wind seems likelier, and the common occurrence of frosted sand grains (Hay and Moiola, 1963, p. 320, 322) supports this premise. If all the fine and very fine sand is windblown, that depositional process accounts for 3.8 percent of the Parting Mud volume in L–12. The Parting Mud in this core is about 3.44 m thick and accumulated during a period of about 13,500 years; this indicates an average depositional rate for sand that was airborne for a distance of several kilometers—to the middle of the basin—of about 1 cm per 1,000 years. As finer material was undoubtedly also introduced during wind storms, aeolian deposition was actually more rapid. If all the acid-insoluble material was transported by wind, aeolian deposits accumulated at the rate of about 6 cm per 1,000 years.

The types of clay included in the clastic fraction of the Parting Mud were studied by Droste (1961, fig. 5) and reported to be predominantly illite, with much smaller percentages of montmorillonite; chlorite or kaolinite were detected only in samples from the edge facies where chlorite was introduced from the adjacent mountain ranges (especially by the Slate Range on the east, where large areas of chlorite-bearing rocks and fault gouge are exposed). R. C. Erd (written commun., 1957) and Hay and Moiola (1963, table 1), however, report montmorillonite as the dominant clay mineral and illite as subordinate.

Organic material in samples from the lower middle part of the Parting Mud in GS–12 was studied by Vallentyne (1957), who reported several types of carotenes and xanthophylls. Samples for depths of 1.46–1.65 m below the top of the Parting Mud in the same core were studied by R. C. Erd (written commun., 1957). In the acid insoluble residue, he noted abundant fragments of chitinous material, apparently derived from the brine shrimp *Artemia*, closely associated with the montmorillonitic (and possibly the aragonitic) mud was an orange-yellow compound that was clearly organic and thought probably a carotenoid. Green stains on some mineral grains suggested algae as a source.

Mankiewicz (1957), in a more recent study, extracted and identified by chromatographic techniques a large number of hydrocarbons, terpenes, and sterols in four cores of the Parting Mud. Green algae, blue-green algae, and vascular plants were the dominant sources of organic components. Their abundances varied in response to changes in stream inflow, lake salinity, and the degree of anaerobic conditions that affect preservation. Zones containing concentrations of vascular plant debris, as indicated primarily by increases in the amounts of straight chain saturated hydrocarbons (n-alkanes) that have odd-carbon numbers in the $C_{23}$–$C_{36}$ range, are interpreted to represent periods of strong inflow which introduced plant remains from other basins. Zones containing high percentages of algal remains, as indicated by concentrations of hydrocarbons that have odd-carbon numbers in the $C_{15}$–$C_{19}$ range, are interpreted as resulting from times of reduced inflow and high algal production within the lake. The extent of diagenetic reaction of original organic compounds to related compounds is used as a measure of the development of anaerobic conditions on the lake floor.

The Parting Mud contains enough brine in its interstices to give the material a moderate plasticity. The percentage of brine in this mud was estimated by recording the weight of water lost when samples were heated to about 60°C[12] for several hours. Amounts of water range from about 10–42 weight percent (fig. 25).

[12] Gaylussite (and presumably pirssonite) is dehydrated to $Na_2Ca(CO_3)_2$ at temperatures approaching 100°C. At 60°C, no dehydration was noted in test samples.

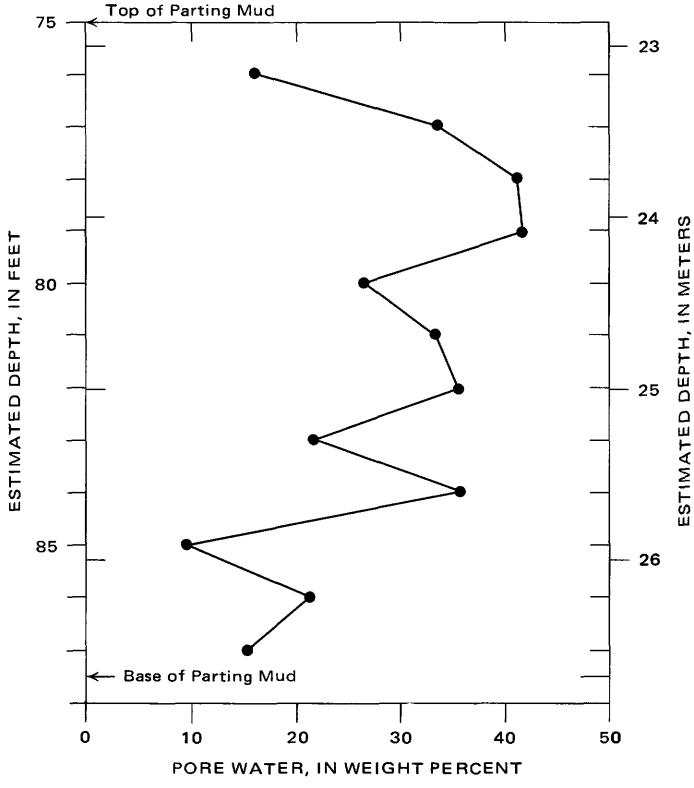


FIGURE 25.—Weight percent of pore water in samples of Parting Mud. Samples from core KM–3; values obtained by measuring weight loss from fresh moist sample during 17 hours of heating at 60°–65°C.

All this evaporated water, though, was in the form of brine that probably had a density of about 1.25 considering the amounts of halite that exist in the sample. For this reason, 10 weight percent water would indicate 12.5 weight percent of entrapped brine, and 42 percent water 52.5 percent brine. The highest percentages are about 1 meter below the top of the unit; distinctly lower percentages are at the top and in the basal zones. The greatest changes occur between units of massive and laminated lithologies; the top three and lower three samples were massive, and the middle six samples were distinctly laminated. These lithologic changes coincide with changes in the amounts of aragonite and calcite in the solids and clearly reflect shifts in the character of deposition. It is likely that the higher percentages of pore water in the middle six samples are products of these changes.

## CHEMICAL COMPOSITION

Nine samples from core GS–16 were partially analyzed to determine their major element composition. Table 13 gives those analyses and lists X-ray diffraction data for the minerals in the same samples. The analyses list the evaporite constituents as "water- and acid-soluble components", and the clastic constituents as "acid-insoluble components."

In making the major element analyses, difficulties were discovered that introduced small errors into the results, and insufficient amounts of the samples remained to complete the analyses or repeat the determinations. For example, one portion of all the samples was heated to 500°C before treatment with acid in an attempt to quantify the percentage of dolomite in the sample. Under correct conditions, dolomite decomposes at this temperature to $CaCO_3$, MgO, and $CO_2$, but the results showed that this reaction was incomplete, possibly because of interference from other components in the mixture. When heated, however, some of the clastic silicate minerals apparently fused with the $Na_2CO_3$ or $Na_2B_4O_7$ in these samples and their components subsequently dissolved in acid. This appears to be the reason that about 65 percent of the total $Al_2O_3$ and 90 percent of the total $Fe_2O_3$ were found in the acid-soluble fraction. Inasmuch as $SiO_2$ was not determined on this fraction and $Al_2O_3$ was determined by difference, all $SiO_2$ in this fraction was reported as $Al_2O_3$ making the total alumina in the acid-insoluble fraction too high. The acid-soluble CaO, MgO, $Na_2O$, and $K_2O$ percentages were determined from this heated fraction. Although the reported amounts of these components seem consistent with the observed evaporite suites, they may be slightly high if they include contributions from the clastic minerals. For the same reason, reported amounts of $SiO_2$ and other elements in the clastic fraction may be low because they represent the concentrations that remained in the acid-insoluble residue after the treatment described above. Total $H_2O$ could not be determined accurately. The samples were first analyzed by heating to about 800°C and the weight loss determined, but the loss was found to include some $CO_2$, organic H, and possibly organic C, as well as $H_2O$ and OH; subsequent analyses on the three samples for $H_2O+$ and $H_2O-$ are given in a footnote to table 13.

The analyses of table 13 show the approximate major-element content of each fraction. On the average, about 20 percent of each sample consists of clastic material, nearly 80 percent is evaporite, and about 1–2 percent is organic. Combining this information with the X-ray diffraction data verifies that the water- and acid-soluble evaporites are clearly dominated by gaylussite, pirssonite, dolomite, calcite, aragonite, and halite.

The acid-insoluble clastic minerals are composed mostly of $SiO_2$, although the X-ray identifications show chlorite, feldspar, mica, and clay to be more abundant than quartz in most samples. The combined percentages of acid-insoluble components (exclusive of organic C) show that the greatest amounts of clastic

TABLE 13.—*Partial chemical analyses of samples from core GS–16 in Parting Mud*

[Major-element analyses by M. J. Cremer, L. B. Schlocker, H. N. Elsheimer, and F. O. Simon; minor-element analyses by Harry Bastron. Analytical techniques: (1) Except for $CO_2$ analysis, water- and acid-soluble components were separated from insoluble components by igniting sample at 500°C for 48 hours, immersing sample in dilute (2N) HCl (ca. 80°C) until $CO_2$ evolution ceased, then filtering. (2) The filtrate included some components that presumably would have remained in the acid-insoluble fraction if the sample had not been heated sufficiently to cause limited $Na_2CO_3$ fusion. Of these, the $R_2O_3$ group was precipitated as hydroxide and total Fe determined as $Fe_2O_3$ by potentiometric titration methods, $TiO_2$ and MnO determined by colorimetric methods, and $Al_2O_3$ by difference. The $AL_2O_3$ and $Fe_2O_3$ percentages were added to the percentages of these components determined on the insoluble fraction. (3) CaO and MgO were determined in this filtrate by gravimetric methods, and $Na_2O$ and $K_2O$ by flame photometer methods. (4) $SO_3$ and $B_2O_3$ were determined on separate samples; they were immersed in boiling water for about 1 hour, $SO_3$ determined on the filtrate by X-ray fluorescence and $B_2O_3$ by volumetric methods. (5) Cl was determined on separate samples by two methods: five samples were immersed in water at 80°C for several hours, filtered, and Cl determined gravimetrically in the filtrate; four samples (values followed by a "?" because considered less reliable) were fused in $LiBO_2$ and total Cl determined by a colorimetric method. (6) Total carbonate determined on dried but unheated sample by adding $H_3PO_4$ and trapping the evolved $CO_2$ in a train. (7) The acid insoluble portion represented by the heated residue after filtering, washing, and drying was fused with $LiBO_2$, dissolved in $HNO_3$, and from this solution, the $Al_2O_3$; total Fe and $Fe_2O_3$, CaO, and MgO determined by atomic absorption methods, the $Na_2O$ and $K_2O$ by flame photometric methods, and the $SiO_2$ by difference. (8) Organic carbon determined by igniting dry sample at 1,000°C, determining evolved $CO_2$ in a train, and subtracting the $CO_2$ present as carbonate from this quantity. (9) Minor elements determined by emission spectrographic techniques on the acid insoluble portion; the results are semiquantitative and are assigned to geometric brackets reported as their midpoints (such as 1, 0.7, 0.5, 0.3, etc.) with their one standard deviation precision estimated at plus or minus one bracket; n.d., not detected. (10) X-ray diffraction analyses of total untreated samples by R. J. McLaughlin and G. I. Smith]

**Major elements (percent of total sample)**

| Sample No. | Depth in core (ft)[1] | Water- and acid-soluble components | | | | | | | | Acid-insoluble components | | | | | | | |
|---|---|---|---|---|---|---|---|---|---|---|---|---|---|---|---|---|---|
| | | CaO | MgO | $Na_2O$ | $K_2O$ | Total Carbonate as $CO_2$ | $SO_3$ | $B_2O_3$ | Cl | $SiO_2$[2] | $Al_2O_3$ | Total Fe as $Fe_2O_3$ | CaO | MgO | $Na_2O$ | $K_2O$ | Organic carbon, as C |
| PM 1[3] | 70.6–71.5 | 13.3 | 8.6 | 14.4 | 2.9 | 20.1 | 1.9 | 0.8 | 9.9 | 13.2 | 2.8 | 1.4 | 0.1 | 0.04 | 0.2 | 0.2 | 1.7 |
| PM 2 | 71.5–72.5 | 14.7 | 5.0 | 19.0 | 2.9 | 18.9 | 2.2 | 0.9 | 11.9 | 12.5 | 2.3 | 1.1 | 0.1 | 0.04 | 0.02 | 0.02 | 1.6 |
| PM 3 | 72.5–73.3 | 12.2 | 5.3 | 19.8 | 3.0 | 13.2 | (4) | 1.1 | 18.8 | 15.4 | 3.1 | 1.4 | .2 | .5 | .3 | .3 | 1.6 |
| PM 4 | 73.3–74.2 | 6.2 | 4.7 | 20.7 | 4.1 | 8.0 | (4) | 1.5 | 15.9? | 19.8 | 4.5 | 1.8 | .3 | .1 | .5 | .5 | 1.8 |
| PM 5 | 74.2–75.1 | 10.7 | 3.9 | 17.6 | 4.3 | 10.8 | (4) | .6 | 19.6? | 19.9 | 4.3 | 2.0 | .3 | .09 | .7 | .5 | 1.6 |
| PM 6 | 75.1–77.0 | 19.6 | 4.3 | 14.6 | 3.0 | 17.6 | 1.3 | .9 | 12.0? | 15.1 | 2.2 | 1.3 | .2 | .06 | .3 | .4 | (4) |
| PM 8[3] | 78.0–79.0 | 17.1 | 4.8 | 13.6 | 3.4 | 16.4 | 1.2 | .6 | 11.5 | 17.3 | 3.6 | 1.6 | .2 | .05 | .3 | .2 | 2.2 |
| PM 9[3] | 79.0–80.0 | 12.9 | 5.3 | 15.8 | 2.9 | 18.4 | 1.5 | .8 | 7.3 | 15.2 | 3.8 | 1.6 | .03 | .01 | .02 | .02 | 1.3 |
| PM 10 | 80.0–81.1 | 11.2 | 6.8 | 17.2 | 2.9 | 18.2 | 1.5 | .8 | 12.0? | 14.0 | 3.1 | 1.5 | .1 | .04 | .3 | .4 | 0.7 |

**Minor elements (parts per million of acid-insoluble portion)**

| Sample No. | B | Ba | Cr | Cu | Ga | Mn | Mo | Nb | Sc | Sr | Ti | Yb | V | Y | Zr |
|---|---|---|---|---|---|---|---|---|---|---|---|---|---|---|---|
| PM 1 | 300 | 500 | 15 | 1.5 | 5 | 50 | 3 | 7 | 3 | 200 | 2000 | 0.7 | 15 | 7 | 150 |
| PM 2 | 300 | 500 | 20 | 2 | 5 | 150 | 7 | 7 | 3 | 200 | 2000 | .7 | 15 | 7 | 200 |
| PM 3 | 300 | 500 | 15 | 2 | 7 | 70 | 5 | 7 | 3 | 200 | 2000 | .7 | 20 | 7 | 150 |
| PM 4 | 500 | 500 | 15 | 1.5 | 7 | 70 | 5 | 7 | 5 | 200 | 3000 | 1 | 50 | 10 | 150 |
| PM 5 | 500 | 500 | 15 | 1.5 | 7 | 70 | 5 | 7 | 5 | 200 | 3000 | 1 | 50 | 10 | 150 |
| PM 6 | 300 | 500 | 15 | 1.5 | 7 | 70 | 5 | n.d. | 5 | 200 | 2000 | 0.7 | 30 | 7 | 150 |
| PM 8 | 100 | 300 | 15 | 0.7 | 5 | 70 | n.d. | 5 | 3 | 200 | 2000 | n.d. | 15 | n.d. | 70 |
| PM 9 | 100 | 50 | 3 | n.d. | n.d. | 30 | n.d. | 5 | n.d. | 10 | 700 | n.d. | 7 | n.d. | 100 |
| PM 10 | 500 | 500 | 15 | 0.7 | 5 | 70 | n.d. | 5 | 3 | 200 | 2000 | 0.7 | 20 | 7 | 100 |

**Minerals identified by X-ray in untreated sample (in approximate order of decreasing abundance)**

PM 1 ———— Dolomite, halite mica, chlorite, clay, calcite(?).
PM 2 ———— Pirssonite, dolomite, halite, mica, clay, chlorite, aragonite, feldspar, calcite.
PM 3 ———— Halite, aragonite, mica, chlorite, clay, dolomite, feldspar, quartz, cacite.
PM 4 ———— Dolomite halite, mica, clay, chlorite, feldspar, quartz, calcite.
PM 5 ———— Halite, aragonite, calcite, mica, chlorite, clay, feldspar, dolomite, quartz(?).
PM 6 ———— Aragonite, dolomite, mica, chlorite, clay, halite, feldspar, quartz, calcite.
PM 8 ———— Aragonite, halite, dolomite, calcite, mica, chlorite, clay, feldspar, quartz.
PM 9 ———— Gaylussite, dolomite, mica, clay, chlorite, halite, calcite, feldspar(?).
PM 10 ———— Dolomite, gaylussite, mica, clay, chlorite, halite, amphibole(?).

[1]Parting Mud in GS-16 lies between 70.6 and 82.2 ft (21.52 and 25.05 m).
[2]Percentage possibly low because of loss during original heating and acid treatment.
[3]Analyses for $H_2O^-$ (weight lost on heating at 100°C) as follows: PM 1 = 6.7, PM 8 = 3.1, PM 9 = 11.1. Analyses for $H_2O^+$ (weight percent of H lost during heating from 100° to 800°C, expressed as $H_2O$) as follows: PM 1 = 1.7, PM 8 = 2.8, PM 9 = 2; percentages may be high because H may have been derived from both $H_2O$ and organic compounds.
[4]Not analyzed because of insufficient sample.

minerals are in a zone just above the middle of the Parting Mud. A high concentration of clastics in these horizons is consistent with the data on sediment sizes in table 12. Slightly increased concentrations of Ga, Sc, Ti, Yb, V, and Y in this zone may also reflect this distribution. Unpublished field observations of the lake sediments exposed in the surrounding valley show that there was a lake recession during this part of its history that would have allowed more and coarser clastic material to be transported into the basin center.

Analyses for U in 29 samples of the Parting Mud by Mankiewicz (1975, table 2–1) shows an average value of 12 ppm with a range from 1 to 42 ppm. The higher values occur near and below the middle of the Parting Mud, a zone he interprets on the basis of the organic content to have been deposited during a period of maximum lake size and inflow.

The analyses of MgO give values that average 5.4 percent but are as high as 8.6 percent; if all the MgO

was contained in dolomite, the dolomite percentage would average 25 percent and be as high as 40 percent. The analyses for carbonate, expressed as $CO_2$, average 15.7 percent. If all the $CO_2$ was in dolomite, the average dolomite percentage would be 33; if it was in calcite or aragonite, their combined average percentage would be 35; if in pirssonite, its average percentage 43; and if in gaylussite, 53. The actual percentages of each are much less because most samples contain two or more of these minerals, but these values provide upper limits. The average $SO_3$ content is 1.6 percent, the $B_2O_3$ content 0.9 percent. These values imply a thenardite content in the analyzed samples of 2.8 percent and a borax content of 2.5 percent. Using the average brine values in table 17, combined with an estimated interstitial brine content in the Parting Mud (fig. 25) of about 25 percent, it appears that desiccation of the entrapped brine could account for all but 1.1 percent of the thenardite and 1.9 percent of the borax. Although borax is commonly observed, thenardite and other sulfate minerals have not been observed in the Parting Mud; some or all of the reported $SO_3$ may have been produced during analysis by oxidation of pyrite, a mineral that has been observed in trace amounts in the Bottom Mud. The Cl content averages 13.1 percent and is as high as 19.6 percent; the implied average halite content is 22 percent with a maximum of 32 percent. As the Cl content of the average brine in the Upper Salt (table 17) is 12.2 percent, the Cl content in the Parting Mud clearly reflects the presence of crystalline halite in the mud.

The CaO content is of special significance in reconstructing the nature of the depositing lake. If the average value of 13.1 percent CaO is not inflated greatly by contribution from the clastic material, it virtually requires the lake to have been stratified with a fresh layer at the surface that introduced additional calcium each year; details of this reasoning are given in the section on the processes of sedimentation of the mud layers.

The average organic C content of 1.6 percent indicates an average content of organic compounds that probably exceeds 2 percent. The Parting Mud in core GS–16 is 12.2 ft (273 cm) thick and has an approximate density of 2.2. If the average organic content is 2 percent, each square centimeter of the Parting Mud represents a column of sediment that contains 16.4 g of organic matter. As the unit was deposited in about 13,500 years, the minimum rate of organic production and accumulation was about $1.3 \times 10^{-3}$ g/cm$^2$/yr. Actual rates were higher because some of the organic material has decomposed and been lost as $CO_2$ and $CH_4$.

These data show that the Parting Mud is a marl dominated by carbonate minerals but containing appreciable quantities of halite and subordinate amounts of clastic components and other evaporites. The organic percentage is low but contributes disproportionately to the physical properties of the mud.

### UPPER SALT

The Upper Salt is the largest of the commercially worked saline layers in the Searles Lake deposit. It extends over an area of about 110 km$^2$ and has typical thicknesses near its center of about 15 m. This unit was the first to be exploited as a source of commercial brine; from it have come the bulk of the industrial chemicals produced from Searles Lake. The salt body is lens shaped; its upper contact with the Overburden Mud is gradational but generally concave downward, and its lower contact is concave upward as it rests in the symmetrically shaped basin formed by the top of the Parting Mud (fig. 26).

Most of the Upper Salt layer is composed of salines. The most abundant minerals are halite, trona, and hanksite. Minerals occurring in smaller quantities are borax, burkeite, pirssonite, thenardite, aphthitalite, sulfohalite, and mud.

Compared with the Lower Salt, the solids of this layer contain more halite and hanksite, about the same amount of borax, and less trona, burkeite, thenardite, and mud. The brine is higher in K and Cl and lower in total $CO_3$ and $B_4O_7$.

#### AREAL EXTENT AND VOLUME

The areal limits of the Upper Salt, are about the same as those given for the saline layers within the Lower Salt (114 km$^2$).

The variations in thickness of the Upper Salt are shown by the isopach map (fig. 27). In making this map, deciding on the position of the contact between the Upper Salt and the Overburden Mud was found to be a very subjective matter. In general, the contact was placed at the top of the uppermost zone in which the salt beds dominate.

According to the isopach map, the configuration of the Upper Salt is symmetrical; it has a zone of rapid thickening near the edges and a large area of more gradual thickening near the center. This distribution of thickness is similar to that of S–5, the largest saline layer in the Lower Salt, but it appears more regular than the other saline layers within that unit. This regularity is partly due to the large contour interval used for the map of the Upper Salt which minimizes the small variations introduced artificially by differences in the measuring techniques used during coring and logging.

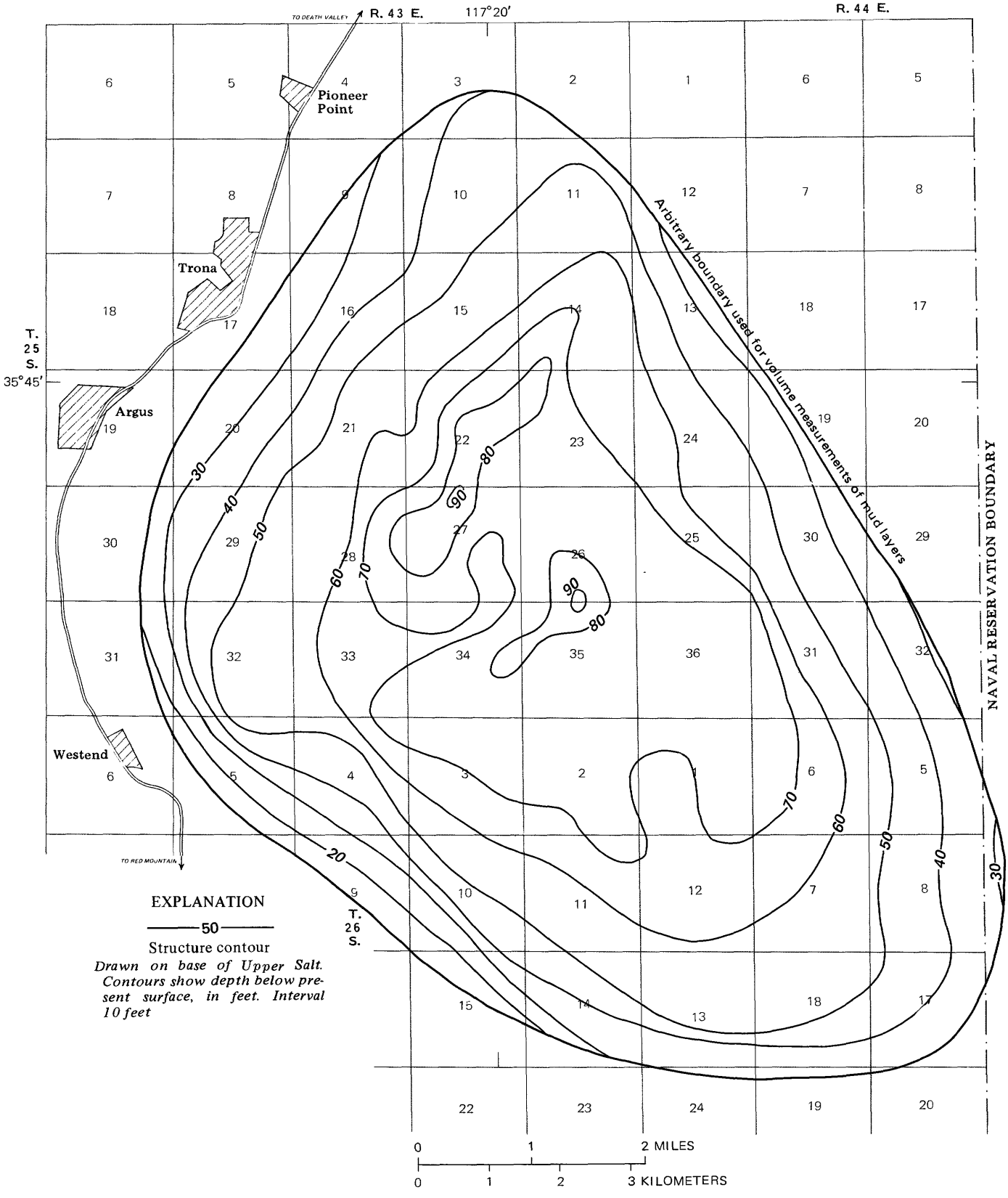


FIGURE 26.—Contour map on base of Upper Salt, Searles Lake.

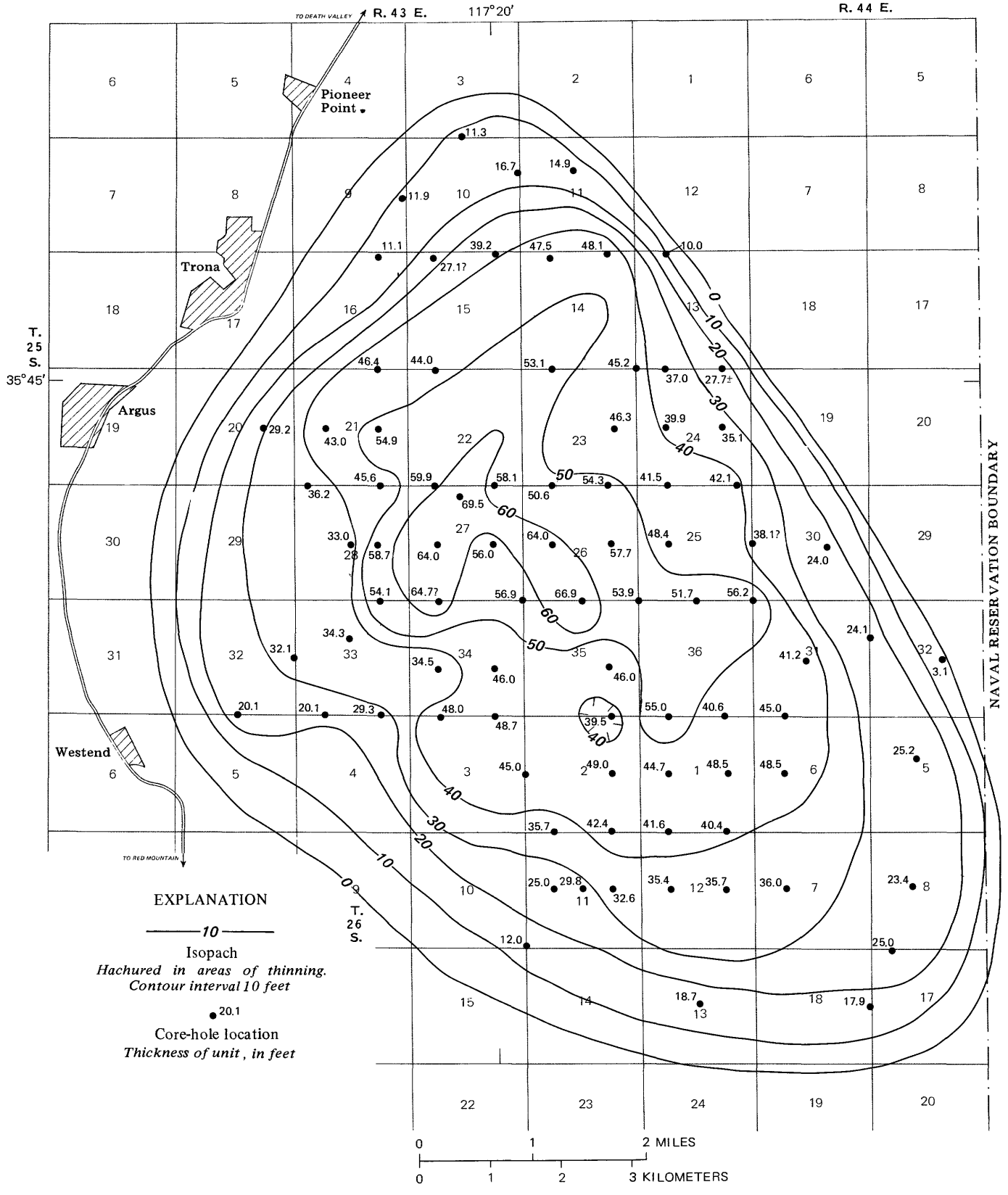


FIGURE 27.—Isopach map of Upper Salt, Searles Lake, Calif.

Using the isopach map of the Upper Salt (fig. 27), the volume is calculated to be about $1,050 \times 10^6$ m$^3$, or about 1 km$^3$, about twice the total volume of the saline layers in the Lower Salt. More than half the total volume of the Upper Salt lies within those parts of the unit that are more than 12 m (40 ft) thick.

## MINERAL COMPOSITION AND LITHOLOGY

Trona and halite are the major mineral components of the Upper Salt, together forming more than three-fourths of the total volume. Hanksite is the third most abundant mineral, borax the forth. Smaller amounts of mud, burkeite, pirssonite, thenardite, aphthitalite, and sulfohalite occur.

Quantitative estimates of the mineral composition of the Upper Salt were made in the same manner as for the saline layers in the Lower Salt. The results of these calculations, given in table 14, illustrate an areal mineral zonation that can be correlated with the unit's thickness. Some of the mineral percentages in individual cores vary markedly. The averaged values indicate the following trends. Trona reaches its maximum percentage in the thinner parts of the layer and diminishes toward the thicker parts.[13] Halite follows the opposite trend. Hanksite, the predominant sulfate mineral in the Upper Salt, is slightly more abundant in the intermediate thickness zones. The highest percentages of borax are normally in the thicker zones. Aphthitalite is concentrated in the thicker parts of the deposits. Thin beds of mud occur sporadically throughout the Upper Salt. Pirssonite is in the mud layers.

Other areal concentrations noted are unrelated to thickness. Hanksite is most abundant in the western, central and eastern parts of the unit, and is deficient to the north and south. Burkeite and thenardite are higher than average along the south and southeast edges of the deposit, apparently because of the source of nearby sulfate in the Slate Range (Smith and others, 1968, p.14). Borax is more common in the western, central, and eastern parts of the Upper Salt body.

The vertical distribution of minerals varies somewhat from one area to the next. A few centimeters of borax occurs at the base of the Upper Salt (or in the top of the Parting Mud) in about half of the GS series of cores, most are from the central part of the deposit. Almost all cores of the Upper Salt have a 1- to 3-m layer of trona at the base. The basal few centimeters of this bed contains major amounts of northupite as a fine-grained interstitial material. This trona layer maintains its thickness toward the edges of the deposit and constitutes the entire Upper Salt in most of the outermost facies. Above the bed of trona, except in the outermost facies, halite is the predominant component. Its percentage increases in an irregular manner toward the top of the Upper Salt. In some parts of the deposit, the halite-rich zone extends to the top of the Upper Salt; in others, in particular in the central facies, it is overlain by a layer 2–5 m thick composed largely of hanksite and borax.

The stratigraphic position of hanksite concentrations in the Upper Salt is variable but is generally related to areal position. In the central part of the deposit, the largest concentrations of hanksite are generally at the top of the Upper Salt, as in GS–15 and GS–16. In the edge facies of the deposit, hanksite is more commonly concentrated just above the basal layer of trona, and may be nearly pure or mixed with halite and trona, a distribution pattern found in GS–10, GS–12, and GS–17. Other cores have distributions of

[13]The one core within the 0–10 contour area, GS–25, is not representative of that facies; it consists of an unusually large amount of borax that is associated with halite, whereas most cores obtained by the chemical companies from that facies mostly contain only trona.

TABLE 14.—*Mineral composition of salines in the Upper Salt by contour interval*

[Based on visual estimates of Haines (1959), compositions in volume percent; calculated for contour shown in figure 27; t = trace]

| Mineral | Between isopach contours | | | | | | | Weighted total percent |
|---|---|---|---|---|---|---|---|---|
| | 0–10 | 10–20 | 20–30 | 30–40 | 40–50 | 50–60 | 60+ | |
| Halite | 61 | 33 | 31 | 46 | 48 | 43 | 46 | 43 |
| Trona | -- | 55 | 43 | 33 | 27 | 33 | 39 | 34 |
| Hanksite | -- | 6.1 | 22 | 19 | 18 | 19 | 10 | 17 |
| Borax | 39 | .8 | 1.0 | .8 | 4.6 | 1.4 | 2.8 | 3.1 |
| Burkeite | -- | .4 | .8 | -- | -- | .8 | -- | .3 |
| Pirssonite | -- | 1.4 | .1 | .1 | .3 | .1 | -- | .2 |
| Thenardite | -- | .8 | .3 | -- | -- | -- | -- | .1 |
| Aphthitalite | -- | -- | -- | t | -- | t | .5 | .03 |
| Sulfohalite | -- | t | t | -- | t | t | .1 | .01 |
| Mud | .3 | 2.7 | 2.0 | 1.0 | 2.2 | 2.6 | 1.3 | 2.0 |
| Number of cores between contours | 1 | 7 | 9 | 4 | 4 | 4 | 1 | -- |
| Percentage of total volume between contours | 2 | 7 | 14 | 20 | 31 | 20 | 6 | -- |

hanksite that are combinations of these two patterns; hanksite may be at both stratigraphic horizons (for example, GS–2, GS–19) or be distributed throughout the section (for example, GS–12, GS–27).

Borax characteristically occurs at two stratigraphic positions in the Upper Salt. The lower and the thinner of the two is at the base of the section, and crystals may extend down into the top few centimeters of the Parting Mud. It is most commonly associated with fine-grained trona and northupite and in some places with a little hanksite. The second characteristic position is a meter or so below the top of the Upper Salt, at the base of the hanksite concentration if any occurs at that level.

The Upper Salt is a porous aggregate of interlocking crystals. Published estimates of the total voids range from 20 to 60 percent, estimates between 40–47 are most common. In this paper, a porosity of 40 percent has been assumed. Visual observations suggest that about half of the total pore space contributes to the useful permeability of the crystal mass.

The permeability varies from one layer to another. The muds or mud-rich zones appear almost impermeable. Burkeite, most commonly in the form of hard massive vuggy material, probably has a very low permeability except where the vugs are numerous. Trona, especially zones composed of fine-grained aggregates, likewise would have a lower permeability (see Haines, 1959, pl. 10); where the coarse-grained bladed or fibrous habit is predominant, the permeability is high. Beds of halite probably have low permeability where they are tightly intergrown but may have a high permeability where the crystals are loosely packed or vuggy (see Smith and Haines, 1964, fig. 8). Hanksite zones have, in many instances, the highest permeability because of the abundant large crystal-faced cavities that characterize the thick beds of this mineral (see Haines, 1959, pl. 9).

Much of the bedding in the Upper Salt is indistinct because the salts have been recrystallized since burial. Some bedding, however, is clearly defined. The best examples of this are in the fine-grained trona beds near the base of the Upper Salt and in scattered zones containing interbedded layers of salines and mud. The bedding in trona is defined either by fluctuations in the percentage of mud impurities or by differences in the transparency of the fine-grained trona (see Haines, 1959, pl.10; and Smith and Haines, 1964, figs. 6 and 7 in which the opaque beds appear white; the more transparent beds appear light gray). Most such layers range in thickness from a millimeter to a few centimeters, but there is wide variation. Calculations based on the solubility of trona and the maximum probable evaporation rate show that layers to a half meter thick could represent annual deposits if no new water was added, but most annual layers would be thinner because there generally was some inflow and rainfall on the lake surface. Beds defined by layers of mud are clearly the result of inflowing muddy water during temporary wet periods. Most of these are found in the upper part of the Upper Salt, and their lack of lateral continuity suggest that they were formed in locally flooded areas rather than in a large lake capable of distributing the sediments evenly throughout the basin.

## CHEMICAL COMPOSITION

### CHEMICAL ANALYSES OF THE SOLIDS

The composition of the solids in the Upper Salt is represented by the analyses of four cores, GS–11, GS–12, GS–16, and GS–21 given in table 15. The sampled profiles include both the Upper Salt and Overburden Mud; the estimated positions of the contacts are indicated by footnotes in table 15. The five samples from GS–16 are representative of the central part of the deposit, the three samples from GS–21 of the edges, and the five from GS–11 and four from GS–12 of facies between the edges and center. The techniques used in sampling and conventions for tabulating the data are the same as the Lower Salt.

The chemical analyses are expressed as weight percent of the hypothetical oxides; X-ray analyses are of the bulk sample. The X-ray data support the areal and stratigraphic trends in mineral composition inferred from the visual estimates (table 14). The most notable tendencies are for the lowest sample to contain large amounts of $CO_2$ in the form of trona; for the middle and upper samples to contain larger amounts of Cl in the form of halite; for the upper samples (that include the Overburden Mud) to contain more acid-insoluble material; and for the base and the middle of the section to contain higher percentages of $B_4O_7$ in the form of borax. The vertical and horizontal distribution of $K_2O$ in the form of hanksite (and aphthitalite?) is erratic.

### CHEMICAL COMPOSITION OF THE BRINES

Most of the production of industrial chemicals from Searles Lake has come from brines from the Upper Salt. Commercial operations using brines from the interstices of the Upper Salt have been in existence on a major scale since the mid-1920's, and some production has come from earlier operations. The brine composition varies from place to place and with depth, partly as a result of its original distribution and partly as a result of the circulation and dilution caused by the pumping.

TABLE 15.—*Chemical analyses of cores from the Upper Salt and Overburden Mud*

[Chemical analyses by L. B. Schlocker, H. C. Whitebread, and W. W. Brannock. Analytical techniques: (1) CaO, MgO, $Na_2O$, $K_2O$, and $B_2O_3$ were determined in solutions prepared by boiling portions of samples in 1+9HCl; (2) Cl was determined in solutions prepared by boiling portions of samples in distilled water; (3) $SO_3$ was determined by X-ray fluorescence of whole samples; (4) acid insoluble was residue obtained by boiling portions of samples in 1+9HCl, dried at 110°C; (5) $H_2O$ was determined by measuring weight of H expelled during combustion. X-ray analyses of total untreated sample by R. J. McLaughlin and G. I. Smith]

| Sample No. | Depth in core (ft) | CaO | MgO | $Na_2O$ | $K_2O$ | $CO_2$ | $SO_3$ | $B_2O_3$ | Cl | $H_2O$ | Acid insoluble | (Oxygen equivalent of Cl) | Sum | Minerals identified by X-ray (in approximate order of decreasing abundance) |
|---|---|---|---|---|---|---|---|---|---|---|---|---|---|---|
| GS–11–A | 0 – [1]17.1 | 1.4 | .49 | 43.8 | 1.1 | 3.2 | 6.8 | .23 | 41.2 | 2.5 | 7.6 | (9.30) | 99.0 | Halite, hanksite, pirssonite? |
| B | 17.1 – 30.7 | 1.5 | .35 | 45.6 | 1.1 | 5.2 | 9.9 | .48 | 38.8 | 2.9 | 2.7 | (8.76) | 99.8 | Halite, hanksite, trona. |
| C | 30.7 – 55.6 | .55 | .16 | 46.3 | 1.2 | 7.8 | 9.6 | 1.2 | 36.1 | 4.4 | .84 | (8.15) | 100.0 | Halite, hanksite, trona, tincalconite?[2] |
| D | 55.6 – 68.6 | .09 | .04 | 49.0 | .47 | 7.6 | 8.3 | .08 | 40.6 | 3.3 | .22 | (9.16) | 100.5 | Halite, trona, hanksite. |
| E | 68.6 – 72.7[3] | .30 | .30 | 42.7 | .65 | 23.5 | 13.6 | 2.2 | 6.9 | 11.6 | .55 | (1.56) | 100.7 | Trona, burkeite, halite, tincalconite[2]. |
| GS–12–A | 26.9 – 33.3[4] | 5.4 | 1.1 | 40.4 | .59 | 9.2 | .71 | .15 | 37.9 | 5.1 | 5.4 | (8.56) | 97.4 | Halite, pirssonite. |
| B | 33.3 – 60.7 | .63 | .16 | 47.8 | .35 | 8.2 | 9.6 | .10 | 38.4 | 3.4 | .51 | (8.67) | 100.5 | Halite, trona. |
| C | 60.7 – 70.8 | .10 | .03 | 45.2 | 2.0 | 9.3 | 23.9 | .10 | 18.8 | 3.6 | .08 | (4.24) | 98.9 | Hanksite, halite, trona. |
| D | 70.8 – 76.3 | .73 | .64 | 37.8 | 1.1 | 24.7 | 5.0 | 7.3 | 7.4 | 16.4 | .35 | (1.67) | 99.8 | Trona, tincalconite[2], halite. |
| GS–16–A | 0 – [5]13.8 | 1.4 | .32 | 43.4 | 1.0 | 3.2 | 9.4 | .12 | 38.3 | 2.0 | 7.6 | (8.65) | 98.1 | Halite, hanksite. |
| B | 13.8 – 25.3 | 1.5 | .16 | 45.8 | 1.4 | 4.6 | 20.2 | .07 | 30.3 | 1.4 | 1.2 | (6.84) | 99.8 | Halite, hanksite. |
| C | 25.3 – 45.8 | .50 | .20 | 45.2 | 1.4 | 8.5 | 11.0 | 2.0 | 31.1 | 5.0 | .44 | (7.02) | 98.3 | Halite, trona, hanksite, tincalconite[2]. |
| D | 45.8 – 64.0 | .13 | .06 | 44.5 | 4.6 | 6.7 | 10.8 | .44 | 37.2 | 3.6 | .22 | (8.40) | 99.8 | Halite, trona, hanksite. |
| E | 64.0 – 70.6 | .19 | .22 | 40.3 | .78 | 31.4 | 2.7 | 1.6 | 7.9 | 16.8 | .14 | (1.78) | 100.2 | Trona, halite, tincalconite[2]. |
| GS–21–A | 5.4 – [6]10.9 | 1.4 | .59 | 37.6 | 1.2 | 13.8 | 25.8 | 2.4 | 2.2 | 8.0 | 3.5 | (0.50) | 96.0 | Hanksite, trona, tincalconite[2], halite? |
| B | 10.9 – 30.6 | .11 | .44 | 40.7 | 1.7 | 14.8 | 24.0 | .85 | 9.4 | 6.8 | 2.0 | (2.12) | 98.7 | Hanksite, trona, halite. |
| C | 30.6 – 35.5 | .15 | .54 | 40.7 | 1.5 | 28.3 | 4.2 | .57 | 10.2 | 15.6 | .51 | (2.30) | 100.0 | Trona, halite, northupite? |

[1] Contact of Overburden Mud at 16.3 ft.
[2] Occurrences of tincalconite represent borax before dehydration in atmosphere.
[3] Includes 0.2 ft of Parting Mud.
[4] Contact of Overburden Mud at 31.3 ft.
[5] Contact of Overburden Mud at 13.8 ft.
[6] Contact of Overburden Mud at 6.3 ft.

The 104 brines analyzed (table 16) are from the Upper Salt portion of 10 core holes, 5 (HH, U, W, X and S–31) in the central part of the deposit, 1 (GS–4) in the outer part, and 4 (MM, S–28, GS–1, and GS–10) in intermediate facies. The samples were collected in the same manner as those from the Lower Salt.

The compositions of the brines listed in table 16 were projected to one face of the tetrahedrons used to represent the two pertinent 5-component systems (fig. 28). Projected boundaries of the mineral stability fields in the $Na_2CO_3$-$NaHCO_3$-$Na_2SO_4$-NaCl-$H_2O$ system at 20°C are shown in figure 28*A*; projected boundaries in the $Na_2CO_3$-$Na_2SO_4$-NaCl-KCl-$H_2O$ system at 20°C in figure 28*B*. The points in figure 28*A* are closely grouped and confirm the equilibrium assemblage in the Upper Salt of trona, halite, and thenardite without burkeite. The points in figure 28*B* are mostly within the boundaries of hanksite field; few are on the hanksite-aphthitalite boundary or in the aphthitalite field, confirming the equilibrium presence of that mineral in the assemblage at the time the analyses were made.

The specific gravities of brines from the central areas are mostly near 1.26 at the top and 1.30 at the base. Those from the edges of the deposit are as low as 1.25. Except for GS–1 and GS–4, which lie nearer the edges than the others, the total percentages of dissolved solids are between 33 and 35 percent. Values of pH from three holes range from 9.1 to 9.4.

The percentage of Na fluctuates over a small range but not systematically. The average is near 11 percent. The K content of the brine increases downward in almost every well. Most of this increase occurs in the top 5–10 m, but further increases generally occur below this zone. Near the top of the sampled profiles, in the Overburden Mud, the percentage of K is generally between 1 and 2 percent; at the base, it is generally about 2.5 percent in the central areas and under 2 percent nearer the edges. Teeple (1929, p. 18), Gale (1938, p. 869), and Ryan (1951, p. 449) list average percentages of K in the brine pumped from the Upper Salt as 2.53, 2.46, and 2.63, respectively.

The analyses list total carbonate expressed as $CO_3$, and in brines having these pH values, almost all the carbonate must actually be in this form. In most core holes, the $CO_3$ percentage shows a marked increase downward. The percentages of $SO_4$ are generally between 4 and 5. The brines in six core holes have increasing percentages of $SO_4$ toward the bottom, in three increase toward the top, and in one $SO_4$ is nearly constant. The percentages of Cl mostly fall between 12 and 13. The Cl content of the brines generally increases upward. Most $B_4O_7$ percentages, which lie near 1, increase downward.

Analyses of minor elements in Upper Salt brines are available for some sets of samples. The phosphate analyses are from brine wells in the intermediate and central parts of the deposit. Although areal position seems to be unrelated to the values, there is considerable variation in $PO_4$ content of brines within and between different wells. Ryan (1951, p. 449) reports an average of 940 ppm $PO_4$ and W. A. Gale (written commun., 1952) reports 920 ppm $PO_4$ in brines from the central part of the Upper Salt. As is reported only for

TABLE 16.—*Chemical analyses of brines from Upper Salt and Overburden Mud*

[Analyses of cores HH, MM, U, W, X, S–28, and S–31 by chemists of American Potash & Chemcial Corp., published with permission of company. Analyses of GS–1, GS–4, and GS–10 by Henry Kramer and Sol Berman, U.S. Geological Survey. Composition in weight percent except where indicated as parts per million (ppm)]

| Sample depth (ft) | Specific gravity | Total dissolved solids (by summation) | pH | Na | K | Total carbonate as $CO_3$ | $SO_4$ | Cl | $B_4O_7$ | $PO_4$ ppm | As ppm | Li ppm | Br ppm | S ppm | F ppm |
|---|---|---|---|---|---|---|---|---|---|---|---|---|---|---|---|
| **Core HH,[1] June 1948** | | | | | | | | | | | | | | | |
| 5 | 1.276 | 32.33 | ----- | 10.81 | 1.95 | 1.74 | 4.02 | 13.02 | 0.72 | ----- | -- | ----- | 700 | ----- | 13 |
| 10 | 1.278 | 32.37 | ----- | 10.80 | 1.98 | 1.83 | 4.05 | 12.88 | .76 | ----- | ----- | ----- | 700 | ----- | 10 |
| 15 | 1.279 | 35.60 | ----- | 10.89 | 1.98 | 1.89 | 4.10 | 14.33 | .77 | ----- | ----- | ----- | 700 | ----- | 13 |
| 20 | 1.280 | 32.66 | ----- | 10.89 | 1.99 | 1.92 | 4.18 | 12.82 | .79 | ----- | ----- | ----- | 700 | ----- | 13 |
| 25 | 1.287 | 33.27 | ----- | 11.03 | 2.03 | 1.98 | 4.87 | 12.50 | .79 | ----- | ----- | ----- | 700 | ----- | 13 |
| 30 | 1.301 | 34.36 | ----- | 11.07 | 2.49 | 2.45 | 5.09 | 12.10 | 1.07 | ----- | ----- | ----- | 900 | ----- | 13 |
| 35 | 1.301 | 34.25 | ----- | 11.04 | 2.48 | 2.45 | 5.03 | 12.09 | 1.07 | ----- | ----- | ----- | 900 | ----- | 13 |
| 40 | 1.301 | 34.34 | ----- | 11.06 | 2.48 | 2.46 | 5.10 | 12.08 | 1.07 | ----- | ----- | ----- | 900 | ----- | 13 |
| 45 | 1.301 | 34.31 | ----- | 11.06 | 2.48 | 2.45 | 5.08 | 12.08 | 1.07 | ----- | ----- | ----- | 900 | ----- | 16 |
| 50 | 1.301 | 34.31 | ----- | 11.05 | 2.48 | 2.45 | 5.10 | 12.07 | 1.07 | ----- | ----- | ----- | 900 | ----- | 15 |
| 55 | 1.301 | 34.34 | ----- | 11.06 | 2.49 | 2.45 | 5.10 | 12.09 | 1.06 | ----- | ----- | ----- | 900 | ----- | 15 |
| 60 | 1.301 | 34.37 | ----- | 11.05 | 2.47 | 2.45 | 5.08 | 12.06 | 1.06 | ----- | ----- | ----- | 900 | ----- | 16 |
| 65 | 1.301 | 34.42 | ----- | 11.05 | 2.49 | 2.45 | 5.08 | 12.09 | 1.06 | ----- | ----- | ----- | 900 | ----- | 1 |
| 70 | 1.301 | 34.46 | ----- | 11.06 | 2.50 | 2.46 | 5.08 | 12.09 | 1.07 | ----- | ----- | ----- | 900 | ----- | 15 |
| 75 | 1.301 | 34.38 | ----- | 11.03 | 2.49 | 2.46 | 5.05 | 12.08 | 1.07 | ----- | ----- | ----- | 900 | ----- | 15 |
| **Core MM,[1] October 1948** | | | | | | | | | | | | | | | |
| 5 | 1.2844 | 32.39 | ----- | 11.34 | 1.06 | 2.20 | 4.55 | 12.06 | 0.82 | 540 | ----- | ----- | 650 | ----- | ----- |
| 10 | 1.286 | 32.60 | ----- | 11.39 | 1.09 | 2.21 | 4.56 | 12.16 | .82 | 540 | ----- | ----- | 670 | ----- | ----- |
| 15 | 1.287 | 32.57 | ----- | 11.38 | 1.06 | 2.21 | 4.55 | 12.13 | .82 | 660 | ----- | ----- | 650 | ----- | ----- |
| 20 | 1.288 | 32.69 | ----- | 11.42 | 1.06 | 2.22 | 4.52 | 12.20 | .81 | 700 | ----- | ----- | 670 | ----- | ----- |
| 25 | 1.292 | 34.26 | ----- | 11.42 | 1.30 | 2.50 | 4.64 | 11.90 | 1.03 | 700 | ----- | ----- | 750 | ----- | ----- |
| 30 | 1.295 | 33.40 | ----- | 11.49 | 1.30 | 2.55 | 4.60 | 11.96 | 1.04 | 700 | ----- | ----- | 740 | ----- | ----- |
| 35 | 1.295 | 33.37 | ----- | 11.47 | 1.27 | 2.54 | 4.66 | 11.91 | 1.04 | 740 | ----- | ----- | 740 | ----- | ----- |
| 40 | 1.292 | 33.39 | ----- | 11.46 | 1.31 | 2.52 | 4.68 | 11.88 | 1.03 | 800 | ----- | ----- | 740 | ----- | ----- |
| 45 | 1.297 | 33.90 | ----- | 11.52 | 1.47 | 2.64 | 4.79 | 11.90 | 1.04 | 860 | ----- | ----- | 720 | ----- | ----- |
| 50 | 1.298 | 34.01 | ----- | 11.42 | 1.65 | 2.72 | 4.69 | 11.86 | 1.07 | 940 | ----- | ----- | 790 | ----- | ----- |
| **Core U,[1] December 1949** | | | | | | | | | | | | | | | |
| 5 | 1.278 | 32.68 | ----- | 11.30 | 1.31 | 2.23 | 4.00 | 12.62 | 0.75 | 740 | ----- | ----- | 630 | ----- | ----- |
| 10 | 1.279 | 32.60 | ----- | 11.29 | 1.28 | 2.25 | 4.00 | 12.55 | .76 | 740 | ----- | ----- | 630 | ----- | ----- |
| 15 | 1.286 | 33.15 | ----- | 11.40 | 1.33 | 2.34 | 4.41 | 12.38 | .78 | 800 | ----- | ----- | 670 | ----- | ----- |
| 20 | 1.293 | 34.40 | ----- | 11.08 | 1.73 | 2.03 | 4.88 | 12.16 | .96 | 900 | ----- | ----- | 680 | ----- | ----- |
| 25 | 1.297 | 34.10 | ----- | 11.38 | 1.73 | 2.52 | 4.95 | 11.91 | 1.04 | 900 | ----- | ----- | 750 | ----- | ----- |
| 30 | 1.297 | 34.10 | ----- | 11.37 | 1.73 | 2.52 | 4.96 | 11.91 | 1.04 | 900 | ----- | ----- | 750 | ----- | ----- |
| 35 | 1.297 | 34.11 | ----- | 11.35 | 1.76 | 2.52 | 4.96 | 11.91 | 1.04 | 900 | ----- | ----- | 760 | ----- | ----- |
| 40 | 1.297 | 34.11 | ----- | 11.35 | 1.77 | 2.52 | 4.96 | 11.91 | 1.04 | 880 | ----- | ----- | 760 | ----- | ----- |
| 45 | 1.297 | 34.11 | ----- | 11.34 | 1.78 | 2.52 | 4.96 | 11.91 | 1.04 | 880 | ----- | ----- | 760 | ----- | ----- |
| 50 | 1.297 | 34.42 | ----- | 11.12 | 2.17 | 2.51 | 4.96 | 11.91 | 1.07 | 880 | ----- | ----- | 760 | ----- | ----- |
| 55 | 1.299 | 34.39 | ----- | 10.99 | 2.37 | 2.51 | 4.96 | 11.91 | 1.09 | 880 | ----- | ----- | 770 | ----- | ----- |
| 60 | 1.301 | 34.76 | ----- | 11.05 | 2.46 | 2.73 | 4.82 | 11.89 | 1.21 | 920 | ----- | ----- | 870 | ----- | ----- |
| 65 | 1.303 | 34.75 | ----- | 11.06 | 2.45 | 2.73 | 4.82 | 11.88 | 1.21 | 920 | ----- | ----- | 880 | ----- | ----- |
| **Core W,[1] February 1935** | | | | | | | | | | | | | | | |
| 5 | 1.256 | 32.62 | ----- | 10.71 | 1.39 | 1.66 | 2.64 | 13.53 | 0.700 | 588 | 70 | ----- | ----- | 40 | ----- |
| 10 | 1.277 | 34.90 | ----- | 11.04 | 1.65 | 2.18 | 3.69 | 12.76 | .950 | 752 | 81 | ----- | ----- | 140 | ----- |
| 15 | 1.284 | 35.65 | ----- | 11.04 | 1.83 | 2.38 | 4.00 | 12.52 | .988 | 830 | 92 | ----- | ----- | 180 | ----- |
| 20 | 1.291 | 36.09 | ----- | 11.14 | 1.88 | 2.41 | 4.25 | 12.32 | 1.067 | 858 | 86 | ----- | ----- | 220 | ----- |
| 25 | 1.292 | 36.25 | ----- | 11.12 | 1.96 | 2.55 | 4.24 | 12.26 | 1.061 | 868 | 32 | ----- | ----- | 270 | ----- |
| 30 | 1.293 | 36.49 | ----- | 11.14 | 1.99 | 2.59 | 4.30 | 12.27 | 1.082 | 896 | 32 | ----- | ----- | 280 | ----- |
| 35 | 1.293 | 36.34 | ----- | 11.05 | 2.06 | 2.57 | 4.29 | 12.17 | 1.097 | 900 | 32 | ----- | ----- | 280 | ----- |
| 40 | 1.294 | 36.72 | ----- | 11.02 | 2.28 | 2.56 | 4.48 | 12.21 | 1.101 | 856 | 54 | ----- | ----- | 270 | ----- |
| 45 | 1.296 | 36.82 | ----- | 10.93 | 2.42 | 2.58 | 4.52 | 12.18 | 1.094 | 872 | 65 | ----- | ----- | 270 | ----- |
| 50 | 1.298 | 37.02 | ----- | 10.92 | 2.51 | 2.62 | 4.52 | 12.19 | 1.099 | 920 | 59 | ----- | ----- | 250 | ----- |
| 55 | 1.298 | 37.19 | ----- | 10.90 | 2.62 | 2.66 | 4.46 | 12.19 | 1.129 | 950 | 92 | ----- | ----- | 200 | ----- |
| 60 | 1.298 | 37.33 | ----- | 10.91 | 2.63 | 2.72 | 4.48 | 12.15 | 1.139 | 988 | 86 | ----- | ----- | 180 | ----- |
| 65 | 1.298 | 37.50 | ----- | 10.98 | 2.60 | 2.74 | 4.54 | 12.17 | 1.143 | 996 | 92 | ----- | ----- | 180 | ----- |
| 70 | 1.298 | 37.42 | ----- | 10.98 | 2.60 | 2.71 | 4.51 | 12.19 | 1.140 | 986 | 92 | ----- | ----- | 190 | ----- |

Footnotes on page 64.

TABLE 16.—*Chemical analyses of brines from Upper Salt and Overburden Mud*—Continued

| Sample depth (ft) | Specific gravity | Total dissolved solids (by summation) | pH | Na | K | Total carbonate as $CO_3$ | $SO_4$ | Cl | $B_4O_7$ | $PO_4$ ppm | As ppm | Li ppm | Br ppm | S ppm | F ppm |
|---|---|---|---|---|---|---|---|---|---|---|---|---|---|---|---|
| **Core X,[1] March 1950** | | | | | | | | | | | | | | | |
| 5 | 1.264 | 30.37 | ----- | 11.16 | 1.05 | 1.96 | 3.36 | 13.05 | 0.57 | 660 | ----- | ----- | 510 | 100 | ----- |
| 10 | 1.265 | 31.59 | ----- | 11.17 | 1.04 | 1.96 | 3.37 | 13.05 | .57 | 660 | ----- | ----- | 520 | 200 | ----- |
| 15 | 1.265 | 31.60 | ----- | 11.18 | 1.04 | 1.96 | 3.37 | 13.05 | .57 | 660 | ----- | ----- | 520 | 200 | ----- |
| 20 | 1.283 | 32.97 | ----- | 11.48 | 1.13 | 2.04 | 5.14 | 12.16 | .60 | 620 | ----- | ----- | 520 | 300 | ----- |
| 25 | 1.294 | 33.88 | ----- | 11.35 | 1.66 | 2.36 | 5.00 | 12.06 | .98 | 720 | ----- | ----- | 610 | 100 | ----- |
| 30 | 1.299 | 34.39 | ----- | 11.25 | 2.05 | 2.47 | 5.10 | 12.02 | 1.03 | 720 | ----- | ----- | 650 | 100 | ----- |
| 35 | 1.300 | 34.49 | ----- | 11.24 | 2.11 | 2.47 | 5.18 | 12.02 | 1.01 | 700 | ----- | ----- | 650 | 100 | ----- |
| 40 | 1.301 | 34.60 | ----- | 11.17 | 2.23 | 2.41 | 5.30 | 12.02 | 1.01 | 700 | ----- | ----- | 630 | 100 | ----- |
| 45 | 1.301 | 34.54 | ----- | 11.17 | 2.23 | 2.41 | 5.26 | 12.02 | 1.01 | 680 | ----- | ----- | 610 | 100 | ----- |
| 50 | 1.301 | 34.59 | ----- | 11.18 | 2.23 | 2.41 | 5.28 | 12.02 | 1.01 | 700 | ----- | ----- | 630 | 100 | ----- |
| 55 | 1.301 | 34.62 | ----- | 11.19 | 2.23 | 2.41 | 5.33 | 11.99 | 1.01 | 700 | ----- | ----- | 630 | 100 | ----- |
| 60 | 1.301 | 34.62 | ----- | 11.19 | 2.23 | 2.41 | 5.33 | 11.99 | 1.01 | 700 | ----- | ----- | 630 | 100 | ----- |
| 65 | 1.300 | 34.60 | ----- | 11.17 | 2.23 | 2.41 | 5.33 | 11.99 | 1.01 | 700 | ----- | ----- | 630 | 100 | ----- |
| 70 | 1.301 | 34.62 | ----- | 11.18 | 2.24 | 2.47 | 5.23 | 11.99 | 1.04 | 700 | ----- | ----- | 720 | 100 | ----- |
| 72 | 1.302 | 34.50 | ----- | 11.13 | 2.24 | 2.46 | 5.10 | 11.99 | 1.06 | 760 | ----- | ----- | 750 | 200 | ----- |
| **Core S-28,[1] August 1950** | | | | | | | | | | | | | | | |
| 30 | 1.290 | 33.57 | ----- | 11.34 | 1.70 | 2.71 | 4.22 | 12.19 | 0.98 | 560 | ----- | ----- | 630 | 500 | ----- |
| 35 | 1.291 | 33.53 | ----- | 11.35 | 1.72 | 2.73 | 4.22 | 12.18 | 1.00 | 560 | ----- | ----- | 640 | 500 | ----- |
| 40 | 1.297 | 34.40 | ----- | 11.32 | 2.15 | 2.99 | 4.16 | 12.09 | 1.21 | 640 | ----- | ----- | 740 | 600 | ----- |
| 45 | 1.301 | 34.78 | ----- | 11.26 | 2.38 | 3.14 | 4.03 | 12.06 | 1.35 | 720 | ----- | ----- | 760 | 800 | ----- |
| 50 | 1.301 | 34.67 | ----- | 11.20 | 2.42 | 3.14 | 4.00 | 12.00 | 1.36 | 700 | ----- | ----- | 770 | 800 | ----- |
| 55 | 1.301 | 34.81 | ----- | 11.24 | 2.42 | 3.16 | 4.05 | 12.01 | 1.37 | 720 | ----- | ----- | 770 | 800 | ----- |
| 60 | 1.302 | 34.81 | ----- | 11.21 | 2.44 | 3.15 | 4.02 | 12.02 | 1.39 | 780 | ----- | ----- | 840 | 700 | ----- |
| 64 | 1.302 | 34.85 | ----- | 11.23 | 2.44 | 3.15 | 4.05 | 12.02 | 1.38 | 780 | ----- | ----- | 840 | 700 | ----- |
| **Core S-31,[1] December 1950** | | | | | | | | | | | | | | | |
| 25 | 1.285 | 32.99 | ----- | 11.49 | 1.30 | 2.51 | 4.23 | 12.33 | 0.76 | 500 | ----- | ----- | 570 | 400 | ----- |
| 30 | 1.285 | 33.02 | ----- | 11.51 | 1.28 | 2.55 | 4.25 | 12.30 | .76 | 500 | ----- | ----- | 590 | 400 | ----- |
| 35 | 1.291 | 34.62 | ----- | 11.44 | 2.06 | 2.97 | 4.31 | 12.12 | 1.20 | 720 | ----- | ----- | 740 | 500 | ----- |
| 40 | 1.306 | 35.20 | ----- | 11.16 | 2.62 | 3.09 | 4.21 | 12.11 | 1.33 | 980 | ----- | ----- | 930 | 500 | ----- |
| 45 | 1.306 | 31.13 | ----- | 11.11 | 2.66 | 3.08 | 4.21 | 12.06 | 1.34 | 960 | ----- | ----- | 940 | 500 | ----- |
| 50 | 1.307 | 35.26 | ----- | 11.13 | 2.68 | 3.11 | 422 | 12.09 | 1.36 | 960 | ----- | ----- | 930 | 500 | ----- |
| 55 | 1.307 | 35.27 | ----- | 11.13 | 2.70 | 3.14 | 4.21 | 12.06 | 1.37 | 940 | ----- | ----- | 930 | 500 | ----- |
| 60 | 1.307 | 35.19 | ----- | 11.10 | 2.71 | 3.12 | 4.20 | 12.06 | 1.37 | 900 | ----- | ----- | 940 | 500 | ----- |
| 65 | 1.307 | 35.17 | ----- | 11.10 | 2.70 | 3.12 | 4.22 | 12.04 | 1.36 | 900 | ----- | ----- | 930 | 500 | ----- |
| 70 | 1.307 | 31.25 | ----- | 11.16 | 2.67 | 3.12 | 4.23 | 12.09 | 1.36 | 880 | ----- | ----- | 930 | 500 | ----- |

brines from core hole W in the central segment of the lake; values range from 32 to 92 ppm with no clear vertical trend. Li was analyzed in brines from intermediate and edge facies but no areal or vertical trend is evident; Ryan (1951, p. 449) reports 70 ppm in pumped brines. The analyses for Br are all brines from the intermediate and central parts of the deposit; Br tends to increase in concentration toward the base of the layer. Ryan reports 810 ppm Br, and Gale estimates 860 ppm Br in brines pumped for commercial use. The amounts of S are variable and tend to increase downward. Ryan and Gale report average amounts of S as 330 and 390 ppm, respectively. Amounts of F in core hole HH are mostly between 10 and 15 ppm; Ryan and Gale estimate 20 and 15 ppm F, respectively. Ryan and Gale estimate the I content of brines pumped from the central part of the Upper Salt to be 30 and 29 ppm. They and Carpenter and Garrett (1959), report W in average amounts near 55 ppm. Hem (written commun., 1960) reports Sr in two samples from 60 and 70 ft (18.3 and 21.3 m) in GS–14 as 4.5 and 3.2 ppm, and in samples from 25 and 30 ft (7.6 and 9.1 m) in GS–26 as 3.7 and 2.2 ppm. The brines from GS–1, GS–4, and GS–10 were analyzed for Ca and Mg but their quantities were found to be below limits of detection.

Vertical variations in brine composition bear a sporadic relation to the mineral composition of the salts although there is a marked increase in the total dissolved solids below the zone immediately below the Overburden Mud. Percentages of $CO_3$ and $B_4O_7$ increase downward in accord with the downward increase of trona and borax, percentages of Cl increase upward as does the percentage of halite. Percentages

TABLE 16.—*Chemical analyses of brines from Upper Salt and Overburden Mud*—Continued

| Sample depth (ft) | Specific gravity | Total dissolved solids (by summation) | pH | Na | K | Total carbonate as $CO_3$ | $SO_4$ | Cl | $B_4O_7$ | $PO_4$ ppm | As ppm | Li ppm | Br ppm | S ppm | F ppm |
|---|---|---|---|---|---|---|---|---|---|---|---|---|---|---|---|
| **Core GS–1,[1] July 1954** | | | | | | | | | | | | | | | |
| 30 | 1.264 | 32.4 | 9.2 | 10.9 | 1.52 | 2.54 | 3.91 | 12.64 | 0.84 | ----- | ----- | 28 | ----- | ----- | ----- |
| 35 | 1.277 | 33.5 | 9.2 | 11.3 | 1.80 | 2.56 | 4.62 | 12.30 | .966 | ----- | ----- | 31 | ----- | ----- | ----- |
| 40 | 1.281 | 34.2 | 9.3 | 11.3 | 2.10 | 2.71 | 4.68 | 12.36 | 1.08 | ----- | ----- | 35 | ----- | ----- | ----- |
| 45 | 1.276 | 34.4 | 9.3 | 11.3 | 2.02 | 3.04 | 4.64 | 12.33 | 1.07 | ----- | ----- | 35 | ----- | ----- | ----- |
| 45.8 | 1.277 | 33.8 | 9.3 | 10.9 | 2.10 | 2.72 | 4.67 | 12.35 | 1.07 | ----- | ----- | 35 | ----- | ----- | ----- |
| **Core GS–4,[1] September 1954** | | | | | | | | | | | | | | | |
| 24.8 | 1.274 | 32.0 | 9.12 | 11.0 | 1.07 | 2.45 | 4.56 | 12.14 | 0.78 | ----- | ----- | 42 | ----- | ----- | ----- |
| 30.0 | 1.278 | 32.3 | 9.18 | 10.9 | 1.19 | 2.62 | 4.62 | 12.08 | .85 | ----- | ----- | 43 | ----- | ----- | ----- |
| 35.0 | 1.277 | 34.0 | 9.23 | 12.8 | 1.20 | 2.50 | 4.72 | 11.99 | .83 | ----- | ----- | 42 | ----- | ----- | ----- |
| 40.0 | 1.282 | 33.0 | 9.28 | 11.3 | 1.22 | 3.03 | 4.73 | 11.81 | .86 | ----- | ----- | 43 | ----- | ----- | ----- |
| 45.0 | 1.284 | 33.0 | 9.31 | 10.9 | 1.78 | 2.81 | 4.42 | 12.01 | 1.11 | ----- | ----- | 72 | ----- | ----- | ----- |
| 48.9 | 1.287 | 32.9 | 9.32 | 10.7 | 1.79 | 2.97 | 4.38 | 11.92 | 1.10 | ----- | ----- | 69 | ----- | ----- | ----- |
| **Core GS–10,[1] January 1955** | | | | | | | | | | | | | | | |
| 36.3 | 1.285 | 33.6 | 9.30 | 10.9 | 1.98 | 2.37 | 5.09 | 12.32 | 0.94 | ----- | ----- | 58 | ----- | ----- | ----- |
| 40 | 1.283 | 33.6 | 9.30 | 10.9 | 1.98 | 2.33 | 5.12 | 12.30 | .94 | ----- | ----- | 58 | ----- | ----- | ----- |
| 45 | 1.285 | 33.5 | 9.30 | 10.7 | 1.93 | 2.32 | 5.11 | 12.28 | .95 | ----- | ----- | 58 | ----- | ----- | ----- |
| 50 | 1.284 | 33.4 | 9.26 | 10.9 | 1.95 | 2.24 | 5.10 | 12.30 | .95 | ----- | ----- | 57 | ----- | ----- | ----- |
| 55 | 1.285 | 33.6 | 9.24 | 10.9 | 1.93 | 2.39 | 5.12 | 12.26 | .95 | ----- | ----- | 57 | ----- | ----- | ----- |
| 60 | 1.282 | 33.7 | 9.25 | 10.9 | 1.95 | 2.40 | 5.19 | 12.28 | .95 | ----- | ----- | 58 | ----- | ----- | ----- |
| 65 | 1.289 | 33.6 | 9.38 | 10.8 | 2.05 | 2.48 | 4.84 | 12.32 | 1.10 | ----- | ----- | 59 | ----- | ----- | ----- |
| 70 | 1.280 | 33.4 | 9.31 | 11.3 | 1.75 | 2.48 | 4.54 | 12.26 | 1.10 | ----- | ----- | 22 | ----- | ----- | ----- |

[1]Depth to top and base of Upper Salt;
HH: 13–78.7 feet.
MM: 6–53.4 feet.
U: 12(?)–65.0 feet
W: 22–71.3 feet.
X: 19–76.7 feet.
S–28: 28.6–64.7 feet
S–31: 23.0–72.0 feet.
GS–1: 28.9–46.0 feet
GS–4: 24.8–48.9 feet.
GS–10: 32.4–70.2 feet

of $SO_4$ do not show any clear trend, and percentages of K increase downward. Both patterns are in contrast with the general tendency for hanksite, the principal mineral in these cores containing these components, to be more abundant near the top of the Upper Salt. The effect of pumping by chemical companies cannot be inferred from data in table 16 because the samples come from widely spaced sites and represent a wide range in dates of collection.

## ESTIMATED BULK COMPOSITION OF THE UNIT

The estimates of mineral composition of the Upper Salt (table 14), the measure of the probable error in the visual estimates (table 8), and analyses of the brines (table 16) provide a basis for calculating the total quantity of the major water-soluble components in the Upper Salt. The total is about $1{,}330 \times 10^{12}$ g of salts. Table 17 gives the quantity of each component and tabulates the steps followed in the calculation. A more detailed study of the boron in Searles Lake (D. V. Haines, unpub. report, 1956) estimates a total of 23 $\times 10^{12}$ g of BO in the Upper Salt, whereas table 17 indicates $28 \times 10^{12}$ g; this discrepancy indicates the approximate accuracy of these estimates. The relative percentages of components, calculated water-free, are:

| | |
|---|---|
| Na | 34.8 |
| K | 2.1 |
| Mg | .4 |
| $CO_3$ | 7.5 |
| $HCO_3$ | 4.9 |
| $SO_4$ | 14.5 |
| Cl | 33.7 |
| $B_4O_7$ | 2.1 |

FIGURE 28.—Compositions of analyzed brines from the Upper Salt (table 16), plotted on diagrams that indicate phase relations in two 5-component systems. *A* Phases in $Na_2CO_3$–$Na_2SO_4$–NaCl–$NaHCO_3$–$H_2O$ system, *B*, Phases in $Na_2CO_3$–$Na_2SO_4$–KCl–NaCl–$H_2O$ system. Brines plotted on the basis of their compositions projected to plane of diagram; some points represent more than one analysis. See figures 35 and 39 and associated text for explanation of phase boundaries and method of plotting.

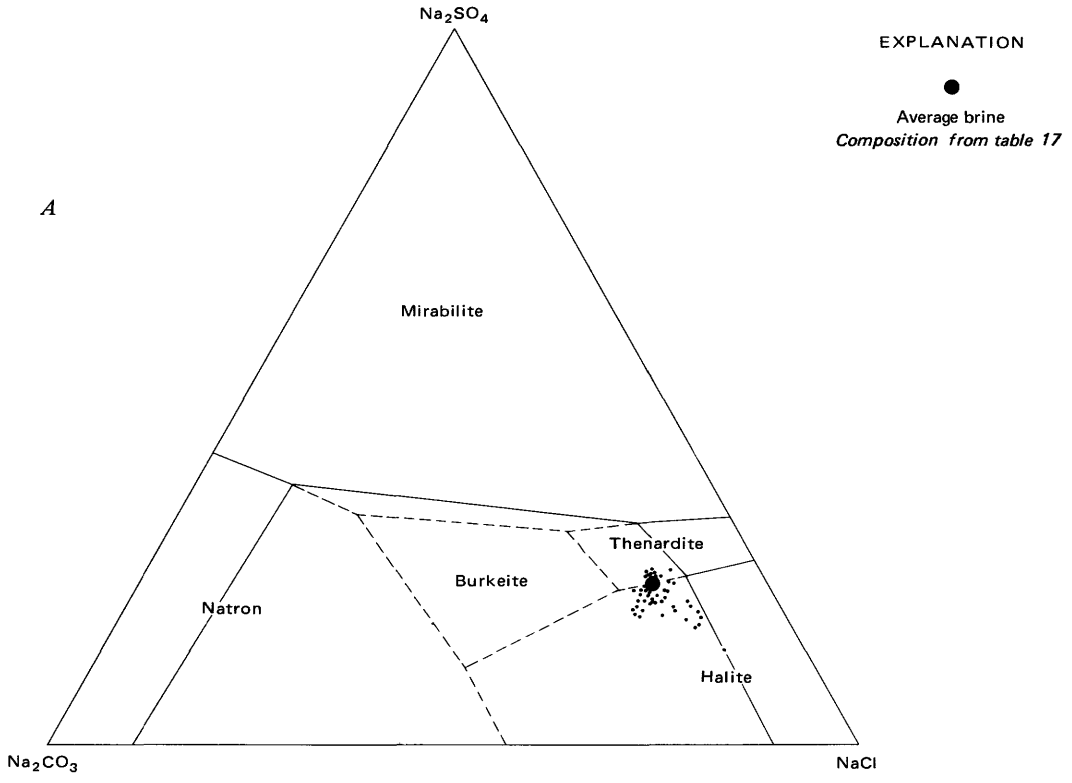
A
$Na_2SO_4$
Mirabilite
Thenardite
Burkeite
Natron
Halite
$Na_2CO_3$
NaCl
EXPLANATION
Average brine
Composition from table 17

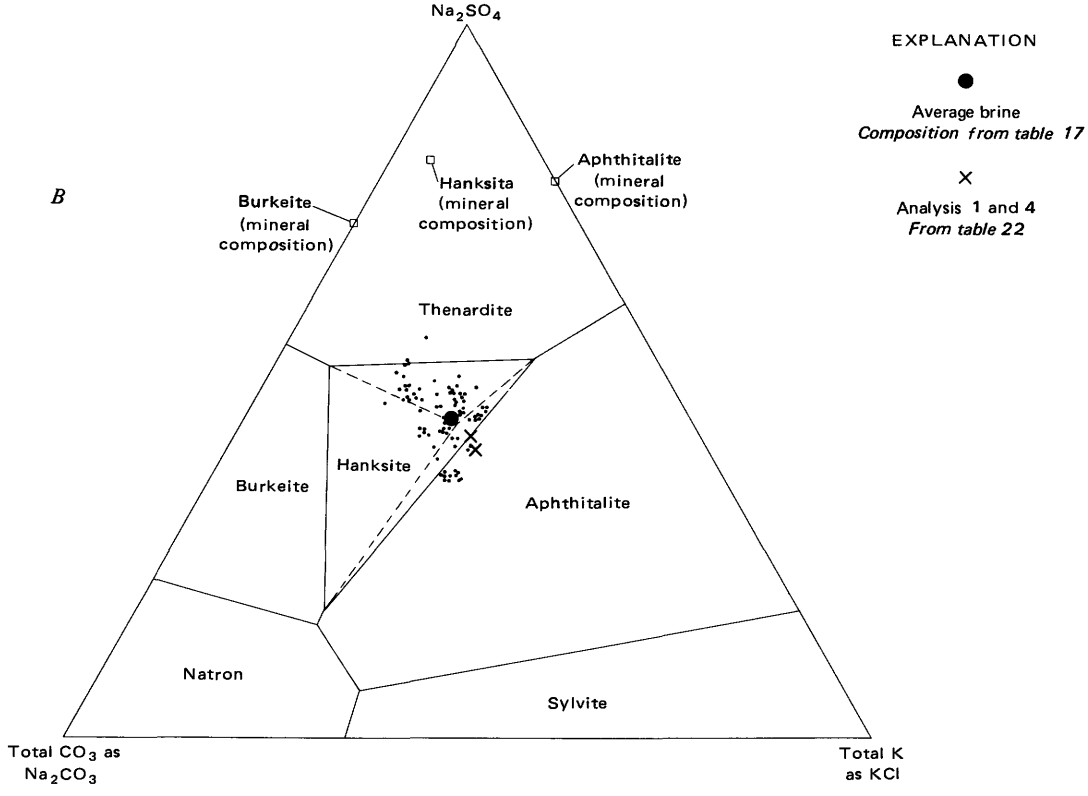
B
$Na_2SO_4$
Hanksita (mineral composition)
Aphthitalite (mineral composition)
Burkeite (mineral composition)
Thenardite
Hanksite
Burkeite
Aphthitalite
Natron
Sylvite
Total $CO_3$ as $Na_2CO_3$
Total K as KCl
EXPLANATION
Average brine
Composition from table 17
Analysis 1 and 4
From table 22

TABLE 17.—*Estimated percentages and total quantities of water-soluble components in the Upper Salt*

| | Na | K | Mg | $CO_3$ | $HCO_3$ | $SO_4$ | Cl | $B_4O_7$ | $H_2O$ |
|---|---|---|---|---|---|---|---|---|---|
| Chemical composition of solids inferred from visual estimate[1] | 34.2 | 0.5 | 0 | 10.5 | 9.1 | 11.4 | 26.8 | 1.0 | 6.5 |
| Average error of visual estimates[2] | −0.8 | +0.6 | +0.5 | −3.4 | [3]−3.4 | +2.6 | +4.8 | +0.8 | [4]−1.6 |
| Chemical composition of solids, in weight percent, adjusted for probable error | 33.4 | 1.1 | 0.5 | 7.1 | 5.7 | 14.0 | 31.6 | 1.8 | 4.9 |
| Chemical composition of brine[5] | 11.2 | 2.0 | 0 | 2.5 | [6]0 | 4.6 | 12.2 | 1.0 | 66.5 |
| Chemical composition of combined solids and brines[7] | 24.5 | 1.5 | 0.3 | 5.3 | 3.4 | 10.2 | 23.8 | 1.5 | 29.5 |
| Total quantity of component in Upper Salt[8], grams × $10^{12}$ | 462 | 28 | 5 | 100 | 64 | 192 | 448 | 28 | 556 |

[1] Data in table 14 converted to weight percent.
[2] Based on comparison of visual estimates and chemcial analyses of cores (converted to ions), data from table 8, average of all samples. Table 8 also lists error in Ca of +0.4, reducing totals in this and underlying columns to 99.6
[3] Error in $CO_3$ listed in table 8 divided equally between $CO_3$ and $HCO_3$.
[4] Reduced by amount of H in $HCO_3$.
[5] Arithmetic average of brine analyses listed in table 16, in weight percent.
[6] Percentage of $HCO_3$ is low, assumed to be 0.
[7] In weight percent, assumed porosity 40 percent.
[8] Assumed specific gravity of salt plus brine filled pores, 1.80; volume from text.

## OVERBURDEN MUD

The Overburden Mud, commonly about 7 m thick in the center of the deposit, is composed of a succession of discontinuous beds of mud and salts. Most of the salt is halite, some as partially dissolved and rounded crystals; locally beds of hanksite, trona, borax, and thenardite are found. Toward the edges of the lake, the Overburden Mud is characteristically a black or dark-gray pirssonite-bearing mud that grades upward into greenish or olive-colored clay and silt; at the surface, when dry, it is a light-tan or pinkish-tan silt. In many parts of the Searles Lake deposit, the subsurface contact between the Overburden Mud and the upper part of the Upper Salt is gradational and not easily identified. Stratigraphic criteria used to place the contact in cores are described in the section on the Upper Salt. Outside the area covered by the Upper Salt, the base of the Overburden Mud is in contact with a sand layer that is the lateral equivalent of the Upper Salt. In most areas, the outcrop of this contact is known or interpreted to be a kilometer or more outside the salt body limits. Along the southwest part of the body, southeast of Westend, this contact is much closer to the inferred edge of the Upper Salt body because the chemical and clastic sediments carried into the basin from upstream formed a delta in this area, steepening the slopes upon which both salt and mud layers were deposited.

### AREAL EXTENT AND VOLUME

The Overburden Mud covers the entire surface of Searles Lake within the area underlain by the Upper Salt (fig. 27), and in most areas extends a kilometer or more beyond this limit. The average thickness of the Overburden Mud in the 88 cores in which it could be measured is 7 m (23 ft). It is only 2–5 m thick in an area of about 10 $km^2$ that lies within a kilometer or two of the northwest edge of the lake, but elsewhere, it is mostly 6–9 m thick. Thickness greater than 9 m were noted only in cores that are near the north, south, and southwest edges of the Upper Salt unit; the unit thins to zero about a kilometer outside this edge.

These thickness data were plotted on an isopach map and the volume of the unit calculated. This information was used in making the very general calculations of the mineral composition of the Overburden Mud. The map is not included in this report because the position of the basal contact of the Overburden Mud, owing to its gradational nature, is chosen by means of a set of arbitrary criteria. As a result, the trends in thickness indicated by subsurface data are relatively unsystematic, and the changes in thickness near the edge of the deposit are too abrupt to allow meaningful extrapolation in areas of no data. The total volume of the unit, calculated from the isopach map and within the arbitrary boundary described previously, is 380 × $10^6$ $m^3$.

### MINERAL COMPOSITION AND LITHOLOGY

The composition of the Overburden Mud is distinctly different from the other mud layers in this deposit. Clastic fragments are commonly larger and make up higher percentages of this layer. Sand is abundant in parts of the Overburden Mud, whereas clastic fragments larger than silt size make up less than 20 percent of the Parting Mud and older mud units. In the outer parts of the deposit, the Overburden Mud is composed almost entirely of mud and this grades into interbedded mud and salt layers in the center. In contrast, the Parting Mud and Bottom Mud are nearly constant in composition between their edge and central facies.

The megascopic composition of the Overburden Mud was estimated by the methods used for older units, although the results are not as reliable for rea-

sons described below. The calculated mean composition (in volume percent) is as follows:

| | |
|---|---|
| Mud (clastic and other fine-grained minerals) | 83 |
| Halite | 13 |
| Pirssonite | 2 |
| Hanksite | 1 |
| Trona | 1 |
| Gaylussite | Trace |
| Borax | Trace |
| Thenardite | Trace |
| Sulfohalite | Trace |

Near the edge of the deposit, evaporite components are generally reported only from the bottom meter, but this is probably not an accurate record of their distribution. Most test holes in those areas did not take cores in the upper part of the Overburden Mud, and the composition of that segment was inferred to be pure mud. Pirssonite and halite are the minerals likely to have been underestimated as a result of this practice. In the central segment of the deposit, evaporite minerals are about evenly distributed vertically throughout the unit.

X-ray diffraction studies of samples from this unit (tables 15 and 18) confirm the megascopic mineral identifications and show that halite, pirssonite, and hanksite are the most common evaporite minerals, and that little dolomite and no aragonite are present. The clastic minerals are mostly quartz, feldspar, mica, and clay. The clay fraction of surface samples, studied by Droste (1961, p. 1,717–1,719), consists mostly of montmorillonite and illite; there is a marked increase in chlorite in the east part of the deposit which receives sediment from the several chlorite-rich zones of fault gouge in the Slate Range.

In the central part of the deposit (Haines, 1959, fig. 6), the surface of the Overburden Mud is generally pure halite. Much of this material is firm enough to support a car or truck, even when covered with water. The cubic crystals of halite are several millimeters to a few centimeters across and are intergrown in a random orientation. As a result of microorganisms that live in the near-surface brine, some of the salt has a light pinkish color. In a few areas where the surface has been modified by the evaporation of waters returned from the chemical plants and towns to the lake, the surface crust includes more thenardite and a number of introduced impurities.

The surface crusts commonly form a pattern of polygonal cracks and ridges (fig. 29). The center of each polygon is saucer shaped, and the edges turn up to form ridges a few millimeters to more than half a meter high. These polygons appear to grow from the center outward, and edges are thrust outward over the adjacent polygon. The zone between polygons is a chaotic zone of slabs broken off when they met crusts growing from the opposing side.

FIGURE 29.—The Polygonal cracks and ridges on surface of northern part of Searles Lake (sec. 11, T. 25 S., R. 43 E.). Metal clipboard is 20 cm long.

A remarkably linear zone of saline crusts and efflorescences known as the "trona reef" occurs along the northeast edge of the lake surface (Gale, 1914, p. 275, 294–296). The efflorescences range from a surface powder to crusts several centimeters thick. Saline minerals constitute the bulk of this material; the percentages of minerals vary from place to place. Gale (1914, p. 294) reports an analysis of a composite sample of crusts that suggests their content to be about 54 percent trona,[14] 20 percent halite, 5 percent thenardite, nearly 3 percent borax, a few percent a K-bearing mineral, and the remainder a material that is insoluble in water. X-ray diffraction analysis of a sample of crust from the northern part of the zone (NW¼ sec. 12) shows it to be composed of halite, a smaller amount of trona, and minor quantities of burkeite and gaylussite(?).

Gale (1914, p. 295) attributed the trona reef to evaporation of saline ground water that rose to the surface at the edge of the playa as a result of the impermeability of the sediments that characterize the playa floor. This does not explain the absence of similar zones around other parts of the playa where ground water is encroaching. Seismic refraction data (Mabey, 1956, p. 846), however, show a velocity discontinuity beneath the trona reef that could be a fault having upward displacement on the east side. It seems likely that this fault extends to the surface, where it acts as a linear barrier to eastward-moving brine.[15] The

[14] The published analysis reports components that total 89.20, not 100 as indicated. However, the percentage of $H_2O$ that would accompany 54.04 percent $Na_2CO_3 \cdot NaHCO_3$ as trona and 1.52 percent $Na_2B_4O_7$ as borax brings the total to 100.77.

[15] As noted by Hardt, Moyle, and Dutcher (1972, fig. 10), as the hydrostatic head of the brines in the center of the valley is greater than in the surrounding areas, brine migrates from the lake into the surrounding ground water reservoir areas.

TABLE 18.—*Partial chemical analyses of core GS–40 from the Overburden Mud*

[Analysts and analytical techniques as listed in table 13]

**Major elements (percent of total sample)**

| | Water-and acid-soluble components | | | | | | | | Acid-insoluble components | | | | | | | |
|---|---|---|---|---|---|---|---|---|---|---|---|---|---|---|---|---|
| Depth in core | CaO | MgO | $Na_2O$ | $K_2O$ | Total carbonate as $CO_2$ | $SO_3$ | $B_2O_3$ | Cl | [1]$SiO_2$ | $Al_2O_3$ | Total Fe as $Fe_2O_3$ | Cao | MgO | $Na_2O$ | $K_2O$ | Organic carbon in C |
| 1.0 | 4.2 | 1.2 | 5.0 | 4.0 | 1.2 | 0.22 | 0.19 | 1.5 | 61.3 | 11.7 | 0.9 | 1.9 | 0.5 | 2.9 | 2.7 | 0.04 |
| [2]30.3 | 9.2 | 6.8 | 14.5 | 2.6 | 15.3 | 1.8 | .64 | 7.9 | 26.9 | 3.0 | .3 | .5 | .1 | .8 | .6 | .5 |

**Minor Elements**

| Depth in core | B | Ba | Cr | Cu | Ga | Mn | Nb | Sc | Sr | Ti | Yb | V | Y | Zr |
|---|---|---|---|---|---|---|---|---|---|---|---|---|---|---|
| 1.0 | 200 | 700 | 15 | 0.7 | 15 | 150 | 5 | 10 | 700 | 3000 | 1.5 | 50 | 10 | 150 |
| 30.3 | 100 | 500 | 15 | 0.7 | 10 | 150 | 7 | 7 | 300 | 3000 | 1.5 | 30 | 10 | 150 |

| Depth in core | Minerals identified by X-ray of untreated sample (in approximate order of decreasing abundance) |
|---|---|
| 1.0 | Feldspar, quartz, mica, amphibole, clay, halite |
| 30.3 | Dolomite, pirssonite, gaylussite, halite, mica, clay, calcite |

[1]Percentage possibly low because of loss during original heating and acid treatment. [2]Base of Overburden Mud in GS–40 at 31.9 feet.

brine is thus forced to the surface and, on evaporation, produces an elongate strip of efflorescences. This explanation accounts for the notable linearity of the feature, and for the absence of similar features along other parts of the lake periphery.

### CHEMICAL COMPOSITION

Analyses of the Overburden Mud segment of four cores are included in the analyses of Upper Salt given in table 15, analyses of individual specimens logged as pure mud in core GS–40 in table 18. Two of the samples given in table 15 (GS–11–A and GS–16–A) are almost entirely Overburden Mud, but samples from GS–12 and GS–21 include only a small part of the unit. The GS–11 and GS–16 cores, from the central segment of the deposit, contain ony 7.6 percent acid-insoluble material. Most of the remaining portions of these cores are halite (as shown by X-ray data combined with the high Na and Cl percentages) with some hanksite (as shown by X-ray data combined with the high $SO_3$ and low $CO_2$ percentages). Some pirssonite is present. The sample from near the top of the unit in core hole GS–40 (table 18) contains 81.8 percent acid-insoluble material, the rest being mostly halite with small amounts of other saline minerals forming the balance.[16] The mud sample from near the basal contact of core GS–40 contains only 32.4 percent acid-insoluble material and larger amounts of dolomite, pirssonite, gaylussite, and halite.

[16] The percentages of acid-soluble $K_2O$ appear too high. The discussion of analytical problems encountered in making analyses of samples from the Parting Mud (p. 54) applies to the two analyses in table 18.

# RADIOCARBON AGES OF STRATIGRAPHIC UNITS

By

MINZE STUIVER[17] and GEORGE I. SMITH

## INTRODUCTION

Radiocarbon ages, together with the stratigraphy and mineralogy, provide a basis for reconstructing the climatically controlled history of Searles Lake. The large number of published $^{14}C$ dates that have been determined on core samples from Searles Lake (fig. 30) are taken from publications by Flint and Gale (1958), Rubin and Berthold (1961), Ives, Levin, Robinson and Rubin (1964), and Stuiver (1964). Of the 74 dates shown in figure 30, 40 are based on carbon from inorganic carbonate minerals, and 2 are on wood fragments.

Fourteen previously unpublished dates on disseminated organic carbon from the Lower Salt and the top of the Bottom Mud are given in table 19.[18] These samples were collected in November 1964 from core L–31 in order to obtain a detailed chronology of the wet-dry episodes in the Lower Salt deposits.

The dated samples plotted in figure 30 are grouped according to the stratigraphic unit from which they came. Stratigraphic assignments were based on the reported sample depths and logs of the sampled cores. The relative positions of samples from the Parting

[17] Quaternary Research Center, University of Washington, Seattle, Wash. 98195.

[18] Support of the $^{14}C$ work was through N. S. F. grant GS–36762 to M. Stuiver.

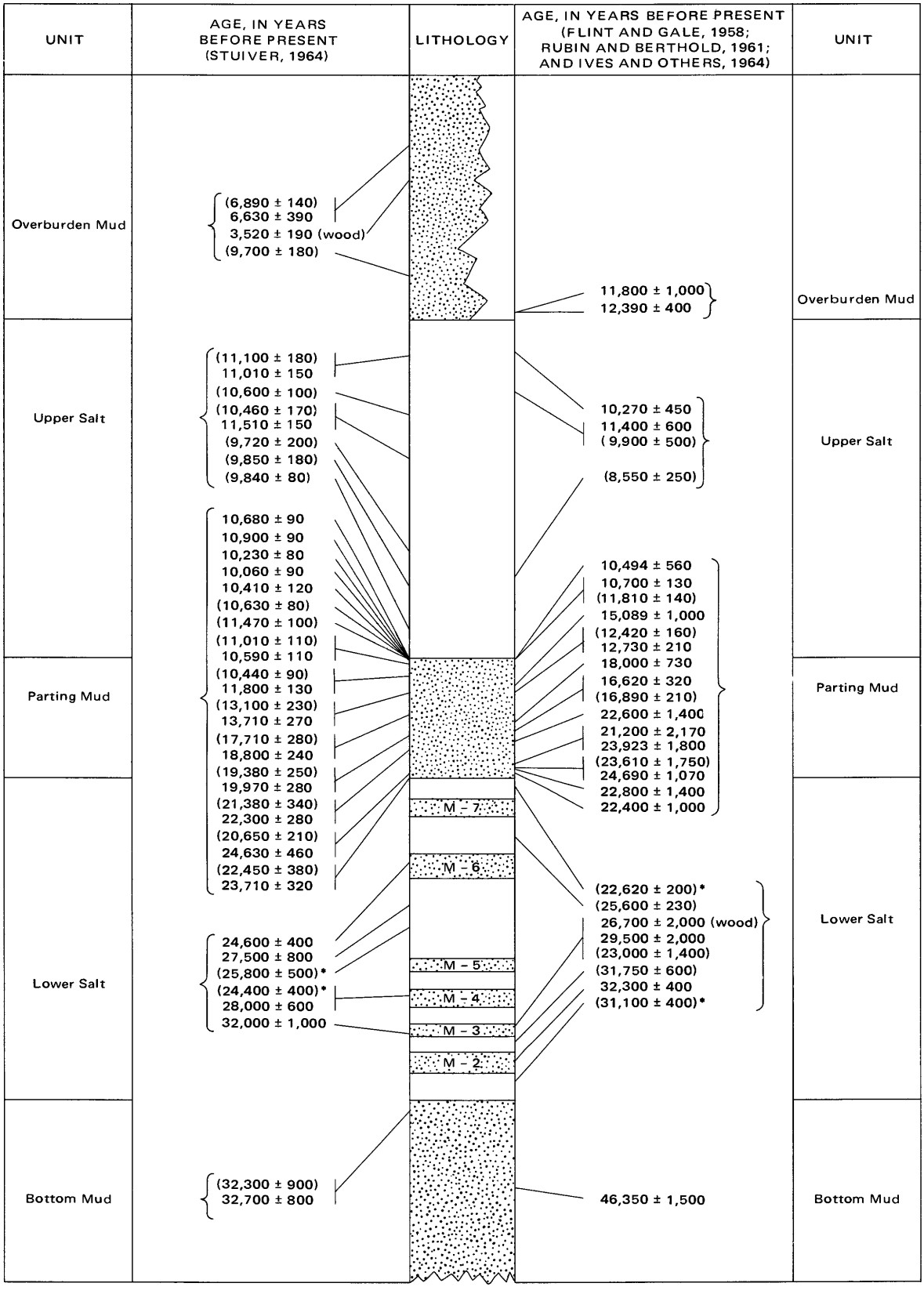


FIGURE 30.—Summary of published $^{14}C$ dates on subsurface samples from Searles Lake. Dates in parentheses are on carbon in inorganic carbonates and are considered relatively unreliable; dates followed by asterisks (*) were suspected by Stuiver (1964) of being contaminated; remaining dates, except for two on wood, are on organic carbon disseminated in lake mud.

TABLE 19.—*New $^{14}C$ dates on disseminated organic carbon in mud layers of Lower Salt and top of the Bottom Mud, core L–31*

| Sample | Depth | Years B.P. |
|---|---|---|
| Y–2230 | Top 5 cm of M–7 | 23,750 ± 300 |
| Y–2231 | Bottom 5 cm of M–7 | 26,350 ± 350 |
| Y–2232 | Top 5 cm of M–6 | 24,760 ± 300 |
| Y–2233 | Bottom 5 cm of M–6 | 28,880 ± 500 |
| Y–2234 | 5 cm thick layer near base S–5 | 27,550 ± 400 |
| Y–2235 | Top 5 cm of M–5 | 28,380 ± 350 |
| Y–2236 | Bottom 5 cm of M–5 | 29,040 ± 350 |
| Y–2237 | Top 5 cm of M–4 | 28,620 ± 350 |
| Y–2238 | Bottom 5 cm of M–4 | 30,160 ± 400 |
| Y–2239 | Top 5 cm of M-3 | 30,510 ± 400 |
| Y–2240 | Bottom 5 cm of M–3 | 30,270 ± 500 |
| Y–2241 | Top 5 cm of M–2 | 30,280 ± 300 |
| Y–2242 | Bottom 5 cm of M–2 | 32,620 ± 500 |
| Y–2243 | Top 5 cm of Bottom Mud | 32,800 ± 600 |

Mud are approximate; dated samples came from many cores, and the level within the unit was estimated and plotted on the basis of its proportionate position between the base and top of the Parting Mud in that particular core hole.

## RELIABILITY OF SAMPLED MATERIALS

Dates on wood are considered to be the most reliable. Dates on disseminated organic carbon are considered less reliable because most are probably somewhat too "old." Dates on carbonate minerals may be either a little too "old" or too "young" and are therefore the least useful. The reasons leading to this ranking of reliabilities are given below.

The dates on wood are considered best because they are on material that is relatively unsusceptible to replacement by younger carbon, and because they presumably derived carbon from atmospheric $CO_2$ rather than from the lake. The only predictable discrepancies between $^{14}C$ dates and true dates are produced by the variation in the atmospheric $^{14}C$ through geologic time which is known for the past 7,400 years from comparison of $^{14}C$ dates with tree-ring dates, and the minor discrepancies that result from fractionation of $^{14}C$ by some plants and trees during their growth. The $^{14}C$ date of 3,520 ± 190 on wood corresponds to a tree-ring age of 3,720–3,800 years (Ralph and others, 1973, p. 11; Stuiver and Suess, 1966, p. 539). The $^{14}C$ date on wood of 26,000 ± 2,000 years is too old for comparison with tree-ring chronologies. Carbon isotope fractionation during plant growth can be calculated by measuring $^{13}C/^{12}C$ ratios. When $^{13}C$ measurements are lacking, age errors of a few hundred years may be introduced.

Dates derived from disseminated organic carbon form the main basis for the time scale used to interpret and correlate the stratigraphic section in Searles Lake. These dates had to be used because wood fragments are rare in the sediments, and a few hundred grams of almost any subsurface sample of mud provides enough disseminated organic carbon for dating. Most mud samples contain several percent carbon in the acid-insoluble fraction that commonly makes up 15–25 percent of the total sample (Stuiver, 1964, table 4; this report, table 13). A sample adequate for dating may therefore be obtained from normal-sized cores by a horizontal slice 1–2 cm thick that probably represents less than 100 years of sedimentation. The organic compounds in these muds do not seem to have changed their composition greatly since deposition (Vallentyne, 1957) although some change is indicated by the secondary organic components noted by Mankiewicz (1975).

Broecker and Kaufman (1965, p. 554) suggest that dates on such material from Searles Lake are likely to be about 2,200 years too "old." An error in this direction is anticipated because the original $^{14}C/^{12}C$ ratios in most lacustrine organisms reflects the ratios in the lake waters, and those ratios were probably not the same as in the contemporaneous atmosphere because of the slow rate at which atmospheric $CO_2$ exchanges with water. The suggested magnitude of error is based on a calculation of the amount of $CO_2$ in solution and the probable exchange rate that indicates that the ratio of $^{14}C$ in the $CO_2$ dissolved in the original lake was only 77 percent that of the atmosphere, giving an apparent age of 2,200 years. The lake area of 250 $km^2$ assumed by them is about correct when the lake stood at a level near 1,750 ft (530 m), and this is reasonable for the lakes that existed during the time the Lower Salt was being deposited (Smith, 1968, fig. 4). At the time the Parting Mud was deposited, however, the average elevation of the lake surface was near 2,000 ft (610 m) and its area about 400 $km^2$. Using their formula and revised values for the average lake area during its expanded stages of 400 $km^2$ and for the number of moles of $Na_2CO_3$ of $2.7\times10^{12}$ (table 17), the percentage of $^{14}C$ in the lake relative to that of the atmosphere becomes 83, indicating an original apparent age of 1,500 years. Broecker and Kaufman (1965) found that modern organic material from Mono and Pyramid Lakes gives apparent ages of 1,800 and 800 years, respectively.

Some confirmation of this magnitude and direction of error predicted by Broecker and Kaufman (1965) results from comparison of two dates from unit M–3 of the Lower Salt (fig. 30). The date of 29,500 ± 2,000 on disseminated organic carbon is 2,800 years older than the date on wood from the same horizon, but the large experimental uncertainty on both samples must be considered in drawing conclusions from this comparison. A similar comparison can be made with the date on wood from the Overburden Mud where one date on disseminated organic carbon from a slightly greater

depth is about 3,000 years older than the dated wood. An age difference twice as large results if other dates on disseminated organic carbon from nearby horizons are compared with the wood date.

It is difficult to assess the extent of disequilibrium between atmospheric and lacustrine $CO_2$ during various stages in the history of Searles Lake. One reason is that some of the lakes appear to have been density stratified (Smith and Haines, 1964, p.52; Smith, 1966, p. 174–176). In such lakes, most organisms live in the less saline and less dense surface layer where photosynthetic activity is greatest. The volume of such a surface layer is only a fraction of the total volume of the lake, and the proportion of total carbonate in it even less because of its lower salinity. The $CO_2$ in the surface layer of a stratified lake, must therefore be more nearly at equilibrium with the atmosphere than is the near-surface concentration of $CO_2$ in an unstratified lake having the same total salinity (Deevey and Stuiver, 1964, p. 6). During the times represented by organic-rich mud layers in Searles Lake, both stratified and unstratified lakes probably existed, but it is not possible to reconstruct the physical and organic regime of the lake at all stages represented by samples.

Additional sources of error come from the fact that during most stages of deposition, older lake deposits were undergoing erosion. They contributed both detrital organic carbon and older $CO_2$ as their carbonate was dissolved. Pre-Quaternary carbonate rocks in Searles Valley are virtually restricted to the north quarter of the Slate Range. Broecker and Walton (1959, p. 24) consider the effects of this process to be negligible in lacustrine environments. Oana and Deevey (1960, p. 265) found evidence based on $^{13}C$ ratios in Searles Lake muds that the process was potentially a major source of error, but with a larger number of samples, Stuiver (1964, p. 389–390) was unable to detect the trend on which their conclusion was based. The many pairs of dates on coexisting carbonate and organic carbon have differences that range from insignificant to 6,500 years. Such differences may be produced in part by variations in the ratio of contaminating carbon introduced in the two forms; dates on both carbonate and organic carbon would reflect the $CO_2$ dissolved from older carbonates, but only the dates on organic carbon would reflect the detrital older carbon.

These diverse sources of error lead to diverse possible combinations. For example, the quantity of carbonate dissolved from older lake sediments and transported as dissolved $CO_2$ into the existing lake was partly a function of the area of sediments preserved and exposed around the lake; the $CO_2$ derived from this source affected both organic carbon and inorganic carbonate in the new lake sediments. The quantity of detrital carbon was influenced by the area of exposure, but it affected only the organic carbon fraction of the new sediments. The rate of new organic carbon production in the lake changed as the concentrations of nutrients and other salts varied, and this variation in productivity affected the ratio of new to reworked organic carbon in the sediments. Moreover, precipitation of $CaCO_3$ was the result of two mechanisms, annual evaporation and mixing with the underlying saline water; the relative importance of the two mechanisms determined how much carbon came from the $CO_2$ in the surface layer of fresh water (and was thus nearly modern) and how much came from the $CO_3$ in the underlying layer (which was less equilibrated and therefore not so modern).

As dates on carbonate minerals involve uncertainties as to the original $^{14}C$ ratio of the $CO_2$ in solution and other factors, neither the direction nor the magnitude of displacement of $^{14}C$ ages on carbonate minerals can be evaluated. Like the organisms that produced the organic carbon in muds, they reflect the $^{14}C$ content of the carbonate and $CO_2$ dissolved in the water, and this ratio was contemporaneous only to the extent that it was equilibrated with the atmosphere. Many of the dated carbonate minerals (such as gaylussite and pirssonite) were formed from moderately saline brines and others (such as trona) came from highly saline brines. Brines represent periods when the lake area was smallest and the rate at which $CO_2$ was equilibrated with the atmosphere at its lowest. Most carbonate minerals formed, therefore, at times when equilibration with the atmosphere was less complete than during periods when the lake contained relatively fresh water and the deposits consisted of organic muds.

Additional change can occur after burial if either younger or older carbon is introduced during recrystallization of the carbonate minerals. Older carbon from deeper horizons may be introduced by carbonate brines that migrate upward during compaction. Carbon from older zones may have come from upward moving $CO_2$ produced by microorganisms that continued to assimilate organic matter after burial (although it is uncertain how long $CO_2$ can avoid being converted to methane in the reducing environment provided by these muds). At some time during the history of Searles Lake, when the hydrostatic brine level became like that of the present, carbon from younger horizons began to be introduced into deeper levels because of the downward movement of brines (Hardt and others, 1972, fig. 10). The hydrogen-deuterium ratios of the interstitial brines and hydrated salts in the mud units

suggest, according to unpublished data, that most of the gaylussite crystallized from brines that had migrated from above; dates on those crystals are therefore expected to be too young.

Many trona layers are bedded and fine grained, and their crystals appear to have stopped recrystallizing soon after the layer was deposited. If the brines in which they grew or recrystallized were near equilibrium with the atmosphere, they are correspondingly reliable carbonate minerals for dating purposes. Whether the brines had reached the required state of near-equilibrium is difficult to determine by an independent method.

All gaylussite and pirssonite crystals in the mud layers were crystallized after the muds in that horizon were deposited and largely compacted (Smith and Haines, 1964, fig. 15; Eugster and Smith, 1965, pl. 1), and all dates on those minerals are suspect. Stratigraphic unit M–3, the unit that provided wood and disseminated organic carbon for dating, contains gaylussite crystals that yielded a $^{14}C$ date (fig. 30) of $23,000 \pm 1,400$ years. This is 3,700 years younger than the wood. If the date on wood is correct, the gaylussite contains about 2.1 percent more modern $^{14}C$ than the wood and may represent contamination to that extent. A liklier mechanism is that the gaylussite formed by the reaction between aragonite or calcite and $Na_2CO_3$-rich brines from above:

$$CaCO_3 + 2Na^+ + CO_3^= + 5H_2O = CaCO_3 \cdot Na_2CO_3 \cdot 5H_2O$$

If the original $^{14}C$ content of the aragonite was the same as the wood, 3.6 percent modern, and the gaylussite is 5.7 percent modern, then by the above equation, the $CO_3^=$ added from brine must have had a $^{14}C$ content of 7.8 percent modern, or an apparent age of 20,500 years.

Most other pairs of carbonate-organic carbon dates do not differ by this much, and about a third differ in the opposite direction. Of the 22 paired dates on carbon and carbonate listed by Flint and Gale (1958, table 2) and Stuiver (1964, tables 1, 2, and 3), 14 of the carbonate ages are younger than the organic carbon (average difference = 1,710 years), and 8 are older (average difference = 520 years).

It seems, therefore, that carbon exchange mechanisms that operate during recrystallization of carbonate minerals are not predictable in terms of either direction or amount. Even when dates on carbonate and organic carbon are determined in pairs, their relative ages cannot be used to indicate whether "old" or "young" carbon was introduced during carbonate recrystallization because the amount of "old" carbon in the organic sample cannot be independently determined.

An opportunity to make a detailed study of paired dates is provided by the 10 pairs listed by Stuiver (1964, table 2) obtained from samples of three cores from the Parting Mud. The three secondary carbonate samples from the top 10 percent of the unit are 200–1,410 years "older" than the organic carbon in the surrounding muds, and the seven samples that lie in the lower 90 percent of the unit are 590–3,980 years "younger". The relation between dates appears too consistent in direction to be accidental.

Stuiver (1964, p. 384–387) suggested that this relation could be explained by the downward diffusion of $^{14}C$ from the top part of the unit, as this isotope had a higher concentration in the brine in that part of the unit and substantial diffusion could have taken place during the 10,000-year period that followed its deposition. Those calculations however, required the top of the Parting Mud to be sealed off by the Upper Salt against post-depositional diffusion of any $^{14}C$ from above, which we now consider unlikely. It seems liklier that the porous carbonate salts at the base of the Upper Salt provide a poor seal, and that the brines in the Upper Salt constitute an available source of carbonate brine having a greater concentration of $^{14}C$ available for diffusion. If this is so, the mechanism is removed by which the carbon as $CO_3$ near the top could have become depleted in $^{14}C$ by downward diffusion while the underlying deposits became enriched and thereby appear younger; downward diffusion of $^{14}C$ from the Upper Salt would instead have maintained or increased the amount of $^{14}C$ in the carbonate of the top part so that its apparent age remained the same or became younger.

It is unlikely that this relation between dates can be entirely explained by the diffusion of high carbonate brines into the Parting Mud. Postdepositional movement of such brines was probably responsible for the recrystallization of aragonite and calcite to form the gaylussite or pirssonite crystals that were dated. This mechanism would have required the migration of carbonate-bearing brines in opposing directions; the carbonate minerals in the top 10 percent of the Parting Mud would have had to incorporate $CO_3$ from older brine that migrated upward from underlying horizons, the carbonate in the lower 90 percent to incorporate $CO_3$ from brine that migrated downward from overlying horizons.

An alternative explanation stems from the possibilities that (1) during deposition, all the original $^{14}C$ ages were too old and that successive $^{14}C$ ages on both carbonates and organic carbon differed from the correct age and from each other by varying amounts, (2) that during diagenesis, all apparent dates on carbonate minerals decreased by a relatively uniform

amount as they incorporated $CO_3$ from downward-migrating brines. The upper 10 percent of the Parting Mud appears to represent a period when the lake was strongly stratified. In those thin and relatively fresh surface layers, organic carbon was probably generated with apparent $^{14}C$ ages that were nearly modern, whereas the submerged and unequilibrated $CO_3$-rich brines of the lower zone (which supplied the carbon for most of the crystallizing $CaCO_3$) was producing apparent $^{14}C$ ages that were substantially old. If those apparent ages were too old for the subsequent recrystallization of carbonate minerals to reverse, the present deposits would have organic carbon dates "younger" than the carbonates--the relation we now see. The lower 90 percent of the Parting Mud, on the other hand, appears to represent a time when the lake was unstratified or less frequently stratified so that most of the organic carbon and carbonate was produced in the same layer and probably slightly old. When more modern carbon was later introduced during diagenesis of the carbonate minerals, it caused the apparent $^{14}C$ age of the minerals to appear less than the organic carbon.

A change in the structure of the lake according to this pattern is reasonable in view of its history during Parting Mud time as deduced from surface mapping (Smith, 1968, fig. 4). The last brief episode of lake expansion (and mud deposition) required introduction of a large amount of new water each year into a basin that had contained smaller and more saline lakes for several thousand years. The new and relatively fresh water introduced by streams was probably nearly in equilibrium with the $CO_2$ of the atmosphere (Broecker and Walton, 1959, p. 32). Carbon in the underlying body of saline water probably would have been "older" because incompletely equilibrated and possibly because large areas of older lake deposits were exposed to erosion so that their carbon and carbonate were added to the lake. Earlier stands of the lake during Parting Mud time were mostly lower and changed less rapidly; new water had more time to mix and form an unstratified lake that was less completely equilibrated and thus depositing both organic and inorganic carbon that was slightly old.

Considering the possible sources of error in most $^{14}C$ dates from Searles Lake, the agreement between dates obtained from different materials and determined in different laboratories is surprisingly good. What the discussion shows is that the dates must be considered individually. The nature of the material, the lake history at the time the sample material was deposited, the subsequent history of the layer, and the size of the experimental uncertainty all must be considered.

The discussion here shows that $^{14}C$ dates on wood samples are best although wood samples from the Searles Lake deposits are rare. They can be used without a correction and with confidence, especially if the experimental uncertainty is doubled, increasing the liklihood from two-out-of-three- to nineteen-out-of-twenty that the correct date lies in this range. Dates on disseminated organic carbon and carbonate are much more abundant, but several factors other than age influence their $^{14}C$ content. Most factors tend to make the disseminated organic carbon samples appear old relative to their true $^{14}C$ age. Present-day analogs and calculations of reasonable models show that this error may range in size from several hundred to a few thousand years. The age assignments that follow are mostly based on disseminated organic carbon; the "corrected" $^{14}C$ ages assume that the reported dates are 500–2,500 years too old. Carbonate mineral samples may have an error of comparable size but either young or old, and these samples provide only a supplementary basis for estimating the ages of units in Searles Lake. With these considerations in mind, the contacts of the mud units are interpreted to have uncorrected and corrected $^{14}C$ ages as follows.

## PROBABLE TRUE AGES OF STRATIGRAPHIC UNITS

In the Overburden Mud, only the one date on wood is regarded as reliable. The wood was recovered from a depth of 2.4 m, about one-third of the depth to the base of this unit, and its age was $3,520 \pm 190$ years (Stuiver, 1964, p.381). The unit was deposited in a much smaller lake than most other mud units (Smith, 1968, fig. 4), and large amounts of older lake beds containing carbon and carbonate minerals were exposed to erosion. Possibly it was contamination from these widespread deposits that accounts for the extreme discrepancy between the date on wood from this unit and the dates on both detrital carbon and carbonate from nearby horizons. The $^{14}C$ age of the basal contact of the Overburden Mud is more than $3,500 \pm 400$ years and less than the age of the Parting Mud.

The seven $^{14}C$ dates from organic carbon derived from the top of the Parting Mud are within a few hundred years of each other (fig. 30). Their average is about $10,500 \pm 165$ years. An earlier estimate of the $^{14}C$ age of this contact was 10,200 years (Stuiver, 1964, p. 382). Quite likely all the dates are too "old" because of the unequilibrated older $CO_2$ that existed in the lake water. The corrected $^{14}C$ age of this contact is therefore likely to be between 8,000 and 10,000 years B.P. The minimum correction leading to the older date is favored because Searles Lake was apparently stratified and the $^{14}C$ that became photosynthetically fixed in the upper layer was therefore more nearly contemporaneous.

The base of the Parting Mud is represented by several dates on organic carbon (fig. 30). The two nearest the base average about 23,000 ± 900 years. The seven dates on the lowest 0.5 m average 23,300 ± 1,175 years. Stuiver (1964, p. 382) estimated the $^{14}C$ age of the basal contact to be about 24,200 years old, the rounded average of the two most reliable dates from the base of the unit. An age of 24,000 years is used here, but the discussion shows that ages spanning more than 1,000 years can be derived. Again, there is reason to suspect that most of the organic carbon was too "old" when deposited the corrected $^{14}C$ age of the base of this unit probably lies between 21,500 and 23,500 years.

Published dates on units within the Lower Salt include six dates on disseminated organic carbon and one on wood (fig. 30). In addition, 13 dates are now available on disseminated organic carbon from core L–31. (table 19). Where possible, samples were collected from the top and bottom sections of the mud layers in the Lower Salt. The ages increase downward from 23,750 ± 300 at the top of M–7 to 32,800 ± 600 at the top of the Bottom Mud, a range of 9,050 years. A minor reversal is represented by the age for the top of M–6 (24,760 ± 300), although it is consistent with the age of 24,600 ± 400 years previously determined on a sample from the upper part of M–6 (Stuiver, 1964 and fig. 30). Plotting this series of $^{14}C$ ages against depth (fig. 31) points up the relatively long periods represented by the muds and the short intervals represented by the salts. For instance, units M–7, M–6, and M–2 together account for approximately 6,500 years of the 9,000 year long Lower Salt episode. The top of unit S–5 represents the only period of desiccation in this unit. It is bracketed by ages of 27,550 ± 400 and 28,880 ± 500 years; its $^{14}C$ age is thus near 28,000 years B.P.

The lake history during Lower Salt time was complex and changed rapidly (Smith, 1968, fig. 4). It is thus difficult to evaluate the probable degree of $CO_2$ equilibration between the atmosphere and the lake waters that contained the majority of organisms or the amount of older carbon and carbonate that was washed into the lake from the surrounding slopes. The difference between dates from unit M–3 on disseminated carbon (29,500 ± 2,000) and wood (26,000 ± 2,000) suggests a 2,800-year lag in the exchange of $CO_2$ in the lake with the atmosphere, but the large experimental uncertainty in both dates makes it unwise to use the size of this difference rigorously. The top of M–6 may represent a time when the $CO_2$ in the lake was close to equilibrium with atmospheric $CO_2$, and its age, 1,500 years younger than the projected age of this horizon in figure 31, may be the ones

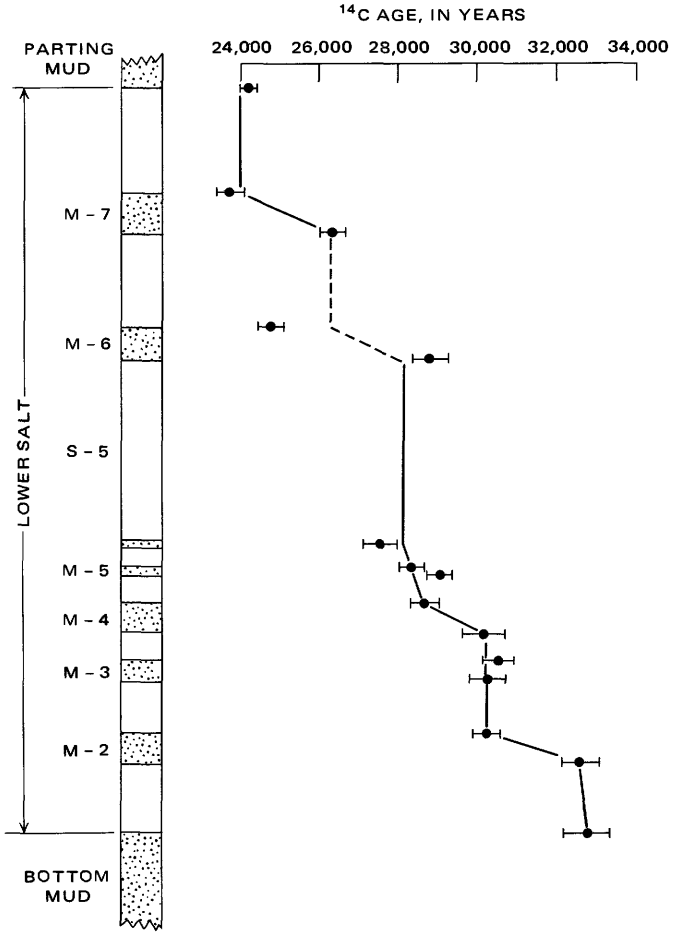


FIGURE 31.—Relation between depth and new $^{14}C$ ages of mud layers in Lower Salt.

that are too old by 500–2,500 years. The corrected $^{14}C$ age of the period of major dessication (S–5) is therefore interpreted to be between 25,500 and 27,500 years, and the age of other mud units to be correspondingly less than reported.

The two $^{14}C$ dates on organic carbon from the top part of the Bottom Mud give ages of 32,700 ± 800 years (fig. 30) and 32,800 ± 600 years (table 19). These ages are interpreted to mean that the uncorrected and rounded age of the contact is about 32,500 ± 700 years, and that the deposition of the Bottom Mud actually ceased some time between 30,000 and 32,000 years ago.

The base of the Bottom Mud is too old for radiocarbon dating. The period of time required for its deposition is inferred by extrapolation of sedimentation rates determined from the Parting Mud (table 20) and from the top 3 m of the Bottom Mud. This period is then added to the age of its top contact, which is approximately 32,500 years. This calculation is not greatly affected by uncertainties about the degree of $CO_2$ equilibration in a lake because the sedimentation

rates are based on the differences between dates on disseminated organic carbon which are subject to comparable errors. As discussed in the next section, it probably should be corrrected on the basis of the percentage of acid-insoluble material, which is higher in the Bottom Mud than in the Parting Mud.

An unpublished study by Goddard (1970) compares dates on salts obtained by $^{230}Th/^{234}U$ techniques with dates obtained by $^{14}C$ techniques.[19] Twenty samples from two cores of the Lower Salt and two samples from the Upper Salt were dated by both methods and found to be in general agreement. Better agreement among dates on the Lower Salt was found when the $^{14}C$ age was reduced by 1,900 years to account for the lag in isotopic equilibrium of lake waters with the atmosphere. He concludes that the absolute ages of salt units in the Lower Salt are as follows:

| *Unit* | *Age ($\times 10^3$ years)* |
|---|---|
| S–7 | $23.0 \pm 1.0$ |
| S–6 | $23.9 \pm 1.0$ |
| S–5 | $26.1 \pm 1.0$ |
| S–4 | $26.3 \pm 1.0$ |
| S–3 | $28.5 \pm 1.0$ |
| S–2 | $29.8 \pm 1.0$ |
| S–1 | $31.3 \pm 1.0$ |

Samples from depths of 7.6 and 21.5 m in the Upper Salt gave $^{230}Th/^{234}U$ dates of $13.8 \pm 1.2 \times 10^3$ and $10.0 \pm 0.2 \times 10^3$ years, respectively.

Using the average sedimentation rates for mud (table 20) without any correction, the base of the Bottom Mud is calculated to have an age of $143{,}000 \pm 6{,}000$ years. (In calculating these numbers, the age of the top contact of the Bottom Mud was rounded to 33,000 years.) (In calculating these numbers, the age of the top contract of the Bottom Mud was rounded to 33,000 years.) The faster and slower sedimentation rates given for cores 129 and X–20 in table 20 indicate ages of $132{,}000 \pm 12{,}000$ and $155{,}000 \pm 9{,}000$ years. Correcting the sedimentation rates on the assumption that the sedimentation rate of acid-insoluble components increased so that they accounted for 30 percent of the sample (while the carbonate sedimentation rate remained constant), the base of the Bottom Mud is calculated to have an age of 129,000 years, with the corrected faster and slower sedimentation rates indicating ages of 119,000 and 139,000 years. Correcting the sedimentation rate on the assumption that the carbonate sedimentation rate decreased enough for the percentage of acid-soluble material to increase to 30 percent indicates the base of the Bottom Mud to be about 195,000 years old. In this paper, an age of 130,000 years, a rounded value based on the corrected average sedimentaion rate, is used for the base of the Bottom Mud, but the above discussion indicates the level of uncertainty.

[19]Data later included in : Peng, T.-H., Goddard, J. G., and Broecker, W. S., 1978, A direct comparison of $^{14}C$ and $^{230}Th$ ages at Searles Lake, Calif: Quaternary Research, v. 9, no. 3, p. 319–329.

## RATES OF DEPOSITION

A knowledge of approximate rates at which salts and muds were deposited in Searles Lake helps interpret the depositional history in the basin. The depositional rates of salts and muds can differ by about three orders of magnitude. Estimates of the rates for each follow.

Salts crystallize from a body of brine at a maximum rate that is determined by the annual evaporation. Some salts (such as natron and mirabilite) crystallize at an accelerated rate during winter because their solubility is markedly reduced by low temperatures, whereas others (such as halite) are virtually unaffected by temperature change. The net accumulation in a year, though, reflects the amount of water lost by evaporation in the preceding year reduced by the amount of new water that was added to the lake during the year. The maximum rate of saline deposition is thus determined by the annual evaporation when no new water is added during the year. Unless the lake begins to expand, the minimum rate is determined by the amount of new dissolved material that is introduced during the year because the water that brought it in must be evaporated and the dissolved salt crystallized out.

Evaporation rates of brines can be derived in two ways: (1) by calculations based on evaporation rates from standard evaporation measurement pans, or (2) by comparison of measured evaporation rates from natural brine bodies. The results, derived below, suggest maximum rates of accumulation of porous salt layers to be between 25 and 40 cm per year. These rates mean that all the salt layers in the Bottom Mud, and all but one of the layers in the Lower Salt could be the result of less than 5 years of crystallization. Unit S–5 of the Lower Salt might represent only a quarter of a century. The Upper Salt might represent half a century.

Rates based on evaporation pan data must first be multiplied by a factor approximated in a desert environment by 0.6 to adjust for the differences in the heat distribution, surface character, circulation, and size of large natural bodies of water relative to small shallow test pans (Blaney, 1955, 1957). The result of this calculation must then be multiplied by a factor that normally lies somewhere between 0.6 and 0.8, depending on the species and concentrations of ions in the solution,[20] as well as the evaporation rate, humidity, and temperature of the brine (Harbeck, 1955). Using rea-

[20] This factor is applicable to most solutions whose anions are dominated by Na and

sonable values for these factors and applying them to the saline lakes that existed in Searles Valley during the periods represented by salt layers suggests maximum depositional rates about 15–25 cm of solid salts per year, or 25–40 cm of porous salts.

A series of measurements on evaporating brine from Owens Lake allows a second means of estimating maximum salt crystallization rates. That lake, 100 km northwest of Searles Lake, is 600 m higher, so therefore has a slightly less arid climate. Owens Lake is normally almost dry, but becomes flooded whenever runoff in Owens Valley greatly exceeds the capacity of the Owens Valley aqueduct, which carries water to Los Angeles. In the winter of 1937–38, Owens Lake flooded, and between mid-April 1939 and mid-April 1940, evaporation lowered the level of Owens Lake by 46.9 inches (119 cm) (Dub, 1947, table 3). During the same period, 6.69 inches (17 cm) of rain fell on the lake, meaning that total evaporation from its surface was 53.6 inches (136 cm). The brine had a $Na_2CO_3$ + $Na_2B_4O_7$ + $Na_2SO_4$ + NaCl content of 154,000 ppm at the beginning of this period and a content of 310,000 ppm at the end. Saturation with sodium carbonate probably occurred during July 1939 when a salinity of about 220,000 ppm was reached. Approximately 29 inches (73 cm) of net evaporation occurred during the 9-month period that followed. A brine body, 73 cm deep and containing 220,000 ppm solids (about 245,000 mg/L), would precipitate 9 cm of solids (assuming a specific gravity of 2.1) or about 15 cm of porous salts containing 40 percent brine. Extrapolating linearly from 9 months to a full year indicates nearly 19 cm of porous salts as an annual accumulation rate, but the actual rate might be nearer 25 cm because the three unrepresented months are May, June, and July, when about 40 percent of the annual evaporation takes place (Lee, 1912, table 50).

Work by Friedman, Smith, and Hardcastle (1976) on Owens Lake following another period of flooding in the spring of 1969 permits another estimate. A maximum water depth of about 2.4 m was reached in August 1969, and this water had virtually all evaporated by September 1971; the net evaporation rate was therefore about 120 cm per year. Sodium carbonate salts began to crystallize in mid-August 1970 from 168 cm of brine. Since the salinity of the brine at that time was near 250,000 mg/L, about 20 cm of nonporous salts (density = 2.1) should have accumulated upon desiccation, which took place a year later. This would be increased to nearly 33 cm if its porosity was 40 percent.[21]

Unless the saline lake begins to expand, the minimum rate of salt deposition is controlled by the amount of dissolved material introduced into the basin each year. If one assumes that the Owens River was the source of all solids that entered Searles Valley during a given year and that the quantity was the same as at present, an estimate can be made of the rate salts would have to be crystallized annually to maintain a steady state. In 1908, at a station in the lower Owens River, the water contained an average of 339 ppm solids and had an annual flow of 218,000 acre feet ($269\times10^6$ m$^3$) (Gale, 1914, p. 263). This flow carried, therefore, about $9\times10^{10}$ g of solids in solution, which, if crystallized in Searles Valley over the area of the Upper Salt (110 km$^2$), would amount to an annual layer of porous salts about 0.06 cm thick (17 yrs/cm). This rate is about three orders of magnitude less than the maximum estimated rate for salts and is comparable to the estimate of depositional rate for muds. Bradley and Eugster (1969, p. B35) used a depositional rate of 0.2 cm/yr (5 yrs/cm) in their calculations of saline depositional rates of trona beds in the Green River Formation. This rate was taken from Fahey's (1962, table 17) estimate based on the percentage of acid insoluble material in the saline beds.

Alternating light and dark beds of trona at the base of the Upper Salt and elsewhere have thicknesses ranging from about 1 to 30 cm (Haines, 1959, pl. 10; Smith and Haines, 1964, p. P22 and figs. 6, 7). These were formerly considered to be annual layers and thus were a means of estimating the rate of saline accumulation. However, the salines deposited in Owens Lake in 1970 and 1971 have many similar layers that apparently reflect weather cycles of a few days or weeks. Similar beds in the Searles Lake saline layers may also represent much less than a year.

Mud layers are deposited at much slower rates. Using thicknesses of the material compacted to its present form, the rate near the middle of the basin is probably near 0.025 cm/yr or 40 yrs/cm. Table 20 gives all of the $^{14}C$ dates from the Parting Mud that used organic carbon and represent a sequence of two or more from the same core. Rates implied by many of the 17 pair are meaningless because the differences between sample ages have large experimental uncertainties, or the intervals in the core were too close to allow the differences in $^{14}C$ dates to be significant. The differences between the uppermost and lowermost samples in cores X–20, X–23, L–U–1, and 129 are considered the most meaningful. They average $38\pm2$ yrs/cm and range from $34\pm4$ to $42\pm3$ yrs/cm. The

K. Solutions containing much Mg have their evaporation rates much more strongly affected by increased salinities because of the very large hydration energy of that ion. Turk (1970) studied the evaporation rate of $MgCl_2$-rich brines from the Bonneville Salt Flats and found that the most concentrated solutions reduced the evaporation rate to as little as 9.5 percent of the freshwater rate. Brines dominated by $CaCl_2$ would exhibit intermediate effects.

[21] Actually, by January 1971, a substantially greater amount of salt had accumulated at the Owens Lake sample site. The discrepancy is apparently caused by wind, which drove crystals growing on the surface of other parts of the lake to the sample site where they sank to the bottom.

TABLE 20.—*Depositional rates in Parting Mud*

[Based on $^{14}C$ dates *in* Flint and Gale (1958, table 2) and Stuiver (1964, table 2). Only dates on organic carbon are used, and only cores with two or more such dates are listed]

| Core | Midpoint of sample (ft below top of Parting Mud) | $^{14}C$ age (years) | Difference between sample depths (feet) | Difference between sample ages (years) | Depositional rates between intervals | | Depositional rates, uppermost to lowermost sample in core | |
|---|---|---|---|---|---|---|---|---|
| | | | | | yrs/ft | yrs/cm | yrs/ft | yrs/cm |
| X-16 | 9.35 | 22,600 ± 1,400 | 4.40 | 200 ± 1,980 | 45 | 1.5 | | |
| | 13.75 | 22,800 ± 1,400 | | | | | | |
| X-20 | .35 | 10,700 ± 130 | 1.28 | 100 ± 184 | 78 | 2.6 | | |
| | 1.63 | 11,800 ± 130 | 1.57 | 930 ± 247 | 592 | 19 | | |
| | 3.20 | 12,730 ± 210 | .20 | 980 ± 342 | 4,900 | 161 | 1,260 ± 97 | 42 ± 3 |
| | 3.40 | 13,710 ± 270 | 3.50 | 2,910 ± 419 | 831 | 27 | | |
| | 6.90 | 16,620 ± 320 | .38 | 3,350 ± 425 | 8,816 | 289 | | |
| | 7.28 | 19,970 ± 280 | 4.17 | 4,720 ± 1,107 | 1,132 | 37 | | |
| | 11.45 | 24,690 ± 1,070 | | | | | | |
| X-23[1] | .16 | [2]10,235 ± 105 | .61 | 355 ± 152 | 582 | 19 | | |
| | .77 | 10,590 ± 110 | 4.68 | 8,210 ± 264 | 1,754 | 58 | | |
| | 5.45 | 18,800 ± 240 | 3.60 | 3,500 ± 369 | 972 | 32 | 1,255 ± 41 | 41 ± 1 |
| | 9.05 | 22,300 ± 280 | 2.58 | 2,330 ± 538 | 903 | 30 | | |
| | 11.63 | 24,630 ± 460 | | | | | | |
| L-U-1[3] | .02 | 10,680 ± 90 | .06 | 220 ± 127 | 3,666 | 120 | | |
| | .08 | 10,900 ± 90 | .07 | −670 ± 120 | | | 1,065 ± 27 | 35 ± 1 |
| | .15 | 10,230 ± 80 | 12.10 | 13,480 ± 330 | 1,114 | 37 | | |
| | 12.25 | 23,710 ± 320 | | | | | | |
| 129 | .50 | 10,494 ± 560 | 3.00 | 4,595 ± 1,146 | 1,532 | 50 | | |
| | 3.50 | 15,089 ± 1,000 | 3.50 | 2,911 ± 1,238 | 832 | 27 | 1,049 ± 122 | 34 ± 4 |
| | 7.00 | 18,000 ± 730 | 5.00 | 4,562 ± 1,478 | 912 | 30 | | |
| | 12.00 | [2]22,562 ± 1,285 | | | | Avg. | 1,157 ± 72 | 38 ± 2 |

[1]Parting Mud assumed to be 12 feet thick.
[2]Average of two dates.
[3]Parting Mud in L-U-1 is 12.3 feet thick.

date of 17,100 ± 700 from a level 2.75 m below the top of the Parting Mud in core B (Mankiewicz, 1975, p. 10) suggests that the depositional rate of mud near the edge of the deposit (fig. 3) was near 24 yrs/cm (assuming the top of the Parting Mud in that area to be 10,500 yrs old).

The $^{14}C$ dates on organic carbon in two samples from the Bottom Mud (fig. 30) indicate a depositional rate of about 46 ± 6 yrs/cm. The upper date of 32,700 ± 800 represents the top 0.1 ft (.03 m) of the unit; the lower date of 46,350 ± 1,500 represents material at about 9.9 ft (3.0 m) depth.

There is a strong lithologic similarity between the dated sediments from the Parting Mud and the sediments in the Bottom Mud. Most of the Bottom Mud is too old for $^{14}C$ dating, but extrapolation by use of these sedimentation rates provides an approximation. The 30 m of sediments in the Bottom Mud contains 3–6 percent bedded salts (mostly nahcolite and mirabilite), probably deposited in very brief periods of time as a result of chilling the lake waters when they were moderately saline. Excluding these salts leaves the equivalent of about 29 m of mud. The average sedimentation rate calculated from dates in the Parting Mud (38 ± 2 yrs/cm) suggests that the Bottom Mud represents a period of deposition about 110,000 ± 6,000 years long. The fastest (34 ± 4 yrs/cm) and slowest (42 ± 3 yrs/cm) rates indicate depositional periods about 99,000 ± 12,000 and 122,000 ± 9,000 years long. The slower sedimentation rate indicated by the two dates at the top of the Bottom Mud (46 ± 6 yrs/cm) suggests a period of deposition about 133,000 ± 17,000 years long.

The variable percentage of acid-insoluble material in the Bottom Mud (fig. 6) shows that the relative importance of various sedimentation processes during Bottom Mud time was not constant. The increases in the percentage of insoluble material may have resulted from an increase in the rate at which water- or air-suspended clastic material was introduced, a very large increase in the rate of organic productivity, or a decrease in the rate of nonclastic precipitation while other rates remained constant. The average of the acid-insoluble percentages plotted in figure 6 is about 30, the average of the percentages given in table 13 for the Parting Mud about 20.

Starting with the balance of nonclastic, clastic, and organic sediments found in Parting Mud, an increase of 70 percent in the depositional rate of acid-insoluble clastic sediments, for example, would increase the total sedimentation rate 14 percent (assuming weight and volume percents are interchangeable) and produce a sediment containing 30 percent acid-insoluble material. An increase of 14 percent above the average sedimentation rate determined for the Parting Mud would change the average sedimentation rate for the Bottom Mud to about 33 yrs/cm. A 500 percent increase in clastic material would double the sedimentation rate and produce a sediment containing the observed maximum of 60 percent acid-insoluble material. Its sedimentation rate would be 19 yrs/cm. An average sedimentation rate of 33 yrs/cm for the 29 m

of mud in the Bottom Mud indicates a depositional interval that was about 96,000 years long.

The increase in the amount of organic material required to change the percentage of acid-insoluble material from 20 to 30 is too large to be a likely mechanism. The average sample of Parting Mud contains about 2 percent organic material, and this would have to increase 3,500 percent to produce the required 70 percent increase in acid-insoluble material.

The observed variation in the percentage of acid-insoluble material in the Bottom Mud might also be caused by a decrease in the sedimentation rate of the nonclastics (mostly carbonates). Again, starting with the balance of sedimentation processes found in the Parting Mud, a reduction of about 40 percent in the depositional rate of carbonate would produce a sediment containing about 30 percent acid-insoluble material. Its sedimentation rate would be about 68 percent that of the Parting Mud, or about 56 yrs/cm. This rate suggests a depositional interval that was more than 160,000 years long.

A final uncertainty in estimating the duration of the period represented by the Bottom Mud by using rates derived from the Parting Mud comes from lack of data on their relative densities and thus the relative extent of compaction. Core samples obtained from freshwater Lake Biwa, Japan, have mud densities at depths of 22–26 m (equivalent to the typical depth of the Parting Mud, although about twice as old) that average about 1.45 g/cm$^3$, whereas samples from depths of 38 m and 68 m (equivalent to depths of the top and base of the Bottom Mud) average about 1.50 g/cm$^3$ and 1.58 g/cm$^3$, respectively (Yamamoto and others 1974, fig. 1). These densities imply a compaction of the deeper samples that increases with depth from 3.5 to 9.0 percent above the value found for the shallower samples. The slope of their age/depth curve (fig. 3) indicates an apparent accumulation rate (after compaction) for the shallower zone of 25 yrs/cm, and rates for the deeper zone that average 28 yrs/cm, an increase of about 12 percent. A similar curve for sediments in Clear Lake, Calif. (Sims and Rymer, 1975, fig. 4) indicates apparent accumulation rates for the same depth zones of about 12.5 yrs/cm and 14 yrs/cm, a 12 percent difference. These data indicate that because of the greater compaction of the Bottom Mud sediments, a correction factor of 3–12 percent is probably required when estimating the period represented by its deposition. Such corrections would increase the age of the base of the Bottom Mud by 5,000–20,000 years and would partially or totally offset the corrections made on the basis of the increased clastic sedimentation rate; it would also explain some of the difference between the 38 yrs/cm average rate determined for the Parting Mud and the 46 yrs/cm rate determined for the top 3 m of the Bottom Mud.

## GEOCHEMISTRY OF SEDIMENTATION

All the late Quaternary lakes that existed in Searles Valley contained an appreciable percentage of dissolved solids (fig. 32). Even at its highest levels, salinities may have exceeded 1.5 percent and pH values probably exceeded 9. Chemical sediments deposited under these conditions consisted mostly of aragonite, calcite, or dolomite. These minerals probably contained most of the calcium, much of the magnesium, and some of the carbonate that was dissolved in those lakes. When the lakes shrank as a result of evaporation, salinities increased and some primary gaylussite may have crystallized. Eventually, saline layers composed of trona, halite, and related minerals formed, and they contain most of the other components originally dissolved in the lake. Only the quantities of those components required for phase equilibrium and the most highly soluble ions remained in solution.

The stratigraphic sequence of mud and salt layers beneath the surface of Searles Lake reflects the gross changes in chemical sedimentation and thus provides a first approximation of the chemical history of the

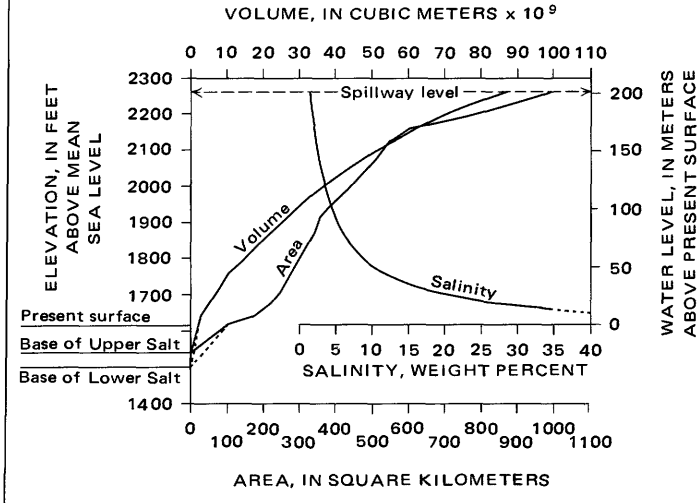


FIGURE 32.—Relation between elevation, area, and volume of the Pleistocene lake surface and approximate salinities of its waters. Based on USGS 15-minute topographic maps, measurements of area enclosed by each contour taken by planimeter, volumes between pairs of contours calculated using the prismoidal formula ($V = \frac{1}{3} C [A_1 + A_2 + (A_1 A_2)^{1/2}]$) where C is the contour interval, and $A_1$ and $A_2$ are areas enclosed by successive contours. Solid lines indicate volume and areas above base of Upper Salt (elev. 1,560 ft, 475 m); dotted portions indicate quantities above base of Lower Salt (elev. 1,500 ft, 457 m). Present surface is about 1,616 ft (493 m) above sea level. Salinity of waters that desiccated to form Upper Salt plotted on a curve based on the assumption that the total quantity of salts (given in table 17) was dissolved in a homogeneous lake having the indicated volume.

lake. Mineral variations within the mud and salt layers mostly indicate variations in the chemistry of the lake waters. When the mineral, chemical, and other lithologic criteria are combined, the lake history and many of the processes of chemical sedimentation can be reconstructed from the chemical sediments now found. In an earlier paper, Smith and Haines (1964) approximated these processes on the basis of mineral assemblages and crystal habits. The data presented here allow a more detailed reconstruction because they include both the relative percentages and the total volumes of minerals that constitute these assemblages.

Mud layers are discussed first because their evaporite composition represents the first components to precipitate from the lake waters. Salt layers represent the components that survived earlier precipitation and were eventually crystallized. Some components in the original lake never crystallized; most of these remained in the brines that filled the interstices of the salts (prior to extensive pumping by the chemical companies that extract chemicals from them) although some were incorporated into the waters of later lakes and lost by overflow. The chemistry of these brines is implicitly considered during discussion of the crystallization of the salts.

## MUD LAYERS

The mud layers beneath the surface of Searles Lake represent deposits formed in relatively fresh lakes that covered much of the floor of Searles Valley. At their maximum size, these lakes covered about 1,000 $km^2$; geologic mapping of the valley floor around the present dry lake shows that carbonate-rich muds were deposited in almost all parts of those expanded lakes. The muds below the present dry lake surface have been affected by diagenesis, but their lateral equivalents exposed around the edge of the valley commonly have similar lithologies, yet do not contain the minerals attributed to diagenesis and thus serve as samples of the original deposits. Their original similarity is not surprising; the chemical compositions of lake waters tend to be uniform over large areas, and primary chemical sediments deposited from them are comparably uniform.

Many of the deposits that crop out are light green, fine-grained, and locally laminated, and most of the samples from the deposits contain high percentages of aragonite, calcite, and (or) dolomite. Halite is commonly present in fresh samples, but not in quantities like those found in subsurface deposits. Analcime, searlesite, K-feldspar, and phillipsite—minerals thought to be produced by authigenesis in the subsurface deposits—have not been found in outcrops. Gaylussite and pirssonite are rarely found in outcrops, and there is no textural evidence in the exposed sediments that large quantities of megascopic crystals like those in subsurface muds ever existed; both minerals are soluble in water, and subaerial leaching normally produces some form of textural expression.

Of the nonclastic minerals in the subsurface mud layers, only aragonite, calcite, dolomite, and northupite are considered primary. Aragonite is most commonly an abundant mineral in the Parting Mud and upper part of the Bottom Mud (pl. 2*B*); the mineral is thermodynamically metastable, and the oldest occurrence is in the Bottom Mud, in sediments estimated to be about 50,000 years old.[22] Possible traces were found in the Lower Salt (table 6); but it is not found in the Overburden Mud (table 18) and Mixed Layer (pl. 2*A*). Calcite is locally abundant in the upper part of the Bottom Mud but is subordinate in the Parting Mud and nearly absent in the Overburden Mud, Lower Salt, and Mixed Layer. It is the only form of calcium carbonate found in sediments older than 50,000 years, and some of the calcite in older sediments may have been produced by diagenetic alteration of primary aragonite. Dolomite is abundant in the Bottom Mud, in some parts of the Overburden Mud, Parting Mud, and Mixed Layer, but it is absent from mud layers in the Lower Salt. Northupite is fairly common in most mud layers of the Lower Salt and apparently is the Mg-bearing mineral in those layers that contain no dolomite. The mineral is found in the top of the Bottom Mud and occurs sporadically throughout the Mixed Layer, but it is absent from the Overburden Mud and Parting Mud.

The amount of Ca that reached the center of the basin virtually required transportation to that area by relatively fresh water (Smith, 1966, p. 173–174). This conclusion results from evidence like the following. The average CaO content of the Parting Mud in core GS–16 is 13.1 percent (table 13). The unit in this core is 12.2 ft (3.72 m) thick and has an average density near 2.0. Each square centimeter of the surface of the Parting Mud in this part of the deposit, therefore, represents a column of mud that weighs 744 g and contains 97 g of CaO. As the Parting Mud was deposited in about 13,500 years, about $7.2\times10^{-3}$ g of CaO was deposited each year over each square centimeter of this part of the lake floor. And as most or all of this was originally deposited as calcite or aragonite, the least-soluble Ca-bearing minerals in the mud, about $12.9\times10^{-3}$ g/$cm^2$/yr of $CaCO_3$was precipitated. Evaporation from the lake surface determines the minimum amount of $CaCO_3$ precipitated each year, and if annu-

[22] Reported occurrences of aragonite in the Mixed Layer (Smith and Haines, 1964, p. P25) were not verified by X-ray diffraction.

al evaporation was 200 cm/yr, each cubic centimeter of evaporated water would have had to contain about 64 ppm $CaCO_3$, or 26 ppm Ca.

This is a reasonable quantity to expect from a freshwater lake in this climate. Pure water in equilibrium with $CO_2$ in the atmosphere (about 0.033 volume percent $CO_2$) at a temperature of 16°C is saturated with $CaCO_3$ at this concentration (Hutchinson, 1957, table 84). With increasing alkalinity, however, smaller concentrations represent equilibrium amounts. Calculating equilibrium quantities of Ca in alkaline brines is difficult, but analyses of comparable natural waters suggest limits. Jones (1965, table 7) cites numerous analyses of stream, spring, and lake waters from Deep Springs Valley, Calif., that have a composition and pH similar to the waters that probably existed in Searles Lake at various stages. Almost all are in contact with $CaCO_3$ or more soluble carbonate minerals. Only a few waters that contain more than 26 ppm Ca have a total dissolved solid content of more than about 1,000 ppm; the few that do have pH values less than 9 and small to unmeasurable amounts of $CO_3$ relative to $HCO_3$. The waters that desiccated to form the salts now in Searles Lake are very unlikely to have had these properties once concentration began.

As noted in the section in diagenesis, microcrystalline halite is found in large quantities in many of the mud layers and is considered the product of diagenesis from highly saline pore waters incorporated in the sediment at the time of deposition. This proposed mechanism conflicts with the evidence for fresh lake waters which was derived from the CaO content of the muds. This enigma can be resolved if one postulates that (1) cool fresh Ca-bearing water flowed into the basin during part of the year and spread as a layer over highly saline waters that occupied the basin during the remaining seasons, and (2) that the calcium in the fresh waters precipitated as aragonite, calcite, or dolomite as a result of both evaporation and mixing in the zone along the interface between the pre-existing saline water and the new fresh water. Salinity stratification seems unavoidable whenever a highly saline lake receives a small supply of new water on a markedly seasonal basis, and it can persist for very long periods with large or uniform inflow volumes because salinity stratification is very stable. The presence of Ca-carbonates in mud layers in the middle of the basin, therefore, is interpreted as an indicator that fresh water flowed into a lake that was chemically stratified.

Aragonite is commonly formed when $CaCO_3$ is precipitated rapidly from solutions with high pH and salinity (Zeller and Wray, 1956; Ingerson, 1962, p. 827–829). Jones (1965, p. A45) reported aragonite "varves" in the older strata of Deep Springs Lake and attributed the crystallization of aragonite to the results of seasonal changes in the lake combined with inflow from fresh springs, possibly as a stratified surface layer. The darker layers were composed of dolomite, calcite, and clastic minerals attributed to deposition during summer periods of high evaporation. Aragonite, along with gypsum and calcite, was also reported by Neev and Emery (1967, p. 82–94) from laminated sediments from the Dead Sea. The white laminae there are composed mostly of gypsum and aragonite, and they form during summer "whitenings" which occur at irregular intervals of several years; necessary conditions are the combined result of several seasons of evaporation followed by a summer warming of the surface waters. The dark laminae are composed of gypsum, calcite, and other components deposited more evenly throughout the intervening periods.

In the Na-carbonate-rich waters that constituted Searles Lake even during its high stands, aragonite was most likely to have been formed when Ca-bearing fresh waters flowed into the basin as a surface layer. Where the aragonite is in the form of distinct laminae, the inflow is interpreted to have been seasonal and to have formed a thin layer so that most of its calcium was precipitated during a small part of the year by a combination of warming, evaporation, and mixing. Where aragonite is disseminated, or calcite is the dominant mineral, the introduction of calcium and crystallization of $CaCO_3$ is interpreted to have been a process that occurred uniformly throughout the year because the surface layer was thick enough to prolong mixing and minimize the importance of seasonal warming and evaporation.

Support for the suggestion that aragonite laminae represent times when the lake was stratified comes from the study by Mankiewicz (1975, p. 115–117). Laminae are most abundant in the Parting Mud above the level dated by him as $17{,}000 \pm 700$ years B.P. That segment also contains a higher percentage of macerated organics and chlorophyll pigments. Mankiewicz interprets this as being partly a matter of preservation and suggests as its cause that a more stable chemical stratification resulted from an increase in the salinity contrast between the upper and lower water layers, and that this reduced the amount of oxygen that could reach the bottom waters and sediments. However, he also attributes the higher percentages of long-chain hydrocarbons (derived from higher plants), aragonite, and uranium in most parts of this zone to vigorous episodes of inflow which brought plant debris, Ca, and U from upstream. The inflow of large volumes of waters into basins containing more saline and unoxygenated waters virtually requires a density stratification.

The dolomite in Searles Lake muds is considered most likely to be primary, or nearly so, although a diagenetic origin at a much later time cannot be disproved. The primary origin seems probable because (1) the mineral occurs chiefly in microcrystalline form; (2) it is found in outcropping lake sediments where other minerals known to be of diagenetic origin are missing; (3) it is concentrated in certain stratigraphic zones as if reflecting episodes when the chemistry of the lake was favorable, (4) dolomite is abundant in samples that apparently had very small percentages of minerals that would have provided Mg during diagenesis (the Mg content of interstitial brines is also very low), and (5) dolomite is absent in zones that contain minerals that could react diagenetically to form dolomite (for example, when the Mg-bearing minerals northupite and tychite occur with calcite, gaylussite, and pirssonite; see Eugster and Smith (1965, p. 497–504)).

Reasoning like that applied here to explain the CaO content of the muds can also be applied to their MgO content. The average percentage of acid-soluble MgO shown in table 13 is 5.4, this percentage implies a depositional rate of $3.0 \times 10^{-3}$ g/cm$^2$/yr from waters containing at least 15 ppm MgO. Since this quantity can be contained in alkaline brines having total salities as high as 300,000 ppm (Jones, 1965, table 7), transport of MgO into Searles Valley by highly saline waters was possible. Solutions containing 15 ppm MgO, however, would also have to contain 21 ppm CaO (15 ppm Ca) to form primary dolomite, and dolomite commonly coexists with other Ca-bearing minerals meaning that the amount introduced by solutions was substantially higher. If twice as much CaO was introduced, Jones' data (1965, table 7) suggest that waters having a total salinity of more than a few percent would be inadequate.

The conditions under which dolomite forms are imperfectly known. In the Overburden Mud and Parting Mud, the mineral commonly occurs in the largest quantities near contacts with salines; in the Bottom Mud and Mixed Layer, though, no correlation is evident. Observations by other workers (Alderman and Skinner, 1957, p. 566; Graf and others, 1961, p. 221; Jones, 1961, p. 201; Jones, 1965, p. 44–45; Peterson and others, 1963; Clayton, Jones, and Berner, 1968; Clayton, Kninner, Berner, and Rubinson, 1968; Barnes and O'Neil, 1971, p. 702–705; Barnes and others, 1973, table 1) present valid reasons for considering dolomite as both primary precipitates and diagenetic products. The studies by Peterson, Bien, and Berner (1963) and by Clayton, Jones, and Berner (1968), though, indicated dolomite to be forming in, or just below the surface of, the muds of Deep Spring Lake, California. That lake represents an environment that is chemically very similar to Searles Lake (Jones, 1965), and the muds that contain dolomite seem to be modern analogs of the muds in Searles Lake that were deposited during times of major inflow and large lakes. In Deep Spring Lake, dolomite is abundant in the area flooded seasonally as the lake rises and falls, and along the side where lake waters mix with perennial, nearly fresh springs (Jones, 1965, p. A44; Clayton, Jones, and Berner, 1968, p. 417). These relations make it additionally plausible to infer that much of the dolomite in the Searles Lake deposit was formed in an environment in which Mg- and Ca-bearing waters mixed with lake waters that had a high pH and total salinity.

The presence of northupite as a primary mineral in the mud layers of Searles Lake has been interpreted as a result of introducing Mg-bearing waters into solutions having relatively high concentrations of sodium carbonate and chloride (Smith and Haines, 1964, p. P51). The mineral has been formed synthetically (Wilson and Ch'iu, 1934, table 4), but the required percentages of carbonate and chloride, relative to magnesium, are not typical of those created by evaporation of normal waters. A likely explanation, therefore, for the occurrence of primary northupite in Searles Lake muds is that there was mixing along the interface between inflowing low density Mg-bearing waters and pre-existing high density saline waters. The mud horizons that contain northupite may indicate times at which the pre-existing saline waters were much more concentrated than those that existed in the basin at the times aragonite, calcite, and dolomite formed by mixing along the interface of a chemically stratified lake.

Thickness variations in the mud units also reflect processes that occurred during deposition. Areal variations were caused by areal differences in the volumes of clastic and chemically precipitated minerals. More than three-quarters of the mud in most units is composed of chemically precipated (acid-soluble) minerals in both subsurface samples and in samples exposed around the edges of Searles Valley. The variations in mud-layer thickness shown on the isopach maps are attributed largely to areal variations in the geochemistry of sedimentation. Chemical sedimentation patterns are influenced by proximity of shorelines, water depth, current patterns, wind directions, and the volume, chemistry, proximity, and entrance point of inflowing water. To some extent, of course, clastic sedimentation patterns also contributed to the thickness variations; they are chiefly influenced by the shape of the preexisting surface of deposition, the total volume and size distribution of clastic material in-

troduced from different directions, the proximity of the shoreline, the depth of water, and the wave energy produced by wind.

Both chemical and clastic sedimentation are influenced by the proximity of the shoreline. The basal and top zones of the mud layers (and possibly some zones in the middle) were deposited immediately after and just prior to saline deposition; therefore, they are deposits formed in lakes that had shorelines only slightly beyond the edges of the salt beds (approximated by the arbitrary boundary line on the isopach maps). The middle zones of the mud layers, however, were mostly deposited in larger lakes in which the areas plotted in the isopach maps represent only the centermost portions. In general, thin mud layers are interpreted to have a higher proportion of material deposited in shallow lakes with nearby shorelines, and thick layers are interpreted to be composed mostly of deep lake deposits.

Isopach maps of the six mud units in the Lower Salt, figures 15–20, seem to show changes in the areal distribution of material, although the lack of many data points near the edges makes contouring and interpretation of these areas very subjective. Unit M–2, the lowermost mud, has evenly spaced isopach contours indicating that the unit thins gradually toward its area of minimum thickness in the central and southern part. Units M–3 and M–5, in contrast, thin abruptly near the edges and have large central areas that are fairly uniform. Unit M–4 is somewhat similar to M–2 except for an anomalous area in the west-central part of the contoured area. Units M–6 and M–7, the upper two mud units in the Lower Salt, again thin uniformly from their edges toward a small central area. In all mud units, those that have the greatest relative volumes (table 3), and therefore probably represent the greatest periods of time, are those that most clearly thin gradually toward the center of the basin. This configuration may be the natural form of deep lake sediments. The layers with smaller relative volumes may have their distribution of thicknesses dominated by the shallower stages at the beginning and end of deposition.

The distribution of sediment in the Parting Mud revealed by the isopach map (fig. 23) shows that the unit tends to have zones of greater thickness near the north, southeast, and south edges, and to be more uniform throughout the middle (although a small thinner area is present near the very center). The thick zone shown by unsubstantiated contours along the southwest edge is based on the assumption that chemical and clastic sedimentation from the southwest—the area receiving most of the inflow—was more rapid than elsewhere. The thick zones near some of the other edges are possibly products of inflowing waters from those directions or of periods where the depositing lakes were relatively small. However, the history of lake fluctuations during the time this unit was deposited was complex (Smith, 1968, fig. 4), and too many episodes are superimposed to make meaningful interpretations.

The pattern of thickness variation in the Overburden Mud was found to be so uncertain that the isopach map used to approximate its volume is not included in this report. Part of the difficulty is in constructing an isopach map from the gradational lower contact of the unit, and part comes from the erosion of this and older units from surrounding areas (determined by geologic mapping of the exposed units) and redeposition of the eroded sediments on the original top surface of the Overburden Mud.

### SALINE LAYERS

The saline layers in the Searles Lake evaporites are composed of relatively soluble salts that crystallized from saline solutions. During the deposition of layers of this type, the minerals that originally crystallize are mostly determined by the compositions and temperatures of the solutions at the surface of the saline lake where they form. Most minerals form on the surface of the lake and float until the crystals founder and sink to the bottom. Although some dissolve at the surface if conditions change before they sink, others do sink and become part of a mineralogically heterogeneous layer that is accumulating on the bottom. Conditions at the surface are changeable, and rapid shifts in temperature, salinity, and $CO_2$ content occur on an hourly, daily, monthly, and seasonal basis. As a result, several different minerals form at the surface from similar solutions. On the bottom, all are exposed to the more uniform environment provided by the accumulating layers of salts on the floor of the lake, and the changes that take place tend to make the mineral assemblage more uniform. Many of these changes occur within the first few hours or days after deposition.

In this section, the present mineral assemblages are used to reconstruct the geochemical environment that existed during their deposition. Many of the following reconstructions, though, apply principally to conditions within the accumulating salt layer, not to the lake that first precipitated them. This is in some ways fortunate because the temperatures in the accumulating salt layer have more meaning; depending on the depth of lake water, they approximate monthly or yearly averages of the lake temperatures and thus can be interpreted more easily as a measure of the climate that prevailed during salt deposition. However, some conclusions regarding the chemistry of the lake waters

can also be made.

The conclusions regarding which temperatures are recorded by saline mineral assemblages are based largely on unpublished observations of salt crystallization processes that occurred in Owens Lake, Calif. during 1970 and 1971. These observations showed (1) that most saline minerals originally crystallized at the water surface and that their geochemical significance was limited to this zone; (2) that some of the crystals that formed at the surface subsequently dissolved whereas others sank to bottom within hours; and (3) that within days to months, most of the carbonate (and sulfate?) minerals that sank to the bottom were altered to another species without any textural or obvious chemical evidence of the change. Had crystals not been collected as they formed or within days thereafter, it would have been virtually impossible to reconstruct the mineralogy of the very first crystals and thus the chemistry of the lake waters in which they formed.

Most of the minerals that recrystallized in Owens Lake without leaving obvious evidence were those sensitive to $P_{CO_2}$. Both nahcolite and natron were primary crystalline phases, and both converted to fine-grained and primary-appearing trona within weeks or months after being deposited on the lake bottom. As explained in more detail by Milton and Eugster (1959), Eugster and Smith (1965), Bradley and Eugster (1969), and later in this section, the changes in $P_{CO_2}$ indicated by these reactions are opposites. Altering nahcolite to trona requires a lowered $P_{CO_2}$ to allow loss of one-third mole of $CO_2$ for each mole of reacting nahcolite; altering natron to trona requires an increased $P_{CO_2}$ to allow the addition of one-third mole of $CO_2$ for each mole of reacting natron. It appeared that the final species of mineral in Owens Lake was determined by the $P_{CO_2}$ in the environment provided by the accumulating layer rather than by the solutions responsible for the primary crystallization. The $P_{CO_2}$ in that environment was partly determined by the extent of organic decomposition within the salt layer and in the salt and mud layers immediately below, partly by the buffering effect of other saline minerals, and partly by the amount of $CO_2$ that was able to migrate between the saline layer pore waters, the overlying waters in the lake, and the atmosphere.

The only sulfate mineral observed in the salines accumulating in Owens Lake was burkeite, but several lines of evidence suggest that mirabilite was originally deposited during the winter. When accompanied by sodium carbonate minerals, the stability fields of mirabilite and burkeite are influenced by $a_{CO_2}$, $a_{H_2O}$, and temperature (Eugster and Smith, 1965, p. 489–497), and it appears that postdepositional reaction of sulfate minerals also occurs in response to the different conditions found in the accumulating sediments.

## PHASE RELATIONS APPLICABLE TO SEARLES LAKE SALTS

The Searles Lake saline layers are composed chiefly of minerals that represent phases in the sodium bicarbonate, carbonate, sulfate, chloride system (fig. 33). Trona, burkeite, mirabilite, thenardite, and halite are now present in the Searles Lake deposit; natron is not. In that system, at 20°C, the field of trona occupies a wedge-shaped volume above all the burkeite and part of the natron, mirabilite, thenardite, and halite fields. The top of the trona field is shown shaded, and the field of nahcolite occupies all the area above both it and the underlying fields that extend outside the edges of the trona field. At temperatures above 20°C, the trona, burkeite, and thenardite fields expand at the expense of the halite, mirabilite, nahcolite, and natron fields. At temperatures below 20°C, the re-

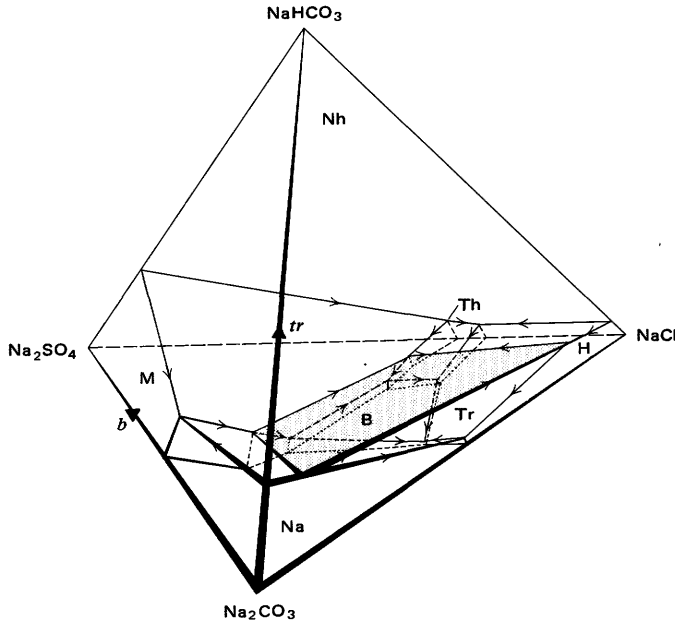


FIGURE 33.—Three dimensional view of phase system $NaHCO_3$-$Na_2CO_3$-$Na_2SO_4$-NaCl-$H_2O$ at 20°C. Solid phases indicated as follows: B, burkeite ($2Na_2SO_4 \cdot Na_2CO_3$); H, halite (NaCl); M, mirabilite ($Na_2SO_4 \cdot 10H_2O$); Na, natron ($Na_2CO_3 \cdot 10H_2O$); Nh, nahcolite ($NaHCO_3$); Th, thenardite ($Na_2SO_4$); Tr, trona ($Na_2CO_3 \cdot NaHCO_3 \cdot 2H_2O$). Shaded area represents top of trona field which occupies a wedge-shaped volume between overlying nahcolite field and parts of underlying natron, mirabilite, thenardite, halite, and burkeite fields. Boundaries of stability fields plotted in terms of weight percent of solid components in equilibrium solutions. Arrows show slopes of boundaries toward base of tetrahedron. Compositions of double salts burkeite (b) and trona (tr) are shown on edges of tetrahedron. Data from Teeple (1929); diagram from Smith and Haines (1964, fig. 16).

verse happens. The thenardite field does not exist below about 17°C; the burkeite field does not exist below 14.4°C. The data in this report show that of the related minerals in figure 33, only trona, halite, burkeite, and thenardite coexist in appreciable quantities; nahcolite is sparsely represented in a few layers, and mirabilite is found only in the Bottom Mud.

The changing composition of the brine during deposition of the salt layers can be theoretically reconstructed from phase diagrams representing the $Na_2CO_3$-$NaHCO_3$-$Na_2SO_4$-NaCl-$H_2O$ system. When data are not available for the 5-component system, the 4-component systems $Na_2CO_3$-$NaHCO_3$-NaCl-$H_2O$ and $Na_2CO_3$-$Na_2SO_4$-NaCl-$H_2O$ are used. Although the laboratory determination of points in a 5-component system is not experimentally difficult, plotting the results in a quantitative manner requires at least four dimensions—which is difficult. However, by limiting boundaries to those in which the $H_2O$ component is saturated, specifying saturation of one or more solid components, and projecting the field boundaries of the saturated solid components onto a two dimensional triangular diagram, all five components can be related.[23]Other components that exist in natural solutions can generally be ignored with only minor uncertainties introduced.

The changing ratios of these components in the lake brines as crystallization and rapid diagenesis proceeded are indicated by the crystallization path. This path represents a greatly simplified version of the chemical events that occurred in the lake because neither the seasonal changes nor the alteration of the initial crystallization products is indicated. The path does show, however, the compositional changes that ultimately occurred when equilibrium was reached as a result of postdepositional interaction between the lake brines and the minerals in the accumulating salt layer. When interaction ceased, the bulk composition of the buried salt layer became largely fixed, and further changes involved only phases allowed by that fixed composition.

The general direction and extent of the crystallization path in a given phase diagram is deduced from the stratigraphic order of the primary minerals[24] that crystallized; its exact path is dictated by the geometry of the stability fields and their boundaries. By combining the stratigraphy of the observed mineral assemblages with the requirements of the phase relations, the composition of primary salt assemblage and the composition of the interstitial brine can be approximately reconstructed. This places limits on the physical conditions under which crystallization took place, and defines both the solids and brines that constituted the starting point for subsequent diagenetic change.

## SALINES IN THE MIXED LAYER

The primary salts in the Mixed Layer apparently represent chemically simple waters. The saline minerals in the Mixed Layers are mostly trona, nahcolite, or halite, meaning that the saline lake waters were dominated by Na, $CO_3$, $HCO_3$, and Cl, and that the brines at the time crystallization began were very close to the $NaHCO_3$-$Na_2CO_3$-NaCl face of the tetrahedron shown in figure 33. The small percentages of burkeite, northupite, sulfohalite, thenardite, and tychite (pl. 2*A*) may indicate brief changes in the chemical composition of the lake waters, but they do not occur in a pattern that seems significant.

Changes in the compositions of the brines that occupied Searles Lake at the times the Mixed Layer was deposited can be inferred from the saline minerals (pl. 2*A*). A few thin beds of trona and a little halite are in unit F, but unit E is the oldest unit that contains thick beds of salt. Units E, D, and C are similar in that they contain much more halite than trona and no nahcolite. In the $NaHCO_3$-$Na_2CO_3$-NaCl-$H_2O$ system at 20°C (fig. 33), the halite field is small; it becomes even smaller above 25° and below 15°C. Many saline beds in units C, D, and E, however, are composed solely of halite. These show that crystallization started from brine represented by a point very close to the NaCl corner, and even though crystallization of halite forced the composition of the remaining brine toward the $Na_2CO_3$-$NaHCO_3$ edge of the phase diagram, it never reached the boundary of the adjoining field. Other saline beds in these units, however, contain both trona and halite. These beds show that the initial brines were represented by points in the trona or ha-

[23] A small uncertainty about the precise relations between stability field boundaries and the compositions of the brines comes from the lack of a satisfactory method for plotting more than one cation percentage in this system. Two major cations (Na and K) were present in the crystallizing solutions in mole ratios of about 10:1, and the diagram dimensions relate hypothetical salts ($Na_2CO_3$, NaCl, etc.) that contain only one. Considering the average brine compositions in table 17 as an example, the anion equivalent sum of $CO_3$, $SO_4$, and Cl is 0.5284 per 100 g of solution, whereas the cation equivalent of Na is only 0.4870, meaning that about 80 percent of the 0.0512 equivalents of K are required to electrically balance the three anions in solution. In this paper, relative percentages in these 4- and 5-component systems have been calculated by converting total $CO_3$, $SO_4$, and Cl to $Na_2CO_3$, $Na_2SO_4$, and NaCl. This overstates the amount of one or more of the hypothetical salts in the reacting solutions by maximum of a few percent. In the example using the average brine given in table 17, if all the K is calculated as KCl and removed from the system, and the amount of NaCl is calculated from the amount of Cl that remains, the point representing the brine composition in the $Na_2CO_3$-$Na_2SO_4$-NaCl-$H_2O$ diagram is shifted by 3 percent directly away from the NaCl corner of the diagram.

[24] For the sake of simplicity in this paper, the term "primary" is used for minerals that appear to have ultimately become the stable phase in the accumulating salt layer even though they may have actually been products of rapid diagenesis from other species. The term "secondary" is reserved for minerals that are thought to have formed many years after deposition and as a result of diagenetic processes not directly related to the geochemistry of the depositing lake.

lite field but near the phase boundary, so that crystallization of the first mineral moved the composition of the remaining brines into the other field before crystallization ceased. It is evident, therefore, that the brines that produced salines in units C, D, and E of the Mixed Layer had initial compositions that were near or inside the boundary of the halite field in the $Na_2CO_3$-$NaHCO_3$-NaCl-$H_2O$ system. Temperature changes and small compositional variations allowed crystallization of other minerals at times, but the bulk composition of the brines was at all times dominated by NaCl.

The composition of salines in units A and B in the Mixed Layer indicate that there was a major change in the composition of water flowing into Searles Valley relative to the waters that desiccated to produce salines in units C, D, and E. In unit B, trona and nahcolite are much more abundant than halite, and in unit A, they are virtually the only saline minerals found. The saline composition of the unit shows that the brines that produce salts in unit B had shifted in composition toward the $Na_2CO_3$-$NaHCO_3$ edge of the diagram shown in figure 33, although extensive crystallization of carbonate minerals still shifted the composition of the remaining brine into the halite field. The brines that produced salts in unit A were either so dominated by Na carbonates that no degree of desiccation could shift the brine composition to the halite field, the brines of unit A were desiccated less extensively than those that produced unit B, or those that crystallized salts did so at lower temperatures.

Evidence of a different type of change in brine composition during deposition of the Mixed Layer comes from the Br content of halite (Holser, 1970, p. 309–315). It abruptly rises and falls in the middle of unit E; more gradually increases to a high level in the lower part of unit C and then decreases. Holser (1970, p. 311) concludes that the gradual rise in Br in the base of unit C represents a gradual net increase in the extent of evaporation, and that the decrease represents a relatively large inflow of new water. The presence of about 13 ft (4 m) of clay and silt in the zone of change (Smith and Pratt, 1957, p. A39) supports this conclusion and might indicate more than 10,000 years of inflow that produced a large lake. The new water in the lake apparently had a high Cl/Br ratio as indicated by their ratio when deposition of salts resumed.

The stratigraphic distribution of nahcolite and trona is a function of the chemical activities of $CO_2$ ($a_{CO_2}$) and water ($a_{H_2O}$). The relation between these controls and minerals has been discussed by Milton and Eugster (1959), Eugster and Smith (1965), Eugster (1966), and Bradley and Eugster (1969). Application of these principles to salts in the Mixed Layer (Eugster and Smith, 1965, fig. 22) demonstrates a gradual but erratic upward increase in $a_{CO_2}$, and an abrupt increase in $a_{H_2O}$ in units B and A. Both changes are consistent with the other evidence of a major change in the chemistry and character of deposition in late Mixed Layer time.

The existence of nahcolite in units A and B indicates values of $a_{CO_2}$ above those provided by equilibrium with the atmosphere. They may be interpreted as a measure of the extent of bacterial production of $CO_2$ at the time deposition was taking place. Observations like those of Siever, Garrels, Kanwisher, and Berner (1961), Siever and Garrels (1962, p. 54), and Jones (1965, p. A48) show that $CO_2$ from bacterial decomposition can increase the $a_{CO_2}$ in uncompacted sediments to a level much above that needed to change any sodium carbonate mineral to nahcolite. Evidence is not available as to whether greater production of $CO_2$ during deposition of the upper part of the Mixed Layer might have resulted from more intense bacterial activity or from a larger amount of organic material available for decomposition. The amount of organic material in the mud layers in units A and B was probably high. This quantity was initially controlled by the chemistry of the lake waters that determined the organic productivity of the lake and thus the organic material that can become available for decomposition. The study of Owens Lake (Friedman, Smith, and Hardcastle, 1976) showed that an alkaline lake concentrated to levels both below and above those necessary to form Na-carbonate salts can have a very high productivity; at salinities ranging from 136,200 mg/L to 387,500 mg/L, the phytoplankton population limited downward visibility to 5 or 10 cm.

### SALINES IN THE BOTTOM MUD

The several layers of salines in the Bottom Mud (pl. 2*B*) are mostly nahcolite or mirabilite; only the zone of salts about a meter below the top of the unit contains other minerals. These salt beds commonly contain more mud than the others do, and the lack of clear correlation between saline layers in the three cores plotted on plate 2*B* suggest that the beds are lenticular. These characteristics indicate that these layers were probably the result of winter cooling of the lake during periods when its salinity had increased to the proper levels.

Deposition in this manner accounts for the monomineralic composition of the beds, the high mud content in some, and the lenticularity of the layers. The original $Na_2CO_3$-minerals were probably natron or nahcolite and the $Na_2SO_4$-mineral was mirabilite. The solubilities of these minerals are markedly sensitive to temperature, and when cooled, solutions containing

mixtures of dissolved salts crystallize these minerals exclusive of the others. Except for borax, which was initially a relatively minor ingredient,[25] no other salts in the applicable systems are similarly affected by chilling. In pure Na-carbonate and Na-sulfate solutions, natron, nahcolite, and mirabilite crystallize at temperatures near 0°C from brines having total salinities between 3 and 7 percent (Makarov and Bliden, 1938, tables 1 and 4; Freeth, 1923, tables 1 and 17); at 15°C, these salts crystallize from solutions having salinities between 8 and 15 percent. Addition of NaCl raises the salinity but lowers the percentage of these components necessary for their crystallization (Makarov and Bliden, 1938, table 8).

The tendency for the salts that are preserved to be mixed with mud and form lenticular beds is interpreted to be a result of a mechanism that allows salts to survive the warmer seasons that follow crystallization. Initially, each salt layer probably covered the floor of the lake, but currents in the relatively shallow lake probably mixed the salts in some parts of the lake with mud, a mixture that would have been relatively impervious. During the following warmer seasons, this property would have protected the salts in these areas from being infiltrated by lake waters and dissolved.

These saline layers, therefore, are considered indicative of crystallization during winter from an intermediate-sized lake. Salinity of the lake water was probably in the range 5–15 percent, the exact value depending on the species and amounts of the other components in solution which depress the saturation point. The data in figure 32 show that lakes having these salinities could have had areas of 400–600 $km^2$ and depths of 70–120 m.

The discontinuous layer about 1 m below the top of the Bottom Mud that contains borax, northupite, trona, nahcolite, and thenardite may also be a result of winter crystallization inasmuch as these minerals are reasonable products of winter crystallization if modified by diagenesis. If the layer was initially composed of salts crystallized during winter, the most likely primary minerals were borax, natron or nahcolite, and mirabilite. The diagenesis that produced the present suite could have been caused solely by a postdepositional decrease in $a_{H_2O}$. Saline brines having a lower $a_{H_2O}$ exist in the overlying Lower Salt, and downward migration of brines from that layer would have mixed with the original interstitial brines and lowered the $a_{H_2O}$. This, with or without a change in $a_{CO_2}$, could have produced the present mineral suite. Remembering that the meter of intervening mud contains dolomite and gaylussite, and using $a_{CO_2}$-$a_{H_2O}$ diagrams of Eugster and Smith (1965, fig. 19), a decrease in $a_{H_2O}$ of brine would have caused minerals of stability field 15 (mirabilite, natron, gaylussite, halite, dolomite, aphthitalite) to alter to those of field 6 (thenardite, nahcolite, gaylussite, halite, dolomite, aphthitalite) or field 18 (thenardite, northupite, trona, gaylussite, halite or dolomite, and hanksite), depending on the $a_{CO_2}$. Note that gaylussite, northupite, and nahcolite do not coexist in any field of those $a_{CO_2}-a_{H_2O}$ diagrams and that they do not coexist in the salt layers being described; gaylussite exists in the muds of all cores, but nahcolite exists in this zone only in cores GS–15 and GS–16, and northupite exists only in cores GS–18 and GS–27.

[25] When the brines that formed the Upper Salt were concentrated to 5 percent, $Na_2B_4O_7$ constituted about 0.15 percent.

## SALINES IN THE LOWER SALT, UPPER SALT, AND OVERBURDEN MUD

The starting compositions of the solutions that produced the Lower Salt and Upper Salt in Searles Lake are now best approximated by the present bulk chemical composition of each salt unit or group of related units. Their compositions are summarized in tables 10 and 17. These calculated compositions are weighted averages of analyses and include the components in both the present salts and the residual brines that fill their interstices. There is the possibility that small quantities of soluble components remained in the surface brines at the time salt crystallization ceased and these components were incorporated into younger saline units or removed from the basin by subsequent overflow. The only evidence of this happening to an appreciable extent is in the deposition of unit S–7.

In the following discussion, the salt layers of the Lower Salt are divided into two groups which represent sequences of crystallization that are interrelated and can be treated almost as if they were continuous. The first is composed of units S–1 to S–5, and the second of units S–6 and S–7. This grouping is emphasized when viewed as a histogram (fig. 34). Crystallization of the Upper Salt is considered as a single continuous event. The crystallization paths followed by the brines during these three episodes are plotted on the phase diagrams shown in figures 35, 36, and 38. The salines in the Overburden Mud were formed by a crystallization sequence similar to the one that formed the Upper Salt.

### LOWER SALT

The phase diagrams shown in figure 35 allow the crystallization of units S–1 through S–5 to be reconstructed. Field boundaries in the 5-component system with all points and boundaries saturated in both $H_2O$ and $NaHCO_3$ are shown in figure 35*A*. To portray this

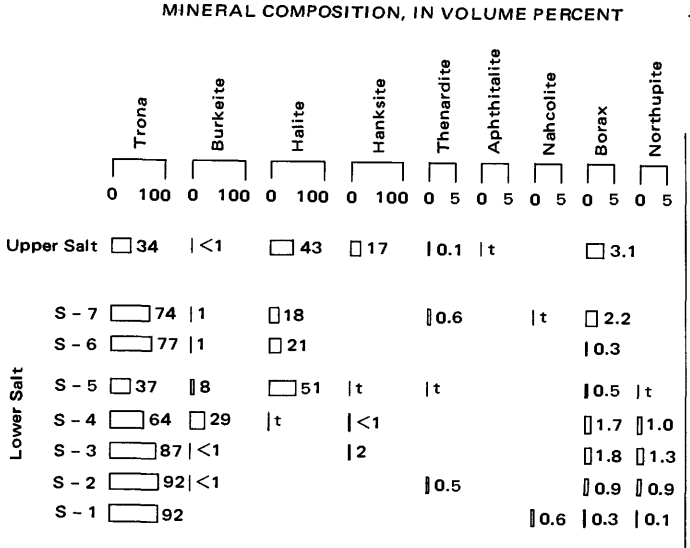


◄FIGURE 34.—Visually estimated volume percentages of major minerals in salt units of Lower Salt and Upper Salt. Data from tables 4 and 14. Percentages rounded, <1 = 0.1 to 1.0 percent, t (trace) = <0.1 percent.

in two dimensions, they are projected from the $NaHCO_3$ corner of the tetrahedron shown in figure 33 to the $Na_2CO_3$-$Na_2SO_4$-NaCl face. The diagram is constructed for a temperature of 20°C, because the positions of the field boundaries at this temperature best satisfy the mineral assemblages found in units S–4 and S–5. The boundaries of fields are probably curved but are drawn straight because of the lack of experimental data.

The boundaries shown in this projection are those of the trona field and those mineral stability fields that lie below and outside of it. Boundaries and triple points within the limits of the trona field, shown with dashed lines because they underlie the trona field as viewed from the $NaHCO_3$ corner of the tetrahedron, represent solutions that are in equilibrium with trona and the two or three adjoining labeled phases. Boundaries outside the limits of the trona field represent solutions that are in equilibrium with nahcolite and the two adjoining labeled phases. The boundaries in this phase diagram are univariant and the triple points are invariant. The composition of burkeite is shown on the $Na_2CO_3$-$Na_2SO_4$ edge; the composition of trona lies on the $Na_2CO_3$-$NaHCO_3$ boundary and is represented by the $Na_2CO_3$ corner of this diagram.

Data on water-soluble components of units S–1 to S–5 (table 10) have been used to determine the composition of the original brine at the time deposition of unit S–1 began. To do this, the percentages of $SO_4$, Cl,

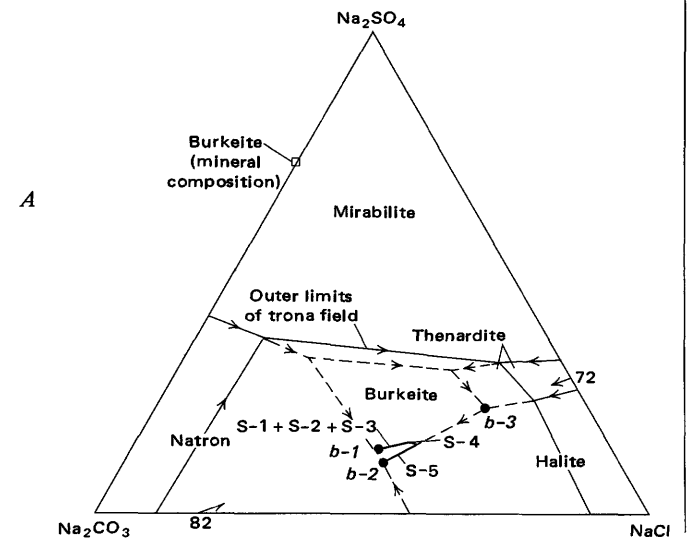


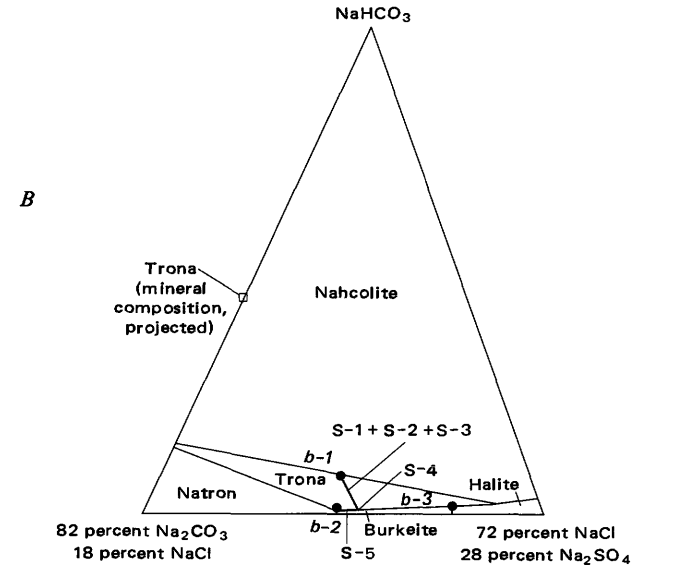


◄FIGURE 35.—Selected mineral stability fields in system $NaHCO_3$-$Na_2CO_3$-$Na_2SO_4$-NaCl-$H_2O$ at 20°C. *A*, Projection from the $NaHCO_3$ corner of tetrahedron toward $Na_2Co_3$-NaCl-$Na_2SO_4$ face. Boundaries represent equilibrium between labeled fields and trona (dashed lines inside limits of trona field) or nahcolite. Arrows show direction of increasing salinity. Starting composition of brine that produced S–1, S–2, S–3, S–4, and S–5 shown by point *b–1*; final composition of brine by point *b–2*; present composition of brine by point *b–3*. Heavy line and arrow indicate changing composition of the brine as units crystallized, with segments of line labeled to indicate units. Arrows labeled 82 and 72 show location of base of section shown in *B*. *B*, Section through a tetrahedron representing $NaHCO_3$-$Na_2CO_3$-$Na_2SO_4$-NaCl-$H_2O$ system in a plane having its base along line between points representing 82 percent $Na_2CO_3$ (18 percent NaCl) and 72 percent NaCl (28 percent $Na_2SO_4$) in diagram *A* and its top at $NaHCO_3$ corner. Boundaries indicate equilibrium between labeled fields. Points *b–1*, *b–2* and *b–3* and crystallization path shown in *A* plotted in this plane. Data from Freeth (1923) and Teeple (1929) as compiled by Smith and Haines (1964, fig. 16*A*) in the form of a 4-component tetrahedron, with all points in equilibrium with $H_2O$. Boundaries plotted in terms of weight percent.

$CO_3$, and $HCO_3$ indicated for the "Chemical composition of combined solids and brines" (line 5 of table 10) were converted to $Na_2SO_4$, NaCl, and total carbonate as $Na_2CO_3$. The result is plotted in figure 35*A* as a point labeled *b–1*. A sufficient supply of Na was assumed. From the same table and by the same method, the "Chemical composition of the present brine" (line 4) was determined and plotted as a point labeled *b–3*. Point *b–2* represents the estimated composition of the final brine at the time primary crystallization ceased. The brine composition moved from point *b–2* to *b–3* as a result of post depositional processes.

The path representing the changing composition of the brine during crystallization of units S–1 through S–5 is plotted between points *b–1* and *b–2* (fig. 35*A*). These points lie approximately along a line that intercepts the edges of the triangle at 72 percent NaCl and at 82 percent $Na_2CO_3$. This line is the base of a scalene triangle that represents a section through the tetrahedron representing the 5-component system (fig. 33). This section is plotted as figure 35*B*, and the changing composition of the brine as it progressed from point *b–1* to *b–2* is plotted on it. This representation is graphic but not precise. Experimental data showing the exact stability fields in these planes are not available; the relations shown are based on linear projections from the 4-component diagrams that make up the faces of the tetrahedron and on scattered control points for the 5-component system within the tetrahedron. Also, the crystallization path curves out of the plane of the diagram and all points must be projected to it.

Point *b–1* (fig. 35*B*) is plotted on the trona-nahcolite boundary because unit S–1 is composed mostly of trona but contains a little nahcolite. As the actual $Na_2CO_3/NaHCO_3$ ratio in the original brines is not known, and the position of that boundary changes rapidly with temperature, the point in figure 35B is more representative of the brine and phase relations that existed in the accumulating salt layer. (In Owens Lake, nahcolite and natron were commonly the first sodium carbonate crystals to form, but they altered to trona a few weeks or months after accumulating on the floor of the lake.) Isotopic evidence (Smith, Friedman, and Matsuo, 1970) suggests that crystallization of units S–1 and S–2 took place at lower temperatures than crystallization of units S–3, S–4, and S–5, so during deposition of the earlier two salt units, the trona field may have been smaller and the nahcolite field may have been larger than shown in figure 35. The phase boundaries are drawn for temperatures near 20°C because their positions best satisfy the relations between brine composition and mineralogy found in units S–4 and S–5.

Units S–1, S–2, and S–3 now consist almost solely of trona (fig. 34), although the first crystals could have been natron, trona, or nahcolite. However, all three sodium carbonate minerals lie on the $Na_2CO_3$-$NaHCO_3$ edge of the 5-component system, and the path representing brine composition during crystallization followed a track that moved away from that edge. Therefore, in figure 33*A* (which projects the $Na_2CO_3$-$NaHCO_3$ edge to the $Na_2CO_3$ corner), units S–1, S–2, and S–3 are plotted along the straight portion of the crystallization path that begins at *b–1* and migrates directly away from the $Na_2CO_3$ corner of the diagram.[26] In figure 35*B*, the path is plotted moving away from the point representing the composition of trona but remaining in the trona field. Other minerals may have been precursors, but trona was the final phase. By the time S–3 was fully crystallized, the composition of the crystallizing brine was very close to the trona-burkeite boundary (fig. 35*B*). That it first touched the trona-burkeite boundary instead of the trona-halite boundary (fig. 35*A*) is indicated by the mineral composition of unit S–4 (fig. 32) in which trona is accompanied by major percentages of burkeite but not halite.

Unit S–4, a thin unit, is mostly trona and burkeite (fig. 33). The composition of brine that was in equilibrium with this assemblage is represented in figure 35*A* by a short curved line that moves along the trona-burkeite boundary and away from a series of bivariant points that lie on the $Na_2CO_3$-$Na_2SO_4$ edge. These points represent mixtures of trona and burkeite and thus lie between the points that define the compositions of pure trona and burkeite. (Pure trona and its precursor sodium carbonate minerals are all represented in figure 35*A* by the $Na_2CO_3$ corner of the diagram, and the composition of pure burkeite is plotted.) The path is curved because the proportions changed. The path representing S–4 stopped at or just prior to reaching the boundary of the halite field. In figure 35*B*, the S–4 segment of the crystallization path follows the trona-burkeite boundary which is plotted straight. In three dimensions, though, its path curves upward from the plane of figure 35*B* and toward the halite field which lies a very short distance "above" the burkeite field in this part of the diagram.

Unit S–5 is represented in both figures 33*A* and 33*B* by a crystallization path that represents a series of univariant points along the trona-burkeite-halite bound-

[26] In detail, the composition of the brine should be plotted with a sawtooth shape; partial reversals in its composition must have occurred during the time represented by the interbedded mud units inasmuch as they represent hundreds or a few thousand years of inflowing water that contained a significant amount of dissolved solids. The reversals would be plotted as short segments traveling back toward point *b–1*, their length being proportional to the amount of solids that were introduced. Space on the diagrams does not allow this detail to be shown.

ary. The direction is toward the invariant point at the junction of the natron, burkeite, halite, and trona fields. This is the assemblage that is in equilibrium with the most concentrated brine, and the crystallization path of S–5 toward it is the only direction that allows the components of trona, halite and burkeite to be removed from solution. Point *b–2* is plotted at the invariant point because most cores from the middle of Searles Lake have some trona in the uppermost part of unit S–5 which is the relation that would be produced by crystallization at this point.

The average composition of the present brine, calculated from table 10, is indicated by point *b–3*. It lies exactly on the trona-burkeite-halite-thenardite invariant point of the fields that are plotted at 20°C. Not all individual brine samples lie at this point (fig. 21*A*), but none remain at the invariant point where crystallization initially ceased. The change in composition from points *b–2* to *b–3* requires the addition of $H_2O$ as well as partial solution of some original phases, and this is discussed in the section on diagenesis.

Changes in brine composition during the crystallization of units S–6 and S–7 are reconstructed by a diagram representing the 4-component system $Na_2CO_3$-$Na_2SO_4$-NaCl-$H_2O$ at 15°C (fig. 36) (data for the 5-component system at this temperature are not available). The trona field would occupy less area than at 20°C (fig. 35) but would probably cover an area that included point *b–2* and the burkeite field. However, the base of the trona field is close to the base of the tetrahedral model of this system (fig. 33) and little error in the position of the burkeite field is introduced by omitting $NaHCO_3$; the difference between the positions of field boundaries in 4-component and 5-component systems at 20°C is illustrated in figure 37. At 15°C, the difference would be even less.

The starting composition of the brine (*b–1*), calculated from data in table 10, is closer to the $Na_2CO_3$ corner of figure 36 than is the starting composition of the brine responsible for the underlying units (b–1 in fig. 35*A*). The first crystals to form may have been natron (as shown in fig. 36), trona, nahcolite, or a mixture of any pair of phases which are represented by the boundaries and fields above trona. As the carbonate mineral crystallized, the composition of the solution, represented by points lying along the line connected to point *b–1* (in figure 36), moved away from the $Na_2CO_3$ corner of the diagram. As soon as it touched the halite field, it coprecipitated trona or natron (but not nahcolite) and halite, the crystallization path following the boundary that separates their fields. The near-lack of sulfate minerals in units S–6 and S–7 shows that crystallization stopped before the crystallization path reached the burkeite (or other sulfate mineral) field and that desiccation was not complete.

The low percentage of sulfate minerals in units S–6 and S–7 is why point *b–2* in figure 36 is likely to represent the brine compositions at the time crystallization of S–6 and S–7 ceased, and why the prevailing temperature of crystallization was at or very near 15°C. At temperatures more than a few degrees above 15°C, the

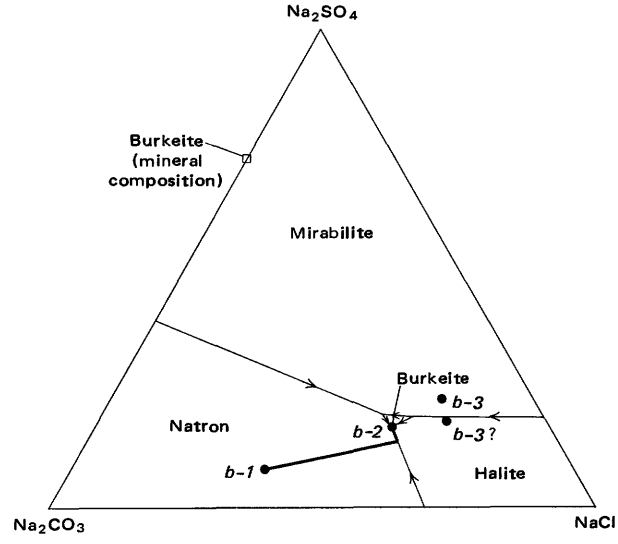


FIGURE 36.—Mineral stability fields in system $Na_2CO_3$-$Na_2SO_4$-NaCl-$H_2O$ at 15°C. Starting composition of brine that produced units S–6 and S–7 shown by point *b–1*; final composition of brines shown by point *b–2*; present composition of brine by point *b–3*. Points *b–1* and *b–3* based on data from table 10. Point *b–3* (?) represents total $CO_3$, $SO_4$, and Cl from analysis of brine from S–7, core hole L–31 (see explanation in text). Heavy line indicates changing composition of brine as salt units S–6 and S–7 crystallized. Arrows show direction ofincreasing salinity. Data from Makarov and Bliden (1938). All boundaries plotted in terms of weight percent.

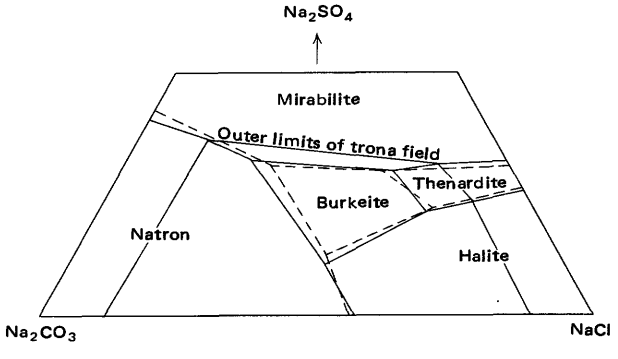


FIGURE 37.—Superimposed stability field boundaries of systems $Na_2CO_3$-$Na_2SO_4$-NaCl-$H_2O$ (dashed lines) and $NaHCO_3$-$Na_2CO_3$-$Na_2SO_4$-NaCl-$H_2O$ (solid lines) at 20°C. Five-component system projected as in figure 35*A*; 4-component system plotted in normal manner. All boundaries plotted in terms of weight percent. Data from Freeth (1923) and Teeple (1929).

burkeite field expanded into the area that would have been reached by solutions precipitating a Na-carbonate mineral before crystallizing halite (as did occur during crystallization of units S–1 to S–5); at temperatures slightly below 15°C, the mirabilite field expands into this zone (Makarov and Bliden, 1938).

The quantity of dissolved solids introduced by fresh water during the times represented by units M–6 and M–7 were probably comparable inasmuch as M–6 and M–7 have similar volumes. Unit S–5 represents desiccation, and the solids in the brine that deposited S–6 resulted from inflow during M–6 time plus those solids dissolved by it from the top of unit S–5. Units S–6 and S–7 have similar percentages of trona and halite suggesting that both crystallized from brines and under conditions that were quite similar. Thus the initial brines that produced units S–6 and S–7 are both approximated by point *b–1* in figure 36, and the paths representing crystallization of units S–6 and S–7 are virtually the same. The sulfates not deposited in unit S–6 because of incomplete desiccation may have been added to the brine that produced unit S–7 and be the cause of the slightly higher percentages of burkeite and thenardite in that unit (fig. 34).

A feature of units S–6 and S–7 unexplained by the inferred crystallization sequence is the present concentration of halite at the base of these units. Initial crystallization in the halite field seems precluded by their present bulk composition. Possibly, the basal layer of each unit represents times when winter crystallization of natron was followed by summer crystallization of halite and solution of all or most of the underlying natron; this sequence would have left a zone of residual halite as the basal layer. During subsequent years, natron crystallized during winter would have converted to trona during the summer warming because of the increased concentration of Na carbonate in the brines. This process would have produced the mixture of halite and trona found in the upper parts of these two units.

Phase data for borax show that cool temperatures strongly favor its crystallization (Teeple, 1929, p. 128–130; Bowser, 1965). The position of borax in the crystallization sequence, therefore, is markedly dependent on temperature as well as the concentration of its components. Borax zones in or near mud layers which indicate deposition in relatively dilute waters thus suggest marked chilling; zones in the middle of saline layers may indicate either chilling or a high total salinity.

The borax content of units S–1 to S–5 of the Lower Salt shows a progressive increase in the lower three units and then a decrease. Previously discussed phase data show that the salinity of the solutions that deposited those five salt units consistently increased. The increase from S–1 to S–3 therefore seems to indicate an environment that was sufficiently cool to allow sodium borate to be crystallized in amounts approximately proportionate to the increasing salinity of the brine. The similar quantities of borax in units S–3 and S–4—a time when the salinities had increased from levels that only crystallized trona to levels where trona and burkeite cocrystallized—indicates a warming trend that increased the solubility of borax about the same amount as its concentration increased in the brines. The sharp decrease in the quantity of borax in unit S–5 probably indicates a more pronounced warming of the lake and the crystals accumulating on its floor.

In units S–6 and S–7, the borax concentration increases upward. The previously discussed phase data for the other components indicate consistently lower crystallization temperatures for these two units than for units S–4 and S–5. The small quantity of borax in S–6 is interpreted as the result of a low concentration of borate in the lake waters, and thus a small quantity of crystals formed in spite of cool conditions (about the same percentage as in S–1). The larger quantity of borax in S–7 is interpreted as the result of the higher borate concentration in the parent brines which resulted from the combination of the quantities not precipitated in S–6 plus those introduced during the long period represented by muds of unit M–7.

Northupite, a common though not abundant mineral, is not represented in any of the phase systems discussed previously. Eugster and Smith (1965, fig. 19) show that northupite may coexist with almost every mineral found in Searles Lake except aphthitalite. It has been synthesized in the laboratory by de Schulten (1896), Watanabé (1933), and Wilson and Ch'iu (1934, table 4). Wilson and Ch'iu added magnesium carbonate to a solution containing much higher amounts of sodium carbonate, sodium bicarbonate, and sodium chloride, and under $CO_2$ pressure about 420 times greater than its pressure in the atmosphere. They synthesized the mineral at temperatures between 100°C and 20°C and noted that high temperatures accelerate the mineral's crystallization, but they did not determine the lower temperature limit of the stability field. In their diagram, the stability field of the synthesized mineral adjoins nahcolite, halite, and a basic magnesium carbonate. However, the required amount of magnesium (100–930 ppm $MgCO_3$) is much higher than in present brines from Searles Lake. In

natural environments, the required concentrations might be attained either by mixing of "fresh" magnesium-bearing waters with saline waters or by evaporation of waters having a low enough pH to permit enough magnesium to stay in solution until the necessary concentrations of other components were attained.

Northupite was reported by Haines (1957, 1959) from units S–1 to S–5 of the Lower Salt but not from units S–6 and S–7. Its percentages in units S–1 to S–5 change systematically with stratigraphy (table 4, fig. 34) and in a pattern similar to that followed by borax. The controls of the northupite percentage, however, can not be the same as for borax if northupite crystallization is promoted by warm temperatures. More likely, controls included the amount of Mg that could be transported to the central part of the basin, and the salinity of the water with which it mixed because this would have affected the proportion of the introduced amount that was crystallized. Eugster and Smith (1965, p. 497–500) show that in the presence of dolomite muds, northupite is not stable at high $a_{CO_2}$ values. The mechanism most likely to explain the presence and progressive change in the amount of northupite in the Lower Salt units is similar to that proposed to explain northupite and Ca-bearing minerals in the muds; that mechanism required a stratified lake with Mg introduced by fresh waters that transported Mg to the center of the basin in a low density fresh layer superimposed on a dense brine, and crystallization by mixing of water from the two layers. Salt layers are inherently the result of climates characterized by more evaporation than inflow, but a seasonal inflow of some fresh water into a salt lake is possible. The increasing percentages of northupite in units S–1 to S–3 are interpreted as the result of sporadic inflow of Mg waters into lakes that had successively greater salinities, and the decrease in units S–4 and S–5 is interpreted as a decrease in the quantity of water introduced by sporadic inflow as final desiccation was approached.

## UPPER SALT

The path representing the changes in brine composition during the crystallization of the Upper Salt is plotted on a phase diagram that shows the boundaries of the stability fields of minerals in the $Na_2CO_3$–$NaHCO_3$–$Na_2SO_4$–NaCl–$H_2O$ system at 20°C (fig. 38). Figure 38*A* projects this system to the base of the tetrahedron, and figure 38*B* is a section through the tetrahedron. A line that represents the changing composition of the brine as crystallization

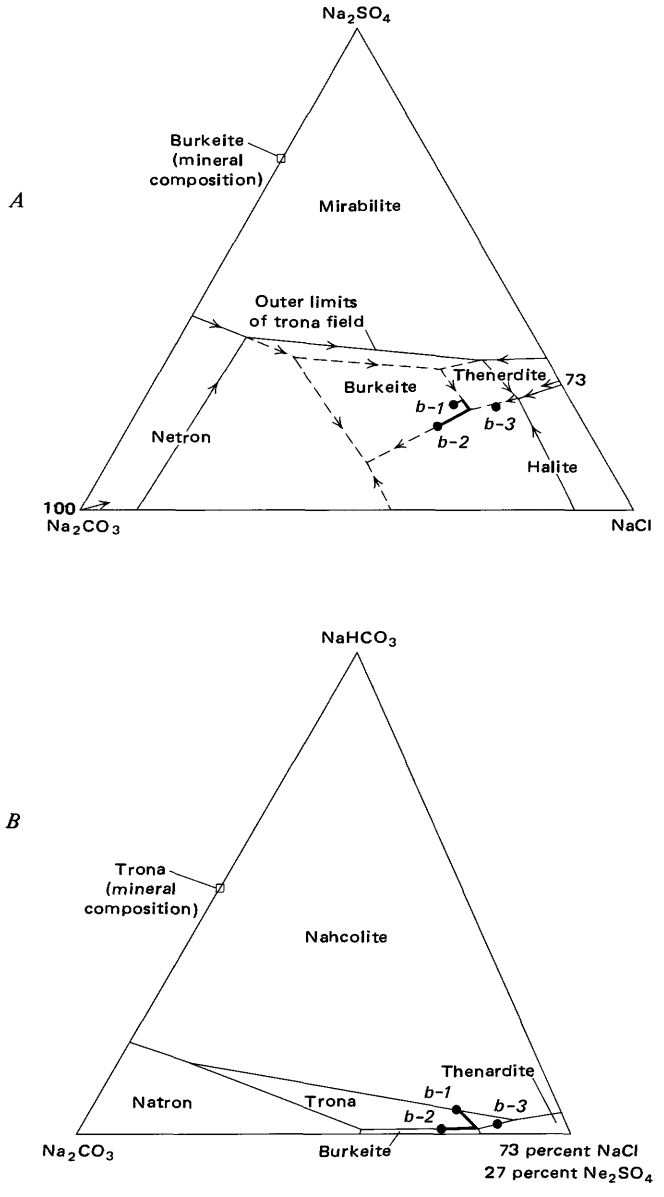


FIGURE 38.—Selected mineral stability fields in system $NaHCO_3$–$Na_2CO_3$–$Na_2$–$SO_4$–NaCl–$H_2O$ at 20°C. *A*, Same projection as in figures 35*A* and 36. Boundaries represent equilibrium between labeled fields and trona (inside limits of trona field) or nahcolite. Starting composition of brine that produced Upper Salt shown by point *b–1*; final composition of brine shown by point *b–2*; present composition of brine shown by point *b–3*. Points *b–1* and *b–2* based on data in table 17. Heavy line indicates changing composition of brine as unit crystallized. Arrows labeled 73 and 100 show location of base of section in *B*. *B*, Section through tetrahedron representing $NaHCO_3$–$Na_2CO_3$–$Na_2SO_4$–NaCl–$H_2O$ system is a plane having its base along line between points representing 100 percent $Na_2CO_3$ and 73 percent NaCl (27 percent $Na_2SO_4$) in diagram *A* and its top at $NaHCO_3$ corner. Boundaries plotted in terms of weight percent indicate equilibrium between labeled fields. Phase data from Freeth (1923) and Teeple (1929).

proceeded connects points *b–1* and *b–2*. As the layer of trona at the base of the Upper Salt shows that a sodium carbonate mineral was the dominant species formed during early stages of crystallization, the initial crystallization path (fig. 38*A*) followed a straight line that started at point *b–1* and led directly away from the $Na_2CO_3$ corner that represents the composition of all sodium carbonate minerals in this system. As noted below, the path probably first touched the boundary of the underlying field about at the boundary between the thenardite and burkeite fields, and trona, thenardite, and burkeite cocrystallized. The path then became a curved line that moved away from a series of points that represent the crystallized mixtures of those minerals plotted along the $Na_2CO_3$–$Na_2SO_4$ edge of the diagram. For the path to move from the trona-thenardite-burkeite-halite invariant point toward the point of maximum salinity under equilibrium conditions, all the thenardite would have to be dissolved. As indicated in the discussion of hanksite that follows, the brines in the central facies may have done so; point *b–2* (fig. 38*A*) is plotted on the assumption that they did, and the final salt assemblage was composed of trona, halite, and burkeite.

The path of crystallization was projected to a plane that cuts a section through the tetrahedron representing the $NaHCO_3$–$Na_2CO_3$–$Na_2SO_4$–NaCl–$H_2O$ system (fig. 38*B*). It intercepts the boundaries of all fields except halite. Point *b–1* is plotted on the nahcolite-trona boundary. Although any of three Na-carbonate minerals may have first crystallized from the lake, trona was the final product after rapid diagenesis, and the net effect of its crystallizations was to move the crystallization path directly away from the point that represents its composition on the edge of the diagram. This results in the crystallization path touching the base of the trona field in the diagram at the top of the boundary between the burkeite and thenardite fields. The next phases to crystallize, therefore, probably included both of those minerals. As most of the thenardite dissolved before the brine moved to point *b–2*, and both burkeite and thenardite apparently became the metastable precursors of the mineral hanksite, their initial ratios had no permanent significance.

The third most abundant mineral in the Upper Salt is hanksite which is not included in the 5-component system plotted in figure 38. A plot of the system $Na_2CO_3$–$Na_2SO_4$–NaCl–KCl–$H_2O$ at 20°C (Teeple, 1929, p. 100–103) illustrates the relation between hanksite and the other sulfate minerals being discussed and shows the inferred path of crystallization in this system followed during deposition of the Upper Salt (fig. 39). Hanksite is stable in a triangular field within the diagram. The ratios of $Na_2CO_3$ to $Na_2SO_4$ that allow hanksite to form, when the solution is saturated in halite and contains the correct percentage of K, are shown by projection from the KCl corner of figure 39*A* to the edge representing those components. However, the slow crystallization rate of hanksite allows minerals from surrounding fields—burkeite, thenardite, and aphthitalite—to form as metastable assemblages controlled by the dashed boundaries, then later react with each other and brine to form hanksite (Gale, 1938, p. 869). For this reason, the crystallization path is shown following the metastable boundaries.

Experimental data for the 6-component system including $NaHCO_3$ are not available. However, the relations shown by Eugster and Smith (1965, fig. 19b) show that increasing percentages of $NaHCO_3$ (proportional to $a_{CO_2}$ in that figure) would cause the thenardite field to encroach on the burkeite field, and the aphthitalite and thenardite fields to encroach on the hanksite field. This means that the burkeite-thenardite boundary and the metastable triple point in the hanksite field (fig. 39*A*) probably are shifted toward the $Na_2CO_3$ corner of the diagram in the 6-component system. The diagrams compiled by Eugster and Smith (1965) show that some combinations of $a_{CO_2}$ and $a_{H_2O}$ allow the boundaries between the hanksite and the burkeite, thenardite, and aphthitalite fields to lie both inside and outside the boundary of the trona field.

Crystallization during deposition of the Upper Salt started at point *b–1* (fig. 39). The crystallization path is plotted in figure 39*A* as if in the 6-component system which included the trona field, and deposition of trona moved the crystallization path away from the $Na_2CO_3$ corner of the diagram. The crystallization path reached the thenardite or burkeite field approximately at the boundary that separates them (then moved along it to the boundary of the halite field, see fig. 38*A*). Trona, thenardite, burkeite, (and halite) then crystallized together until the path reached the aphthitalite field, forming a metastable triple point. Further increase in salinity required solution of the previously crystallized thenardite prior to following the metastable burkeite-aphthitalite boundary. Thenardite is still found in the outermost parts of the deposit (cores GS–5 and GS–23), meaning that crystallization ceased in that area before the phase was destroyed. It is probable, however, that the central facies crystallized further, and that burkeite and aphthitalite crystallized simultaneously until brine concentration ceased. At that time, the composition of the brine

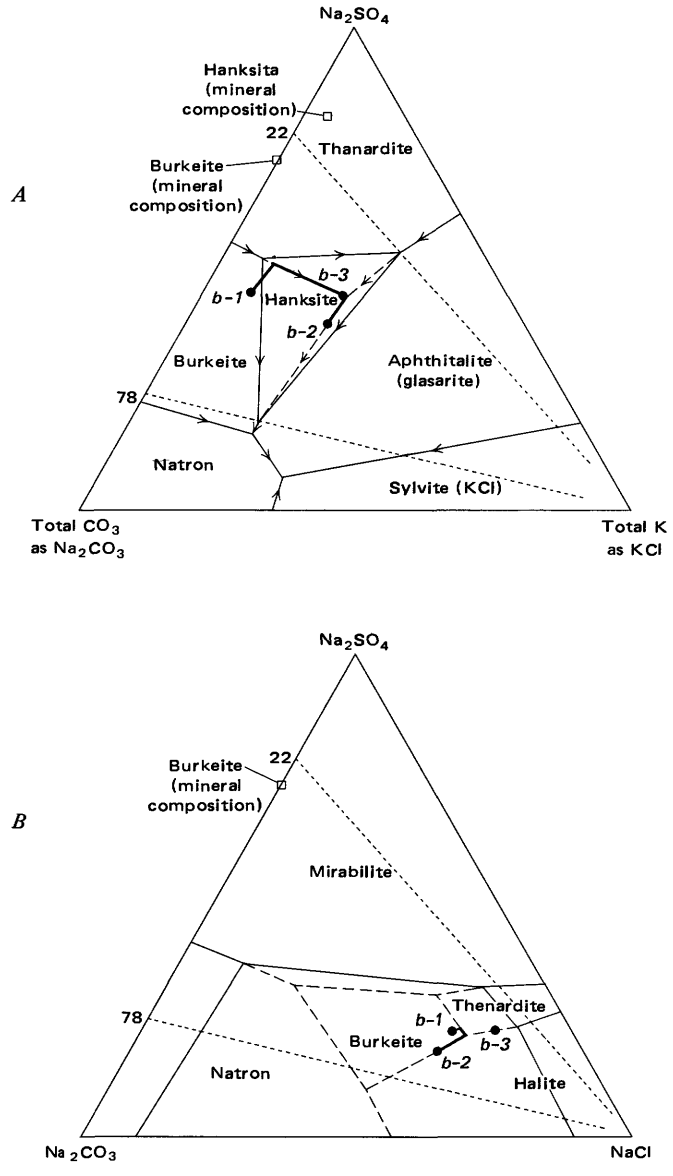


FIGURE 39.—Stability field of hanksite (9 $Na_2SO_4 \cdot 2\ Na_2CO_3$ KCl). *A*, Positions of hanksite and other fields in $Na_2CO_3$–$Na_2SO_4$–NaCl–KCl–$H_2O$ system at 20°C. Boundaries (solid lines) represent equilibrium in aqueous solutions between labeled components plus halite; dashed lines within hanksite field are boundaries between metastable assemblages of burkeite, thenardite, and aphthitalite plus halite. Points *b–1* and *b–3* derived from data in table 17. Point *b–2* is inferred. Projections of edges of hanksite field to $Na_2CO_3$–$N_2SO_4$– NaCl–$H_2O$ edge of diagram, shown by dotted lines labeled 22 and 78 percent $Na_2CO_3$ along edge. *B*, Part of diagram shown in figure 38 for $Na_2CO_3$–$NaHCO_3$–$Na_2SO_4$–NaCl–$H_2O$ system at 20°C showing points *b–1*, *b–2*, and *b–3*. Projection of hanksite field to $Na_2CO_3$–$Na_2SO_4$–NaCl–$H_2O$ edge in figure 39*A* is projected back by dotted lines in figure 39*B* to boundary of halite field; this approximates zone along halite-burkeite and halite-thenardite boundaries that can coexist with hanksite and (in all but a small segment) trona. All points and boundaries plotted as weight percent. Data from Teeple (1929).

was represented by a point (*b–2*) somewhere on the burkeite-aphthitalite boundary. That crystallization of the Upper Salt involved the aphthitalite field is confirmed by the small amounts of the mineral that are still present. If crystallization had reached the natron-burkeite-aphthitalite-halite point (or the invariant point for the system), we would be unable to account as satisfactorily for the massive concentrations of secondary hanksite because both points are outside the zone in which mixtures containing burkeite, aphthitalite, and halite would react spontaneously to form it.

Figure 39*B* is a phase diagram adapted from figure 38*A*. Because all points in figure 39*B* are saturated in halite, one can consider it as a diagram projected from the NaCl corner of figure 38*A* to the "walls" of the halite field. In figure 39*B*, this projection is made, and the zone containing the hanksite field falls between the projection lines. All other points and fields in figure 39*A* can be projected in the same manner. As required by the mineralogy of the Upper Salt and the data used to construct figure 38*A*, points *b–2* and *b–3* plotted in the 5-component system lie within the projected zone of the hanksite field (fig. 39*B*).

The early part of the reconstructed crystallization path (figs. 38 and 39) is consistent with stratigraphy of the Upper Salt, which is characterized by a basal layer of nearly pure trona. The later parts of the path are not so easily correlated with the observed stratigraphic sequence. Above the basal trona layer, halite is most abundant, and the only common sulfate mineral, hanksite, occurs in the highest concentrations near the top. Burkeite, thenardite, and aphthitalite make up less than 1 percent of the unit. However, hanksite clearly resulted from an episode of diagenesis that required aphthitalite, halite, and either burkeite or thenardite as precursors. As burkeite and thenardite probably crystallized before most of the halite and aphthitalite crystallized after it, it is clear that some of the components of hanksite migrated during diagenesis and therefore can not be easily related to the stratigraphic sequence of the precursor minerals. Other characteristics of the hanksite distribution that are probably also a result of this migration are the tendency for the mineral concentrations to have variable stratigraphic positions in the same parts of the deposit, and the lack of relation between the stratigraphic distribution of the high mineral concentrations and distribution of potassium in the brine.

Of the cores that contained large amounts of both hanksite and halite, about two-thirds had a small concentration of hanksite resting on the basal trona layer (Haines, 1957, 1959), and those concentrations may

represent the original stratigraphic position of aphthitalite. The hanksite crystals in the middle and lower horizons of the Upper Salt (and in units S–3, S–4, and S–5 of the Lower Salt) tend to have dominant basal pinacoid faces whereas crystals in the upper parts of the Upper Salt tend to have prominent pyramidal and prismatic faces (Smith and Haines, 1964, p. 17–18). Possibly the pinacoid form is favored by crystallization in high-sulfate environments (solid thenardite or burkeite reacting with K-bearing brine) and the pyramid form is favored by high potassium environments (solid aphthitalite reacting with $CO_3$-bearing brine).

The change of the metastable assemblage composed of thenardite, aphthitalite, burkeite, and halite to hanksite is a form of diagenesis. It would normally be discussed in the discussion of diagenesis but the process consumed some minerals and produced others, and these changes should be considered when comparing the inferred phase relations with present stratigraphy. The reaction of aphthitalite (Ap), thenardite (Tn), and halite (H) to form hanksite (Hk) also consumes trona (Tr) and produces $CO_2$ and $H_2O$ according to the following reaction:

$$4Tr + Ap + 3H + 25Tn = 3Hk + 10H_2O + 2CO_2.$$

Substituting burkeite (B) for thenardite, however, results in a reaction that has the opposite requirements:

$$6Ap + 18H + 75B + 65H_2O + 13CO_2 = 18Hk + 26Tr.$$

Both reactions produce and consume $H_2O$ and $CO_2$ in the same ratios, so the two reactions can offset each other as follows:

$$Ap + 3H + 13Tn + 6B = 3Hk.$$

These relations mean that thenardite and burkeite must be initially present in mole ratios of 13:6 to avoid the involvement of $H_2O$, $CO_2$, and trona in their conversion to hanksite.

The zone immediately above the trona layer at the base of the Upper Salt is inferred to represent the stage when primary sulfate minerals should have started to crystallize (see figs. 38 and 39), yet thenardite and burkeite are almost absent. Haines (1957, 1959) found neither of these minerals at this horizon except for one core, GS–11, which contains burkeite in beds 5–10 ft (1.5–3 m) above the top of the trona layer. Conversely, no K-bearing mineral should have crystallized at this level (fig. 39*A*), yet hanksite is common. It seems clear that the original suite of minerals recrystallized to form hanksite, deriving the required amounts of potassium from the ionic $K^+$ in the interstitial brines and consuming all the primary sulfates. The production of hanksite (Hk) from burkeite (B) or thenardite (Th), halite (H), and $K^+$-bearing interstitial brine also involves trona (Tr), $H_2O$, $CO_2$, and $H^+$ (ionic hydrogen) according to the following relations:

$$6K^+ + 6H + 27B + 33H_2O + 9CO_2 = 6Hk + 12\,Tr + 6H^+$$

or

$$K^+ + H + Tn + Tr = Hk + 2H_2O + H^+$$

and with mixtures of burkeite and thenardite as follows:

$$7K^+ + 7H + 27B + Tn + 31H_2O + 9CO_2 = 7Hk + 11Tr + 7H^+$$

All reactions release $H^+$ which would have reduced the pH of the remaining brine and promoted partial solution of carbonate-bearing phases. The salinity of present brine in this zone is as great or greater than other brines in the Upper Salt, and this salinity is consistent with the possibility of water being extracted from it during diagenesis according to the reactions that involve chiefly burkeite. At the time of reaction, trona and halite were certainly present to excess in this zone, and the reaction was limited by the amount of sulfate mineral of K-rich brine. As K-bearing brine is still present and sulfates are absent, the reaction apparently ceased because the original sulfate minerals were exhausted.

The upper part of the Upper Salt is the zone inferred to have been deposited when the crystallization path reached the metastable triple point (fig. 39*A*). It should have originally consisted of aphthitalite, burkeite, halite, and possibly thenardite; some or all of these must have converted to hanksite during diagenesis. The central parts of the deposit now have thick beds of vuggy hanksite and no other sulfate mineral; however, a few areas near the edge of the deposit have small amounts of thenardite (cores GS–5 and GS–23) and burkeite (cores GS–3, GS–4, and GS–5). This distribution seems to indicate that aphthitalite was exhausted in the edge facies before all of the original burkeite or thenardite and that both of those minerals were exhausted in the central facies before the aphthitalite. In the central facies, some trona occurs in or near the hanksite concentrations, and these zones appear to be products of reaction from a suite that included enough burkeite for trona to be produced. This reaction also requires sources of $H_2O$ and $CO_2$; additional $H_2O$ was undoubtedly available at the time the Overburden Mud was deposited, and $CO_2$ may have

been available from the same waters or from $CO_2$ released by bacterial action on underlying units.

Hanksite is abundant and aphthitalite is locally common in the Upper Salt, whereas hanksite is rare and aphthitalite missing in the Lower Salt. The concentration of potassium and sulfate in the brines that formed the Lower Salt was apparently high enough for some aphthitalite to form because that mineral was necessary for the formation of the local concentration of hanksite that are observed. The quantities of both components were higher in the brines that produced the Upper Salt. The increase may have occurred because the Upper Salt brines inherited a substantial amount of the sulfate and all the potassium that remained after crystallization of S–6 and S–7 of the Lower Salt. Those two Lower Salt units are nearly free of potassium- and sulfate-bearing minerals, and the brines that remained when crystallization ceased were correspondingly enriched. The enriched brines probably would have been preserved if the dense layer of brine that had formed during deposition of S–7 continued to occupy the lowermost levels in the series of the enlarged but stratified lakes that deposited the Parting Mud. In this way, all the potassium and sulfate would have stayed in Searles Lake rather than being partly lost during overflow. Those components would then have been added to the brines that ultimately desiccated to form the Upper Salt.

Borax is concentrated at the base of the Upper Salt and near the top, where it is associated with the large amounts of hanksite. The basal layer is interpreted as the result of chilling just prior to and coincident with the first deposition of a Na-carbonate mineral; the marked effect of low temperatures on solubility of borax was noted in the previous section. Its concentration in the zone now occupied by hanksite is interpreted as the result of crystallization of those horizons at high temperatures when borax solubility increased to levels that allowed it to remain in solution until very late stages in the sequence.

## OVERBURDEN MUD

The saline components in the Overburden Mud came from two sources. Some were dissolved from the top of the Upper Salt; and others were introduced by the inflowing waters that formed the lake. The exposed surface of the Upper Salt was largely halite and hanksite, and since hanksite dissolves very slowly in solutions saturated with halite, the components added to the lake waters from this source were dominated by Na and Cl. The components introduced by the inflowing waters were presumably similar to those of earlier episodes.

Extensive solution of the exposed surface of the Upper Salt and the tendency for hanksite to dissolve slowly could also explain the notably irregular and concave-downward contact between the Overburden Mud and Upper Salt. The thickest layers of hanksite were probably near the surface of the central facies of the Upper Salt. These hanksite zones may have retarded the solution rate of the Upper Salt in these facies, and their absence in the edge facies would have allowed more extensive solution in those areas. In the central facies, this would have produced a hummocky and irregular lake floor that was little lower than the original surface, and the floor would have been covered by concentrations of disaggregated, subhedral to anhedral, hanksite crystals. This is a lithology that is commonly found near the contact between the units in the central facies (Haines, 1959, see logs of GS–14 and GS–16). More extensive solution of the edge facies would have produced a concave-downward shape to the overall surface. Clastic sediments from nearby shorelines would probably have quickly filled in this deep trough around the edge of the partially dissolved salt body, producing the wedge of abnormally clastic-rich sediments we now see in this zone (pl. 1).

Evidence from cores and outcrops suggests that the lake that was responsible for deposition of the Overburden Mud was quite different from previous lakes. It was a perennial lake, yet small and highly saline, and contained more suspended sediment. The hydrologic details and climatic cause of this different type of lake are not understood. Beneath the outer parts of the present dry lake surface, most of the Overburden Mud consists of sand- and silt-sized clastic material, and even near the center, discontinuous beds of clastics make up 10–50 percent of the unit. Clearly, large quantities of the older lake sediments that cropped out around the edges of the relatively small lake were washed into it. Halite crystals eroded from the exposed surface of the Upper Salt are commonly found embedded in mud. The crystals are rounded as if partially dissolved, and this could mean that the lake waters were so near saturation in NaCl that the amount dissolved from those crystal edges brought the solutions to the saturation point. Many outcrops of sediments deposited at the same time are solidly cemented by halite; this characteristic further suggests a highly saline lake.

The mineral composition of salts in the Overburden Mud suggests that the composition of the brines that formed the salts would have plotted well inside the halite field in the phase diagrams (figs. 38 and 39*B*). Initial crystallization of halite is consistent with the geologic evidence showing that all the saline layers in this unit include halite, and that the clastic sediments

exposed around the edges of the lake are cemented by halite in a manner suggesting that they were permeated by saturated brine at the time of deposition. Probably there were several episodes of saline deposition that alternated with clastic deposition caused by renewed inflows of sediment-laden water. Each episode that started with the crystallization of halite would have moved the point representing the composition of the remaining brine toward other fields (figs. 38 and 39). The areal distribution of saline minerals in cores from the Overburden Mud (Haines, 1957, 1959) suggests that the trona and thenardite fields were touched first, and the fields of the other minerals that were precursors to hanksite touched last. Trona is most common, and thenardite is found only in cores near the edge of the deposit; hanksite is most abundant in the center. This distribution seems best explained if trona an thenardite were deposited during an earlier stage, when the lake covered a larger area, and the other precursor minerals for hanksite and K-rich brines were products of a later lake that covered a smaller central area. Most of the previously formed trona and thenardite in the center should have been consumed by the reaction of halite and aphthitalite to form hanksite, $H_2O$, and $CO_2$. Borax in this unit is distributed similarly to trona.

### GEOCHEMICAL INFLUENCE ON SHAPE AND THICKNESS OF SALT BODIES

The shapes of the saline layers as indicated by isopach maps are largely products of conditions that existed at the time chemical sedimentation was taking place. They can be interpreted on the basis of examples provided by present-day saline lakes and evaporating ponds constructed for commercial production. In the zone around the edges of saline lakes and ponds that are crystallizing salt but not evaporating to dryness, saline layers tend to be thin and uneven; the edges are more affected by seasonally fluctuating brine levels and wave erosion, and the salts that crystallize from dilute brines are controlled more by seasonal fluctuations in temperatures. The zone in the middle, however, is characterized by saline layers that have more uniform thickness because the salts are affected less by these variables and the crystal layers tend to be draped over topographic irregularities of the underlying mud.

Some small-scale relief in both zones is probably produced initially by winds. On Owens Lake, an irregular surface having a relief of half a meter seemed to be largely a result of wind-generated currents which were observed moving clumps of crystals on the brine surface into certain parts of the lake. Where these crystals foundered and sank, apparently because of turbulence caused by irregularities on the lake floor, they "piled up" to make the mounds even larger, and eventually made "islands." These processes were most active during mid-winter when rapid crystallization occurred with nighttime chilling, and during the final stages of desiccation when mid-day evaporation produced massive crops of crystals.

Saline lakes and ponds that eventually become dry most of the year produce saline layers that are nearly flat on top. This is because when the lake floods or when rain falls on the exposed salts, the water dissolves and transports salts from the higher areas to the lowest areas, eventually filling them in. As almost all the thickness variation in a desiccated saline layer is attributable to its lower surface, its shape as depicted by an isopach map is that of an inverted mold of the mud surface on which it rests.

After deposition, other processes may alter the original shape and thickness of saline units. If the saline lake receives an inflow of fresh water and becomes larger and fresher, erosion and solution of the salines probably creates new variations in thickness. Even after a protective layer of mud has been deposited, further volume and thickness changes may result from postburial recrystallization of salines under new temperatures and pressures and from solution by encroaching groundwater or undersaturated brines from other horizons. In Searles Lake, solution and volume change caused by the removal of interstitial brines by the chemical companies may have created new variation in thickness.

The most critical control of the shape of thick saline layers that resulted from desiccation is the topographic surface provided by the underlying muds. This is partly a result of the depositional pattern in the preceding lake and partly a result of compaction of the underlying deposits. Variation in the distribution of thickness in mud units is indicated by the isopach maps (figs. 15–20 and 23). The effect of postdepositional compaction is demonstrated by the present shape of the top of unit S–5 that was almost certainly flat at the end of its desiccation. The cross sections shown on plate 1 show more than 40 ft(12 m) of relief on this surface between the center and edge of the unit, and more than 10 ft(3 m) of relief in the central area between adjacent cores. Both local and overall relief seem best attributed to differential compaction of underlying material since deposition of the unit.

All saline units in the Lower Salt except S–5 were deposited on the floors of incompletely evaporated brine bodies rather than in lakes that desiccated. Isopach maps of the saline beds in the Lower Salt show that unit S–1 (fig. 8) has relatively small area near the center of the layer in which intermediate to maximum

unit thicknesses are attained and a wide peripheral zone in which the bed is less than 1 ft (0.3 m) thick; relief in the central part is irregular and commonly amounts to half a meter. Units S–2, S–3, and S–4 (figs. 9, 10, and 11) have near-maximum thicknesses over larger areas; local relief appears less in units S–2 and S–3 but is pronounced in some part of S–4. The diminishing amount of local relief, and increasing tendency toward uniform distribution of salts as units S–1 to S–3 were deposited may reflect the decreasing proportion of the total crystallization that occurred rapidly because of night-time chilling. Units S–4 (and S–5) crystallized more during the summer, when massive crops of crystals are produced during mid-day, causing the bottom topographic irregularities to grow rapidly. Units S–1, S–2, and S–4 have thin areas that trend from the southwest edge northeastward. Salt units in this area may be thin because they were partially dissolved by inflowing fresh waters which entered Searles Valley from China Lake via Poison Canyon (Salt Wells Canyon on old maps) which lies to the southwest.

The thickest of the saline units in the Lower Salt is S–5. It has a more symmetrical shape than any of the other units in the Lower Salt (fig. 12); its sides thicken rapidly and uniformly near the edge toward a large central area of irregular thickness. Unit S–5 was a product of complete desiccation; the major features of its isopach map reflect the topographic surface that preceded it, a basin with sloping sides and a flat central area. The marked local relief in the central area is likely to be the result of irregularities produced by solution of the flat surface during the initial stages of flooding that produced M–6.

Units S–6 and S–7 (figs. 13 and 14) have differences in their thickness distributions comparable to the differences between units S–2 and S–1. Thicknesses near average extend over much of the total extent of units S–6 and S–2; thicknesses below average characterize a wide area around the edge of units S–7 and S–1. These units represent the first two and last two periods of salt deposition in the Lower Salt sequence, and the explanation for their shapes may be the same. Thick concentrations of salts near the center suggest that most of the deposits formed after the lakes had shrunk to their minimal sizes because their brines were less concentrated or because the depositional basins had nearly flat edges and central depressions. Uniform distribution of thickness suggests opposite conditions. Neither possibility appears reasonable for these pairs of units. Possibly wind erosion of nearshore facies was more active during S–1 and S–7 times as a result of the major transition in climate that was taking place at that time. Solution by inflowing fresh water appears inadequate as an explanation because there is no relation between the sizes of thin areas and major sources of inflow.

The pattern of thickness distribution of the Upper Salt (fig. 27) is similar to that of S–5. The sides of the saline body thicken uniformly and rapidly toward a large central area of near-maximum thickness. The relief in this central area also is pronounced (although less obvious because fig. 27 has a 10-ft contour interval). Most of the overall shape of the Upper Salt is attributed to the shape of the basin at the time deposition of the Parting Mud ceased. Some of the overall shape and much of the irregular relief was apparently produced by the solution of the upper surface that occurred when the Overburden Mud was deposited. As plate 1 shows, though, relief along the basal contact of the Upper Salt is substantial, and some of the irregularities in the top contact seem to be reflections of irregularities in the basal contact (for example, note cores GS–12, GS–15, GS–18 on pl. 1*A*, and cores EE and N on pl. 1*B*). These irregularities partially cancel out each other and reduce the variation shown in the isopach map (fig. 27); this probably means that some of the irregularity now present in the basal contact was produced by differential compaction since the Upper Salt and Overburden Mud were deposited.

The areal extent and position in the basin of the seven saline units in the Lower Salt as plotted in figures 8–14 are notably similar. Their zero contours lie within about half a kilometer of each other in most places. The zero contour of the Upper Salt also lies within these limits. There is no systematic shifting of position with age, and each unit covers within 10 percent of the same area, regardless of thickness (table 3). Although in many areas the zero contour is not bracketed by data points, possible changes are mostly limited to those that increase the extent indicated.

It seems likely that the area of each salt layer was about the same as the area of the lake toward the end of crystallization. Lakes that shrank to the point of desiccation must have had early salt deposition in areas that became exposed to weathering. The exposed salts were presumably dissolved by surface runoff and their components recrystallized in the upper parts of the desiccating body. This process would have produced an inverted chemical stratigraphy for some of the dissolved components; those crystallized early from the larger lake were dissolved and redeposited with (or above) the components that crystallized last from the smallest lake (Smith and Friedman, 1975, p. 138). The final areal extent of the salt unit, therefore, is considered to be approximately the area of the lake that followed maximum concentration of the brine and solution of all exposed salts.

Deposition of the Upper Salt apparently followed this process. When Searles Lake began to shrink just prior to depositing the Upper Salt, salinities of 5 percent (that would allow deposition of salts during winter) were reached when the lake level was about 110 m deep (90 m above the present surface) and covered an area 3.5 times the present extent of the Upper Salt body (fig. 32). Salinities of 25 percent (that would have allowed trona to form all year from a $Na_2CO_3$–$NaHCO_3$ solution at 25°) were reached when the lake was about 40 m deep (20 m above the present lake surface) and covered an area almost 2.5 times the present extent of that body. A salinity of 35 percent, which is equivalent to the present brine, was reached when the lake was 33 m deep (13 m above the present surface), and this was apparently the original extent of the Upper Salt. As no salt beds are now exposed at these levels, they must have dissolved prior to, and during, deposition of the Overburden Mud. At present, the zone between the present lake surface and a level about 13 m above it is nearly free of vegetation except along washes; the Upper Salt, deposited initially over this larger area of the lake floor, apparently "poisoned" the soil, thereby preventing most plant growth since its solution and redeposition.

The differences in the reconstructed maximum salinities of units S–1 to S–3 relative to S–4 and S–5 suggest that the areas of saline deposits should decrease. As table 3 demonstrates, however, there is no change. Apparently, as successive layers of salts crystallized, they filled and flattened the central depression in the basin such that the area-to-volume ratio changed. In this way, the lakes that crystallized units S–4 and S–5 were shallower and more saline but occupied about the same area as the lake that deposited S–1. Some support for this model comes from calculating the quantity of salt in unit S–5 and applying it to the area-to-volume curve shown in figure 32 for the Upper Salt.[27] The present shape of the base of the Lower Salt cannot be used because as much as 10 m of compaction has occurred since deposition of units S–5 which must have been originally almost flat (pl. 1).

A similar calculation of units S–6 and S–7 shows that they should have crystallized from a 30-percent brine that had a volume of about $0.6\times10^9$ $m^3$ and covered an area of only about 30 $km^2$. Their actual area is about 100 $km^2$. Part of the discrepancy results from the flattening of the basin caused by deposition of units S–1 to S–5. A larger factor may be that more salts were dissolved in those lakes than table 10 indicates—the sodium, potassium, sulfate, and chloride that were retained in the brine and ultimately incorporated in the Upper Salt.

[27] When the dissolved solids in units S–1 to S–5 were in a brine that had a salinity of 20 percent (the approximate salinity of multicomponent solutions at 10°C when they precipitate sodium carbonate minerals but not halite), it occupied about $2.0\times10^8$ $m^3$. The curves for volume extrapolated to the base of the Upper Salt in figure 32 show that these volumes occupied about 100 $km^2$.

## SOURCE OF SALT COMPONENTS

The large volume of components in the salt bodies of Searles Lake were clearly introduced into the valley by water. Many of the components are found in almost all waters draining from bedrock terrane, among them Ca, Na, K, and Mg. All natural waters also contain $CO_3$ and $HCO_3$ contributed by the atmosphere. Many natural waters in the Great Basin drain areas underlain by Cenozoic lacustrine sediments that contain halite and gypsum, and those waters contain higher-than-average amounts of Cl and $SO_4$. The unusual components in Searles Lake—many of them the components that make the brines so unusual and valuable—must have come from sources that occur only infrequently in the headwaters of streams in the Great Basin. Thermal springs, mostly in the Long Valley area near Mammoth, apparently provided that source. The reasons leading to this conclusion are described in another paper (Smith, 1976); a summary of that information follows.

The Owens River and its headwaters probably contributed most of the dissolved solids because they account for most of the volume of water, and their drainage includes geologically favorable areas. Most of the uncommon components probably came from thermal springs, and the quantities of elements now issuing from those springs, plus those derived by the Owens River from other sources, are adequate to account for the amounts of most components now in Searles Lake. Data available for seven components — Na, K, $CO_3$, $SO_4$, Cl, B, Li—allow comparison of the total quantity of dissolved solids that would be carried by the present Owens River in 24,000 years, and the amounts estimated to have accumulated in Owens Lake and Searles Lake during the same period (table 21). From the concentrations of those components now present in the Owens River where it enters the Los Angeles aqueduct (or Owens Lake), the approximate amounts that would be contributed annually to a system of closed lakes today are estimated. It is reasonable to assume that the total amounts dissolved in the river during the Pleistocene were comparable or greater, and that since deposition of the Lower Salt in Searles Lake ceased 24,000 years ago, most of those components crystallized as salts in the Upper Salt of Searles Lake or were trapped in Owens Lake. Overflow of Searles Lake during Parting Mud time apparently carried few dissolved solids, for on desiccation, neither borates nor potassium salts crystallized in

TABLE 21.—*Comparison of amount of selected components carried by Owens River in 24,000 years with amount now in Owens Lake and Upper Salt of Searles Lake*

[Quantities expressed as parts per million (ppm) and grams (g)]

| Component | Present concentration in Owens River[1] (ppm) | Amount carried annually[2] by Owens River (x $10^9$g) | Amount carried by Owens River in 24,000 years (x $10^{12}$g) | Amount now in Upper Salt, Searles Lake (x $10^{12}$g)[3] | Amount in Owens Lake in 1912 (x $10^{12}$g)[4] | Total amount now found in Searles and Owens Lakes (x $10^{12}$g) |
|---|---|---|---|---|---|---|
| Na | 26 | 10.9 | 262 | 462 | 54 | 516 |
| K | 3.4 | 1.4 | 34 | 28 | 3 | 31 |
| Total $CO_3$ | 137 | 57.5 | 1,380 | 163 | 30 | 193 |
| $SO_4$ | 17 | 7.1 | 170 | 192 | 15 | 207 |
| Cl | 14 | 5.9 | 142 | 448 | 38 | 486 |
| | | [5]7.8 | 187 | | | |
| B | [5].77 | .32 | 7.7 | 7.9 | .8 | 8.7 |
| | | [5].23 | 5.5 | [6]6.4 | | 7.2 |
| Li | .11 | .046 | 1.1 | [7].06 | [1].0005 | .06+ |

[1]Friedman, Smith, and Hardcastle (1976) except value for B.
[2]Average annual flow of river $4.2 \times 10^{14}$ g/yr (calculated for period before irrigation in Owens Valley, using data of Gale, 1914, p. 254–261).
[3]Values from table 17 except as indicated.
[4]Recalculated from Gale (1914, p. 259); he incorrectly calculated quantities in this report but corrected them in later reports (Gale, 1919).
[5]Data from Wilcox (1946); value for concentration, from his table 12, is mean for the years 1929–1945 at the inlet to the aqueduct near Aberdeen. Values of amounts of Cl and B carried annually compiled by methods described by Smith (1976).
[6]Data from unpublished administrative report by D. V. Haines, entitled "Borate reserves of Searles Lake, San Bernardino County, Calif.", U.S. Geological Survey, July 1956.
[7]Calculation assumes average value 60 ppm Li in brine and 20 ppm in salts.

Panamint Valley, whereas they are abundant in Searles Valley (Smith and Pratt, 1957).

Such a comparison shows that three of the seven components are now present in Owens and Searles Lakes in quantities close to those expected to be carried by the Owens River in 24,000 years. The quantity of K in the two lakes is within 10 percent of that expected, and the quantity of B now found may be as close (depending on which combinations of the amounts listed in table 21 are used). The quantity of $SO_4$ is about 20 percent greater than predicted.

In the Upper Salt, only about 15 percent of the predicted amount of $CO_3$ and 5 percent of the Li are accounted for. Large quantities of calcite precipitated in Owens and China Lakes (Smith and Pratt, 1957) and the carbonates in the mud layers of Searles Lake account for additional quantities. Some of the lost $CO_3$ was probably restored as the lakes and streams dissolved atmospheric $CO_2$, but the original quantities were never fully replaced. The amount of Li now found in Searles Lake indicates even more loss, presumably by adsorption on clays. The amounts of Na and Cl now in Searles Lake are two to three times greater than the present Owens River seems likely to have supplied. The excess of Na in the Upper Salt is less because part of the quantity in the brine reacted after burial to form gaylussite and pirssonite in the interbedded mud layers. The excess of Cl came from erosion of older lake beds as well as from springs and atmospheric sources.

Calculations like those in table 21 can also be made for the quantities of $PO_4$ and F. The amounts of $PO_4$ and F in the Owens River are at least 0.11 ppm and 0.5 ppm (Smith, 1976, table 41). The quantity of $PO_4$ contributed by the river to Searles and Owens Lakes in 24,000 years is about $1.1 \times 10^{12}$ g, whereas, the amount present is near $0.5 \times 10^{12}$ g. The discrepancy seems significant but its cause uncertain because downstream movement of $PO_4$ was affected by biological factors in each lake of the chain. The quantity of F now found in the Owens River is very large. The analysis cited by Friedman, Smith, and Hardcastle (1976) indicates the amount to be about 1 percent of the total solids, although data from the Los Angeles Department of Water and Power suggest 0.25 percent as a more typical content. This amount, nevertheless, means that $5 \times 10^{12}$ g of F should be present in the Upper Salt of Searles Lake, yet only about $14 \times 10^9$ g is present. Those brines contain $8 \times 10^9$ g of F, and the salts would have to be composed of about 8 percent sulfohalite to account for the remaining quantity of F. That is three orders of magnitude greater than the amount estimated (table 14), and clearly a large amount of F is unaccounted for.

The quantity of W in the brines of Searles Lake has been attributed to the combined influence of springs and drainage from the many tungsten deposits in the Owens River drainage (Carpenter and Garrett, 1959). They estimated a total of $6 \times 10^{10}$ g of W in the Upper and Lower Salts of Searles Lake; data from this present report suggest about $3 \times 10^{10}$ g in the Upper Salt. One analysis of Owens river water reports 0.07 mg/L of W (Smith, 1976, table 41), and this would provide about $7 \times 10^{11}$ g in 24,000 years to Searles Lake. Only a small portion of this came from drainage of tungsten-bearing bedrock. A water sample collected November 8, 1958, from Morgan Creek, 28 km west of Bishop, Calif., at a point below the Pine Creek tungsten mine

(in one of the largest scheelite-bearing pendants in the Owens River drainage), contained 0.003 ppm W and 0.08 ppm Mo (F. S. Grimaldi, analyst, May , 1960). The flow was not measured, but an estimate made during a comparable season (December 12, 1975, by W. Hobbs of the Los Angeles Department of Water & Power, Independence, Calif.) suggests the flow in Morgan Creek at this time of year to be about 9 cfs ($8 \times 10^{12}$ g/yr) with most of that coming from one or more of the tungsten mine adits. That flow, for 24,000 years, would contribute about $6 \times 10^{8}$ g of W to the Owens River. About $1.5 \times 10^{10}$ g of Mo would be transported in the same period. The quantity of W from Morgan Creek would account for less than 0.1 percent of the total in the Owens River.

The amount of W issuing from springs in the Long Valley area can be estimated on the basis of two unpublished neutron activation analyses for W in water samples from Hot Creek and Little Hot Creek (L. A. Eccles, written commun., March 1976). These samples contained 0.035 and 0.9 mg/L of W, respectively, and average flow rates for those streams are estimated to be $3.2 \times 10^{13}$ and $3.6 \times 10^{11}$ g/yr. In 24,000 years, those two sources would contribute a total of $3.4 \times 10^{10}$ g of W, which is 5 percent of the calculated contribution by the the Owens River for that period but slightly more than is present in the Upper Salt of Searles Lake. Carpenter and Garrett (1959, p. 302) reported that W in water from Keough Hot Spring (on the west side of Owens Valley) averages 0.2 mg/L but no discharge data are available.

## GEOCHEMISTRY OF DIAGENESIS

Both salts and muds in Searles Lake have undergone change since first deposited. In both, new minerals have developed, and some original minerals have recrystallized into larger euhedral crystals of the same mineral. It is difficult to identify the times of most diagenetic changes; many could have taken place within weeks or months of first deposition although some clearly followed long periods of burial.

In theory, diagenesis of primary sediments takes place as a result of one or both of the following: (1) when postburial changes in the pressure, temperature, or composition of the interstitial fluids create conditions that favor the creation of new phases, or (2) when the original crystals or phases are thermodynamically metastable so that time alone results in spontaneous changes to form larger crystals or new phases.

Changes in pressure are proportional to changes in depth of burial plus the depth of the overlying lake, and in the Searles Lake sediments described here, they were relatively minor. The deepest samples obtained in core L-W-D come from 875 feet. Considering only the sediments, confined load pressures are about 60 bars, the unconfined hydrostatic pressures about 35 bars (Eugster and Smith, 1965, p. 480, 485). During times the basin was filled by a large lake, loads would have been about 30 bars greater. Pressures of this magnitude have been shown to have little effect on the mineral pair mirabilite-thenardite (Gibson, 1942, p. 195). The great contrast in density between mirabilite and thenardite suggests that they are likely to be as sensitive to change in pressure as any mineral pair found in Searles Lake. Pressure, therefore, is virtually neglected as a possible cause of changes described in this report.

Changes in temperature were probably more important as a cause of diagenesis. Temperatures at the time of original crystallization and for a short time after deposition probably varied over a range of 30°C or more, depending on the contrast between seasons, the depth of water, the salinity of the water, and the continentality of the climate. After deposition, temperatures within the accumulating layers fluctuated less and converged toward a level approximated by the mean annual air temperature in the basin during that period. As burial continued, these temperatures slowly changed to conform to the geothermal gradient. As the geothermal gradient is about three times normal—29°C/1,000 ft or 95°C/km—reactions caused by increased temperatures are likelier to occur in the Searles Lake evaporites than at similar depths in other deposits. A plot of the measurements in one core hole (fig. 40) shows that the projected mean temperature at the surface of the lake is about 20°C (the mean annual temperature today at Trona is about 19°C) and the base of the Bottom Mud a temperature of about 26°C. Projecting this trend downward suggests that the base of core L-W-D (875 ft, 267 m) is at a temperature of about 45°C, and the base of the sedimentary fill in the deepest part of the basin (3,300 ft, 1,000 m) about 115°C.

Changes in the composition of the interstitial solutions probably account for the most diagenetic changes. Several processes led to these compositional changes, some almost immediately after deposition, others much later. As most of the processes operative in the mud layers were not operative in the saline layers and vice versa, generalizations about them are given separately in the sections that follow.

### MUD LAYERS

Diagenetic reactions appear to have occurred in the mud layers as a result of several factors. Most of the diagenetic changes are attributed to disequilibrium between the original minerals and the brines that sur-

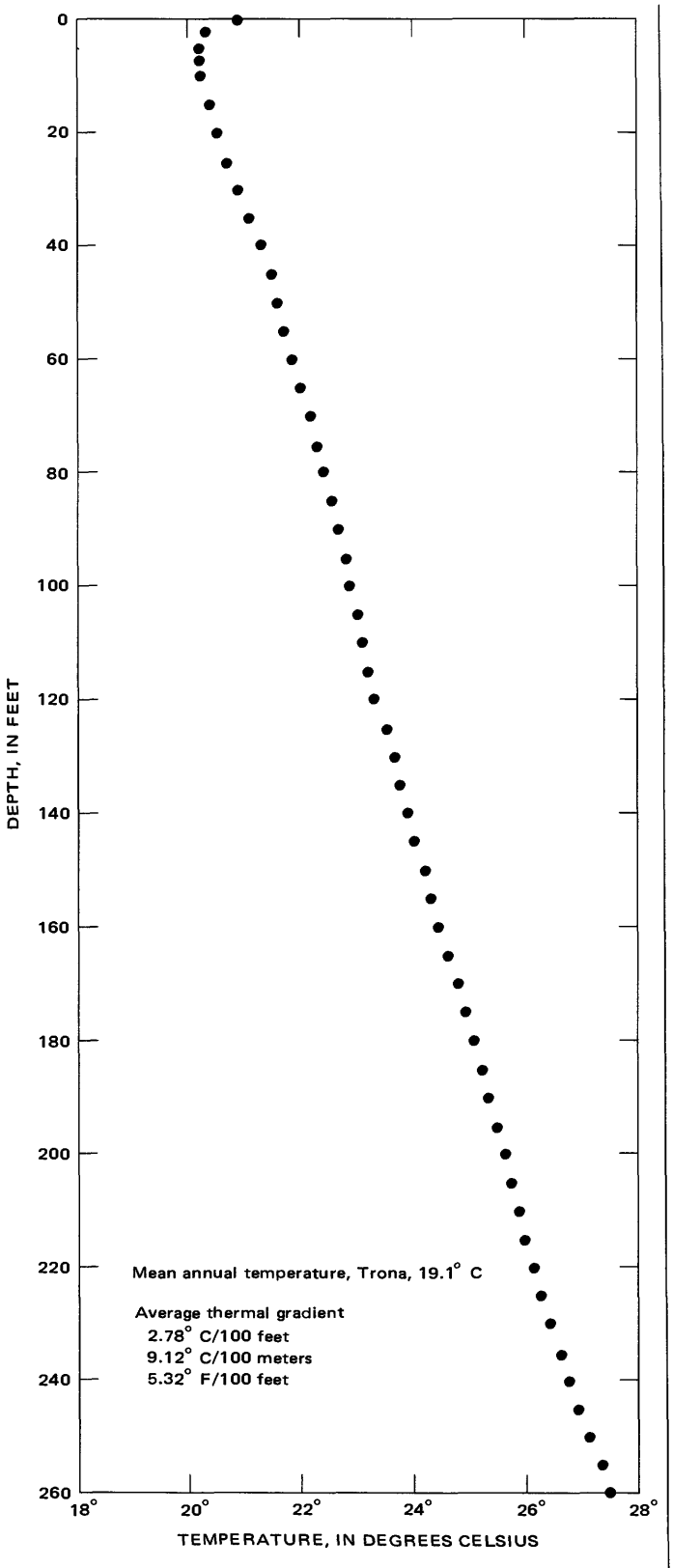


FIGURE 40.—Relation between temperature and depth in Searles Lake. Measured in core hole KM–8 with thermistor probe on insulated cable, on April 8, 1970, by G. I. Smith, W. J. Mapel, and R. L. Bornemann. Estimated accuracy ±0.2°C.

round them after burial. Others are attributed to chemical disequilibrium that resulted when temperatures within the mud layers changed significantly after burial. Still others are attributed to the fact that some of the initial precipitates were thermodynamically metastable and thus subsequently altered spontaneously to stable forms.

Some of the states of disequilibrium between the original minerals and brine occurred almost immediately after the original minerals were formed. Some minerals probably crystallized originally in stratified lakes along the zone of mixing and then sank to the bottom where they were surrounded by interstitial solutions of a different composition. Other states of disequilibrium occurred much later when brines migrating through the mud layer changed the composition of the previous interstitial brines or replenished the components that had been exhausted from them. Others occurred when organic decomposition altered the partial pressures of confined $CO_2$ and thus the quantities of dissolved $HCO_3$ and $CO_3$ in the interstitial solutions. Still others probably occurred during compaction when pore waters were eliminated more rapidly than were the salts dissolved in them, resulting in an increase in the relative percentage of dissolved ions. Changes may have occurred whenever major differences in the chemical compositions of contiguous brine zones caused ionic diffusion to occur.

Nearly all gaylussite and pirssonite crystals in the muds of Searles Lake appear to be diagenetic products of reactions between primary calcium carbonate minerals and sodium- and carbonate-rich solutions according to the equation (for gaylussite):

$$CaCO_3(s) + 2Na^+ + CO_3^= + 5H_20 = Na_2Ca(CO_3)_2 \cdot 5H_2O$$

This process was inferred by Jones (1965, p. A45) to explain gaylussite crystals in Deep Springs Lake, Calif., because of the tendencies for calcite and gaylussite to have inverse abundances and for gaylussite to be more abundant in older deposits. Both types of evidence for this reaction are found in Searles Lake. Aragonite occurs most prominently as laminae in these deposits, and although the number or thickness of the laminae does not seem to determine the zones that contain a high percentage of gaylussite or pirssonite, the percentage of aragonite obviously decreases in the gaylussite- and pirssonite-rich zones as segments of the aragonite laminae are replaced by the larger crystals during their volume-for-volume growth (see Smith and Haines, 1964, fig. 15). In the Bottom Mud, the percentage of aragonite and calcite decreases downward whereas the percentage of gaylussite increases (pl.2*B*); in the underlying Mixed Layer, calcium carbonate minerals are virtually nonexistent

whereas gaylussite and pirssonite are common.

Several diagenetic processes were probably involved in the formation of those minerals. Textural evidence shows that the most of the gaylussite and pirssonite crystal growth occurred after the muds had been compacted to their present state (Smith and Haines, 1964, fig. 15; Eugster and Smith, 1965, pl. 1), but other evidence suggests that some growth started immediately after the aragonite (or calcite) was deposited on the bottom. As described earlier (p. 79), much of the aragonite was apparently crystallized in the zone of mixing between a layer of calcium-bearing fresh water at the surface and a more saline layer below it. Crystals of aragonite formed in this way must have then settled to the bottom in a mud layer that had interstitial solutions of a higher salinity than the solution they formed in. If the sodium carbonate concentration in the solution was sufficient (between 14 and 22 percent $Na_2CO_3$ in the 3-component system) and the temperature high enough (between 15° and 40°C), a spontaneous diagenetic reaction to form gaylussite would have started (Bury and Redd, 1933, p. 1162). Higher salinities and temperatures would have produced pirssonite. Inasmuch as evidence derived from the existence of halite in the muds (described below) suggests that the initial salinity of some interstitial brines was nearly high enough to form halite, those brines probably also had concentrations greater than the minimum required to initiate the alteration of aragonite to gaylussite.

Most of the gaylussite and pirssonite crystallized after burial. The supply of $CaCO_3$ was generally more than adequate, for some is still preserved in most mud layers. Therefore, limits on the rate of gaylussite growth were imposed by the rate at which Na-bearing brines were able to migrate through the muds to the site of crystal growth and the availability of $CO_3$ from the same solutions or from nearby bacterial production of $CO_2$.

The rate at which Na in the solution that surround the growing crystal was able to reach the site of crystal growth must have been retarded by the low porosity of the muds. The quantity of Na in the original interstitial solutions should have been adequate. In the brines that permeate the salt layers (tables 9 and 16), the number of moles of Na is an order of magnitude greater than of $CO_3$ although about half the Na in solution was electrically balanced by $SO_4$, Cl, or $B_4O_7$ ions; K-, Mg-, and Ca-salts of those ions are not now found in the muds showing that the quantities of Na required to balance these anions were not extracted, and calculations outlined below show that only about a third of the total Na appears to be in gaylussite and pirssonite.

If the ionic ratios in the salts are representative of the pore brines in the mud layers, $CO_3$ ions in solution seem likely to have been exhausted first. Once the $CO_3$ was exhausted, the rate at which gaylussite crystallization could proceed probably depended in part on the rate at which $CO_2$ was formed by postburial decomposition of organic matter in the sediments so it could react with water and replenish the $CO_3$ in the interstitial solutions. Production of $CO_2$ by this process is effective but not necessarily rapid. Siever, Garrels, Kanwisher, and Berner (1961) and Siever and Garrels (1962, p. 54) report that in recent marine muds, there may be an order of magnitude increase in the partial pressure of $CO_2$ ($P_{CO_2}$) over solutions equilibrated with the atmosphere. Jones (1965, p. A466, A48) noted that fetid organic muds and $CO_2$-bearing gas from vents accompanied some occurrences of nahcolite, a mineral that requires the $P_{CO_2}$ to be at least four times that of solutions in equilibrium with the atmosphere (Eugster, 1966, fig. 3).

The crystallization of gaylussite and pirssonite from calcium carbonate and dissolved ions depleted the interstitial solutions in Na, $CO_3$, and $H_2O$. The average of Na values reported in analyses of the Parting Mud (table 13) is 12.6 percent (17.0 percent $Na_2O$); after subtracting 8.6 percent of the Na which is combined with the average of 13.2 percent Cl to form 21.8 percent halite, 4.0 percent of the muds consists of Na which is in gaylussite and pirssonite. The volume of the Parting Mud within the areal limits used for isopach plotting (fig. 23) is about $480 \times 10^6$ $m^3$. Assuming an average density of the Parting Mud of 2.0, about $80 \times 10^{12}$ g of Na is in halite and $35 \times 10^{12}$ g of Na is in gaylussite and pirssonite. This is about 20 percent of the amount of Na now found in the Upper Salt. Although the crystallization of this amount of Na caused a relative increase in the amount of dissolved K in the brines, it is probably not great enough to account for the exceptional concentration of K in the Upper Salt. At greater depths, where so much Na has been extracted from interstitial solutions to form gaylussite and pirssonite that $CaCO_3$ is almost nonexistent, this process might explain the creation of authigenic K-silicate phases in the muds, a mechanism suggested as the cause of these phases in the Green River Formation (Goodwin, 1973, p. 103).

Gaylussite and pirssonite in the Parting Mud are more abundant near the top and bottom contacts than in the middle (Haines, 1959, pls. 7, 8), and there is a tendency for the pirssonite that is found in the Parting Mud to be concentrated in these zones (Eugster and Smith, 1965, p. 519). Concentrations of more than a few percent of diagenetic gaylussite or pirssonite required additional Na, $CO_2$, and $H_2O$ from nearby sa-

line layers because the quantities of these components in the original interstitial brines were small. Concentrations of either pure gaylussite or pure pirssonite had to form in an open system. This is because the reaction responsible for diagenetic gaylussite removes five moles of $H_2O$ from the surrounding brines for each three moles of dissolved components, and if this process occurred in a closed system, it would raise the salinity, lower the chemical activity of water, and eventually result in the cocrystallization of pirssonite. Reactions of brine with aragonite to form pirssonite removed only two moles of water for each three moles of dissolved components, so its crystallization in a closed system would have decreased the salinity, increased the $a_{H_2O}$, and promoted the cocrystallization of gaylussite.

In most other mud layers that are shallower than 545 ft (166 m), though, the distribution of gaylussite and pirssonite seems to be controlled by the original salinities of the interstitial solutions and thus $a_{H_2O}$ (below 166 m it seems controlled by temperature, see below). Individual mud units (such as those in the Lower Salt) characteristically contain gaylussite, pirssonite, or a mixture without regard to the proximity or composition of the brine in the overlying and underlying saline layers. It seems likely that the salinities of the interstitial solutions at the time crystal growth occurred reflect the variations in the original bottom waters to a larger extent than waters introduced later by diffusion. Possibly seed crystals that grew in the original bottom waters determined which phase would later become abundant during diagenesis.

The maximum depth at which diagenetic gaylussite has been preserved is apparently controlled by temperature. In the $Na_2CO_3$-$CaCO_3$-$H_2O$ system, pirssonite is stable within a certain range of compositions above a boundary that lies between 37.3° and 40°C and gaylussite is stable within a similar range of compositions below these temperatures (Bury and Redd, 1933, p. 1162). Additional components in the solution will lower the chemical activity of water ($a_{H_2O}$) and thus lower the temperature range of this boundary (Eugster and Smith, 1965, p. 478–480). In core L-W-D, at levels above 545 ft (166 m), both gaylussite and pirssonite exist, apparently because of local variations in $a_{H_2O}$. Below 166 m only pirssonite is found. Projecting the geothermal gradient shown in figure 40 to 166 m indicates 35°C as the approximate temperature at that depth. Although this is 2°–5° below the range containing the gaylussite-pirssonite stability field boundary in the three component system, other components exist in the interstitial solutions, and the lower $a_{H_2O}$ resulting from their presence probably depresses the temperature range of the field boundary to about 35°C. At greater depths, temperatures would be above this point and only pirssonite would be stable.

Several other diagenetic minerals in the muds seem best explained by postburial changes in the partial pressure of $CO_2$ ($P_{CO_2}$) as a result of fluctuations in the biologically generated $CO_2$ from organic rich mud. A postdepositional increase of $P_{CO_2}$ in muds that contain sodium-rich pore brines seems the most likely explanation of rosettes and isolated clumps of nahcolite and trona in the muds of Searles Lake; this mechanism was proposed by, and supported by data of, Bradley and Eugster (1969, p. B9, B43) to explain similar features in the Green River Formation. In fact, the preservation of nahcolite in contact with brine requires the postdepositional addition of $CO_2$ such that the $P_{CO_2}$ is raised and maintained above that provided by equilibrium with the atmosphere. A postburial decrease in $P_{CO_2}$ in the mud layers of Searles Lake is possibly indicated by octahedra and nodules of finely crystalline northupite and tychite that cut bedding and are inferred to be diagenetic (Smith and Haines, 1964, p. P30–P33). These minerals can result from the interaction of brines and dolomite (or other minerals containing the necessary ingredients) when the $P_{CO_2}$ is lowered, although it is equally possible that the critical change in environment consisted of a decrease in the chemical activity of $H_2O$ (Eugster and Smith, 1965, p. 497–504; Bradley and Eugster, 1969, p. B60).

Microcrystalline halite, identified by X-ray diffraction techniques, is present in many of the mud units. This is one of the diagenetic products that seems most likely a result of postdepositional increases in the salinity of the interstitial brine during compaction (Smith and Haines, 1964, p. P39). Some of the observed halite in the muds may have crystallized from the interstitial brines that were evaporated to dryness prior to X-ray diffraction, but crystalline NaCl must also exist in the undried muds. The Parting Mud is the most carefully studied mud unit that contains major quantities of halite in most samples, and the conclusion that halite exists as a solid phase in the fresh moist samples is virtually unavoidable; the maximum brine content in the samples of this unit from core KM–3 was about 50 percent (fig. 25), and assuming that the unit in core GS–16 had a similar porosity, and the interstices were filled with brine that was saturated with NaCl, the maximum amount of Cl in the analyzed samples (table 13) should be only about 8 percent. All but one contain more than this amount and some contain more than twice as much.

Dissolved solids are commonly concentrated by several percent after they are deeply buried in sediments (White, Hem, and Waring, 1963, p. F9). Many work-

ers—DeSitter (1947, p. 2039–2040), Wyllie (1955, p. 288–301), Bredehoeft, Blyth, White, and Maxey (1963), and Von Engelhardt and Gaida (1963)—consider the postdepositional concentration of NaCl solutions in deeply buried marine sediments a probable result of the salt-filtering effect of compacting clay, which acts as a membrane that allows $H_2O$ to escape during compaction more rapidly than the salts dissolved in it. Bradley and Eugster (1969, p. B65) add the suggestion that the organic content may enhance the filtering effectiveness of sediments. Emery and Rittenberg (1952, p. 788–789) found no change in the NaCl concentration of brines of very shallowly buried (5–10 ft) muds, although Siever, Garrels, Kanwisher, and Berner (1961) and Siever and Garrels (1962) note a slight tendency for such concentration. Jones, Van Denburgh, Truesdell, and Rettig (1969, p. 257–258) report a downward increase in dissolved solids in muds from the bottom of Abert Lake, Oreg., and attribute it to the entrapment of more saline waters during an earlier period when the lake was more saline; Van Denburgh (1975, p. C24–C27, table 9) reports similar data from the muds beneath Abert Lake but no trend (or a weak trend in the opposite direction) in muds from nearby Summer Lake. Neev and Emery (1967, fig. 50, p. 96) noted the presence of halite crystals up to 10 cm in size that grew beneath the sediment surface in muds from the Dead Sea, but no explanation of their origin is suggested.

While the above observations show that increases in the salinities of interstitial brines do occur during compaction, they do not indicate increases of more than a few percent. The inference that halite in the mud layers of Searles Lake is product of this mechanism is therefore tenable only if the salinity of the pore brines from which halite crystallized was high. This is part of the reason for concluding that the lake was chemically stratified during some stages (see p. 54) with the densest and most saline waters, produced during previous episodes of near-desiccation or by solution of underlying salts, forming a layer on the bottom of the lake. The concentration of halite in the upper-middle part of the Parting Mud (table 13) is reasonably correlated with the episode of partial desiccation that geologic mapping indicates for this part of the lake's history (Smith, 1968, fig. 4) but it cannot be correlated with the present stratigraphic proximity of saline layers.

It is difficult to conceive of a mechanism other than diagenesis that could explain halite in the Parting Mud which was deposited on the bottom of a lake 100–200 m deep (Smith, 1968, fig. 4). If the lake was unstratified, and assuming that it contained the quantity of dissolved salts that later crystallized to become the Upper Salt, its average salinity while standing at these levels would have been at most only 5 percent—20 percent of that necessary to precipitate halite. If the lake was stratified, much denser brines near saturation could have existed on the floor of the lake. There is, however, no mechanism that allows a dense brine in this position to become supersaturated with halite. Further concentration could not occur as a result of evaporation because the lower brine layer did not have an exposed surface; supersaturation could not occur as a result of mixing along the interface between the brine and the overlying water layer because halite is one of the last minerals to precipitate from waters of these compositions, so both of its components would be concentrated in the denser lower layer.

In addition to diagenesis that is attributable to changes in the composition of the interstitial solutions and the temperature, some changes occurred because the original phases were thermodynamically metastable. The most common reaction of this type was probably the conversion of aragonite to calcite. Aragonite is a metastable compound, and if in contact with fluids, converts spontaneously to calcite (Berner, 1971, p. 138–147). In Searles Lake, aragonite in contact with interstitial solutions is in the Parting Mud, possibly in some mud layers in the Lower Salt and in the upper part of the Bottom Mud.[28] The oldest aragonite occurrences confirmed by X-ray are in muds from core L–30 at 136 ft (41 m), about 5 m below the top of the Bottom Mud and in deposits estimated to be about 50,000 years old. The similarity of laminae in older layers to those composed of aragonite in the younger layers suggests that they were originally aragonite but that the mineral converted spontaneously to calcite as a result of its thermodynamic metastability. If this is so, the conversion appears to require about 50,000 years under conditions of pressure and temperature found in these deposits.

Another diagenetic process related to thermodynamic forces is the long-term growth of large crystals of a given mineral species at the expense of very small crystals of the same species. This is promoted by the fact that the free energy of large crystals is slightly less than crystals less than a few microns in size (see Berner, 1971, p. 27–34). In a deposit containing very small crystals composed of moderately soluble phases, this thermodynamic drive probably results in some change. Most large crystals in the mud layers presumably contain some ions that become available by this process. Most of their postdepositional growth, however, was probably the result of the other processes

[28]Smith and Haines (1964, p. P25) reported laminae—presumed to be aragonite—in the lower part of the Bottom Mud, but these laminae were subsequently found by X-ray diffraction to be composed of other minerals.

that have been discussed.

Much slower diagenetic reactions between brines and (or) clastic silicates have produced a suite of authigenic silicate minerals. All these reactions were caused by disequilibrium between the interstitial brines and the silicates in the muds, although some were probably accelerated by the thermodynamic metastability of the amorphous silicates—tuffs—that lie at several horizons. Monoclinic K-feldspar, two types of searlesite, and two zeolites—analcime and phillipsite—occur in the subsurface deposits of Searles Lake. Hay and Moiola (1963) studied 72 carefully selected samples from cores GS–2, GS–14, GS–17, and L-W-D and found authigenic silicates in 54. None of the five samples they collected from the Overburden Mud contained authigenic silicate minerals. Two of the nine samples from the Parting Mud were from a 2 1/2 mm tuff bed that is about half a meter below the top of the unit; the tuff was almost entirely converted to phillipsite. R. L. Hay reports (written commun., June 1964) that two tuff laminae at a level 1 m below the top of the Parting Mud in core GS–27, possibly representing the same ash fall, were altered to phillipsite. One clayey dolomite sample from near the base of the Parting Mud contained a trace of analcime. Three of the six samples from the mud beds in the Lower Salt contained traces of analcime (their sample from GS–2 at 99 ft (30 m) is probably from the Bottom Mud rather than the Lower Salt as indicated in their table 1); the three containing analcime came from M–7 and M–6(?), and the three remaining samples came from M–6(?) and M–4. All but one of the 12 samples from the Bottom Mud contained authigenic minerals. A thin tuff bed 8.3 ft (2.5 m) below the top of the Bottom Mud consisted almost totally of phillipsite, but a tuff of similar thickness at the base of the Bottom Mud was altered to analcime. Analcime was detected in clayey samples from the upper and lower parts of this unit; authigenic K-feldspar was found mostly in the middle; and what Hay and Moiola (1963, p. 324–325) call "type B" searlesite was found in the lower part of that middle zone. Samples from the Mixed Layer contained analcime, both their "A" and "B" types of searlesite, and authigenic K-feldspar (data on Mixed Layer samples from table 1 of Hay and Moiola are summarized here on pl. 2*A*). Analcime appears to decrease in abundance downward through the Mixed Layer; K-feldspar clearly increases in abundance. Occurrences of both types of searlesite seem random. Two relatively thick (40 mm and 150 mm ) tuff beds in the Mixed Layer were altered to analcime, "type B" searlesite, and (or) K-feldspar.

In the study described by this present report, authigenic silicates were sought systematically only in samples from the Bottom Mud. They have been confirmed to be present in the Parting Mud and in mud layers of the Lower Salt, as reported by Hay and Moiola (1963), but their percentages are commonly too low to allow detection by X-ray diffraction unless especially favorable sample material is selected. Authigenic silicates are common in the Mixed Layer, but very few samples from that unit were studied, as Hay and Moiola had thoroughly studied the only available core.

The authigenic silicates in the Bottom Mud of cores L–30, L-W-D, and 254 were sampled, X-rayed, and their distribution plotted on plate 2*B*. Few or no authigenic silicates are in the top 20 ft (6 m). Analcime is a prominent component in a 10 m zone below that, with authigenic(?) K-feldspar coexisting with analcime in the lower 3–6 m of this zone. Authigenic K-feldspar is found as a component in the underlying 5 m of sediments, and in part of this zone, it coexists with "type B" searlesite of Hay and Moiola (1963, p. 324–325). Except for a basal zone, authigenic silicates are not detected in the bottom 10 m. This zonation is similar to that reported by Hay and Moiola (1963, table 1).

The phases present in the clastic silicate fraction of Searles Lake muds are presumably about the same throughout the section, even though the original percentages of clastic minerals may have varied by a factor of three. The distinct zonation of authigenic silicate minerals in the Bottom Mud would therefore seem to be most likely a result of differences in the chemistry of the pore waters. Differences in the composition of interacting solutions that would be critical can be inferred from the compositions of the new phases. Analcime ($NaAlSi_2O_6 \cdot H_2O$) and searlesite ($NaBSi_2O_8 \cdot H_2O$) require environments that have high chemical activities of Na and $H_2O$, but searlesite environments require a higher activity of B or a lower activity of Al than analcime. Zones of K-feldspar ($KAlSi_2O_8$) indicate higher ratios of K/Na activities than zones composed solely of analcime and searlesite. In the Bottom Mud (pl. 2*B*), authigenic K-feldspar occurs alone and also coexists with analcime and with searlesite; analcime and searlesite rarely coexist with each other, and only analcime occurs alone. This shows that the K/Na activity ratios in the reacting interstitial solutions are those required by the K-feldspar or analcime fields, or by the boundaries between the K-feldspar/analcime and K-feldspar/searlesite fields. The activites of Al apparently are those required by the K-feldspar and analcime fields and the K-feldspar/searlesite boundary, but not the searlesite field or the analcime/searlesite boundary. Variations in the chemical activity of B partially control the distribution of searlesite, but the necessary combination

of high Na and B, combined with low values of Al, that would allow searlesite and analcime to coexist, are rarely present. Conditions that allow searlesite to occur alone apparently are never present.

Pyrite was noted (and confirmed by X-ray diffraction) in one sample from the Bottom Mud as a cluster approximately 0.1 mm in diameter of intergrown euhedral crystals. It is surprising that it was undetected in nine other samples subjected to similar study from the Parting Mud, Lower Salt, and other parts of the Bottom Mud. Pyrite in these sediments is almost certainly the product of diagenesis by reaction of Fe compounds in the clastic sediments with hydrogen sulfide produced by sulfate-reducing bacteria that consumed $SO_4$ from the salts or brines. Neev and Emery (1967, p. 86, 94) infer that this process is responsible for the pyrite found in almost all dark laminae in sediments from the bottom of the Dead Sea.

## SALT LAYERS

The most obvious result of diagenesis in the salt layers is the postdepositional increase in the size of some crystals. This increase may be due partly to the thermodynamic drive supplied by the small difference in the free energy of large crystals relative to small ones, but this factor is probably negligible. The energy difference is a result of the larger surface-to-volume area of small crystals, but the differential is minute when the crystals are more than a few microns in size. Even with geologic spans of time involved, it does not seem likely that the typical "primary" crystals in the salt layers, most of which are 1,000 microns (1 mm) or more in size, would be affected.

It seems likely that the solution of small crystals and recrystallization of their ingredients on the surfaces of larger crystals is a result of cycles that first cause slight undersaturation and then supersaturation. Periods of slight undersaturation would result in some solution of all crystals, but smaller crystals would tend to be destroyed while larger crystals would tend to be partially preserved. Because supersaturation is required to start new nuclei, most of the ions from the destroyed crystals would recrystallize on the surfaces of the remnants of the larger crystals (along with the ions that had been previously dissolved from those crystals). The net effect would be for the large crystals to grow larger and small crystals to disappear. Cycles of this type can be created by daily or seasonal changes in temperature (while the salt layer is still near the surface), by the long-term changes in temperatures that occurred during the Pleistocene, or by cyclic changes in brine chemistry (caused, for example, by cycles in the $P_{CO_2}$ related to fluctuations in the rate of biological decomposition). The addition of brines having different composition or of fresher waters would also cause changes in the degree of saturation, but as changes caused by these mechanisms are inherently irreversible, their effects would have to be counteracted by other processes to complete the cycle.

Evidence of other forms of diagenesis of the salt layers in Searles Lake is rare, although most of the processes that created diagenesis in the mud layers were active in the salt layers. There are no convincing examples of one mineral being pseudomorphous after another. There is evidence that one suite of original minerals was thermodynamically metastable and that it recrystallized later to form a new mineral—hanksite. There are, however, only isolated examples of evidence indicating changes in mineralogy caused by postdepositional disequilibrium between the original minerals and new interstitial brines or by changes in temperature. However, as noted earlier (see section on "Saline Layers"), studies at Owens Lake show that the recrystallization that occurs immediately after some of the crystals first sink to the bottom leaves almost no physical evidence, so the lack of evidence of later change in salines of this type is not very significant.

The convincing example of diagenesis caused by a thermodynamically metastable suite of primary minerals that recrystallized spontaneously into a new mineral phase is provided by large crystals of hanksite. These crystals occur commonly as vuggy clusters, beds, and as relatively isolated euhedral crystals in several parts of the Upper Salt, less commonly as isolated crystals in units S–3, S–4, and S–5 of the Lower Salt (Smith and Haines, 1964, p. P16–P18). Hanksite crystals grow very slowly, and solutions that have compositions within its stability field commonly precipitate metastable assemblages of burkeite, aphthitalite (glaserite), and thenardite (Gale, 1938, p. 869) . Hanksite crystals in Searles Lake are almost all large and euhedral and occur in vuggy configurations that are virtually impossible to relate to conditions provided by the bottom of a saline lake. Recrystallization may have taken place within a relatively short time of the original deposition of the precursor minerals; some crystals contain inclusions of orange micro-organisms likely to have been most abundant during and immediately after salt deposition. The earliest core logs and descriptions of salts from Searles Lake (Hidden, 1885; Hidden and Mackintosh, 1888; Gale, 1914, p. 304; and company data made available to the author) report hanksite crystals in the form in which they now occur; their distribution and habit cannot be related to changes resulting from commercial operations on the lake.

Small percentages of anomalous minerals are mostly interpreted here as products of diagenesis rather than original depositional conditions. Some may have resulted from changes in bulk composition that can occur after deposition when brines from overlying or underlying sediments migrate into a layer. Others may have been caused by differences in temperature that occured between the time the initial layer was deposited and the present. New phases created because of postdepositional changes in temperature, however, were crystallized only to the extent that their components were available in the brines. Since about 15 percent of the evaporite components are estimated to be in the brines (tables 10 and 17, footnote 7), new phases containing components that were initially only in brines cannot exceed this percentage and are likely to contribute much lower percentages. Examples of diagenetic minerals probably formed in this way are indicated by analyses of Lower Salt cores (table 7). In most cores, units S–1, S–2, S–3, S–6, and S–7 do not contain sulfate minerals that are detected visually or by X-ray (fig. 34), yet the analyzed samples do contain a few percent $SO_4$ indicating the presence of a small percentage of such minerals. It seems likely that these sulfate minerals, present consistently but in small amounts, are products of post-burial diagenesis.

The $CO_2$ that was organically generated in muds after burial may have locally changed the species of carbonate minerals in overlying saline layers because $CO_2$ (and methane) tends to escape upward. Changes in the rate at which $CO_2$ is produced could change the $P_{CO_2}$ in those solutions, and, as indicated by Eugster and Smith (1965, p. 486–512), numerous reactions are promoted by such changes. For example, assuming reasonable assemblages of Searles Lake minerals, increasing the $P_{CO_2}$ (which is nearly proportional to $a_{CO_2}$) may promote reactions that will change thermonatrite to trona, burkeite to mirabilite, or natron to trona (Eugster and Smith, 1965, figs. 19A, B). Decreasing the $P_{CO_2}$ could have the opposite effect. Since all these reactions are also promoted by changes in $a_{H_2O}$, evidence of alteration is not necessarily a sign of change in the $CO_2$ in the postdepositional environment, therefore, the conclusions may be ambiguous.

It is difficult to evaluate the importance of this mechanism. There is very little physical evidence in the saline layers of the Searles Lake deposits of diagenetic changes caused by changes in $P_{CO_2}$, yet as noted previously, such evidence is sometimes missing even where reactions are known to have taken place. Coarsely crystalline aggregates of some sensitive minerals are clearly recrystallized after burial, but they do not appear to be replacing or growing at the expense of another species of mineral; in many instances, in fact, they coexist with finely crystalline layers of the same mineral (Smith and Haines, 1964, p. P45).

Any diagenesis of the salt layers must cause corresponding changes in the brines. The present brines, indicated by point *b–3* in figures 35, 36, 38 and 39, are all different from the brines as they existed at the end of crystallization (point *b–2* in those figures). All the points labelled *b–3* lie on a phase boundary or triple point for the applicable system at 20°C (which is within 3°C the present temperature of the salt bodies), but in a position that requires that they have a slightly lower percentage of dissolved solids than when crystallization ceased at point *b–2*. Clearly, water has been added to the brines since deposition of the salt bodies, and partial solution of the original salts has produced brines whose compositions are controlled by the boundaries of the remaining phases.

The deuterium-hydrogen content of the salts and present interstitial brines in Searles Lake (Smith, Friedman, and Matsuo, 1970, p. 258) confirms the fact that water has been added to the saline units since their deposition. The question is: Did the addition of water cause diagenesis or did diagenesis produce the additional water? It is clear that some water was added as the present hydrostatic head (Hardt and others, 1972, fig. 10) is forcing relatively dilute brines from near the surface of the lake into the underlying layers, thus producing an increase in the $a_{H_2O}$ of the interstitial brines. Diagenetic reactions that require water would be favored by this change. Two of the post-depositional reactions that probably occurred have this requirement. Nahcolite (Nh) reacts to form trona (Tr) as follows:

$$3Nh + H_2O = Tr + CO_2$$

and burkeite (B), aphthitalite (Ap), and halite (H) react to form hanksite (Hk) and trona as follows:

$$75B + 6Ap + 18H + 65H_2O + 13CO_2 = 18Hk + 26Tr$$

However, other post-depositional reactions that probably occurred release water; they would have produced a more dilute brine but might have been inhibited by the dilution of the brine by other processes. Natron (Na) reacts to form trona as follows:

$$3Na + CO_2 = 2Tr + 25H_2O;$$

and thernadite (Tn) and other minerals react to form hanksite as follows:

$$25Tn + 4Tr + Ap + 3H = 3Hk + 10H_2O + 2CO_2$$

At this time, there is no clear way to tell which processes were most active. The net result, though, was

that the brines were diluted after initially being formed and that their present compositions are controlled by the phase relations between the surviving mineral species at about 20°C.

The position of point *b–3* in figure 39*A* is almost exactly on the metastable triple point of that system. This is probably coincidence. Once the metastable suite of minerals has altered to hanksite, the triple point has no meaning. Moreover, the actual position of the triple point in the system that contains $NaHCO_3$ and thus trona was inferred (p. 92) to be positioned more toward the $Na_2CO_3$ corner of that diagram. It is more likely the Upper Salt brines are on the aphthitalite-thenardite-trona-halite boundary in the 6-component system at 20°C. Burkeite, therefore, would not be expected to exist in the Upper Salt, but a few pockets remain. Point *b–3* represents an average, however, and the scatter of brine compositions indicated by figures 21 and 28 means that local assemblages may exist that are not in equilibrium with a brine having this average composition.

## RECONSTRUCTED DEPOSITIONAL HISTORY

The history of lakes in Searles Valley is partially documented by the sequence and nature of the sediments beneath the present dry-lake surface. The mud layers represent large, relatively deep lakes that were fresh or brackish, and variations in the lithology and mineralogy of those layers reveal changes in the composition, concentration, and distribution of dissolved solids in those lake waters. The salt layers represent either small, relatively shallow lakes that were highly saline or dry lakes. Some saline lakes crystallized salts during part of the year only; others crystallized salts all year; still others desiccated. Beds of monomineralic salt of a type that probably crystallized as a result of winter cooling indicate a moderately saline lake (approximately 3–15 percent salinity); beds of monomineralic or bimineralic salts that probably crystallized during much of the year but did not include the most soluble species indicate a shallower(?) more saline lake (approximately 15–30 percent); and beds of salts that include the most soluble species of salts indicate a highly saline lake that approached or reached desiccation (more than about 30 percent).

In the following reconstruction of Searles Lake history, the ages of the inferred events are mostly based on the ages discussed in the section on $^{14}C$ dates. The positions of salt layers in the Bottom Mud are based on core 254 (pl. 2*B*), and the period of time represented by that unit is based on the depositional rate determined for the Parting Mud, as corrected for the greater amount of acid-insoluble material found in the Bottom Mud.

The Mixed Layer represents a long period during which there was a gradual shift from nearly continuous mud sedimentation to salts, and from a NaCl- to a $Na_2CO_3$-dominated water chemistry. Nearly continuous mud sedimentation is represented by unit F (pl. 2*A*). Salt deposition started as a mixture of mud and halite (unit E), then progressed to alternating beds of mud, halite, and trona (unit D), then to beds of nearly pure trona and halite that grade up to halite (unit C), and finally shifted to beds dominated by trona and nahcolite (units B and A).

Although the mud layers in the units F and E represent perennial lakes, the salinities of the interstitial waters appear to have been high inasmuch as they contain large amounts of authigenic K-feldspar, analcime, and searlesite. These minerals occur more consistently and in larger amounts than in younger salt-bearing units, either because the mud in units E and F provided more adequate sources of silica and alumina for diagenesis, or because their greater age allowed diagenesis to progress further. The other minerals present in fine-grained form in the muds of the Mixed Layer seem to indicate no trends in sedimentation history that are not evident from the megascopic lithology of the mud and salt units.

Several mud layers in the Mixed Layer are characterized by mottled coloration that includes reddish hues. Mottled zones are inferred to represent times when the lake was dry and the sediments were exposed to oxidation by the atmosphere. The surface was probably dry at many other times when oxidation of the clastic sediments was prevented by an overlying layer of salt that contained entrapped brine. However, salts exposed at the surface of modern salt flats tend to become tan to pink as they are mixed with or covered by silt of these colors that is introduced by winds and seasonal floodings. Salt surfaces that have been dry for more than a few thousand years are likely to be identifiable in cores by the intermixed clastic sediments that have these colors.

Sands, silts, and clays exposed on the present surface of Searles Lake have hues in the 5YR to 10YR category of standard rock-color charts. These colors do not characterize any layers of muds or salts in the units above the Mixed Layer (Smith and Pratt, 1957, p. 25–33; Haines, 1959) but do occur at six horizons in core L-W-D. One horizon (534 ft, 163 m) is in unit C, five (at approximate depths of 715, 722, 763, 768, and 783 ft, or 218, 220, 233, 234, and 239 m) are in unit E. None occur in units A, B, D or F. These data combined with those described above suggest that the center of Searles Valley contained a deep lake during much of the time unit F was deposited, a fluctuating lake that desiccated several times and remained dry for long

periods while units C, D, and E were deposited, and a shallow saline lake that commonly produced salts but dessicated rarely or only for relatively brief periods during the times units B and A were being deposited.

Calculations described by Smith (1976, table 1) show (1) that Searles Lake was likely to have been dry only when it received no overflow from Owens Lake meaning that the flow of the Owens River did not exceed about 3 times that of the present, (2) that it was likely to have been a small saline lake when the Owens River flow into Owens Lake was approximately 4 times that of the present, and (3) that it was likely to have been a maximum-sized or overflowing lake when the river was flowing at a rate 7 to 10 times that of the present. Using these categories of relative flow of the Owens River, the lithology of unit C of the Mixed Layer represents an episode that was dominantly like category 1 (interpluvial), the lithology of unit F represent an episode that was clearly like category 3 (pluvial), and units A, B, D, and E represent episodes that were mostly intermediate between these extremes.

The period of time represented by the Mixed Layer can only be approximated on the basis of sedimentation rates. In core L-W-D (Smith and Pratt, 1957), the Mixed Layer is about 200 m thick of which about half was recovered as core. As the cumulative thickness of mud recovered from the Mixed Layer was about 45 m, about 90 m of mud may occur in this part of the section. The sedimentation rate derived for the Bottom Mud (about 33 yrs/cm) suggests that 90 m of mud represents about 300,000 years. As the top of the Mixed Layer is about 130,000 years old, the age of the base of unit F might be about 430,000 years plus whatever time was required to deposit 110 m of salts. Reasonable guesses of the age of that horizon probably lie between 500,000 and 1,000,000 years.

The larger amounts of data pertaining to the Bottom Mud and younger deposits allow more details of their depositional processes to be reconstructed. The curve shown in figure 41 indicates the inferred lake history during the past 150,000 years. The levels labeled C, D, E, and F are represented in cores by saline layers, with each level representing a range of salinities that would result in deposition of the observed suites. The levels labeled A and B represent large perennial lakes that had a wide range of depths, and some probably had relative depths which were the opposite of those implied by the curve because the choice of levels is based on criteria that are only suggestive of depth. Segments of lake history plotted at level B are based on the presence in cores of authigenic silicates (indicative of higher salinities in the bottom waters and presumably also those of the entire lake), or aragonite laminae (indicative of pronounced chemical stratification and thus probably a more saline lower layer and a smaller total lake volume). The segments plotted at level A are mostly based on the absence of these suggestions of moderate salinity. Some portions of lake history are plotted at levels between the labeled horizons because the available data do not allow a clear choice.

The Bottom Mud mostly consists of mud that was deposited in deep lakes, although several low stands are documented by salt layers. The deep lakes are represented by mud. A plot of its fine-grained components (pl. 2*B*) shows marked variations in the amounts of the four Ca-bearing minerals, aragonite, calcite, dolomite, and gaylussite, but these variations are not used as a primary basis for inferring a succession of lacustrine environments. The amount of Ca

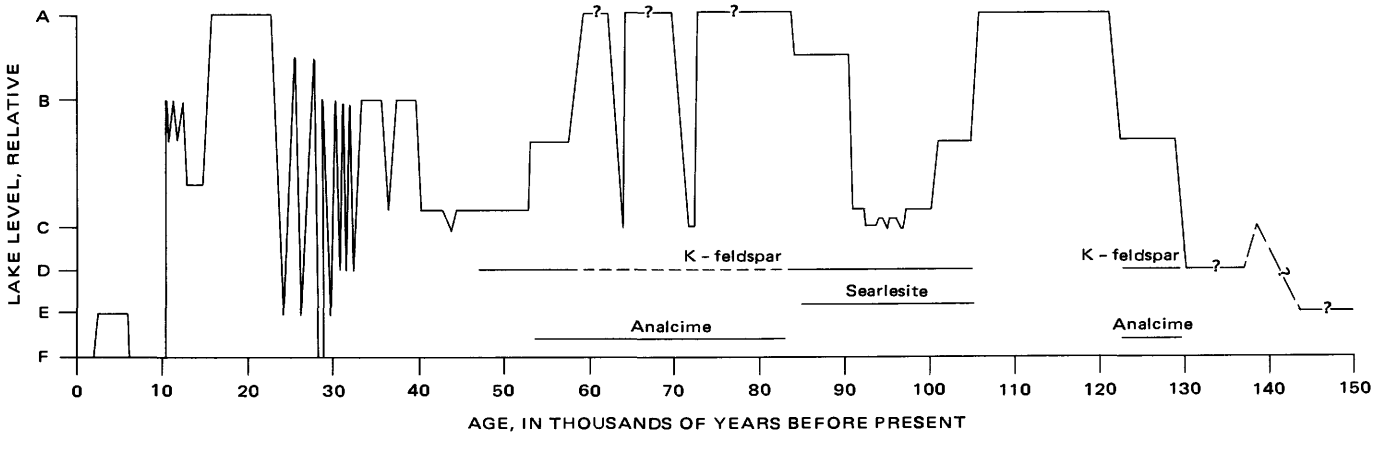


FIGURE 41.—Inferred history of fluctuations in Searles Lake, 0–150,000 years ago. A, Deep lake, unstratified or stratified with thick surface layer; B, Deep lake, stratified with thin surface layer; C, Intermediate-depth lake, salinity of interstitial brine 3–15 percent; D, Shallow lake, salinity 15–30 percent; E, Very shallow lake, salinity 30–35 percent; F, Dry lake, salt surface exposed part of year, salinity of interstitial brine mostly greater than 35 percent.

that was transported into the lake basin and precipitated theoretically provides a measure of the volume of inflow, but the percentages of Ca in those minerals (40, 40, 22, and 14, respectively) vary so much that it is almost impossible to estimate the total amount from the semiquantitative estimates of mineral abundance, and chemical analyses that report total Ca are not available.

In younger units, the existence of a stratified lake is inferred from the abundance of aragonite laminae or the dominance of aragonite over calcite. Aragonite laminae are found in the upper few meters of the Bottom Mud, but calcite is the more abundant of the two minerals. These proportions suggest that the lake in which the upper part of the Bottom Mud was deposited was occasionally stratified but that conditions favorable for slow crystallization of $CaCO_3$ as calcite existed during most of the year; presumably this required a large, relatively fresh lake. Calcite percentages diminish downward in the Bottom Mud, but it is not clear if this is because its original percentage was low or because the extent of its reaction to form gaylussite is more nearly complete.

The distribution of dolomite and gaylussite in the Bottom Mud apparently also reflects too many processes to make it useful for reconstruction. In the Parting Mud, the distribution of dolomite suggests that it is favored by brines that are intermediate in salinity, but its coexistence in the Bottom Mud with gaylussite, calcite, and aragonite, combined with its proximity to saline layers, means that there is either broad overlap of stability fields, that there were rapid fluctuations between environments, or that some is diagenetic. The quantity of gaylussite must partly reflect the original amount of calcite (or aragonite) and partly indicate the amount of Na in the original or introduced interstitial brines. In the lower part of the Bottom Mud, there is a fair correlation between the large percentages of gaylussite (pl. 2*B*) and the high stands of the lake inferred from other data (fig. 41). In the upper part of core 254 (pl. 2*B*), a zone containing abundant calcite approximately coincides with a zone low in gaylussite, and this suggests a deficiency in the amount of Na-bearing brine that was required for the diagenetic reaction. This interval also contains trace amounts of Na-bearing saline minerals meaning that the Na percentages in the interstitial brines must be high. Inconsistencies like this make interpretations of the original depositional condition based on gaylussite percentages seem tenuous.

Lake levels plotted at or below the horizon labeled B in figure 41 are mostly those represented by mud containing analcime, searlesite, or authigenic K-feldspar. Exceptions to this are the three queried intervals between 55,000 and 85,000 years which are tentatively plotted at horizon A, even though the sediments contain authigenic K-feldspar and analcime, on the basis of correlations with unpublished geologic mapping; this shows that greater thicknesses of sediments were deposited at the highest lake levels in the period that followed a low stand (presumed to be the one plotted at 95,000 years) than before it.

Analcime in the Bottom Mud is clearly concentrated in certain zones (fig. 41). They are interpreted as of diagenesis resulting from times when the original lake and resultant pore waters had higher chemical activities of Na and $H_2O$. The tendency for these zones to characterize the mud layers above and below nahcolite layers suggests that the lakes at these times had Na-rich brines in contact with the accumulating mud layers for long periods of time, either because the lake was stratified or because it was shallow and uniformly saline. The lack of frequent zones of winter-crystallized salines throughout the analcime zones argues against shallow saline lakes.

Changes in the abundance of searlesite in the Bottom Mud must in part indicate variations in the abundance of B in the interstitial waters. The one searlesite zone in the interval plotted (fig. 41) between 85,000 and 105,000 years probably reflects a period of abnormally high B in the inflowing waters. A high B content might also result from concentration by evaporation of lake waters, but searlesite is missing from other zones known to have been deposited in lakes having high salinities.

Concentrations of authigenic K-feldspar occur in the Bottom Mud in two or three distinct zones (fig. 41), that probably indicate higher K/Na ratios in the pore waters than zones containing only analcime or searlesite. As K-feldspar occurs with analcime and searlesite as well as without either of these minerals, these zones probably indicate periods characterized by both intermediate and high K/Na ratios in the pore waters.

Several times the lakes that deposited the Bottom Mud decreased in size and deposited salts during part of each year. Zones in the Bottom Mud that contain disseminated salines appear to represent lakes that were too deep for salt crystallization during normal winters, but which deposited small quantities of salts during exceptionally cold winters or dry years. Zones that are composed of more nearly pure salines are interpreted to represent the culmination of those periods when the lakes were a little shallower and more saline so that salts crystallized out during most winters. Periods represented by these nearly pure saline layers are plotted in figure 41 at level C. The prominent saline layers are mostly composed of mirabilite

or of nahcolite that was probably altered from primary natron. They are mostly overlain and underlain by zones of mud that is mixed with minor amounts of similar salts that are detected only by X-ray (pl. 2*B*, column Sx), and these are shown in figure 41 at a level slightly above C. For example, in core 254, mirabilite occurs as a minor component in muds above and below the layer of salines at 134 ft (41 m); these and other saline minerals are intermixed with muds that are interbedded with the thin layers of salines near 164 ft (50 m) and 190 ft (58 m). Similar zones occur in core L-W-D at depths of 150 ft (46 m) and 216 ft (66 m), and they provide the only evidence of the saline layers that probably lie at depths near 190 ft (58 m).

The depositional history of the Lower Salt is one of conditions that alternated between large perennial lakes that deposited muds and small saline lakes that either deposited salts or dried up to form salt flats. The details come largely from the mineralogy of the layers. The successively greater degrees of desiccation indicated by the mineralogy of saline units S–1 to S–5 and the partial desiccations indicated by units S–6 and S–7 allow the salinities and relative levels of the small highly saline lakes to be approximated. The progressive changes in the volume of inflow into the perennial lakes are indicated by the quantities of gaylussite plus pirssonite. Their percentages decrease gradually from units M–2 to M–5 and increase markedly in units M–6 and M–7. Because there are virtually no other Ca-bearing minerals in these layers, these percentages are interpreted as being proportional to the volumes of Ca-bearing water that annually flowed into the lakes.

The presence or absence of laminar bedding also indicates progressive changes in the character of the larger lakes during Lower Salt time. Well developed laminar bedding occurs in units M–2 and M–3, less well developed laminar bedding occurs in units M–4 and M–5, and massive bedding occurs in units M–6 and M–7. Distinctly laminated muds are interpreted as the products of stratified lakes that periodically (seasonally?) received influxes of Ca-bearing fresh water that formed thin surface layers that quickly warmed, evaporated, or mixed with the underlying dense saline layers; this would have resulted in most of the $CaCO_3$ being crystallized rapidly during a small part of the depositional year. Unlaminated mud layers are interpreted as products of unstratified lakes or stratified lakes that received Ca-bearing waters throughout the year or had thicker surface layers; this would have resulted in $CaCO_3$ being crystallized more uniformly throughout the year.

These criteria suggest that the mud units in the Lower Salt were deposited under the following conditions. Units M–2 and M–3 are interpreted to have been deposited in stratified lakes that seasonally received moderate volumes of Ca-bearing water which formed thin layers over the brine bodies that developed during the preceding salt deposition episodes (S–1 and S–2). Units M–4 and M–5 were deposited in stratified lakes that received less fresh water each year but received it more evenly throughout the year. Unit M–6 was presumably deposited in a lake that annually received large volumes of water but was unstratified because no residual brine layer existed at the close of S–5 time. Unit M–7 was probably deposited in a lake that was stratified but received such a large annual inflow that the surface layer was too thick to precipitate its $CaCO_3$ during only part of the year.

The Parting Mud represents a long period of deposition in fluctuating but perennial lakes. Variations in the lithologic details of the unit indicate the nature and approximate duration of the fluctuations. The lower 40 percent of the unit consists mostly of massive black mud. The upper 60 percent of the unit consists of prominently laminated aragonitic mud, and an interval low in $CaCO_3$ and high in acid-insoluble components occurs near the middle of this zone. The change from unlaminated to laminated sediments occurs at a horizon dated as about 17,100 years (Mankiewicz, 1975, p. 10). Interpreting the presence or absence of laminar bedding, as in the Lower Salt muds, it appears that during the period that lasted from about 24,000 to 17,100 $^{14}C$ years ago (uncorrected), deposition took place in a lake that generally was either unstratified or stratified with a thick zone of fresher water forming the upper layer, and that during the period that lasted from 17,100 to 10,500 $^{14}C$ years ago, deposition took place in a stratified lake that produced laminae.

Contacts between the four subdivisions of the laminated zone described by Mankiewicz (1975, p. 7–8) lie at levels whose estimated ages (using the sedimentation rate in his core "B" of 24 yrs/cm) are 14,460 years, 12,300 years, and 11,220 years. The unit deposited between 17,100 and 14,460 years ago is interpreted, on the basis of mud lithology plus evidence from outcrops, to represent the waning stages of the lake which had reached its maximum expansion slightly before that time. The unit deposited between 14,460 and 12,300 years may represent a persistent period of low stands during which no salts were deposited but widely spaced dolomite(?) laminae resulted from the decreased frequency of inflow and increased salinity. In outcrops, deposits correlated with this stage, or its end, consist of lag gravels and a characteristic soil (Smith, 1968, figs. 4 and 7). The two units above that horizon, covering the age range of 12,300 to 11,220 and

11,200 to 10,500 years, are probably correlative with the two high stands shown by Smith (1968, fig. 4) for this period. A brief final lake expansion, represented by about 50 cm of unlaminated mud in most cores (but not in core B of Mankiewicz) and by similar deposits in outcrop, occurred after these events; its duration is unknown but must have been small.

The Upper Salt records an almost uninterrupted desiccation. The succession of minerals follows that expected from crystallization of a brine having its bulk composition. Crystallization temperatures were initially low when winter chilling produced borax and probably natron (now trona), and temperatures rose when the lake became shallower and summer evaporation accounted for most of the salts. A few thin discontinuous mud layers in the Upper Salt indicate temporary floodings that covered part of the lake with sediments, but there is no evidence of a significant break in salt deposition within the unit.

The lithology and mineral composition of the Overburden Mud show that much of it was deposited in a shallow saline lake. Clastic fragments in some samples from the edge facies constitute more than 80 percent of the Overburden Mud, although in the central facies they make up less than 10 percent of most samples. In samples from all but the basal layer, fine-grained carbonate minerals are missing and pirssonite and gaylussite are rare. The organic carbon fraction is lower than in any of the other mud layers studied in detail. Halite is abundant, especially in the central facies, and partially dissolved crystals characterize some horizons. All indications are that relative to the lakes that deposited other mud layers, the lake responsible for the Overburden Mud was smaller, more saline, lower in organic productivity, and characterized by deposition of more clastic material relative to chemical sediments. Geologic mapping of outcrops suggests that the lake that deposited the Overburden Mud never reached levels greater than about 45 m above the present surface.

## CORRELATIONS WITH DEPOSITS IN OTHER AREAS

The subsurface stratigraphic units of Searles Lake reflect distinct climatic episodes. Major climatic changes are widespread; they certainly affected areas comparable in size to several western states and are likely to have been recorded over areas the size of a continent, a hemisphere, or throughout the world. In-

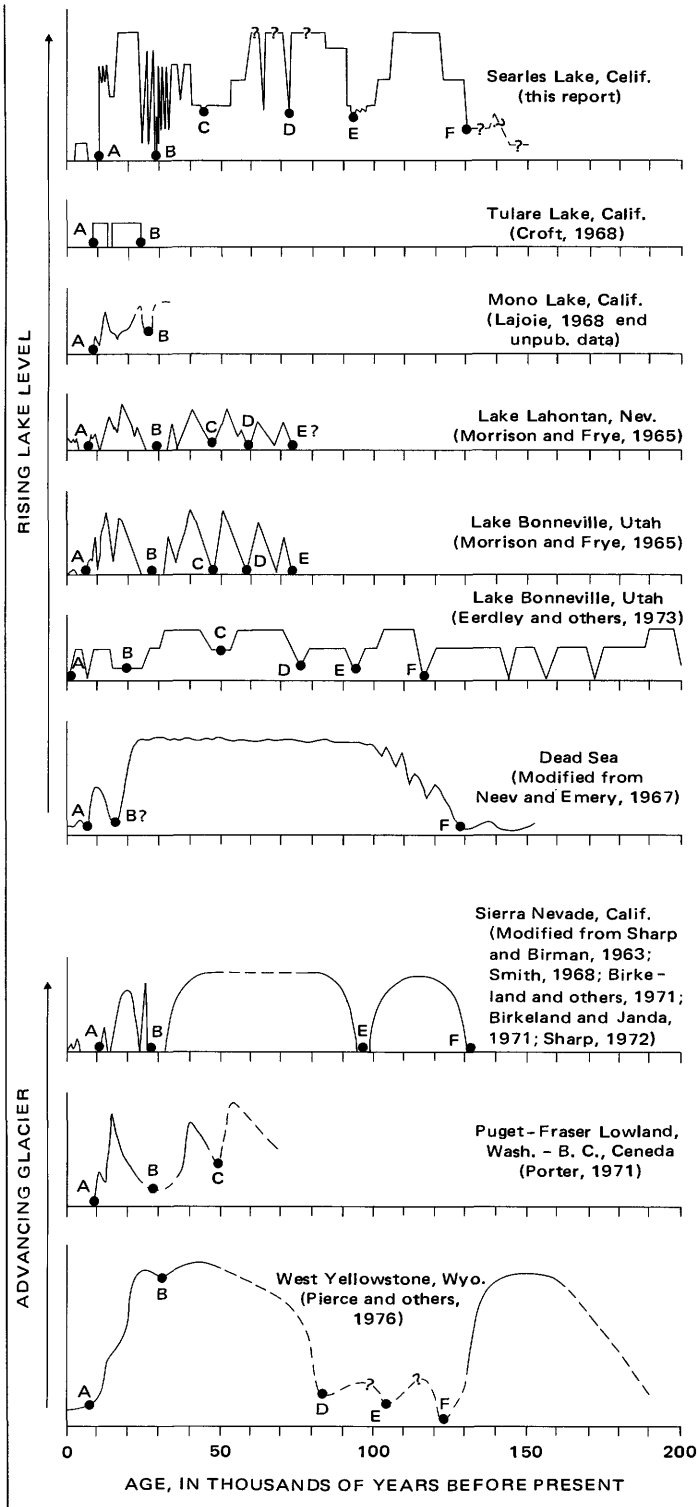


FIGURE 42.—Comparison of lake-fluctuation curve for Searles Lake (fig. 41) and other lacustrine and glacial chronologies that extend over much or all of the past 150,000 years. Data from sources indicated. Lettered points are inferred correlative events.

dividual stratigraphic units in Searles Lake are therefore expected to be correlative with deposits that reflect climatic events in many other areas.

Possible correlation between the fluctuations of Searles Lake over the past 150,000 years and the histories reconstructed for 16 other areas (figs. 42 and 43) are based on various criteria of climatic change. Figure 42 compares it with other Pleistocene lake fluctuations and glacial advances and retreats; figure 43 with records of variations in atmospheric temperatures, pollen, sea-surface temperatures, and sea levels. Lake expansions, glacial advances, cooling trends, and sea-level lowering are considered most likely to occur in phase, and the curves are drawn so as to have similar shapes when this relation exists. A summary of these correlations was presented in another paper (Smith, 1976). Other and more complete discussions of possible correlations between deposits of this age in western North America are presented by Porter (1971) and Birkeland, Crandell, and Richmond (1971).

The curve for Searles Lake shows six low stands, labelled A through F. Low stands are more reliably documented by subsurface data of the type presented here, so are used as points of correlation. Most records from other areas, however, are least reliable for these times. Lacustrine records are based mostly on sediments exposed on the valley sides, and a low stand is recorded as a period of erosion, alluvial deposition, or soil formation; glacial records are mostly based on evidence of extensive or maximum advances, and a retreat is indicated by different degrees of weathering and erosion on successive deposits. None of these criteria indicate the time of the lake's lowest level or the glacier's maximum retreat. Points in the fluctuation curves from other areas that are considered reasonably correlative with the selected Searles Lake low stands are labelled with the same letters. A similarity in assigned ages was sought but not used as a basis for correlation—partly because almost all age estimates older than about 45,000 years are based on assumptions and projections, and partly because some glaciers and lakes probably did not respond synchronously owing to their size, hydrologic setting, or latitude.

A similarity is evident between Searles Lake fluctuations and several of the other curves in figure 42.

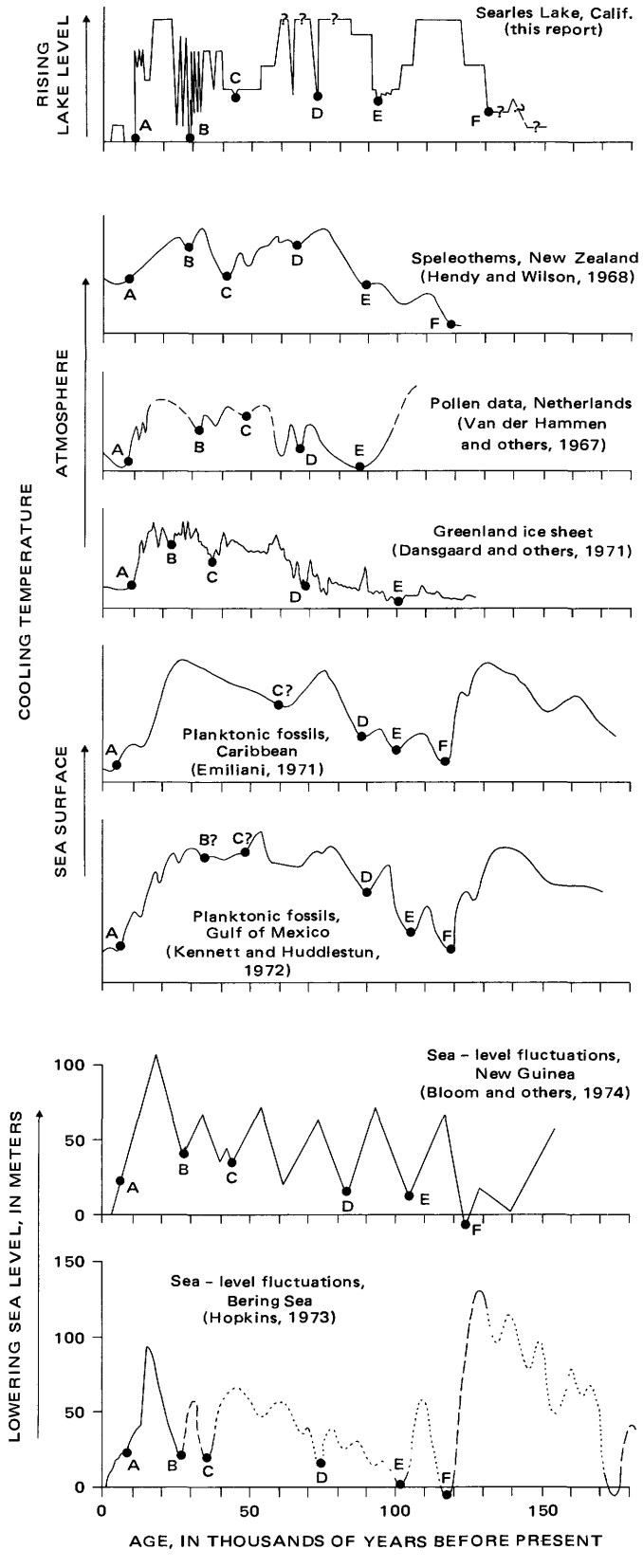


FIGURE 43.—Comparison of lake-fluctuation curve for Searles Lake (fig. 41) and other climatically sensitive geologic indicators; included are criteria that are sensitive to fluctuations in air temperature, sea temperature, and sea level. Lettered points indicate inferred correlative events.

Points labelled A and B are assigned to every curve, and many curves show a similarity in their detailed shapes between these two points. Point A (base of Upper Salt) lies between 5,000 and 10,000 years in all but the Lake Bonneville curve by Eardley and others (1973), and their lithic log (fig. 1) shows a soil at the top that suggests an extensive closing period of nondeposition. Point B (top of unit S–5) lies between 20,000 and 35,000 years in all but the curve for the Dead Sea, which may be too distant for detailed correlation of climatic cycles. Points C, D, and E represent three sets of salt beds in the Bottom Mud. The three are correlated with comparable recessions of Lakes Bonneville and Lahontan, and one or more of them are correlated with recessions shown in the three glacial records. Correlation between point E in the Searles Lake curve and the curves for Lake Bonneville, Lake Lahontan, and the glacial deposits in the Sierra Nevada[29] is based on the stratigraphic position of a prominent fossil soil on the deposits of this age around Searles Lake and in the other three areas.

Point F in (fig. 42) represents the base of the Bottom Mud and of the first of the late Pleistocene lacustrine rises in Searles Valley that followed a very long period that was lacking these events. The Lake Bonneville curve by Eardley and others (1973) shows a period preceding point F during which there were moderate to large lakes, but their lithic log (fig. 1) shows coarse sand deposits and a succession of soils that seem to indicate more strongly a period of relative aridity. The curve (fig. 42) for the Dead Sea was modified from the version published by Neev and Emery (1967, fig. 16) such that the lake history at the time marked by point F is placed at about 140,000 years instead of 75,000 years; this modification was made because they suggested the possibility of a greater age for this event (p. 26), and recalculation of sedimentation rates from their data (p. 25) suggested the age plotted here. The significance of the position of point F in the curve representing glacial advances in the West Yellowstone area is discussed below.

The curves of figure 43 compare the history of Searles Lake for the past 150,000 years with other criteria of climatic change. Speleothems, pollen data, and the isotopic composition of ice sheets reflect atmospheric temperature changes; planktonic fossils reflect sea-surface temperature change; and sea levels reflect the partitioning of the earth's water between the major ice caps and the oceans. The points labelled A to F on the curve for Searles Lake are the same as in figure 42. Points A and B can be correlated with reasonable confidence to most of the other curves at times that are within a few thousand years of each other. Points C, D, and E seem reasonably correlated as shown, although the prominence of the correlated events differs between curves. The best correlations appear to be between Searles Lake and the pollen data from the Netherlands and the two records of sea-level change.

Point F on the curve of figure 43 is correlated with the warmest points in the two sea-surface temperature curves and the highest stands in the two sea-level curves that are of similar age. In figure 42, it is correlated with the maximum recession of the West Yellowstone glacier. These curves, however, show cooler temperatures, lower sea level, and advancing glaciers during the preceding period, and these histories are inconsistent with the climate that seems likely to explain the history inferred for Searles Lake prior to 130,000 years. It is possible that the time scale used for the Searles Lake diagram (and the Sierra Nevada glacier diagram which has its time scale based on the Searles scale) is too short, or that the scales used for the other curves are too long; alteration of these scales might allow the point labelled E in the Searles and Sierra Nevada diagrams to be correlated with the points labelled F in the other five curves. However, changes of 50,000 years or more would be necessary to allow the curves to have this relation, and it seems unlikely that any of the scales are in error by this amount. Admittedly, the subsurface and outcrop data in Searles Valley do not entirely eliminate the possibility of lakes of moderate salinity and depth in the valley during part of the time prior to point F, but they do make it clear that the period that preceded point F was conspicuously less pluvial than the 100,000-year period that followed it. If the correlations in figures 42 and 43 are correct, the growth of major ice sheets during the period prior to point F required a different climatic regime than during the several glacial periods that followed. Relative to the later periods, that earlier regime would have required glacial growth to be caused more by lower temperatures than by increased precipitation.

The record of fluctuations in Searles Lake and the North American (Laurentide) ice sheet is very similar for the last 45,000 years, but problems arise in correlating events before that time (fig. 44). Points in the fluctuation curves that seem correlative in terms of their magnitude and character, and their positions among other events, are labeled the same. The single

[29]Almost no $^{14}C$ dates from glacial deposits in the Sierra Nevada are available. The ages of glaciation shown for the Sierra Nevada were adjusted to fit the chronology of the Searles Lake curve.

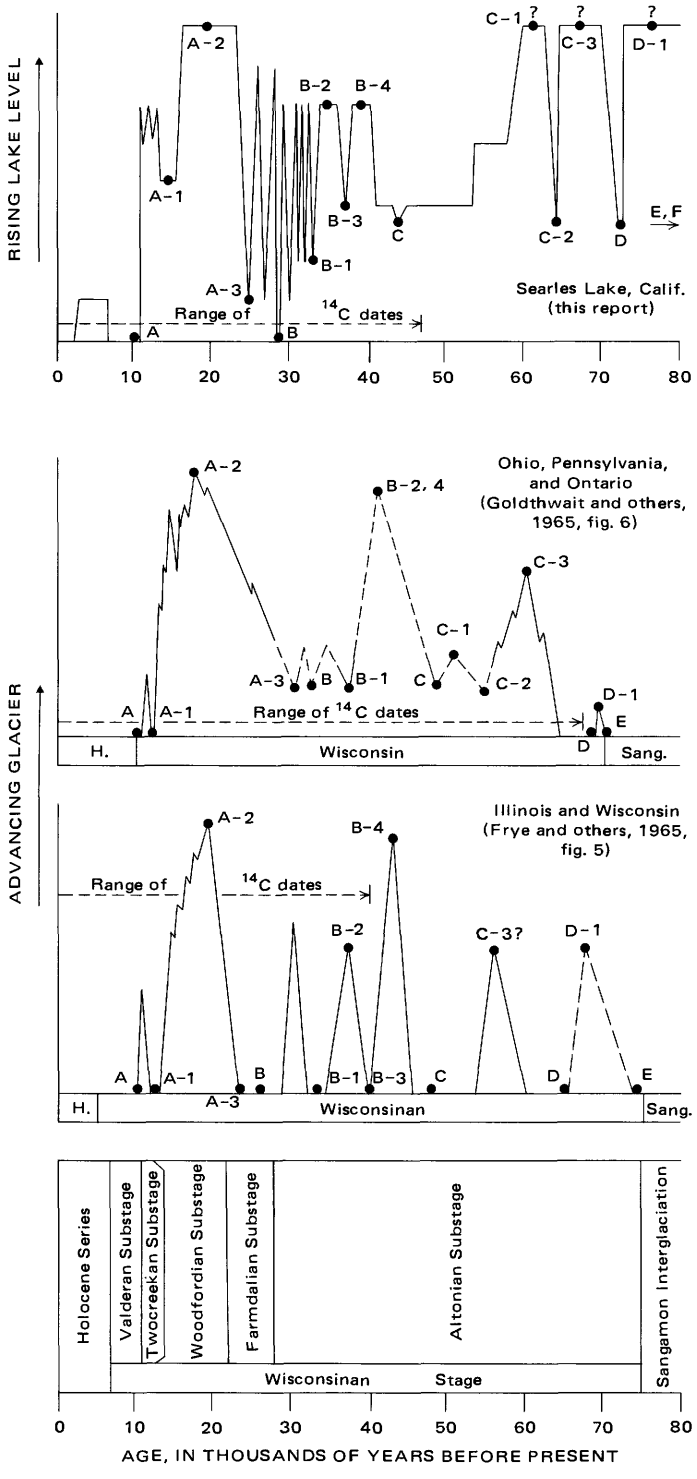


FIGURE 44.—Correlation of fluctuations in Searles Lake during the past 80,000 years with those of Laurentide ice sheet and with time-stratigraphic units commonly used in those areas (Frye, Willman, Rubin, and Black, 1968). Ranges of $^{14}C$ dates available in each area also shown. Lettered points indicate inferred correlative events; single letters placed at same points in Searles Lake diagram as in figures 42 and 43.

letters have the same position as in figures 42 and 43, and the letter-number pairs indicate additional points of correlation. Correlation points between A and C all lie within five thousand years of each other and most are closer. For most of the time shown, a close coincidence of glacial and lacustrine events is evident. Several fluctuations in Searles Lake probably represent climatic episodes that were too short for the larger ice sheet to reflect but were widespread, and tentatively they should be considered part of the North American Pleistocene climate chronology.

There is less similarity between the shapes of the older parts of these curves, and there are larger discrepancies in the ages of points between C–1 and D. A major discrepancy exists between the ages of the points labelled E in in the Searles Lake and Laurentide ice sheet curves. Point E in the Searles Lake diagram (figs. 42 and 43) is plotted at 93,000 years, where the Laurentide ice sheet diagrams (fig. 44) have the correlated event—the end of the Sangamon Interglaciation—plotted at about 75,000 years. The oldest $^{14}C$ date in the Laurentide chronology, on deposits in Ontario at the horizon labelled D, is 67,000 years (Goldthwait and others, 1965, p. 92), and glacial till correlated with the Wisconsin sequence underlies that horizon. This means that the age of the Sangamon-Wisconsin boundary is significantly older, and it seems quite possible that it should be nearer the 93,000 years age estimated for point E in the Searles Lake chronology.

If this correlation is correct, it requires revision of an earlier suggestion (Smith, 1968, fig. 5, p. 307, 308) that tentatively equated the Sangamon Interglaciation with the Mixed Layer of Searles Lake. The revised correlation in figures 42 and 43 would now place the Sangamon Interglaciation near point E, the Yarmouth Interglaciation prior to point F, and the Illinoian Glaciation between them. Future dating of deposits in the Laurentide area may confirm or refute this revised correlation, but the age estimated for point F in the Searles Lake chronology shown in figures 42 and 43 seems too old to correlate with the Sangamon if it ended less than 100,000 years ago.

The Pleistocene chronology of northeast North America is commonly expressed in terms of time-stratigraphic units. The stages, substages, and ages recommended by Frye, Willman, Rubin, and Black (1968) are plotted along the base of figure 44. The substages (Altonian, 75,000 to 28,000 years B.P.; Woodfordian, 22,000 to 12,500 years B.P., and Valderan, 11,000 to 7,000 years B.P.) correlate clearly with major periods of lake expansion in Searles Lake (except for

the age of the Sangamon-Wisconsinan boundary which was discussed earlier). The substages that separate them (Farmdalian and Twocreekan) correspond closely to identifiable episodes of recession in Searles Lake.

Such close correlations raise the question of whether the amount of water stored in glaciers in the Pleistocene Searles Lake drainage area should have been enough to significantly delay the shrinking of Searles Lake as the glaciers retreated in response to regional climatic change. Calculations show that the delay could amount to only a few hundred years. Topographic and geologic maps of the Sierra Nevada show that the areal extent of glaciers in that part of the Sierra Nevada that drained into Searles Lake was about 1,000 $km^2$—the same as the maximum area of the lake. For purposes of an example we can postulate that evaporation from Searles Lake was 1.5 m/yr and that glaciers in the Sierra Nevada system had vertical walls and averaged 300 m in thickness. This would mean that the entire volume of water produced by the complete melting of the glaciers could be evaporated from Searles Lake in 200 years. Retreat of Searles Lake from a high stand, relative to when the glaciers started their retreat, could be delayed only by that much.

Correlation of the deposits in the Mixed Layer of Searles Lake with other areas is not attempted in any detail because of the lack of time control. The estimate that the base of the Mixed Layer in core L-W-D is probably 500,000–1,000,000 years old permits the tentative correlation of the pluvial deposits in the lower 25 m or more of the Mixed Layer with the Sherwin Glaciation in the Sierra Nevada. Sharp (1968, p. 361) considers them to be about 750,000 years old and correlative with the Kansan Glaciation in northeast North America. He and several other workers infer a relatively long interval between the Sherwin and the younger Mono Basin and Tahoe Glaciation, and the long period of relatively nonpluvial deposition represented by the salts in units A to E in the Mixed Layer of Searles Lake represents a compatible climatic history. In figure 42, point F is plotted at the base of the Mono Basin Till in the Sierra Nevada diagram, and the long interglacial period that appears to have preceded that point, and the succession of glaciations that followed it, is the major reason for correlating events in the Sierra Nevada and Searles Lake in this way. As noted earlier, though, there are several valid reasons for concluding that points E and F in figures 42 and 43 should be correlated in other ways. The decision revolves around the reliability of ages, the quality of the geologic evidence indicative of glacial and pluvial climates, and the likelihood that the sequence of climatically controlled events was similar in different areas. Several alternative correlations are almost equally reasonable.

## ECONOMIC GEOLOGY

The chemicals produced each year at Searles Lake, valued at $30 million, come from the brines. The original and post-diagenesis compositions of the brines and salts have been discussed in this paper. Since the beginning of commercial operations on the deposit, however, the average brine compositions have undergone some change, for the chemical companies pump large quantities of it and the volume occupied by the pumped brine is mostly replaced by groundwater, surface runoff, and plant effluent. Those waters, which range from nearly fresh to brines having various salinities and compositions, react with the salts. The resulting new brines (called "replacement brines" in this paper) have compositions controlled by the phase relations discussed.

The post-diagenesis compositions of the brines plotted as points *b–3* in figures 35, 36, 38, and 39 are averages of brines analyzed in the late 1940's and early 1950's, and are actually intermediate between the brines present in the lake prior to any commercial production and present-day replacement brines. Older analyses of brines (Gale, 1914, p. 6276–277) do not appear to be sufficiently reliable; when plotted on the above diagrams, some of the points lie near points *b–3*, whereas others lie in positions relative to the more modern analyses that are highly improbable. The brines on which points *b–3* are based, probably did not differ greatly from the original brines because less than a quarter of the total amount of brine pumped by 1974 had then been extracted. Hardt, Moyle, and Dutcher report 1972 pumping rates of $19.2\times10^{12}$ g of brine (density about 1.3) per year. Dyer reports 1950 pumping rates of $10.0\times10^{12}$ g of brine per year from the lake, of which the plant at Trona (Ryan, 1951) used about $8\times10^{12}$ g. Assuming that brine pumping increased linearly from 1926 to 1974, and that pumping extracted $10\times10^{12}$ g per year by 1950 (24 years after it began) and $20\times10^{12}$ g by 1974 (48 years after), a total of about $120\times10^{12}$ g of brine had been pumped by 1950 (approximately when the analyses used for points *b–3* were made) and $480\times10^{12}$ g of brine had been pumped by 1974.

Simple extrapolation of the historical increase in pumping rates would suggest that the original brine would be entirely exhausted shortly after the year 2000. However, this is not a valid approach to estimating the commerical life of the salt body for four reasons—three of which tend to extend it and one to shorten it. One factor that extends it is that continued

improvements in technology allow lower grade brines to be utilized. The second is that as pumping continues, the remaining brine becomes a mixture of original brine and replacement brine, and the proportion of original brine decreases such that the rate of its depletion is slower than assumed in this extrapolation. The third is that pumping rates are presently limited by the U.S. Geological Survey to the amount of fluid available to replace the pumped brines; the present pumping rate nearly equals the recharge rate from natural sources and present plant effluent (Hardt and others 1972, p. 34–48), and large increases would require modified plant processes and/or increased amounts of water imported from other nearby valleys. The factor that decreases the commercial life expectancy of this body is that the brines preferred by the chemical companies have compositions that are found only in some parts of the deposit, and a significant proportion of the brines included in the preceding calculations are not considered adequate by present standards.

The total quantity of chemicals that have been extracted from the brines of Searles Lake, valued at more than $1 billion, has been estimated at about $57\times10^{12}$ g (Hardt and others, 1972, p. 50). This is about 3 percent of the total quantity of salts in the Upper and Lower Salt bodies (table 10 and 17) and may represent substantially less than half of the potential production from the salt bodies. Since existing plant processes use only brine, and it contains only about 15 percent of the total components in the salt bodies, approximately 20 percent of the original quantity of dissolved solids has been extracted. As about half of the dissolved solids are NaCl, not now considered a commercial product, so the salts extracted to date account for about 40 percent of the commercially extractable salts that were in the original brine. Some, possibly a large part, of the extracted salts have been replaced as a result of solution of solid salts by the waters that form the replacement brine, and the extractable salts in these bodies have theoretically been increased by this amount. How much of the replacement brine can be used for commercial purposes depends on future refinements in extraction technology and the proportions of components in the brines required for it.

Three complete and three partial analyses of the brines considered by the companies to be of commercial grade during and prior to 1950 are given in table 22. Analyses 1 and 4 are plotted in the $Na_2CO_3$-$Na_2SO_4$-KCl-NaCl-$H_2O$ system at 20°C in figure 28*B* and analysis 6 is plotted in figure 21*B*. The brines of the Upper Salt used at that time are represented by points that are on (or near) the hanksite-aphthitalite boundary (fig. 28*B*), but it is evident that many of the individual brine samples from the Upper Salt body contained different ratios of those ions. The commercially attractive brines from the Lower Salt (table 22) are represented by a point within the hanksite field, (fig. 21*B*) and many of the other brines in that unit contain different ratios of those ions.

TABLE 22.—*Analyses of brines pumped to chemical plants, 1938–51*

[Analyses of major components expressed as weight percent, minor components (Li, S, $PO_4$, F, Br, and I) as parts per million. Sodium not listed for partial analyses because original analyses expressed as hypothetical salts. Sources of data noted below]

| Components | Upper Salt | | | | Lower Salt | |
|---|---|---|---|---|---|---|
| | 1 | 2 | 3 | 4 | 5 | 6 |
| Na | 11.07 | --- | --- | 11.00 | --- | 11.86 |
| K | 2.46 | 2.63 | 2.73 | 2.63 | 1.44 | 1.54 |
| Li | --- | --- | --- | 70 | --- | 30 |
| $CO_3$ | 2.66 | 2.70 | 2.84 | 2.71 | 3.82 | 3.84 |
| $SO_4$ | 4.71 | 4.58 | --- | 4.56 | --- | 4.43 |
| Cl | 12.16 | --- | --- | 12.13 | --- | 10.81 |
| $B_4O_7$ | 1.16 | 1.22 | 1.32 | 1.26 | 1.54 | 1.51 |
| S | --- | --- | --- | 330 | --- | 1560 |
| $PO_4$ | 930 | --- | --- | 940 | --- | 590 |
| F | 40 | --- | --- | 20 | --- | 20 |
| Br | --- | --- | --- | 810 | --- | 540 |
| I | --- | --- | --- | 30 | --- | 20 |
| W | --- | --- | --- | 55 | --- | 32 |
| Specific gravity | 1.30 | 1.30 | --- | --- | --- | --- |
| pH | 9.4 | --- | --- | | | |

NOTE.—1. Gale, 1938, p. 869.
2. Dyer, 1950, p. 41, "pumped brine."
3. Dyer, 1950, p. 41, typical analysis, Upper zone, 35–70 ft. depth.
4. Ryan, 1951, p. 449.
5. Dyer, 1950, p. 41, typical analysis, Lower zone, 85–125 ft. depth.
6. Ryan, 1951, p. 449.

The amount of scatter in the 1950 brine compositions shown in figures 21 and 28 shows that despite the constraints imposed by the phase relations, considerable variation in composition does occur. Part of this variation is a result of the areal difference in the solid phases present in the Lower Salt and Upper Salt; the relative percentages of minerals vary in a broadly concentric pattern (tables 4 and 14), and the edge facies appear devoid of many minerals. As a reduction in the number of minerals removes constraints on possible brine compositions, brines from the edge facies (which apparently lack some phases present in the central facies) are likely to be more variable.

Implicit in this conclusion is the suggestion that brines in the salt bodies do not mix freely. The density and compositional profiles in the Upper Salt brines support this suggestion, but two other lines of evidence suggest that the brines have mixed over periods of time that are unknown but could be short. The first consists of isotopic data (G. I. Smith, S. Matsuo, and I. Friedman, unpub. data) showing that the deuterium-hydrogen ratios of the brines from the Upper Salt are nearly uniform from the top to base of the unit despite

a marked density and compositional contrasts over the same range. Significant lateral variation in deuterium percentages do exist, but vertical variations do not. The present brines in a given area are clearly replacements of the original brines and are evidently made from similar mixtures of original and replacement waters. The second line of evidence, which suggests that the brines move freely and that the migration and mixing times might be short, comes from the records of brine levels in wells which responded in periods of several weeks or a few months to the onset of heavy pumping several kilometers away (Hardt and others, 1972, p. 45–48).

Several lines of study need to be pursued to test the possibility that brines in the Upper Salt migrate over periods of less than a year in response to manmade or natural changes in the hydraulic regime of the lake. If found valid, the areal variations in the brines must be largely inherited from the assemblage of salts that exist in the various parts of the lake. Properly used, this property could become the basis for extracting much greater quantities of chemicals from the lake than simple reliance on original brines would allow.

The scatter of brine compositions found in the Lower Salt (fig. 21) is greater than in the Upper Salt. This difference is largely a result of the effect of the mud units, M–2 to M–7, which isolate each of the interbedded salt layers from the others, originally allowing seven slightly different salt deposits to coexist. After drilling and pumping of the Lower Salt commenced in the mid-1940's, though, some mixing of their brines occurred because most of the pumped wells were uncased from the top of unit S–7 to the base of S–1. Isotopic investigations in progress show that the $H_2O$ contained by the brines in the Lower Salt is isotopically nearly homogeneous from the top of the unit to the base, and that it is also different from the brines that crystallized some of the salts. The present isotopic ratios of the $H_2O$ seem, partly at least, to be the result of geologic processes that occurred before pumping began, but some of the change may have been the result of pumping.

Despite this mixing, however, distinct compositional differences still exist between the brines of each salt unit in the Lower Salt. Selective pumping and mixing of them would allow relatively precise control of the ratios of ions in the brines reaching the plants. Solution mining of individual layers in this unit would allow more controlled and restricted leaching than in the Upper Salt.

The overall shapes of the Upper Salt and Lower Salt result in marked differences in the probable response to the addition of low-density water. The upper contact of the Upper Salt has a shape that is crudely concave-downward (pl. 1), and any low density waters and brines introduced to produce replacement brines will, if they do not mix, migrate or remain in the higher part of the body, which is near the middle of the lake. The salts of the Lower Salt, however, have lens shapes with upturned edges (pl. 1), and comparable low-density waters and brines will migrate or remain in the higher parts of those bodies that are at the edges. Fluids entering the Lower Salt and Upper Salt brine bodies as natural and artificial recharge therefore probably migrate in opposite directions.

Pumping of brines and production of soda ash from the trona and nahcolite bodies in units A and B of the Mixed Layer are planned and construction of a new plant to process them is now underway (1977). Deeper units seem to present no commercial prospects.

## REFERENCES CITED


Alderman, A. R., and Skinner, H.C.W., 1957, Dolomite sedimentation in the southeast of south Australia; Am. Jour. Sci., v. 255, p. 561–567.

Bailey, G. E., 1902, The saline deposits of California: California State Mining Bur. Bull. 24, 216 p.

Barnes, Ivan, and O'Neil, J. R., 1971, Calcium-magnesium carbonate solid solutions from Holocene conglomerate cements and travertines in the Coast Range of California: Geochim. et Cosmochim. Acta, v. 35, p. 699–718.

Barnes, Ivan, O'Neil, J. R., Rapp, J. B., and White, D. E., 1973, Silica-carbonate alteration of serpentine—Wall rock alteration in mercury deposits of the California Coast Ranges: Econ. Geology, v. 68, no. 3, p. 388–390.

Berner, R. A., 1971, Principles of chemical sedimentology: New York, McGraw-Hill, p. 240.

Birkeland, P. W., Crandell, D. R., and Richmond, G. M., 1971, Status of correlation of Quaternary stratigraphic units in the western conterminous United States: Quaternary Research, v. 1, no. 2, p. 208–227.

Birkeland, P. W., and Janda, R. J., 1971, Clay mineralogy of soils developed from Quaternary deposits of the eastern Sierra Nevada, California: Geol. Soc. America Bull., v. 82, no. 9, p. 2495–2514.

Bixler, G. H., and Sawyer, D. L., 1957, Boron chemicals from Searles Lake brines: Indus. and Eng. Chemistry, v. 49, p. 322.

Blaney, H. F., 1955, Evaporation from and stabilization of Salton Sea water surface: Am. Geophys. Union Trans., v. 36, no. 4, p. 633–640.

_____1957, Evaporation study at Silver Lake in the Mojave Desert, California: Am. Geophys. Union Trans., v. 38, no. 2, p. 209–215.

Bloom, A. L., Broecker, W. S., Chappell, J.M.A., Matthews, R. K., and Mesolella, K. J., 1974, Quaternary sea level fluctuations on a tectonic coast—New $^{230}Th/^{234}U$ dates from the Huon Peninsula, New Guinea: Quaternary Research, v. 4, no. 2, p. 185–205.

Bowser, C. J., 1965, Geochemistry and petrology of the sodium borates in the nonmarine evaporite environment: California Univ. at Los Angeles, Ph.D. thesis, p. 282

Bradley, W. H., and Eugster, H. P., 1969, Geochemistry and paleolimnology of the trona deposits and associated authigenic minerals of the Green River Formation of Wyoming: U.S. Geol.

Survey Prof. Paper 496–B, 71 p.
Bredehoeft, J. D., Blyth, C. R., White, W. A., and Maxey, G. B., 1963, Possible mechanism for concentration of brines in subsurface formations: Am. Assoc. Petroleum Geologists Bull., v. 47, no. 2, p. 257–269.
Broecker, W. S., and Kaufman, Aaron, 1965, Radiocarbon chronology of Lake Lahontan and Lake Bonneville II, Great Basin: Geol. Soc. America Bull., v. 76, no. 5, p. 537–566.
Broecker, W. S., and Walton, A., 1959, The geochemistry of $C^{14}$ in fresh-water systems: Geochim. et Cosmochim. Acta, v. 16, nos. 1–3, p. 15–38, 200.
Bury, C. R., and Redd, R., 1933, The system sodium carbonate—calcium-carbonate—water: Chem. Soc. Jour. [London], p. 1160–1162.
California Geology, 1972, Salt—San Bernardino County: California Geology, v. 25, no. 10, p. 233.
Carpenter, L. G., and Garrett, D. E., 1959, Tungsten in Searles Lake [Calif.]: Mining Eng., v. 11, no. 3, p. 301–303.
Chilton, C. H., 1958, Crystallization—Key step in sodium sulfate process: Chem. Engineering, p. 116–119.
Clayton, R. N., Jones, B. F., and Berner, R. A., 1968, Isotope studies of dolomite formation under sedimentary conditions: Geochim. et Cosmochim. Acta, v. 32, p. 415–432.
Clayton, R. N., Kninner, H.C.W., Berner, R. A., and Rubinson, M., 1968, Isotopic compositions of recent south Australian lagoonal carbonates: Geochim. et Cosmochim. Acta, v. 32, p. 983–988.
Croft, M. G., 1968, Geology and radiocarbon ages of Late Pleistocene lacustrine clay deposits, southern part of San Joaquin Valley, California, *in* Geological Survey research 1968: U.S. Geol. Survey Prof. Paper 600–B, p. B151–B155.
Dansgaard, W., Johnsen, S. J., Clausen, H. B., and Langway, C. C., Jr., 1971, Climatic record revealed by the Camp Century Ice Core, *in* Turekian, K. K., ed., The late Cenozoic glacial ages: New Haven and London, Yale Univ. Press, p.37–56.
Deevey, E. S., and Stuiver, Minze, 1964, Distribution of natural isotopes of carbon in Crinsley Pond and other New England lakes: Limnology and Oceanography, v. 9, no. 11, p. 1–11.
De Groot, Henry, 1890, The Searles borax marsh: California State Mining Bur., 10th Ann. Rept., p. 534–539.
De Sitter, L. U., 1947, Diagenesis of oil-field brines: Am. Assoc. Petroleum Geologists Bull., v. 31, no. 11, p. 2030–2040.
Dolbear, C. E., 1913, The Searles Lake potash deposit: Eng. and Mining Jour., v. 95, p. 259–261.
Dolbear, S. H., 1914, The saline deposits of Searles Lake, California: Mining and Eng. World, v. 41, p. 797–800.
Droste, J. B., 1961, Clay minerals in sediments of Owens, China, Searles, Panamint, Bristol, Cadiz, and Danby lake basin, California: Geol. Soc. America Bull., v. 72, p. 1713–1722.
Dub, G. D., 1947, Owens Lake, source of sodium minerals: Mining Technology, v. 11, no. 5, 13 p.
Dyer, B. W., 1950, Searles Lake development: Colorado School Mines Quart., v. 45, no. 4B, p. 39–44.
Eardley, A. J., Shuey, R. T., Gvosdetsky, V., Nash, W. P., Dane Pichard, M., Gray, D. C., and Kukla, G. J., 1973, Lake cycles in the Bonneville Basin, Utah: Geol. Soc. America Bull., v. 84, no. 1, p. 211–216.
Emery, K. O., and Rittenberg, S. C., 1952, Early diagenesis of California basin sediments in relation to origin of oil: Am. Assoc. Petroleum Geologists Bull., v. 36, no. 5, p. 735–806.
Emiliani, C., 1971, The last interglacial—Paleotemperatures and chronology: Science, v. 171, p. 571–573.
Eugster, H. P., 1966, Sodium carbonate-bicarbonate minerals as indicators of $P_{CO_2}$: Jour. Geophys. Research, v. 71, no. 14, p. 3369–3377.
Eugster, H. P., and Smith, G. I., 1965, Mineral equilibria in the Searles Lake evaporites, California: Jour. Petrology, v. 6, pt. 3, p. 473–522.
Fahey, J. J., 1962, Saline minerals of the Green River Formation: U.S. Geol. Survey Prof. Paper 405, p. 50.
Fairbanks, H. W., 1896, Notes on the geology of eastern California: Am. Geologist, v. 17, p. 63–74.
Flint, R. F., and Gale, W. A., 1958, Stratigraphy and radiocarbon dates at Searles Lake, California: Am. Jour. Sci., v. 256, no. 10, p. 689–714.
Free, E. E., 1914, The topographic features of the Desert Basin of the U.S. with reference to the possible occurrence of potash: U.S. Dept. Ag. Bull. 54, 68 p.
Freeth, F. A., 1923, The system—$Na_2O$-$CO_2$-NaCl-$H_2O$, considered as two four-component systems: Philos. Trans. Royal Soc. London, ser. A, v. 223, p. 35–87.
Friedman, I., Smith, G. I., and Hardcastle, K., 1976, Studies of Quaternary saline lakes—II. Isotopic and compositional changes during desiccation of the brines in Owens Lake, California, 1969–71: Geochim. et Cosmochim. Acta v. 40, p. 501–511.
Frye, J. C., Willman, H. B., and Black, R. F., 1965, Outline of glacial geology of Illinois and Wisconsin *in* Wright, H. E., Jr., and Frey, D. G., eds, The Quaternary of the United States—A review volume for the 7th Cong. Internat. Assoc. for Quaternary Research: Princeton, N.J., Princeton Univ., p. 43–62.
Frye, J. C., Willman, H. B., Rubin, Meyer, and Black, R. F., 1968, Definition of Wisconsinan stage: U.S. Geol. Survey Bull. 1274–E, p. E1–E22.
Gale, H. S., 1913a, Papers on potash and other salines: U.S. Geol. Survey Bull., 540–N, p. N1–37.
_____1913b, Searles Lake, California [potash]: U.S. Geol. Survey Mineral Research, pt. 2, p. 884–890.
_____1914, Salines in the Owens, Searles, and Panamint basins, southeastern California: U.S. Geol. Survey Bull. 580–L, p. 251–323.
_____1919, Searles Lake, *in* Salt Resources of the United States, by Phalen, W. C.: U.S. Geol. Survey Bull. 669, p. 164–174.
Gale, W. A., 1938, Chemistry of the trona process (from the standpoint of the phase rule): Indus. Eng. Chemistry, v. 30, no. 8, p. 867–871.
_____1945, Lithium from Searles Lake: Jour. Chem. Industries, v. 57, p. 442–446.
Gan, T. L., 1961, Heavy minerals in sediments from Owens, China, Searles, and Panamint basins, southern California: Indiana Univ., Bloomington, Ph.D. dissert., 95 p.
Garrett, D. E., 1960, Borax processing at Searles Lake, *in* Industrial minerals and rocks: New York, Am. Inst. Mining, Metall., and Petroleum Engineers, p. 119–122.
Garrett, D. E., and Phillips, J. F., 1960, Sodium carbonate from natural sources in the United States, *in* Industrial minerals and rocks (Nonmetallics other than fuels), Seeley W. Mudd Series: New York, Am. Inst. of Mining, Metall., and Petroleum Engineers, p. 799–808.
Gibson, R. E., 1942, Effect of pressure on phase equilibria in binary condensed systems: Geol. Soc. America Spec. Paper 36, p. 187–202.
Gilbert, G. K., 1875, The glacial epoch: Explor. and Surveys West 100th Meridian, (Wheeler) Rept. v. 3, chap. 3, p. 86–104.
Goddard, J. G., 1970, $Th^{230}/U^{234}$ dating of saline deposits from Searles Lake, California: Queens College, City Univ. New York, New York, M.A. thesis, 50 p.
Goldthwait, R. P., Dreimanis, Aleksis, Forsyth, J. L., Karrow, P. F., and White, G. W., 1965, Pleistocene deposits of the Erie Lobe *in* Wright, H. E., Jr., and Frey, D. G., eds., The Quaternary of

the United States—A review volume for the 7th Cong. Internat. Assoc. for Quaternary Research: Princeton, N. J., Princeton Univ. Press, p. 85–98.

Goodwin, J. H., 1973, Analcime and K-feldspar in tuffs of the Green River Formation, Wyo: Am. Mineralogist, v. 58, p. 93–105.

Goudge, M. F., and Tomkins, R. V., 1960, Sodium sulfate from natural sources, *in* Industrial minerals and rocks (Nonmetallics other than fuels), Seeley W. Mudd Series: New York, Am. Inst. of Mining, Metall., and Petroleum Engineers, p. 809–814.

Graf, D. L., Eardley, A. J., and Shimp, N. F., 1961, A preliminary report on magnesium carbonate formation in glacial Lake Bonneville: Jour. Geology, v. 69, no. 2, p. 219–223.

Haines, D. V., 1957, Core logs from Searles Lake, San Bernardino County, California: U.S. Geol. Survey open-file report.

———1959, Core logs from Searles Lake, San Bernardino County, California: U.S. Geol. Survey Bull. 1045–E, p. El39–E317.

Hamman, W. D., 1912a, Potash solutions in the Searles Lake region: Mining Sci., v. 65, p. 372–373.

———1912b, Potash solutions in the Searles Lake region—II: Mining Sci., v. 65, p. 391–392.

———1912c, The Searles Lake potash deposit: Eng. and Mining Jour., v. 93, p. 975–978.

Hanks, H. G., 1883, Report of the borax deposits of California and Nevada: California State Mining Bur., 3rd Ann. Rept. State Mineralogist for the year ending June 1, 1883, 111 p.

———1889, On the occurrence of hanksite in California: Am. Jour. Sci., ser. 3, v. 37, p. 63–66.

Harbeck, G. E., Jr., 1955, The effect of salinity on evaporation: U.S. Geol. Survey Prof. Paper 272–A, 5 p.

Hardt, W. F., Moyle, R. W., Jr., and Dutcher, L. C., 1972, Proposed water-resources study of Searles Valley, Calif.: U.S. Geol. Survey open-file report. 69 p.

Hay, R. L., and Moiola, R. J., 1963, Authigenic silicate minerals in Searles Lake, California: Sedimentology, v. 2, no. 4, p. 312–332.

Hellmers, H. S., 1938, Borax, soda ash, lime hydrate—Their recovery by West End Chemical Co., Searles Lake, California: Pacific Chem. and Metall. Industries, v. 2, no. 9, p. 3–11.

Hendy, C. H., and Wilson, A. T., 1968, Paleoclimatic data from speleothems: Nature (London), v. 219, p. 48–51.

Hidden, W. E., 1885, On Hanksite, a new anhydrous sulphato-carbonate of sodium from San Bernadino County, California: New York Acad. Sci., Annals 3, p. 238–241.

Hidden, W. E., and Mackintosh, J. B., 1888, On a new sodium sulphato-chloride, sulphohalite: Am. Jour. Sci., 3d ser., v. 36, no. 216, p. 463–464.

Hightower, J. V., 1951, New carbonation technique—more natural soda ash: Chem. Engineering, v. 58, p. 162–169.

Holser, W. T., 1970, Bromide geochemistry of some non-marine salt deposits in the southern Great Basin: Mineralog. Soc. America Spec. Paper 3, p. 307–319.

Hopkins, D. M., 1973, Sea level history in Beringia during the past 250,000 years: Quaternary Research, v. 3, no. 4, p. 520–540.

Hutchinson, E. G., ed., 1957, A treatise on limnology; V. 1, Geography, Physics and Chemistry; New York, John Wiley & Sons, 1015 p.

Industrial Minerals, 1971, Occidental's Searles Lake Borax. p. 35.

Ingerson, E., 1962, Problems of the geochemistry of sedimentary carbonate rocks: Geochim. et Cosmochim. Acta, v. 26, p. 815–847.

Ives, P. C., Levin, Betsy, Robinson, R. D., and Rubin, Meyer, 1964, U.S. Geological Survey radiocarbon dates VII: Radiocarbon, v. 6, p. 37–76.

Jennings, C. W., Burnett, J. L., and Troxel, B. W., 1962, Geologic map of California, Olaf P. Jenkins edition, Trona sheet: California Div. Mines and Geology Map Sheet.

Jones, B. F., 1961, Zoning of saline minerals at Deep Spring Lake, California; *in* Geological Survey research 1961: U.S. Geol. Survey Prof. Paper 424–B, p. B199–B202.

———1965, The hydrology and mineralogy of Deep Spring Lake, Inyo County, California: U.S. Geol. Survey Prof. Paper 502–A, 56 p.

Jones, B. F., Van Denburgh, A. S., Truesdell, A. H., and Rettig, S. L., 1969, Interstitial brines in playa sediments: Chem. Geology, v. 4, p. 253–262.

Kallerud, M. J., 1966, Advances in solar salt—Solar evaporation in multicomponents processes, *in* Rau, J. L., and Dellwig, L. F., eds., 3rd Symposium on Salt, Vol. 2: Cleveland, Ohio, Northern Ohio Geol. Soc., p. 41–46.

Kennett, J. P., and Huddlestun, Paul, 1972, Late Pleistocene paleoclimatology, foraminiferal biostratigraphy and tephrochronology, Western Gulf of Mexico: Quaternary Research, v. 2, no. 1, p. 38–69.

Lajoie, K. R., 1968, Quaternary stratigraphy and geologic history of Mono Basin, eastern California: California Univ. (Berkeley), Ph.D. thesis, 271 p.

Lee, C. H., 1912, Water resources of a part of Owens Valley , California: U.S. Geol. Survey Water-Supply Paper 294, 135 p.

Leonardi, M. L., 1954, American Potash and Chemical Corp., main plant cycle: Am. Inst. Mining Engineers Tech. Pub. 3728–H, v. 199.

Leopold, E. B., 1965, Late Quaternary and modern pollen rain at Searles Lake, California [abs.]: Internat. Assoc. Quaternary Research, 7th Internat. Cong., Boulder and Denver, Colo., 1965, p. 289.

Mabey, D. R., 1956, Geophysical studies in southern California basins: Geophysics, v. 21, no. 3, p. 839–853.

Makarov, S. Z., Bliden, V. P., 1938, The polytherm of the Quaternary system $Na_2CO_3$-$Na_2SO_4$-NaCl-$H_2O$ and solid solutions of the burkeite type: Akad. Nauk SSSR Izv., Otdeleniyle, Mat. i Yestestven. Nauk ser. chem. p. 865–890. [In Russian, with English Summary.]

Mankiewicz, P. J., 1975, An organic geochemical investigation of a glacial sequence at Searles Lake, California: California Univ. at Los Angeles, M.S. thesis, 122 p.

Milton, C., and Eugster, H. P., 1959, Mineral assemblages of the Green River Formation, *in* P. H. Abelson, ed., Researches in geochemistry: New York, John Wiley and Sons, p. 118–150.

Morrison, R. B., and Frye, J. C., 1965, Correlation of the Middle and Late Quaternary successions of the Lake Lahontan, Lake Bonneville, Rocky Mountain (Wasatch Range), Southern Great Plains, and Eastern Midwest areas: Nevada Bur. Mines Rept. 9, 45 p.

Moyle, R. W., Jr., 1969, Water wells and springs in Panamint, Searles, and [Pilot] Knob valleys, San Bernardino and Inyo Counties, Calif.: California Dept. Water Resources Bull. 91–17, 110 p.

Neev, David, and Emery, K. O., 1967, The Dead Sea—Depositional processes and environments of evaporites: Israel Ministry Development Geol. Survey Bull. 41, 147 p.

Norman, L. A., Jr., and Stewart, R. M., 1951, Mines and mineral resources of Inyo County: California Jour. Mines and Geology, v. 47, no. 1, p. 17–223.

Oana, Shinya, and Deevey, E. S., 1960, Carbon 13 in lake waters, and its possible bearing on paleolimnology: Am. Jour. Sci., Bradley Volume, v. 258–A, p. 253–272.

Pabst, A., and Sawyer, D. L., 1948, Tincalconite crystals from

Searles Lake, San Bernardino County, California: Am. Mineralogist, v. 33, p. 472–481.

Peterson, M.N.A., Bien, G. S., and Berner, R. A., 1963, Radiocarbon studies of recent dolomite from Deep Spring Lake, California: Jour. Geophys. Research, v. 68, no. 24, p. 6493–6505.

Phosphorus and Potassium, 1971, Company Reports: Phosphorus and Potassium, no. 56, p. 50.

Pierce, K. L., Obradovich, J. D., and Friedman, Irving, 1976, Obsidian hydration dating and correlation of Bull Lake and Pinedale glaciations near West Yellowstone, Montana: Geol. Soc. America v. 87, Bull., p. 703–710.

Porter, S. C., 1971, Fluctuations of Late Pleistocene alpine glaciers in western North America, *in* Turekian, K. K., ed., The late Cenozoic glacial ages: New Haven and London, Yale Univ. Press, p. 307–330.

Ralph, E. K., Michael, H. N., and Han, M. C., 1973, Radiocarbon dates and reality: MASCA Newsletter Applied Sci. Center for Archeology, Pennsylvania Univ., Philadelphia, v. G, no. 1, 20 p.

Rubin, Meyer, and Berthold, S. M., 1961, U.S. Geological Survey radiocarbon dates VI: Radiocarbon, v. 3, p. 86–98.

Ryan, J. E., 1951, Industrial salts—Production at Searles Lake: Mining Eng., v. 3, p. 447–451.

Schulten, M. A., 1896, Production artificielle du chlorocarbonate de sodium et de magnesium: Soc. Française Mineralogie [Paris] Bull., v. 19, p. 164–169.

Sharp, R. P., 1968, Sherwin till-Bishop tuff geological relationships, Sierra Nevada, California: Geol. Soc. America Bull., v. 79, no. 3, p. 351–364.

———1972, Pleistocene glaciation, Bridgeport Basin, California: Geol. Soc. America Bull., v. 83, no. 8, p. 2233–2260.

Sharp, R. P., and Birman, J. F., 1963, Additions to classical sequence of Pleistocene glaciations, Sierra Nevada, California: Geol. Soc. America Bull., v. 74, no. 8, p. 1079–1086.

Sheppard, R. A., and Gude, A. J., 3d, 1968, Distribution and genesis of authigenic silicate minerals in tuffs of Pleistocene Lake Tecopa, Inyo County, California: U.S. Geol. Survey Prof. Paper 597, 38 p.

———1969, Diagenesis of tuffs in the Barstow Formation, Mud Hills, San Bernardino County, California: U.S. Geol. Survey Prof. Paper 634, 35 p.

Siever, Raymond, and Garrels, R. M., 1962, Early diagenesis—Composition of interstitial waters of recent marine muds: Am. Assoc. Petroleum Geologist-Soc. Econ. Paleontologists and Mineralogists Mtg., San Francisco, Calif., 1962, Program, p. 54–55.

Siever, Raymond, Garrels, R. M., Kanwisher, John, and Berner, R. A., 1961, Interstitial waters of recent marine muds off Cape Cod: Science, v. 134, p. 1071–1072.

Sims, J. D., and Rymer, Michael, 1975, Preliminary description and interpretation of cores and radiographs from Clear Lake, Lake County, California; Core 4: U.S. Geol. Survey open-file report.

Smith, G. I., 1962, Subsurface stratigraphy of late Quaternary deposits, Searles Lake, Califonia—A summary; in Geological Survey research 1962: U.S. Geol. Survey Prof. Paper 450–C, p. C65–C69.

———1964, Geology and volcanic petrology of the Lava Mountains, San Bernardino County, California: U.S. Geol. Survey Prof. Paper 457, 97 p.

———1966, Geology of Searles Lake—A guide to prospecting for buried continental salines, *in* Symposium on salt, 2d—v. 1, Geology, geochemistry, mining: Cleveland, Ohio, Northern Ohio Geol. Soc., p. 167–180.

———1968, Late Quaternary geologic and climatic history of Searles Lake, southeastern California: Internat. Quaternary Cong., 8th, Proc. 7, p. 293–310.

———1976, Origin of lithium and other components in the Searles Lake evaporites, California, *in* Vine, J. D., ed., Lithium resources and requirements by the year 2000: U.S. Geol. Survey Prof. Paper, 1005, p. 92–103.

———, 1976, Paleoclimatic record in the upper Quaternary sediments of Searles Lake, Calif., U.S.A., *in* Horie, S., ed., Paleolimnology of Lake Biwa and the Japanese Pleistocene; v. 4, Kyoto Univ., Kyoto, Japan, p. 577–604.

Smith, G. I., and Friedman, Irving, 1975, Chemical sedimentation and diagenesis of Pleistocene evaporites in Searles Lake, California, U.S.A., *in* Theme 2—Les divers aspects geochimiques de la sedimentation continentale: Congres Internat. de Sedimentologie, 9th, Nice 1975, p. 137–140.

Smith, G. I., Friedman, Irving, and Matsuo, Sadao, 1970, Salt crystallization temperatures in Searles Lake, California: Mineralog. Soc. America Spec. Paper 3, p. 257–259.

Smith, G. I., and Haines, D. V., 1964, Character and distribution of nonclastic minerals in the Searles Lake evaporite deposit, California: U.S. Geol. Survey Bull. 1181–P, 58 p.

Smith, G. I., and Pratt, W. P., 1957, Core logs from Owens, China, Searles, and Panamint basins, California: U.S. Geol. Survey Bull. 1045–A, 62 p.

Smith, G. I., Troxel, B. W., Gray, C. H., Jr., and von Huene, Roland, 1968, Geologic reconnaissance of the Slate Range, San Bernardino and Inyo Counties, California: California Div. Mines and Geology Spec. Rept. 96, 33 p.

Stuiver, Minze, 1964, Carbon isotopic distribution and correlated chronology of Searles Lake sediments: Am. Jour. Sci., v. 262, no. 3, p. 377–392.

Stuiver, Minze, and Suess, H. E., 1966, On the relationship between radiocarbon dates and true sample ages: Radiocarbon, v. 8, p. 534–540.

Teeple, J. E., 1921, The American potash industry and its problems: Ind. and Eng. Chemistry, v. 13, p. 249.

———1929, The industrial development of Searles Lake brines with equilibrium data: Am. Chem. Soc., Mon. Ser., no. 49, 182 p.

Thompson, D. G., 1929, The Mohave Desert region, California, a geographic, geologic, and hydrologic reconnaissance: U.S. Geol. Survey Water-Supply Paper 578, 759 p.

Turk, L. J., 1970, Evaporation of brine: A field study on the Bonneville Salt Flats, Utah: Water Resources Research, 6, no. 4, p. 1209–1215.

Vallentyne, J. R., 1957, Carotenoids in a 20,000-year-old sediment from Searles Lake, California: Archives Biochemistry and Biophysics, v. 70, p. 29–34.

Van Denburgh, A. S., 1975, Solute balance at Abert and Summer Lakes, south-central Oregon; Closed-basin investigations: U.S. Geol. Survey Prof. Paper 502–C, 29 p.

Van der Hammen, T., Maarleveld, G. C., Vogel, J. C., and Zagwijn, W. H., 1967, Stratigraphy, climatic succession and radiocarbon dating of the last glacial in the Netherlands: Geologie en Mijnbouw, v. 46, no. 3, p. 79–95.

Ver Planck, W. E., 1957, Salines, *in* Wright, L. A., ed., Mineral commodities of California: California Div. Mines Bull. 176, p. 475–582.

Von Engelhardt, Wolf, and Gaida, K. H., 1963, Concentration changes of pore solutions during the compaction of clay sediments: Jour. Sed. Petrology, v. 33, no. 4, p. 919–930.

Watanabe, Tokunosuke, 1933, Synthese de la northupite, de la tychite et de nouveaus mineraux artificiels du même groupe:

Inst. Phys. and Chem. Research Sci. Papers [Tokyo], v. 21, p. 35–39.

White, D. E., Hem, J. D., and Waring, G. A., 1963, Chemical composition of subsurface waters: U.S. Geol. Survey Prof. Paper 440–F, 67 p.

Wilcox, L. V., 1946, Boron in the Los Angeles (Owens River) aqueduct: U.S. Dept. Agr., Bur. Plant Research Dept. 78, 66 p.

Wilson, E. O., and Ch'iu, Yü-ch'ih, 1934, Brine purification: Indus. and Eng. Chemistry, v. 26, no. 10, p. 1099–1104.

Wyllie, M. R. J., 1955, Role of clay in well-log interpretation, *in* Pask and Turner, eds., Clays and clay technology: California Div. Mines Bull. 169, p. 282–305.

Yamamoto, Atsuyuki, Kanari, Seiichi, Fukuo, Yoshiaki, and Horie, Shoji, 1974, Consolidation and dating of the sediments in core samples from Lake Biwa, *in* Horie, Shoji, ed., Paleolimnology of Lake Biwa and the Japanese Pleistocene (2d issue; Contr. Paleolimnolgoy of Lake Biwa and Japanese Pleistocene), no. 43, p. 135–144.

Young, G. J., 1914, Potash salts and other salines in the Great Basin region: U.S. Dept. Agri. Bull. 61, 96 p.

Zeller, E. J., and Wray, J. L., 1956, Factors influencing precipitation of calcium carbonate: Am. Assoc. Petroleum Geologists Bull., v. 40, no. 1, p. 140–152.

# INDEX

[Italic page numbers indicate major references]


Page

A

Albert Lake, Oreg., muds, dissolved solids ---- 104
$a_{CO_2}$ ---- 83, 85, 86, 92
$a_{H_2O}$ ---- 83, 85, 86, 92, 103, 107
Age, estimates, basis ---- 113
Algae ---- 53
American Potash and Chemical Corp ---- 5, 8, 20
  brines pumped ---- 45
American Trona Co ---- 5
Analcime ---- 10, 13, 14, 15, 16, 17, 18 37, 52, 79, 105, 108
  formation ---- 105
  Mixed Layer ---- 105, 108
  tuff ---- 105
Apatite ---- 14
Aphthitalite ---- 10, 37, 43, 56, 59, 90, 92, 93, 94, 95, 106, 107
  phase diagrams ---- 92
  Upper Salt ---- 92
Aragonite ---- 10, 14, 16, 17, 18, 37, 43, 47, 51, 54, 72, 78, 79, 80, 102, 104, 110
  alteration ---- 102
  beds ---- 48
  Bottom Mud ---- 79, 101, 104, 110
  conversion to calcite ---- 104
  crystallization ---- 80
  formation ---- 81, 102
  laminae ---- 110
    significance ---- 109
  Lower Salt ---- 79
  Mixed Layer ---- 79
  oldest occurence ---- 79
  Overburden Mud ---- 79
  Parting Mud ---- 104
  precipitation ---- 80
  primary ---- 79
  recrystallization ---- 72
  varves ---- 80
Argus Range ---- 3
*Artemia* ---- 53
Ash, volcanic ---- 14, 15
Atmospheric temperature changes ---- 114
*Atriplex hymenelytra* ---- 3

B

Bacteria, sulfate-reducing ---- 106
Bacterial production, $CO_2$, measure ---- 85
Bedding laminar, significance ---- 111
Berthold, S.M., cited ---- 68
Biotite ---- 13, 52
Blackmon, P. D., cited ---- 52
Blue-green algae ---- 53
Borate Playas, Nevada ---- 4
Borates ---- 98, 99
Borax-4, 5, 10, 16, 17, 18, 34, 36, 37, 39, 40, 43, 47, 48, 51, 56, 59, 60, 64, 66, 67, 86, 90, 95, 96, 112
  beds ---- 16
  crystals ---- 34, 37, 39, 40, 47
  crystallization ---- 90, 95
  Lower Salt ---- 47, 90
  Overburden Mud ---- 96
  zones ---- 90
Boron, Lower Salt ---- 47
  Searles Lake ---- 47, 64
Bottom Mud ---- 10, 12, *15*, 79
  acid-insoluble material, percentage ---- 77
  age ---- 15, 75, 109

Page

*Bottom Mud—Continued*
  analcime, zones ---- 110
  aragonite ---- 79, 104
    laminae ---- 110
    percentage ---- 101
  areal extent ---- *16*
  authigenic K-feldspar ---- 105, 110
  authigenic minerals ---- 14, 18, 105
  base ---- 16
    age ---- 74, 78
    temperature ---- 110
  B content ---- 100
  brines, salinities ---- 86
Ca-bearing minerals ---- 109
calcite ---- 79, 101
  chemical composition ---- *17*
  clastic, sedimentation, ---- 78
  core, logs ---- 16
  core L-W-D ---- 16
  dated sediments ---- 77
  deposition ---- 74, 110
  depositional history ---- 109, 110
  depositional interval ---- 78
  depositional processes ---- 109
  depositional rate ---- 77
  diagenesis ---- 86
  disseminated salines, zones ---- 110
  dolomite ---- 79, 81, 110
  evaporite minerals ---- 18
  gaylussite, crystals ---- 16
    distribution ---- 110
    quantity ---- 110
  lithology ---- 16
  mineral composition ---- *16*, 37, 86
  minerals, alteration ---- 86
  mud densities ---- 78
  nahcolite ---- 86
  northupite ---- 86
  organic carbon, dates ---- 74, 77
  pyrite ---- 10, 56
  saline layers ---- 16, 85
  salines ---- *85*
  salt layers, accumulation rate ---- 75
    correlation ---- 114
    depositional process ---- 85, 86
    formation ---- 85
    mineral composition ---- 85
    positions ---- 108
  searlesite ---- 105, 110
  sedimentation rates ---- 75, 77, 109
  sediments ---- 77
  silicate minerals, authigenic ---- 14
  thickness ---- *16*
  top ---- 16, 78
  tuff, analcime ---- 105
Bradley, W. H., cited ---- 83, 85
Brine ---- 8, 18
  carbonate ---- 71
    total ---- 44
  changing ratios of components ---- 84
  chemical composition ---- *60*
  chemistry ---- 79
  commercial grade ---- 56, 117
  composition, changes ---- 197
    post-diagenesis ---- 116
  depletion rate ---- 117
  economic value ---- 43, 98
  interstitial, hydrogen-deuterium ratios ---- 71
  evaporation, rates ---- 75
    salinities ---- 104

Page

*Brine—Continued*
  major elements ---- 43
  minor elements ---- 45
  original, exhausted ---- 116
    extractable salts ---- 117
  Owens Lake ---- 76
  Parting Mud ---- 53, 56, 72
  post-depositional changes ---- 45
  pumping rates ---- 116
  shrimp ---- 53
  test pumping ---- 5
Broecker, W. S., cited ---- 70
Burkeite ---- 10, 13, 15, 16, 18, 34, 36, 37, 39, 40, 43, 56, 59, 60, 67, 83, 84, 92, 93, 94, 106, 107, 108
  Lower Salt ---- 89
  mineral percentages ---- 34
  phase diagrams ---- 89, 92
  stability fields ---- 83
  Upper Salt ---- 92, 94
Burro-bush ---- 3

C

Calcite ---- 13, 14, 15, 16, 17, 18, 43, 51, 54, 72, 78, 79, 80, 81, 110
  Bottom Mud ---- 79, 101
  diagenetic alteration ---- 79
  formation ---- 81
  Lower Salt ---- 79
  Mixed Layer ---- 79
  Overburden Mud ---- 79
  Owens Lake ---- 99
  precipitation, significance ---- 109, 110
  Parting Mud ---- 79
  recrystallization ---- 72
Carbon, detrital, $^{14}C$ age ---- 73
Carbon exchange mechanisms ---- 72
Carbonate, wood samples, $^{14}C$ dates ---- 73
Carbonate minerals ---- 17
  dates ---- 70, 71
  diagenesis ---- 73
  recrystallization ---- 71, 72
Carbonates ---- 18, 78
  X-ray determinations ---- 14
Carotenes ---- 53
Carpenter, L. G., cited ---- 63
Chemicals, industrial ---- 56, 60
Chemicals, potential production ---- 117
Chemistry, lake waters ---- 85
China Lake ---- 97, 99
Chlorite ---- 52, 53, 54
Chlorophyll pigments ---- 80
Chronology, Searles Lake ---- 115
Clastic minerals ---- 16, 17, 37, 56
Clastic silicates ---- 13, 37, 47, 52
Clay minerals, Mixed layer ---- 14
  Parting Mud ---- 51
Clays ---- 8, 13, 53, 54, 67
Clear Lake, Calif., sediments, accumulation rates ---- 78
Climate chronology, North American, Pleistocene ---- 115
Climatic change, criteria ---- 113, 114
$CO_2$, bacterial decomposition ---- 85
Core L-W-D ---- 14, 16, 105
  authigenic silicate minerals ---- 105
  base, temperature ---- 100
  gaylussite ---- 103
  pirssonite ---- 103
  saline layers ---- 111

Page

Core samples, mineral composition ---17
Correlation, Dead Sea ---114
glaciers ---113
lake fluctuations, Pleistocene ---113
mud and saline units ---10
pollen ---113
sea levels ---113
sea-surface temperatures ---113, 114
West Yellowstone glacier ---114
Creosote bush ---3
Current marks ---39

D

Dead Sea, correlation ---114
fluctuation curve ---114
mineral composition ---80
muds ---104
pyrite ---106
sediments, laminated ---80
Death Valley ---3
Deep Spring Lake ---80, 81
gaylussite crystals ---101
muds ---81
similarity to Searles Lake ---81
Deposition rates ---*75*
Depositional history, reconstructed ---*108*
Deposits, correlations with other areas ---*112*
Desert holly ---3
Diagenesis, geochemistry ---*100*
Lower Salt ---88
primary sediments ---100
temperature, changes ---100
Diagenetic minerals ---107
Diagenetic processes, mud layers ---100
salt layers ---106
Dissolved solids, quantity extracted ---117
Dolomite ---10, 13, 14, 15, 16, 17, 37, 43, 47, 51, 54, 67, 68, 78, 79, 81, 86, 110
Bottom Mud ---79, 81, 110
coexistence ---110
diagenetic origin ---81
distribution, Bottom Mud ---110
formation ---81
Lower Salt ---79
Mixed Layer ---79, 81
Overburden Mud ---79, 81
Parting Mud ---79, 81
primary origin ---81
Droste, J. B., cited ---8, 14, 53, 67
Dutcher, L. C., cited ---8, 116
Dyer, B. W., cited ---44

E, F

Economic development, Searles Lake ---*4*
Economic geology ---*116*
Emery, K. O., cited ---80, 106, 114
Erd, R. C., cited ---37, 53
Eugster, H. P., cited ---7, 83, 85, 86, 90, 92
Evaporation pan, rates ---75
Evaporation ponds ---5
Evaporite content, Parting Mud ---54
Evaporite deposits ---56
Mixed Layer ---*13*
stratigraphy ---*8*
Evaporite mineralogy ---13
Evaporite minerals, Overburden Mud ---67
Evaporites, Lower Salt ---37
Searles Lake ---4, 8, 82, 100
Fahey, J. J., cited ---76
Feldspar ---13, 52, 54, 67
Flint R. F., cited ---7, 16, 68
Flora, surrounding area ---3
Flourine, Owens Lake ---99
Searles Lake ---99
Fossil soil ---114
*Franseria dumosa* ---3
Friedman, I., cited ---76, 99

Page

G

Gale, H. S., cited ---7, 13, 67
W. A., cited ---7, 16, 45, 61, 68
Galeite ---10, 37
Garrett, D. E., cited ---63
Gaylussite ---10, 13, 14, 15, 16, 17, 18, 34, 37, 39, 40, 43, 47, 48, 51, 54, 67, 68,72, 78, 79, 81, 86, 101, 102, 103, 110, 111, 112
Bottom Mud ---16, 110
cocrystallization ---103
composition, stability ---103
crystallization ---72, 110
rate ---102
crystals ---16, 34, 37, 39, 40, 47, 48, 72, 101
diagenetic ---103
maximum depth ---103
formation ---72
mineral percentages ---34
Mixed Layer ---101, 102
Parting Mud ---102
pirssonite stability field boundary ---103
quantities ---111
quantity, significance ---110
Geochemistry, diagenesis ---*100*
sedimentation ---*78*
Geologic environment, Searles Lake ---*5*
Geologic studies, previous, Searles Lake ---*6*
Glacial advances ---113, 114
Glacial retreats ---113, 114
Glacial deposits, correlation ---114
Glacial records ---113, 114
Glaciation, Illinoian ---115
Mono Basin ---116
Glacier, West Yellowstone ---114
Glacier diagram, time scale ---114
Galciers, Pleistocene, Searles Lake drainage area 116
Glaserite ---10, 106
Glass, devitrified ---15
Glass shards ---52
Goddard, J. G., cited ---75
*Grayia spinosa* ---3
Great Basin, streams, headwaters ---98
Green algae ---53
Green River Formation, authigenic K-silicate phases ---102
nahcolite, rosettes ---103
trona beds, saline depositional rates ---76
Ground water, Searles Valley ---8
Gude, A. J., cited ---17
Gypsum ---45, 80, 98
Gypsum-bearing fault gouge ---6

H

Haines, D. V., cited ---7, 12, 20, 34, 39, 40, 47, 51, 95
Halite ---10, 13, 14, 15, 16, 17, 18, 34, 36, 37, 42, 43, 47, 48, 51, 54, 56, 59, 60, 61, 64, 66, 67, 68, 75, 78, 79, 80, 83, 84, 85, 90, 93, 94, 95, 96, 98, 103, 104, 107, 108, 112
beds ---60, 108
crystallization ---75, 84, 90, 95, 96
crystals ---47, 48, 51, 84, 104
cubic ---15
diagenesis ---80
Lower Salt ---90
Mixed Layer ---108
microcrystalline ---80, 103
mineral percentages ---34
Overburden Mud ---67, 112
Parting Mud ---103, 104
phase diagrams ---95
Upper Salt ---95
Hanksite ---10, 18, 34, 36, 37, 39, 43, 56, 59, 60, 64, 66, 67, 68, 92, 93, 94, 95, 96, 106, 107, 108
crystallization rate ---92
crystals ---94, 95, 106
diagenesis ---94

Page

Hanksite—Continued
formation ---92, 93, 106, 107
Lower Salt ---106
mineral percentages ---34
Overburden Mud ---96
phase diagrams ---92, 93
recrystallization ---106
secondary ---93
Upper Salt ---60, 92, 93, 94, 95, 106
Hardcastle, K., cited ---76, 99
Hardt, W. F., cited ---8, 116
Hay, R. L., cited ---8, 14, 17, 52, 53, 105
Hem, J. D., cited ---45, 63
Hop Sage ---3
Hot Creek ---100
flow rate ---100
tungsten, amounts ---100
Hydrocarbons ---53

I, J, K

Ice sheet, Laurentide ---114, 115
Ice sheets, isotopic composition ---114
major, growth ---114
Illinoian Glaciation ---115
Interstitial solutions, composition, changes ---100
Introduction ---*2*
Isopach map, Overburden Mud ---82
Isopach maps, Lower Salt ---82, 96
mud units ---20
saline units ---20
Ives, P. C., cited ---68
Joshua trees ---3
Kaufman, Aaron, cited ---70
Keough Hot Spring ---100
tungsten, amount ---100
Kerr-McGee Chemical Corp ---16
chemical analyses ---8
cited ---10
logs ---8
K-feldspar ---10, 13, 14, 15, 17, 18, 79
authigenic ---16, 102, 105, 108, 110

L

Lacustrine facies, areal extent ---13
Lacustrine records ---113
Lacustrine sediments, Cenozoic ---98
Lake, chemical stratification ---80
mud, deposition ---82
organic productivity ---85
saline ---108
stand, low, definition ---113
stratified ---110, 111
Lake basin, inflow, volume ---110
Lake surface, saline minerals ---67
Lake Biwa, Japan ---78
Lake Bonneville ---114
lake-fluctuation curve ---114
recessions, correlated ---114
Lake brines, crystallization path ---84
Lake deposits, gypsum-bearing ---45
Lake efflorescences ---67
Lake fluctuations, Pleistocene ---113
Lake Lahontan, recessions, correlated ---114
Lake levels, related to sediments, thickness ---110
Lake salinity, stratification ---80
Lake waters, chemistry ---83, 84, 85
Lakes, deposition, Bottom Mud ---110
larger, Lower Salt ---111
perennial ---108, 111
saline, deposition ---96
formation ---96
layers ---96
recrystallization ---96
solution ---96
volume changes ---96
zones ---96
stratified ---101
unstratified ---111

Page

Laminar bedding, significance ---111
*Larrea tridentata* ---3
Laurentide chronology ---115
Laurentide ice sheet, correlation with Searles Lake 114
fluctuations ---114, 115
Leopold, E. B., cited ---8
Levin, Betsy, cited ---68
Little Hot Creek ---100
flow rate ---100
tungsten, amounts ---100
Long Valley area, springs, thermal ---98
tungsten, amount ---100
Los Angeles aqueduct ---98
Lower Salt ---10, *18*, 75
age ---18, 74
aragonite occurrences ---79, 104
areal extent ---*20*
authigenic silicate minerals ---105
borax ---47
brine, densities ---18
brine composition ---45
average ---89
variation ---117, 118
brines, analyses ---43
commercial grade ---117
mixing ---118
post-depositional changes ---45
saline ---86
total carbonate ---44
calcite ---79
chemical analyses ---*43*
chemical composition ---*40*, 86
core samples, chemical analyses ---40
X-ray analyses ---40
deposition ---98
dry-lake stage ---45
salinity ---90
wet-dry episodes ---68
depositional history ---111
deposits, volumes ---18
diagenesis ---88, 90
dolomite ---79
estimated bulk composition ---*47*
hanksite crystals ---94
inferred environment ---90
lake history ---74
lakes, large ---111
lithology ---*34*
mineral compositon ---*34*
mineral distribution ---*34*
mud beds, analcime ---105
mud deposits ---18
mud layers ---18, 47
mud units ---20, *37*
depositional conditions ---111
evaporites ---37
isopach maps ---82
mineral composition ---37
relative volumes ---82
M-2 ---*37*, 82
deposition, inferred ---111
laminar bedding ---111
M-3 ---*37*, 81
dates, different ---74
deposition, inferred ---111
laminar bedding ---111
M-4 ---*39*, 82
deposition, inferred ---111
laminar bedding ---111
M-5 ---*39*, 82
deposition, inferred ---111
laminar bedding ---111
M-6 ---*40*, 82
age ---74
deposition, inferred ---111
dissolved solids ---90
laminar bedding ---111
M-7 ---*40*, 82
age ---74
deposition, inferred ---111

Page

Lower Salt, M-7—Continued
dissolved solids ---90
laminar bedding ---111
muds, laminar bedding ---111
northupite ---79
organic carbon, dates ---74
Parting Mud ---*47*
phase diagram, burkeite field ---89
trona field ---87, 89
4-component system ---89
5-component system ---86, 88
pumped wells ---118
pyrite ---105
saline beds, isopach maps ---96
saline deposits ---18
saline layers ---18
saline units ---*20*, *34*
areal extent ---97
basin position ---97
deposition ---96
mineral content, volume percentage ---34
salines ---*86*
salt depositional sequence ---97
salt layers ---47
accumulation rate ---75
borax ---47
crystallization sequences ---86
salt units, absolute ages ---75
$^{230}Th/^{234}U$ age ---75
samples ---68
selective pumping ---118
shapes ---118
sodium carbonate minerals ---88
solids, chemical analyses ---*40*
solutions, initial compositions ---86
stratigraphic subdivisions ---18
S-1 ---16, *34*
borax content ---90
brine, composition ---88
crystallization ---97
crystallization, path ---88
crystallization, temperature ---88
deposition, final ---88
original brine ---87
mineral assemblage ---88
mineralogy ---111
northupite, percentage ---91
phase diagrams ---86
thickness distribution ---97
trona ---88
S-2 ---*36*
borax content ---90
brine, composition ---88
crystallization ---97
crystallization, path ---88
crystallization, temperature ---88
mineralogy ---88, 111
northupite, percentage ---91
phase diagrams ---86
thickness distribution ---97
trona ---88
S-3 ---*36*
borax content ---90
brine, composition ---88
crystallization ---97
crystallization, path ---88
crystallization, temperature ---88
hanksite, crystals ---106
mineralogy ---88, 111
northupite, percentage ---91
phase diagrams ---86
thickness distribution ---97
trona ---88
S-4 ---*36*
borax content ---90
brine, composition ---88
crystallization ---97
crystallization, path ---88
crystallization, temperature ---88
hanksite, crystals ---106

Page

Lower Salt, S-4—Continued
mineral assemblage ---88
mineralogy ---111
northupite, percentage ---91
phase diagram, field boundaries ---87
phase diagrams ---86
thickness distribution ---97
S-5 ---*36*, 56
accumulation rate ---75
age ---74
borax content ---90
brine, composition ---88, 89
crystallization ---97
crystallization, path ---88
crystallization, temperature ---88
compaction, post-depositional ---96
desiccation ---90, 97
dessication period ---74
hanksite, crystals ---106
mineral assemblage ---89
mineralogy ---111
northupite, percentage ---91
phase diagram, field boundaries ---87
phase diagrams ---86
thickness ---97
S-6 ---*37*
borax concentration ---90
brine, composition ---89
crystallization, summer ---90
crystallization, temperature ---89, 90
crystallization, winter ---90
crystallization sequence ---89, 90
final ---89
original ---89, 90
halite ---90
mineralogy ---111
natron, crystallization ---90
sulfate minerals ---89
thickness distribution ---97
trona ---90
S-7 ---*37*
borax concentration ---90
brine, composition ---89
crystallization, summer ---90
crystallization, temperature ---89, 90
crystallization, winter ---90
crystallization sequence ---89, 90
final ---89
original ---89, 90
halite ---90
mineralogy ---111
natron, crystallization ---90
sulfate minerals ---89
thickness distribution ---97
trona ---90
water-soluble components, major ---47
wood, date ---74
units ---10, 12
solution mining ---118
upper contact ---118
visual estimates, percent error ---42
volume ---*20*
water, isotopically homogeneous ---118

M

Mabey, D.R., cited ---12
Magnesium ---78
Mankiewicz, core B, age ---111, 112
P. J., cited ---48, 52, 53, 55, 80, 111
Manly party ---4
Marine muds, recent ---102
Marine sediments, NaCl solutions, postdepositional concentration ---104
Marl ---56
Marls, organic-rich ---37
Megascopic minerals, volume percentages ---34
Methane ---71
Microorganisms ---71, 106
Milton, C., cited ---83, 85

Page

Mineral assemblages, geochemical environment
of deposition ---82
saline, temperatures---83
Mineral species, crystals, large, growth---104
Minerals---17
anomalous, formation---107
diagenetic ---107
related, coexistence ---84
sulfate---107
Mining, solution, Lower Salt ---118
Mirabilite---10, 16, 17, 18, 77, 83, 100, 107, 111
beds ---16
Bottom Mud ---85
crystallization ---75, 86
layers---110, 111
stability fields ---83
Mixed Layer---10, 12
age ---13, 109
analcime---108
abundance---105
aragonite ---79
areal extent---*13*
authigenic K-feldspar ---108
authigenic silicate minerals ---105
base, age ---116
brines ---84
composition---15, 85
initial---84
calcite ---79
chemical analyses, water-soluble fraction---14
chemistry, major change ---85
clay minerals ---14
core L-W-D---13
thickness ---109
correlated with Sherwin Glaciation---116
correlation, revised---115
deposition ---84
change ---85
nonpluvial---116
dolomite ---79, 81
evaporite deposits---*13*
evaporite minerals, coarse-grained---14
gaylussite---101, 102
lacustrine deposits ---13
lithology---*13*
mineral composition ---*13*, 14
minerals, stratigraphic distribution---14
mud, sedimentation ---108
muds, color ---108
northupite ---79
pirssonite---101, 102
saline layers ---13, 15
salines---*84*
salt deposition ---108
salts, color---108
primary---84
searlesite ---108
sedimentation history ---108
sedimentation rates---109
silicate minerals, authigenic---14
stratigraphic units ---13, 14
thickness ---13
tuff beds, analcime---105
K-feldspar ---105
type B searlesite ---105
unit A ---*14*
brine composition ---85
brines, pumping ---118
nahcolite ---85
nahcolite beds ---108, 118
organic material ---85
saline composition ---85
trona beds ---108, 118
unit B ---14
brine composition ---85
nahcolite ---85
nahcolite beds ---108, 118
organic material ---85
saline composition ---85
soda ash production---118
trona beds ---108, 118

Page

Mixed Layer—Continued
unit C ---*15*, 84, 85
horizons, color ---108
interpluvial ---109
halite beds---108
trona beds ---108
unit D ---*15*, 84, 85
halite deposition ---108
mud deposition ---108
trona deposition ---108
unit E ---*15*, 84, 85
brine composition, change---85
horizons, color ---108
mud ---108
unit F ---*15*, 84
base, age ---109
mud sedimentation---108
pluvial---109
units---10
volume percentages ---13
zones ---13
mottled ---108
Moiola, R. J., cited ---8, 14, 17, 52, 53, 105
Mono Basin Glaciation---116
Mono Basin Till ---116
Mono Lake, age---70
Monomineralic salt, beds---108
Morgan Creek, flow, rate---100
water analysis, tungsten ---99, 100
Moyle, R. W., cited ---8, 116
Mud ---48, 56, 59
Mud deposition, rates ---76
unit E, halite ---108
Mud layer, aragonite, formation---102
pirssonite, formation ---102
Mud layers ---13
authigenic K-silicate phases---102
borax zones, significance---90
brine, interstitial, salinity ---103
brines, disequilibrium ---101
ionic ratios ---102
chemical disequilibrium ---101
$CO_2$, rate of formation ---102, 103
compaction ---103
diagenetic changes---*100*
disequilibrium between original minerals and brines---100
dissolved solids, concentration ---103
gaylussite, concentrations---103
distribution ---103
formation, limits---102
halite, microcrystalline---103
interstitial solutions, salinities ---103
ionic diffusion ---101
large crystals, growth ---104
lithology---34
organic decomposition, partial pressures---101
pirssonite, concentrations ---103
distribution ---103
pore water elimination ---101
Mud samples, dating---70
Mud units, areal extent ---*20*
areal variations---81
bedding character---12
brines, interstitial, H D ratios---71
crystal habit---12
crystal size ---12
depositional processes---81
hydrated salts, H D ratios ---71
isopach maps---20
mineralogy ---10, 12
minerals, quantitative analyses ---37
saline minerals ---37
thickness ---12, 20
distribution, variation---96
variations ---81
volume ---*20*
Muds, CaO content ---81
laminated, significance ---111
marine, recent ---102
MgO content---81

Page

Muds, CaO content—Continued
unlaminated, significance---111
M-2, megascopic lithology ---37
nodules ---37
thickness ---37
M-3, current marks ---39
megascopic lithology---37
thickness ---39
M-4, megascopic lithology ---39
thickness ---39
M-5, megascopic lithology ---39
ripple marks ---39
thickness ---39
M-6, megascopic lithology ---40
thickness ---40
total volume ---40
M-7, megascopic lithology ---40
thickness ---40
total volume ---40

N

Nahcolite---10, 13, 14, 15, 16, 18, 34, 37, 40, 77, 83, 84, 85, 86, 103, 107, 108, 118
alteration to trona ---83
beds ---16, 17, 108, 118
Bottom Mud ---85, 86
crystallization ---86
crystalline phases, primary ---83
formation---102
layers---110, 111
Mixed Layer ---85, 108, 118
preservation, brine---103
rosettes, Green River Formation---103
stratigraphic distribution ---85
Natron ---83, 90, 107, 112
alteration to trona ---83
crystalline phases, primary ---83
crystallization ---75, 86, 90
Lower Salt---90
Neev, David, cited ---80, 106, 114
North American ice sheet, correlation with Searles Lake---114
fluctuations---114
North American Pleistocene climate chronology ---115
Northupite---10, 13, 14, 15, 18, 34, 36, 37, 39, 40, 43, 52, 59, 79, 81, 84, 86, 90, 91, 103
beds ---16, 37, 38, 39, 48
Bottom Mud ---79, 86
crystallization ---91
crystals---34, 48
Lower Salt---79, 91
Mixed Layer ---79
nodules ---38, 39
Overburden Mud---79
Parting Mud ---79
primary material---81
stability field ---90
synthesis ---90
synthetic formation ---81

O

Old Searles deep well ---12, 13, 16
Organic carbon, disseminated, dates ---70
disseminated, Lower Salt---74
wood samples, $^{14}C$ dates---73
production, rate---71
Organic compounds, muds, composition ---70
Organic material---10, 13, 16, 18, 37
decomposition ---85
Organic productivity, lake---85
Overburden Mud---10, *66*, *95*
aragonite ---79
areal extent---*66*
basal contact, $^{14}C$ age---73
borax, distribution ---96
brines, composition ---95

Page

Overburden Mud—Continued
- calcite ---- 79
- chemical composition ---- *68*
- clastic minerals ---- 67
- composition, megascopic ---- 66
  - megascopic, mean, calculated ---- 67
- contact ---- 95
- crystallization sequence ---- 86
- deposition ---- 66, 95, 97, 98
  - lake ---- 95
- dissolved solids, total ---- 64
- dolomite ---- 79, 81
- evaporite minerals ---- 67
- halite, abundant ---- 112
  - surficial ---- 67
- hanksite, distribution ---- 96
- isopach map ---- 82
- lake, levels ---- 112
- lake, perennial ---- 95
- lithology ---- *66*
- mineral composition ---- *66*
- northupite ---- 79
- polygons ---- 67
- saline components, sources ---- 95
- saline minerals, areal distribution ---- 96
- salines ---- *86*
- salts, mineral composition ---- 95
- sand ---- 66
- stratigraphic contact ---- 56, 66
- thenardite, distribution ---- 96
- thickness, average ---- 66
  - variation ---- 82
- trona, distribution ---- 96
- volume ---- *66*
- wood sample, reliable date ---- 73

Owens Lake ---- 85, 88, 98
- accumulation rate, annual ---- 76
- brine, evaporation rate ---- 76
- brine content ---- 76
- calcite precipitation ---- 99
- crystallization process ---- 96
- dissolved solids, total quantity ---- 98
- evaporation rate, net ---- 76
- fluorine, amount ---- 99
- minerals, recrystallized ---- 83
- overflow ---- 109
- $P_{CO_2}$ environment ---- 83
- $PO_4$, amounts ---- 99
- phytoplankton population ---- 85
- recrystallization ---- 106
- salinities ---- 85
- salt crystallization ---- 83
- surface, irregular ---- 96
- water depth ---- 76

Owens River ---- 76, 99
- components, compared to Searles Lake ---- 99
  - concentrations ---- 98
  - sources ---- 98
- dissolved solids, total quantity ---- 98
- flow, Pleistocene ---- 109
- fluorine, amounts ---- 99
- headwaters, dissolved solids ---- 98
- $PO_4$, amounts ---- 99
  - contributed to Owens Lake ---- 99
  - contributed to Searles Lake ---- 99
- water analysis, tungsten ---- 99

Owens Valley aqueduct ---- 76

Owens Valley, runoff ---- 76

P

Panamint Valley ---- 3, 98

Parting Mud ---- 10, 12, 79
- age ---- 47
- algae ---- 53
- aragonite ---- 104
- areal extent ---- *47*
- authigenic silicate minerals ---- 105
- base, organic carbon, dates ---- 74
- brine ---- 53
  - desiccation ---- 56

Page

Parting Mud—Continued
- brines, diffusion ---- 72
- calcite ---- 79
- CaO content ---- 56, 79
- carbonate minerals ---- 56
- chemical composition ---- *54*
- chemical stratification ---- 80
- chlorine content ---- 56
- chlorophyll pigments ---- 80
- clastic content ---- 54
- clastic minerals, distribution ---- 55
  - grain-size distribution ---- 51
- clay minerals ---- 51, 53
- core B ---- 48
- core samples, dated ---- 70
- crystallization ---- 51
- dated sediments, lithologic similarity ---- 77
- density, average ---- 102
  - lake water stratification ---- 80
- deposition ---- 79, 95, 97
  - aeolian ---- 53
- depositional rate ---- 108
- deposits correlated with outcrops ---- 111
- dolomite ---- 54, 79, 81, 105, 110
  - decomposition ---- 54
  - distribution ---- 110
- dolomite sample, analcime ---- 105
- evaporite content ---- 54
- gaylussite, abundance ---- 102
- halite ---- 103
  - concentration ---- 104
  - diagenesis ---- 104
- interstitial brine content ---- 56
- laminae ---- 51, 80
  - calcium carbonate, thickness ---- 51
- laminated zone, subdivisions ---- 111
- lateral equivalents ---- 1, 47
- lithology ---- *48*
- Lower Salt Contact ---- *47*
- major element analyses ---- 54
- marl ---- 56
- MgO analyses ---- 55
- mineral composition ---- 37, 47, *48*
- mineral distribution ---- 48
- minerals ---- 51
- mud, densities ---- 78
  - depositional rate ---- 77
  - matrix ---- 47
- northupite ---- 79
- organic carbon, $^{14}C$ dates ---- 73, 76
  - content ---- 56
- organic content ---- 53, 54, 80
  - average ---- 56
- organic material ---- 51, 78
- organic production rate ---- 56
- paired dates ---- 72
- prissonite, abundance ---- 102
- pore water, percentages ---- 54
- pyrite ---- 105
- sand grains, frosted ---- 53
- sediment, distribution ---- 82
- sedimentation rate ---- 51
  - average ---- 77
- sediments, laminated ---- 111
  - unlaminated ---- 111
- silicates, authigenic ---- 51
- sodium content average ---- 102
- stratified lakes ---- 95
- stratigraphy ---- 47
- textural characteristics ---- 51
- thickness ---- 47
- tuff bed ---- 105
- uranium ---- 55, 80
- volume ---- *47*, 102

$P_{CO_2}$ ---- 83, 102, 103, 106, 107

Perennial lakes, Searles Valley ---- 15

Phase diagram, crystallization path, extent ---- *84*
- crystallization path, direction ---- 84

Phase diagrams ---- 84, 86, 87, 91, 92, 93, 95
- 4- component system ---- 84
- 5-component system ---- 84, 92, 93

Phase diagrams—Continued
- 6-component system ---- 92
- halite field ---- 95
- Lower Salt ---- 86, 87

pH, brine ---- 43, 61, 78, 80, 81, 94

Phillipsite ---- 10, 14, 17, 52, 79, 105

Phytoplankton, Owens Lake ---- 85

Pine Creek tungsten mine ---- 99

Pinyon Pine ---- 3

Pirssonite ---- 10, 13, 14, 15, 18, 34, 37, 39, 40, 43, 47, 48, 51, 54, 56, 59, 67, 68, 72, 79, 81, 101, 102, 103, 112
- cocrystallization ---- 103
- composition, stablility ---- 103
- crystallization ---- 72, 102
- crystals ---- 34, 39, 47, 48, 72
- diagenetic ---- 102
- mineral percentages ---- 34
- Mixed Layer ---- 101, 102
- Parting Mud ---- 102

Planktonic fossils ---- 114

Plant growth, carbon isotope fractionation ---- 70

Plants, lower Sonoran zone ---- 3
- vascular ---- 53

Playa lake ---- 13

Pleistocene, temperature, long-term changes ---- 106

Pleistocene climate chronology ---- 115

Pleistocene lake fluctuations, correlation ---- 113

Pollen, correlation ---- 113, 114
- data ---- 114
- fossil ---- 8

Ponds, evaporation ---- 5
- saline, deposition ---- 96

Potassium salts ---- 5, 98, 99

Pratt, W. P., cited ---- 7

Pumping, selective, Lower Salt ---- 118

Pyramid Lake, age ---- 70

Pyrite, Bottom Mud ---- 10, 56
- crystals ---- 17, 106
- Dead Sea ---- 106
- diagenesis ---- 106
- Lower Salt ---- 105
- Parting Mud ---- 105

Q, R

Quaternary lakes, chemical sediments ---- 78
- pH values ---- 78
- salinities ---- 78
- Searles Valley ---- 78

Radiocarbon dates, carbonate minerals ---- 68
- carbonate vs. organic carbon ---- 71
- error ---- 70
- organic carbon, disseminated ---- 68
- reliability ---- 70
- sources of error ---- 73
- wood fragments ---- 68
- wood vs. disseminated organic carbon ---- 70

Ripple marks ---- 39

Robinson, R. D., cited ---- 68

Rubin, M., cited ---- 68

Ryan J.E., cited ---- 44, 45, 61, 63

S

Saline crust, X-ray diffraction analysis ---- 67

Saline crusts ---- 67

Saline deposition, rate ---- 76
- rate, maximum ---- 75
  - minimum ---- 75

Saline deposits ---- 18

Saline lakes ---- 108
- deposition ---- 96
- erosion ---- 96
- formation ---- 96
- solution ---- 96
- zones ---- 96

Saline layers, borax, significance ---- 90
- burkeite ---- 83
- distribution ---- 16

Page

Saline layers—Continued
evaporites ---*82*
geochemical environment of deposition ---82
lithology ---34
Lower Salt ---18
mirabilite ---83
Mixed Layer --- 13, 15
shape affected by underlying muds ---96
sulfate mineral ---83
water-soluble fraction, analysis ---14
zones ---13
Saline mineral assemblages ---83
Saline minerals, crystallization ---83
lake surface ---67
Mixed Layer ---84
mud units, formation ---37
Overburden Mud ---96
relative volume percentages ---34
Saline units, areal extent ---*20*
bedding character ---12
crystal habit ---12
crystal size ---12
isopach maps ---20
Lower Salt --- *20*, *34*, 96, 97
megascopic minerals, volume percentages ---34
mineral components ---34
mineralogy --- 10, 12
minerals, volume percentage, method ---34
mud layers ---12
thickness --- 12, 20
volume ---*20*
Salines, in Bottom Mud ---*85*
Lower Salt ---*86*
Mixed Layer ---*84*
Overburden Mud ---*86*
pure, zones ---110
Upper Salt ---*86*
Salt, surfaces ---108
Salt bodies, geochemical influence, shape ---*96*
geochemical influence, thickness ---*96*
Salt components, source ---*98*
Salt deposition, Mixed Layer ---108
Salt depositional rate ---75
Salt depositional sequence, Lower Salt ---97
Salt flats, modern ---108
Salt layers, accumulation, rates ---75
crystals, large, growth ---106
primary ---106
size, postdepositional increase ---106
deposition, brine, changing composition ---84
diagenetic changes ---*106*
Lower Salt --- 47, 75, 86
significance ---108
Salt units, areal extent, final ---97
Lower Salt ---75
Upper Salt ---75
Salt Wells Canyon ---97
Salts ---18
crystallization, winter ---110
rates ---75
phase relations ---*83*
Sampled materials, reliability of dates ---*70*
Sand Canyon thrust fault ---45
Sangamon Interglaciation ---115
Sangamon-Wisconsin boundary, age ---115
Schairerite --- 10, 18, 37
Sea levels ---114
Sea-level curves, correlation --- 113, 114
Sea surface temperature, correlation --- 113, 114
Searles basin ---12
Searles Lake --- 105, 114
aragonite ---104
laminae ---101
assigned ages, similarity ---113
atmospheric and lacustrine $CO_2$ disequilibrium 71
boron --- 47, 64
brine ---18
borate concentration ---90
Cl/Br ratio ---85
compositions --- 79, 84, 85, 108

Page

Searles Lake, brine—Continued
dilution ---108
economic value ---43
interstitial, present ---107
magnesium ---90
pH ---43
phases ---107
present ---107
replacement ---116
specific gravities ---43
tungsten ---99
valuable ---98
burkeite field --- 83, 84
chemical sedimentation, changes ---78
chemical stratification ---81
chemicals, total quantity ---117
value ---116
chronology ---115
climatic episodes, fluctuations ---115
components compared to Owens River ---99
confined load pressures ---100
core L-W-D, depth ---100
correlated with pollen data, Netherlands ---114
correlated with sea-level change ---114
correlation with events in
Sierra Nevada ---116
correlation with Laurentide ice sheet ---114
density, stratified ---71
deposition, episodes ---96
desiccation ---74
diagram, time scale ---114
discovery ---*4*
dissolved solids, total quantity ---98
dolomite ---81
drainage area, Pleistocene glaciers ---116
dry surface, present ---95
economic development ---*4*
evaporation ---116
evaporite deposit, value ---4
evaporites, extent ---8
logs of cores ---8
mineral composition ---8
saline layers ---*82*
samples ---8
temperature effects ---100
expansion, correlation with Pleistocene
chronology, northeast North America --115, 116
fluorine, amount ---99
fluctuation curves ---115
fluctuations, correlation ---113
correlation with Laurentide ice sheet ---114
fossil soil, stratigraphic position ---114
geologic environment ---*5*
geologic studies, previous ---*6*
halite crystallization ---84
halite field --- 83, 84, 85
hanksite, crystals ---106
history --- *5*, 68, 114
chemical ---78
inferred --- 108, 109
industrial chemicals ---56
production ---60
low stands ---113
Lower Salt, deposition ---98
micro-organisms, orange ---106
mirabilite field ---83
Mixed Layer, correlation ---116
correlation, revised ---115
deposition ---84
mud, depositional rate ---75
mud deposition ---73
mud layers --- *79*, 81, 108
carbonates ---99
halite ---104
muds, diagenetic changes ---100
gaylussite ---101
northupite ---81
pirssonite, crystals ---101
mud units, contacts, $^{14}C$ ages ---73
Na-carbonate-rich waters ---80

Page

Searles Lake—Continued
nahcolite field ---83
nahcolite, rosettes ---103
natron field ---83
organic carbon, production rate ---71
overflow --- 98, 109
phases, muds ---105
original ---104
$P_{CO_2}$, alteration minerals ---107
$PO_4$, amount ---99
post-depositional reactions ---107
Quaternary lakes ---78
recession, correlation, northeast North
America ---116
reducing environment ---71
saline layers --- 76, 108
changes in $P_{CO_2}$ ---107
crystallizaion conditions ---82
mineral composition ---83
salinity --- 98, 109
average ---194
salt, depositional rate ---75
salt components, source ---*98*
salt layers deuterium-hydrogen content ---107
diagenesis ---106
salts, diagenetic changes ---100
phase relations ---*83*
sediments, pressure, changes ---100
seismic refraction data ---67
solution, change ---96
stratification ---104
chemical ---105
stratigraphic section ---70
stratigraphic sequence ---78
stratigraphic units, subsurface ---112
structure change --- 73
surface, clays, color ---108
elevations, average ---70
temperature ---100
present ---108
projected mean temperature ---100
sands, color ---108
silts, color ---108
thenardite field --- 83, 84
trona, rosettes ---103
trona field --- 83, 84
unstratified lake water ---73
Upper Salt, tungsten ---99
volume, change ---96
water, depth ---98
salinity ---86
source ---98
Searles Lake basin, depositional history ---75
Searles Lake deposits, correlation ---14
old, erosion ---71
Overburden Mud ---66
Upper Salt ---56
Searles Valley --- 76, 79, 99
climate ---2
deposits, subsurface ---79
surface ---79
drainage area ---2
fresh lakes, maximum size ---79
fresh water, inflowing ---97
Searles Valley, ground water ---8
lacustrine rises, late Pleistocene ---114
lakes, history ---108
muds, diagenesis ---79
lateral equivalents ---79
saline deposition, rate ---76
water composition, change ---85
Searlesite --- 10, 13, 14, 15, 16, 17, 18, 79, 105, 108
Bottom Mud --- 105, 110
Mixed Layer ---108
type B ---105
Sea-surface temperature ---114
Sedimentation, geochemistry ---*78*
Sedimentation history, Mixed Layer ---108
Sedimentation patterns, chemical --- 81, 82
clastic --- 81, 82

Page

Sedimentation patterns—Continued
acid-insoluble components---75
ages, estimated---111
Bottom Mud---75, 77, 109
carbonate components---75
Clear Lake, Calif---78
Mixed Layer---109
Parting Mud---51
Sediments, varved---80
Sheppard, R.A., cited---17
Sherwin Glaciation, Sierra Nevada---116
Sierra Nevada, glacial deposits, correlation---114
glaciers, areal extent---116
Silicates---10, 18
authigenic---14, 17, 47, 51, 102, 105, 109, 195
Slate Range---3, 45
chlorite-bearing rocks---53
fault gouge---53, 67
sulfate source---59
Smith, G. I., cited---7, 12, 34, 76
Soda ash---5
production---118
Sodium bicarbonate system---83
Sodium carbonate salts, crystallization---76
Sodium sulfate, production techniques---5
Speleothems---114
Springs, thermal---98
Sterols---53
Stratigraphic units, probable true ages---*73*
Strontium, Lower Salt---45
Stuiver, M., cited---7, 72, 74
Sulfate minerals, formation---107
Lower Salt---89
postdepositional reaction---83
Sulfate system---83
Sulfohalite10, 13, 14, 15, 18, 34, 36, 37, 39, 40, 56, 59, 84
Summer Lake, dissolved solids---104
S-1, mineral composition---34
mud---34
salinity, maximum, reconstructed---98
S-2, mineral composition---36
mud---36
salinity, maximum, reconstructed---98
S-3, mineral composition---36
mud---36
salinity, maximum, reconstructed---98
S-4, mineral composition---36
mud---36
salinity, maximum, reconstructed---98
S-5, mineral composition---36
mud---37
salinity, maximum, reconstructed---98
S-6, mineral composition---37
mud---37
S-7, mineral composition---37
mud---37

T

Tahoe Glaciation---116
Teepleite---10
Temperature, postdepositional changes---107
Temperatures, crystallization, original---100
geothermal gradient---100
Terpenes---53
Thenardite---10, 13, 15, 16, 18, 34, 36, 37, 56, 59, 61, 66, 67, 83, 84, 86, 93, 94, 96, 106, 107
beds---16
cocrystallization---92
density---100
Overburden Mud---96
phase diagram---92
Upper Salt---92
Thermal springs, Long Valley area---98
Thermonatrite---107
Thompson, D. G., cited---8
Till, Mono Basin---116
Tincalconite---10, 16, 34, 43
Tree-ring dates---70

Page

Trona---10, 13, 14, 15, 16, 18, 34, 36, 37, 39, 40, 42, 52, 56, 59, 60, 61, 64, 66, 67, 78, 83, 84, 85, 86, 88, 90, 93, 94, 96, 103, 107, 108, 112, 118
beds---15, 16, 48, 60, 76, 108, 118
deposition---72
Green River Formation---76
Upper Salt---60, 76
cocrystallization---92
crystallization---72
crystals---38, 39, 48, 72
fibrous---15, 36
formation---107
Lower Salt---87, 88, 89, 90
mineral percentages---34
Mixed Layer---108, 118
Overburden Mud---96
phase diagrams---87, 89, 92
plant---116
stratigraphic distribution---85
Upper Salt---92
Trona reef, formation---67
Tuff, altered to phillipsite---52
andesitic---15
Tuff beds---17, 105
analcime---105
K-feldspar---105
rhyolitic---48
searlesite, type B---105
Tungsten, Hot Creek---100
Keough Hot Spring---100
Little Hot Creek---100
Long Valley area---100
Morgan Creek---99, 100
neutron activation analyses---100
Owens River---99
Pine Creek mine---99, 100
Searles Lake---99
sources, compared---100
Upper Salt---99
Tychite---10, 13, 14, 15, 18, 34, 37, 39, 81, 84
crystals---38, 103

U

Unit A, deposition, saline lake---109
lake, perennial---109
mud layers---14
nahcolite beds---108
saline layers---14
trona beds---108
Unit B, deposition, saline lake---109
lake, perennial---109
mud layers---14
nahcolite beds---108
saline layers---*14*
trona beds---108
Unit C, deposition, saline lake---109
halite beds---15
mud layers---15
salinity, range---109
trona beds---15
Unit D, tuff bed---15
mud layers---15
saline layers---15
salinity, range---109
tuff bed---15
Unit E, deposition, fluctuating lake---109
saline layers---15
salinity, range---109
volcanic ash bed---15
Unit F, deposition, deep lake---108
halite---15
mud layers---15
saline layers---15
salinity, range---109
trona beds---15
Unit S-5, top, correlation---114
Upper Salt---10, 12, *56*, 59, 75, *91*

Page

Upper Salt—Continued
aphthitalite---95
areal extent---*56*
areal mineral zonation, correlated with thickness---59
base, correlation---114
bedding---60
borax, concentration---95
distribution pattern---60, 64, 95
brine---56
composition, variation---117
vertical variations---64
salinity---94
brines, areal variations---118
boron---63
carbonate source---72
carbonate total---61
chemical composition---*60*
chloride---61
commercial grade---117
compositions---61, 93, 117
density profile---117
deuterium-hydrogen ratios---117
dissolved solids, total percentages---61
fluoride---63
iodide---63
lithium---63
major elements, analyses---61
migration---118
pH values---61
phosphate---61
sulfide---63
sampling---61
6-component system---108
sulfate---61
specific gravities---61
strontium---63
tungsten---63
burkeite---92, 94
central facies---95
chemical composition---*60*, 86
compared to Lower Salt---95
contact, base---97
upper---97
core samples, chemical analyses---42
crystallization sequence---86, 92, 93, 98
deposition---56, 92, 98, 112
diagenesis---92, 93, 94
distribution---56
equilibrium assemblage---61
estimated bulk composition---*64*
flourine amount---99
halite---95
hanksite---92, 95
beds---94
concentration---93
crystals---94, 106
distribution---60, 93, 95
secondary---93
permeability---60
lateral equivalent---66
lithology---*59*
metastable assemblage---94
mineral assemblage, recrystallization---94
mineral composition---*59*
estimates---64
minerals---56
vertical distribution---59
minor elements---61
mud---59
mud layers, discontinuous---112
formation---60
original extent---98
overall shapes---118
permeability---60
phase diagram---91
burkeite field---92
aphthitalite field---92
5-component system---92, 93

Page
Upper Salt, phase diagram—Continued
halite---95
hanksite field---92, 93
6-component system---92
thenardite field---92
trona field---92
porosity---60
potassium amount---102
salines---*86*
salt layers, accumulation rate---75
salt units, $^{230}Th/^{234}U$---75
shape related to basin---97
sodium amount---102
sodium carbonate mineral, dominant species -92
solids, chemical analyses---*60*
composition---60
solutions, initial compositions---86
stratigraphic contacts---56, 60, 66
Upper Salt—Continued
sulfate minerals, primary---94
temperatures, crystallization---112
thickness---56
thickness distribution---97
trona beds---60, 76
trona layer---93, 94
upper zone---94
volume---*56*, 59
water-soluble components, major, total---64
X-ray analyses---60
Uranium---55, 80

V, W

Vallentyne, J. R.,cited---53
Volcanic ash, andesitic---14, 15
basaltic---14
Volume, computation method---20
Waters, calcium, total dissolved solid content---80
natural, components---98
Great Basin---98
pH values---80
Well, Old Searles---12, 13, 16
Wells, pumped, Lower Salt---118
West End Chemical Co.---5
West Yellowstone area, glacial advances---114
West Yellowstone glacier, recession, maximum --114
Wood, dates---73

X,Y, Z

Xanthophylls---53
Yarmouth Interglaciation---115
Zeolite---17, 105
Zones, salines, pure---110

GPO 689-035